RESEARCH AND DEVELOPMENT TECHNICAL REPORT
CECOM — DRSEL-TR-80-0588F

FREQUENCY HOPPING TRANSCEIVER MULTIPLEXER

GTE Sylvania Systems Group
Communication Systems Division
Needham Heights, MA 02194

Final Report for 1 August 1980 — 1 March 1983

March 1983

Distribution Statement

Approved for public release:
distribution unlimited.

Prepared for

Center for Communication Systems

CECOM

US ARMY COMMUNICATIONS – ELECTRONICS COMMAND
FORT MONMOUTH, NEW JERSEY 07703

NOTICES

Disclaimers

The citation of trade names and names of manufacturers in this report is not to be construed as official Government endorsement or approval of commercial products or services referenced herein.

Disposition

Destroy this report when it is no longer needed. Do not return it to the originator.

SECURITY CLASSIFICATION OF THIS PAGE *(When Data Entered)*

REPORT DOCUMENTATION PAGE		READ INSTRUCTIONS BEFORE COMPLETING FORM
1. REPORT NUMBER DRSEL-TR-80-0588F	2. GOVT ACCESSION NO. AD-A126736	3. RECIPIENT'S CATALOG NUMBER
4. TITLE *(and Subtitle)* Frequency Hopping Transceiver Multiplexer		5. TYPE OF REPORT & PERIOD COVERED Final Report Aug 1980 – Mar 1983
		6. PERFORMING ORG. REPORT NUMBER
7. AUTHOR(s) Colin B. Weir		8. CONTRACT OR GRANT NUMBER(s) DAAK80-80-C-0588
9. PERFORMING ORGANIZATION NAME AND ADDRESS GTE Sylvania Systems Group Communication Systems Division 77 "A" Street, Needham Heights, Mass 02194		10. PROGRAM ELEMENT, PROJECT, TASK AREA & WORK UNIT NUMBERS IL161102AH48
11. CONTROLLING OFFICE NAME AND ADDRESS CENCOMS US Army CECOM, DRSEL-COM-RN-3 Fort Monmouth, NJ 07703		12. REPORT DATE March 1983 13. NUMBER OF PAGES 384
14. MONITORING AGENCY NAME & ADDRESS*(if different from Controlling Office)*		15. SECURITY CLASS. *(of this report)* Unclassified 15a. DECLASSIFICATION/DOWNGRADING SCHEDULE

16. DISTRIBUTION STATEMENT *(of this Report)*

Approved for Public Release, Distribution Unlimited

17. DISTRIBUTION STATEMENT *(of the abstract entered in Block 20, if different from Report)*

18. SUPPLEMENTARY NOTES

19. KEY WORDS *(Continue on reverse side if necessary and identify by block number)*

frequency hopping, quadrature coupler, bandpass filter, coupling circuit, filter, helical resonator, matching network, PIN diode switch, binarily related capacitance tuning array, transceiver multiplexer, frequency hopping transceiver multicoupler, antenna multicoupler, antenna coupler

20. ABSTRACT *(Continue on reverse side if necessary and identify by block number)*

This final report summarizes the activity on contract DAAK80-80-C-0588, which investigated the concept and feasibility of a 30MHz to 88MHz frequency hopping transceiver multiplexer. An approach which uses helical resonator filters, PIN diode switched capacitors and quadrature couplers for combiner and antenna matching circuits represents the most optimistic design.

DD FORM 1 JAN 73 1473 EDITION OF 1 NOV 65 IS OBSOLETE

SECURITY CLASSIFICATION OF THIS PAGE *(When Data Entered)*

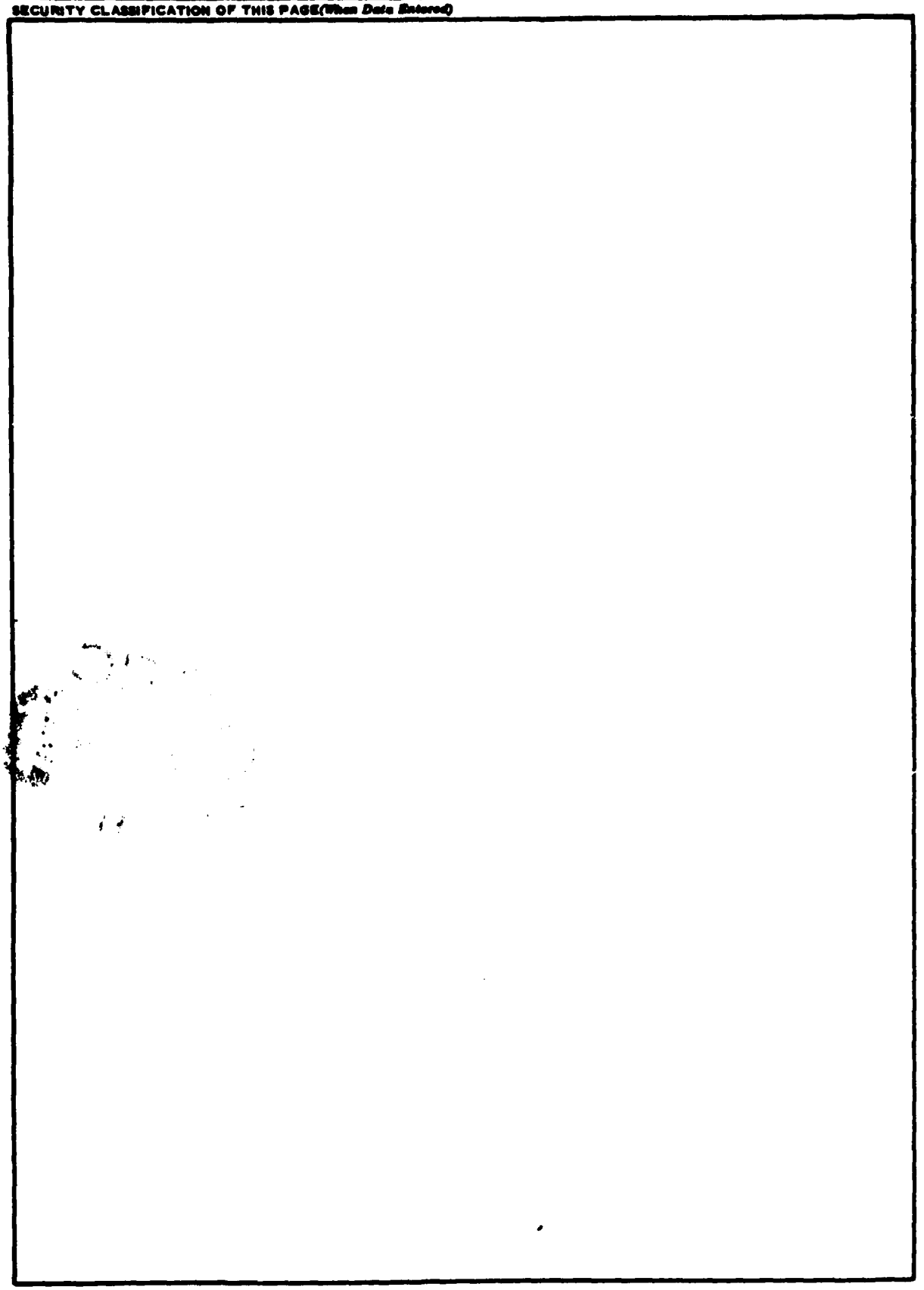

FREQUENCY HOPPING MULTIPLEXER DESIGN ASSESSMENT

FINAL REPORT

AUGUST 1982

PREPARED FOR
USA CORADCOM
ON CONTRACT
DAAK80-80-C-0588

GTE Systems

Communication Systems Division
GTE Communications Products Corporation
77 "A" Street
Needham Heights, MA 02194
Area Code 617 449-2000
TELEX: 922497

FREQUENCY HOPPING MULTIPLEXER

DESIGN ASSESSMENT

FINAL REPORT

AUGUST 1982

Prepared for:

USA CORADCOM
Contract No. DAAK80-C-0588

Communication Systems Division
GTE Communications Products Corporation
77 "A" Street
Needham Heights, Mass. 02194

ABSTRACTS

DESIGN ASSESSMENT

This GTE Final Report for a Frequency Hopping Multiplexer (FHMUX) Design Assessment completes a 12 month study to investigate its concept and feasibility. This report develops and explains an approach to permit the operation of up to five frequency hopping transceivers, in the 30 to 88 MHz frequency range, with a common wideband antenna.

The results of the study are positive. The FHMUX can perform as desired and also enhance certain transceiver performance parameters such as broadband transmitter noise rejection, more constant transmitter loading, and increased receiver selectivity. These positive results should encourage the design and development of an advanced engineering model.

This report is supported by a Reference Document which discusses work performed early in the FHMUX program.

FEASIBILITY MODEL

This GTE Final Report completes a successful program to prove the design concept and demonstrate equipment feasibility for a VHF Frequency Hopping Multiplexer (FHMUX). This is a continuation of the FHMUX Design Assessment program.

The results of the program are positive. The FHMUX will perform as required and also enhance certain transceiver performance parameters such as broadband transmitter noise rejection, more constant transmitter loading, and increased receiver selectivity. These positive results should encourage the design and development of an FHMUX advanced engineering model.

TABLE OF CONTENTS

Section	Title	Page
	Abstracts	iii
1	INTRODUCTION	1
1.1	Program Description	1
1.2	Report Organization	1
2	JUSTIFICATION OF A SINGLE ANTENNA SYSTEM	3
2.1	Tradeoffs Between Single and Dual Antenna Approaches	3
2.2	Block Diagram Discussion	3
2.3	Dual Antenna Approach Conclusions	3
3	SYSTEM STUDIES AND BER ANALYSIS	7
3.1	Introduction	7
3.2	Block Diagram Discussion	7
3.3	Isolation Requirement	7
3.3.1	IMD Performance	10
3.4	Load Pulling Effects	10
3.5	Antenna Study	12
3.6	Antenna Compensation	12
4	BIT ERROR RATE PERFORMANCE OF THE FHMUX	13
4.1	Introduction	13
4.2	Derivation of a Reference System	13
4.3	FHMUX Self Blocking	17
4.3.1	An FHMUX Model	18
4.3.2	Four-Port Coupler Model	20
4.4	The BER Model	24

TABLE OF CONTENTS (Cont.)

Section	Title	Page
4.5	The BER Model vs. the Reference System	35
4.6	Combined Effects	38
4.7	Description of the Baseline System	40
4.8	Model Errors	43
5	EVALUATION OF HARDWARE CONFIGURATION	45
5.1	Introduction	45
5.2	An Additional Combining Scheme	45
5.3	Load Pulling	47
5.4	Quad Combiner Analysis	48
5.5	Laboratory Verification	71
5.6	Power Combining Properties	75
5.7	Filter Interaction	81
5.8	High Q Resonator Study	85
5.8.1	Introduction	85
5.8.2	Bounding the Problem	85
5.9	Computer Aided Design and Analysis	90
5.9.1	Helical Resonator	90
5.9.2	Shunt Capacitance Binary Bus Discussion	94
5.9.3	Resonator Design Decisions	97
5.9.4	Results and Conclusions	108
5.10	Packaging Concept	110
5.10.1	Mechanical Concept	110
5.10.2	Power Consumption	112

TABLE OF CONTENTS (Cont.)

Section	Title	Page
6	CONCLUSIONS AND RECOMMENDATIONS	115
6.1	Comment	115
6.2	Final Configuration	115
6.3	Alternate Configuration	116
7	BIBLIOGRAPHY	121
7.1	Referenced Documents	121
7.2	Jamming - Frequency Hopping - Spread Spectrum	121
7.3	Devices	122
7.4	Ferrite Circulators	122
7.5	Active Circulators	123
7.6	Distortion	123
7.7	Circuits	124
7.8	Miscellaneous	124
APPENDIX E	RESONATOR STUDY	129
E.1	Introduction	129
E.2	Flauto-C Resonator Model	131
E.3	Helical Resonator Model	132
E.4	Shortened-Line Resonator Model	133
E.5	Flauto-C Results	135
E.6	Helical Resonator Results	142
E.7	Conclusions	142
E.8	References	148

TABLE OF CONTENTS (Cont.)

Section	Title	Page
APPENDIX F	SHUNT CAPACITANCE BINARY BUS DESIGN	149
F.1	Introduction	149
F.2	Initial Results	149
F.3	Analysis of Problem Areas	153
F.4	Comment	156
APPENDIX G	BLOCKAGE RATE OF THE FHMUX	159
Appendix A through D are contained in Reference Document August 1982.		
APPENDIX A	CIRCULATOR CIRCUIT TECHNIQUES	A-1
A.1	Circulator Multiplexing Schemes	A-1
APPENDIX B	DISCUSSION OF DUAL ANTENNA SYSTEMS	B-1
B.1	Circulator Discussion	B-1
B.2	Switching Considerations	B-4
B.3	Active Circulator	B-4
B.4	Two Antenna Systems with Linear Amplifiers	B-4
B.5	Alternate Approaches	B-14
B.6	Hybrid Two Antenna System	B-16
B.7	System Requirements	B-19

TABLE OF CONTENTS (Cont.)

Section	Title	Page
APPENDIX C	LOAD PULLING STUDY	C-1
C.1	Filter Application & Load Pulling Study	C-1
C.2	Load Pulling	C-3
APPENDIX D	ANTENNA STUDY	D-1
D.1	Antenna Description	D-1
D.2	Antenna Impact on System Design	D-8
D.3	Analysis of Antenna Parameter Variation	D-9
D.4	Possible Value of Phase Correction	D-12
D.5	The Self-Calibrating Single Antenna FHMUX	D-16
D.6	Advantage of Self-Calibration	D-16
D.7	Block Diagram Description	D-17
D.8	Alignment Procedure	D-19
D.9	Impedance Measurement Techniques	D-21
D.10	Operational Scenario	D-21

LIST OF FIGURES

Figure	Title	Page
2-1	Block Diagram, Two Antenna System	4
3-1	Block Diagram, Single Antenna System	8
3-2	Isolation Requirements	9
3-3	IMD Analysis	11
4-1	Reference System	14
4-2	Frequency Spacing vs. Acceptable S_2/S_D Ratio	16
4-3	Frequency Hopping Multiplexer for a Five Transceiver System	19
4-4	Four-Port Coupler	21
4-5	Average Blockage Rate for User #5 with the Indicated Number of Transmitters on the Air, Fixed Priority	31
4-6	Average Blockage Rate vs. 40 dB Bandwidth, Rotating Priority, Worst Case	32
4-7	Transmit Duty Cycle vs. Probability that N of Five Transmitters are Active in a Five Channel FHMUX in Time Coincidence with a Remote Transmitter	33
4-8	Combined Effects, Scaled to 80 MHz	39
4-9	Combined Effects, Scaled to 30 MHz	42
5-1	RF Combining Scheme	46
5-2	General Two-Port Block Diagram	49
5-3	S Parameter Definitions	49
5-4	Block Diagram for Analysis of Interface Conditions Between FHMUX and Antenna System	50
5-5	Block Diagram for Hybrid Coupled Bandpass Filters	56
5-6	Hybrid Coupler	57
5-7	Hybrid Coupler System	63
5-8	Test Circuit	72
5-9	Comparison of Short and Open Circuit Swept Response	74

LIST OF FIGURES (Cont.)

Figure	Title	Page
5-10	Quadrature Hybrid Relationships	76
5-11	Combining Loss Due to Filter p1 and p2 vs. Filter Skirt Attenuation	82
5-12	Means of Connection	84
5-13	Loss Analysis	86
5-14	Insertion Loss in dB vs. QU/QL	87
5-15	Resonator Model	89
5-16	Q Inductor vs. Q Capacitor for a Loaded Q of 50, with Insertion Loss as Parameter	91
5-17	Resonator Design Aid High Band Resonator	93
5-18	Frequency Hoppable Bandpass Filter	96
5-19	Schematic, 50-88 MHz Frequency Hoppable Bandpass Filter	100
5-20	Explanation of Calculator Program	101
5-21	Preliminary Mechanical Concept	111
6-1	Five-Channel FHMUX	117
6-2	Five-Channel FHMUX Alternate Configuration	118
E-1	Series Resonant Bandpass Filter	130
E-2	Parallel Resonant Bandpass Filter	130
E-3	Flauto-C Resonator Model	131
E-4	Helical Resonator Model	133
E-5	Shortened Line Resonator	133
E-6	Odd-Even Mode Model for Shortened Line Resonator	134
E-7	Schematic and Computer Printout, Flauto-C Resonator Tuned at 59 MHz	136
E-8	Schematic and Computer Printout, Flauto-C Resonator Tuned to 88 MHz	137

LIST OF FIGURES (Cont.)

Figure	Title	Page
E-9	Schematic and Computer Printout, Flauto-C Resonator Tuned to 59 MHz	138
E-10	Schematic and Computer Printout, Flauto-C Resonator Tuned to 88 MHz	139
E-11	Schematic and Computer Printout, Flauto-C Resonator Tuned to 30 MHz	140
E-12	Schematic and Computer Printout, Flauto-C Resonator Tuned to 88 MHz (30 MHz with Diode "ON")	141
E-13	Schematic and Computer Printout, Flauto-C Resonator with Two Tuning Capacitors Tuned to 59 MHz	143
E-14	Schematic and Computer Printout, Flauto-C Resonator with Two Tuning Capacitors Tuned to 88 Mhz	144
E-15	Schematic and Computer Printout, Flauto-C Resonator Showing Absence of Second Passband	145
E-16	Schematic and Computer Printout, Helical Resonator Tuned to 59 MHz	146
E-17	Schematic and Computer Printout, Helical Resonator Tuned to 88 MHz	147
F-1	Preliminary Model Capacitance Bus	151

REFERENCE DOCUMENT

LIST OF FIGURES

Figure	Title	Page
A-1	Summation of 3 Transmitters	A-2
A-2	Summation of 4 Transmitters	A-5
A-3	Five Way Combiner	A-7
A-4	Nine Way Combiner	A-8
A-5	16 Way Combiner	A-9
B-1	Three Port Circulator Preliminary Specification	B-2
B-2	Specification Response	B-3
B-3	Switching Considerations	B-5
B-4	Active Three-Port Circulator	B-6
B-5	Alternate Circuit - Transmit Multi-Coupler	B-7
B-6	IMD Analysis	B-10
B-7	Noise Floor Analysis	B-11
B-8	Channelized Amplifier	B-15
B-9	Hybrid Two Antenna RF Block Diagram	B-17
B-10	Dual Antenna System Model Derivation	B-20
C-1	Tuned Circuit Response	C-5
C-2	Range of Element Values	C-6
C-3	Loads 3 and 4	C-8
C-4	Loss vs. Bandwidth, Load #3	C-9
C-5	Loss vs. Bandwidth, Load #4	C-10
C-6	Impedance vs. Frequency, Loads 5 and 6	C-11
C-7	Loss vs. % Bandwidth Load #5	C-12
C-8	Loss vs. % Bandwidth Load #6	C-13
C-9	Antenna Load #1 Impedance vs. Frequency	C-15

LIST OF FIGURES (Cont.)

Figure	Title	Page
C-10	Impedance vs. Frequency Load #2	C-17
C-11	Locus Points for Load 3, 4, 5, and 6. Taken every 10 degrees	C-20/C-21
D-1	Antenna Characteristics	D-2
D-2	As 3166/GRC Antenna Impedance	D-3
D-3	Antenna Group OE-254/GRC R + JX at Input to 50 ft. Cable. Resistance vs. Frequency	D-6
D-4	Antenna Group OE-254/GRC Reactance vs. Frequency	D-7
D-6	Variation in Input Impedance for +/-10% Variation in Load Impedance	D-10
D-7	Variation in Input Impedance as Length is Varied from 80'-2% to 80'+2%	D-11
D-8	Block Diagram, FHMUX Single Antenna Scheme with Antenna Phase Correction	D-15
D-9	Block Diagram, Self Calibrating FHMUX	D-18

LIST OF TABLES

Table	Title	Page
4-1	Path Loss Data	15
4-2	Ratio of Undesired to Desired Signals	15
4-3	Minimum Spacing vs. Frequency	17
4-4	Average Blockage Rate (Expressed as a Fraction) vs. 40 dB Percentage (of User Operating Frequency) Bandwidths. Expressed Under Worst Case Fixed Priority Conditions	26
4-5	Average Blockage Rate for User Number 5 with Indicated Number of Transmitters (Expressed as a Fraction) vs. 40 dB Percentage (of User Operating Frequency) Bandwidths. Expressed Under Worst Case Fixed Priority Conditions	28
4-6	Average Rate of Blockage (expressed as a fraction) vs. 40 dB BW, Rotating Priority, Worst Case	30
4-7	Probablistic Effects, Fixed Priority System	34
4-8	Required Guard Bandwidth for 10% BER, Four Transceivers Transmitting on Line, Fixed Priority	36
4-9	Required Guard Bandwidth (%) for 10% BER, with Four Tranceivers Transmitting Rotating Priority	37
4-10	Derivation of Curve C	40
4-11	Response of a System with a -40 dB Bandwidth of +/-5%	40
5-1	Helical Resonator Design	92
5-2	Helical Resonator Design and Analysis	99
5-3	"On/Off" Values at 53 MHz	102
5-4	"On/Off" Value at 70 MHz	103
5-5	"On/Off" Values at 87 MHz	104
5-6	Filter Analysis at 53 MHz	105
5-7	Filter Analysis at 70 MHz	106
5-8	Filter Analysis at 87 MHz	107

LIST OF TABLES (Cont.)

Table	Title	Page
5-9	PIN Diode Specification	109
5-10	Power Consumption	112
F-1	Filter Analysis at 30 MHz	152
F-2	Filter Analysis at 88 MHz	154
F-3	Filter Performance with Low Capacitance Relay Parameters	155
F-4	Filter Performance with High Capacitance Relay Parameters	157

SECTION 1

INTRODUCTION

1.1 PROGRAM DESCRIPTION

This Final Report describes the evaluation and final design assessment of a frequency hoppable multiplexer (FHMUX) to operate in the 30-88 MHz frequency range.

Three Quarterly Reports have preceded this Final Report. The first Quarterly Report describes initial concepts and system concepts for both single and dual antenna systems. The dual antenna system provides separate antennas for transmitting and receiving, whereas the single antenna scheme multiplexes the transmitters and/or receivers on a single antenna. Preliminary work indicates antenna VSWR as a possible problem area.

The Second Quarterly Report describes the continued investigation of system concepts and preliminary hardware implementation. A Bit Error Rate(BER) performance analysis was initiated. (This final report concludes this BER analysis and takes into account the transmit-receive duty cycle.) The Second Quarterly Report analyzes the antenna system and its effect on the FHMUX, and justifies the selection of a single antenna system.

The Third Quarterly Report provides introductory hardware design concepts for the helical resonator and the shunt capacitive bus used to tune the resonator. A third means of channel combining was introduced which was soon recognized to be superior to the others.

This Final Report summarizes the successes and failures of the previous work. As noted, the BER analysis is completed. Also, new work is introduced to justify the final system configuration.

1.2 REPORT ORGANIZATION

This Final Report is intended to be a stand alone document which describes the full thrust of the FHMUX design assessment, and the logical flow of the task. It is however, supported by a Reference

Document containing Appendices A, B, C, and D, which are referred to in the main text. These Appendices describe work performed early in the program. The report is organized as shown below:

Section 2 - Decision to specify a single, rather than a dual antenna system

Section 3 - System studies and BER analysis

Section 4 - BER performance of the FHMUX

Section 5 - Evaluation of hardware configuration

Section 6 - Comment and recommendation

Section 7 - Bibliography

Appendix E - Resonator Study

Appendix F - Shunt Capacitance Binary Bus Design

Appendix G - Blockage Rate of the FHMUX

SECTION 2

JUSTIFICATION OF A SINGLE ANTENNA SYSTEM

2.1 TRADEOFFS BETWEEN SINGLE AND DUAL ANTENNA APPROACHES

Tradeoffs between single and dual antenna approaches were conducted; the single antenna approach was selected. This section contains the reasons for not selecting the dual antenna solution. The basic dual antenna block diagram and various circulator multiplexing schemes are shown, the results of a circulator literature search, and a circulator specification are discussed. Also included are preliminary RF switching considerations.

2.2 BLOCK DIAGRAM DISCUSSION

Figure 2-1 shows the Dual Antenna System Simplified Block Diagram. This circuit will take advantage of circulator techniques to eliminate any tuned circuits for the combining of the transmitters to a single antenna. Since the inherent characteristics of ferrite circulators prevent reciprocity, a second antenna and filter multiplexer must be used for the receiving mode. As shown in Figure 2-1, this dual antenna scheme requires a T/R controlled switching system to separate the transmitted and received signals for routing to the correct multiplexer. A description of these circulator circuit techniques is given in Appendix A. Appendix B discusses the reasons for the elimination of the dual antenna system (see Reference Document).

2.3 DUAL ANTENNA APPROACH CONCLUSIONS

- The FHMUX Design Assessment program plan calls for a decision regarding the selection of a single or dual antenna system to be made during the midpoint of the program. The remaining time in the project will be spent assessing and refining the surviving system. At the time of the decision, the load insensitive quadrature coupled combining scheme described later herein was not yet under consideration. Antenna loading was then considered to be a major problem

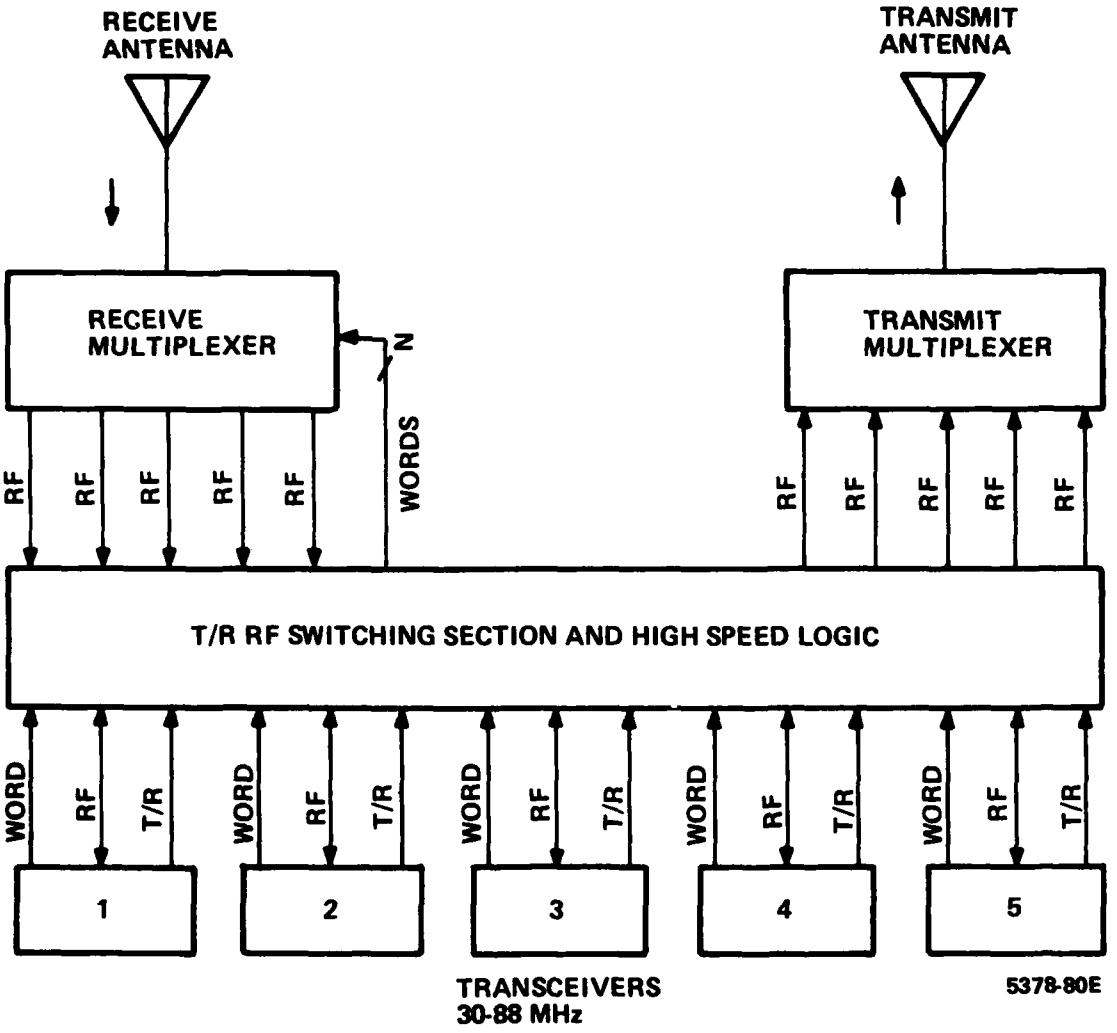

Figure 2-1. Block Diagram, Two Antenna System

area, and a high powered linear amplifier was considered as a buffer amplifier and channel combiner to isolate the antenna from the filters. Because of the large amount of dc power required, and the need for excellent amplifier linearity, this version of the dual antenna scheme was discarded

- GTE has also concluded that ferrite devices will not be available for a 30-88 MHz dual antenna FHMUX
- The dual antenna concept was set aside. Later, a quadrature coupler channel combining scheme was developed which was insensitive to changes in antenna impedance. This scheme is explained in Section 5 of this report, and is used in the final version of the single antenna FHMUX
- A dual antenna FHMUX can be configured to use this quadrature combining scheme and thus eliminate the high powered linear amplifier
- This "new" version of the dual antenna system has not been assessed in detail. However, if approximately 15 dB of antenna isolation can be obtained, a very flexible system is possible
  - If the transmit section of this multiplexer is of equal quality as the single antenna design, IMD suppression will be the same as that of the single antenna system
  - The volume and weight requirements of this system will be almost double that of the single antenna system, if the receiver and transmitter sections have equal performance capability. Overall system insertion loss will be slightly higher because of the need for a transmit/receive switch for each transceiver. Overall Bit Error Rate performance will be better due to the approximate 15 dB of "built in" antenna isolation, which will result in a narrower guard band
  - The receiver section filtering requirements can be reduced if improved BER performance is not required.

For this case, the receiver section will have to withstand about one to two watts of RF power without generating excessive IMD products

- Because of the complexity and size of this system, the single antenna system as described later on, still appears to be more workable
- The Dual Antenna FHMUX really seems best suited for separate receiver and transmitter operation. That is, the driving transceivers will provide direct access to the transmitters and receivers rather than an additional external T/R switch
- The dual antenna system may be the basis for a complete radio system rather than a field operated unit. The inherent flexibility of this system will tend to drive its use to accommodate five or more sets of separate receivers and transceivers.

SECTION 3

SYSTEM STUDIES AND BER ANALYSIS

3.1 INTRODUCTION

This section is concerned with a frequency hopping multiplexer which combines five transceivers with a single antenna. Discussed are: the original proposed block diagram, isolation requirements, load pulling effects, and evaluation of the BER model.

3.2 BLOCK DIAGRAM DISCUSSION

The preliminary block diagram is shown in Figure 3-1. As shown, this implementation is a single broadband system using quadrature coupled tuned filter elements in both the transmiting and receiving path. The tuning of these filter elements will be microprocessor-controlled to prevent collisions of tranmissions and receptions on the same frequency. The circuit uses the unique and well known quadrature couplers characteristics of always presenting a 50 ohm impedance match at the input (or output) port. Cascaded special purpose RF filters are used to multiplex the RF energy to the antenna.

If a transmitter is energized and the quad coupled filters are tuned to the transmitter frequency, the RF energy will pass through the filters with only slight attenuation. If the filters inside the quad-couplers are not tuned to the transmitter frequency but are identically tuned to each other, the RF energy will be dissipated in the quad-coupler terminating resistor. This protects the transmitter and permits rapid tuning of the filters without the need to shutdown the transmitter.

3.3 ISOLATION REQUIREMENT

The design assessment stated goal is to achieve system performance equivalent to that achieved with separate antennas spaced 100 meters apart. Figure 3-2 shows the amount of isolation required by the multiplexer to provide this equivalent performance, given certain assumptions regarding antenna gain and the ground plane. As shown,

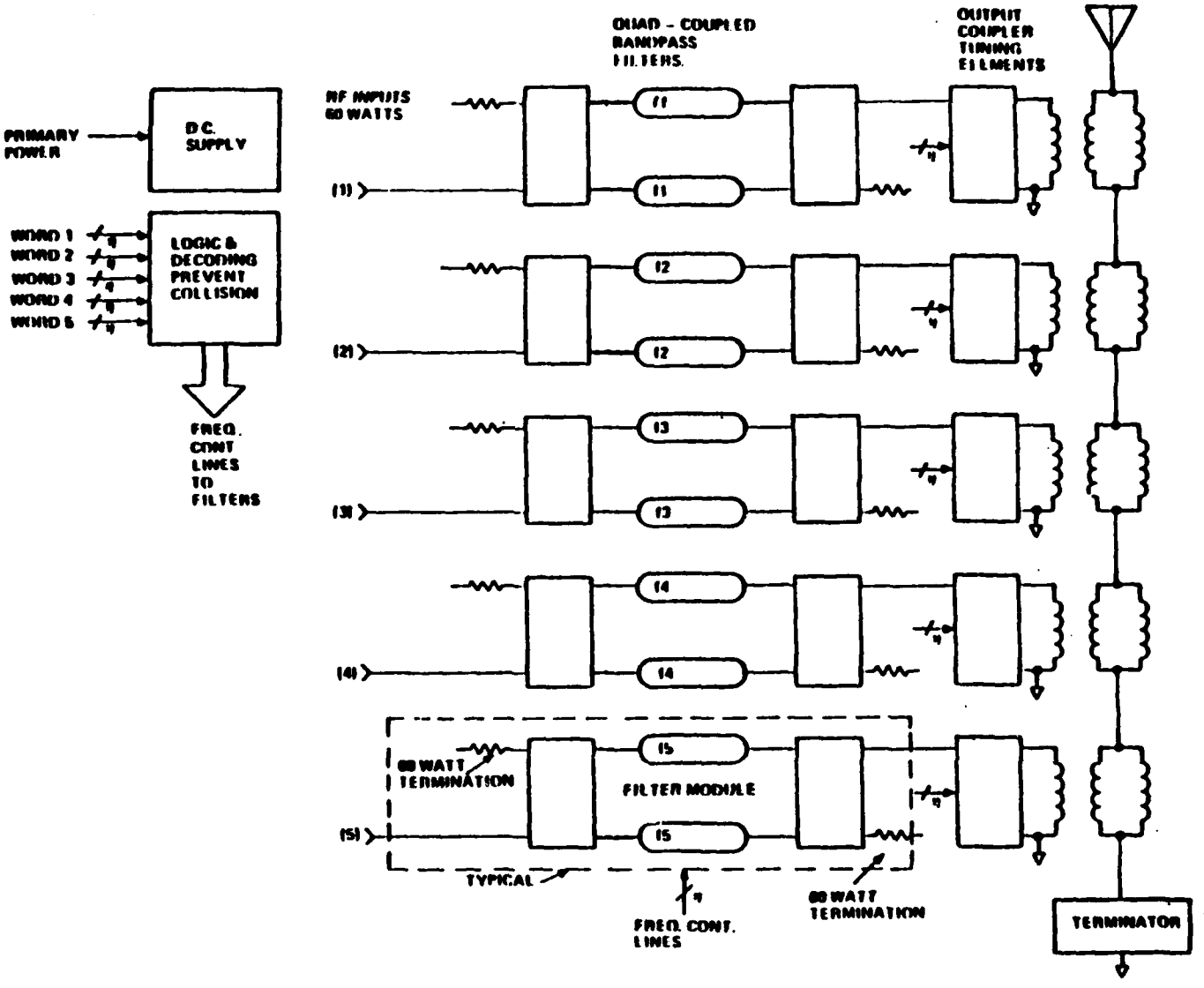

Figure 3-1. Block Diagram, Single Antenna System

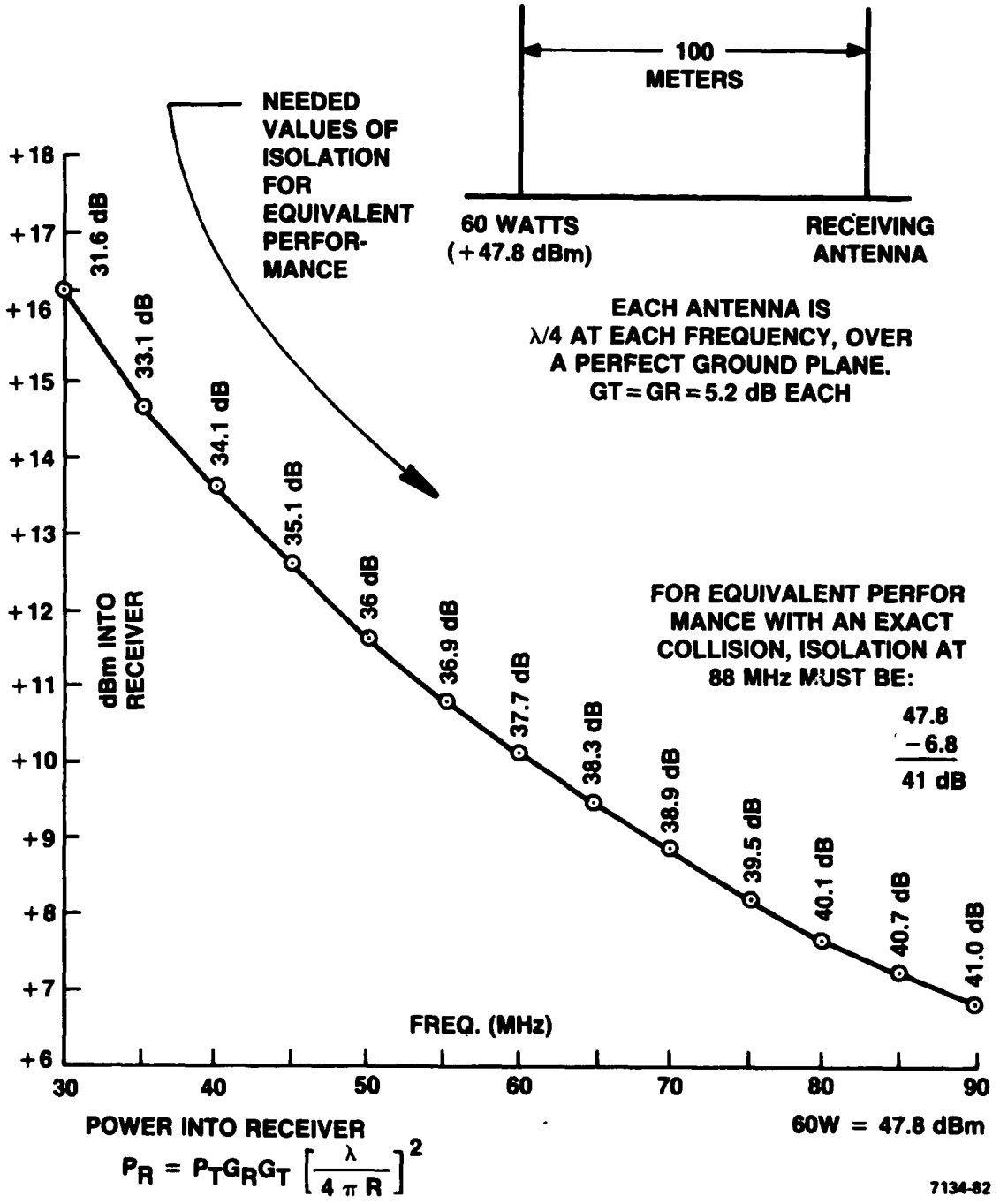

Figure 3-2. Isolation Requirements

the required isolation appears to vary from 31.6 dB at 30 MHz to 41.0 dB at 90 MHz. However, it appears that a more realistic assumption is a minimum of 40 dB isolation between any two channels spaced ±5% apart, across the full 30-88 MHz bandwidth.

3.3.1 IMD Performance

Figure 3-3 shows that when two transceivers are both in the transmit mode, and separated by 5% in frequency, a zero dBm interfering signal will appear at the output of both transmitters. This is based on having 46 dB of isolation between channels. The degree of transmitter back intermodulation is unknown at this time, but it is hoped that it will be at least 40 dB below the interfering signal, or at -40 dBm. The intermodulation signal ($2F_1-F_5$, or $2F_5-F_1$) will be attentuated by an additional 46 dB as it travels back through the filters. Thus, the intermodulation signals will be at a level of about -86 dBm, or at -132 dBc, which is better than the design goal by approximately 12 dB. Thus, it appears that if this scheme can be designed such that it does not generate excessive IMD products of its own, it can greatly improve the IMD situation in the field. At this time, the generation of IMD products in the single antenna system will probably concentrate in the RF switches.

3.4 LOAD PULLING EFFECTS

During the early months of this design assessment, lumped element filters were considered in lieu of helical resonators. The basic design of these distributed filters lead to a load pulling study. The results of this study indicate that load pulling is potentially a severe problem. This led to a series of antenna tuning and calibration schemes which complicates the FHMUX design. A channel combining scheme has been chosen to obviate the need to measure the antenna and compensate for the impedance variation. The lumped filter evaluation and the load pulling study are contained in Appendix C of the Reference Document.

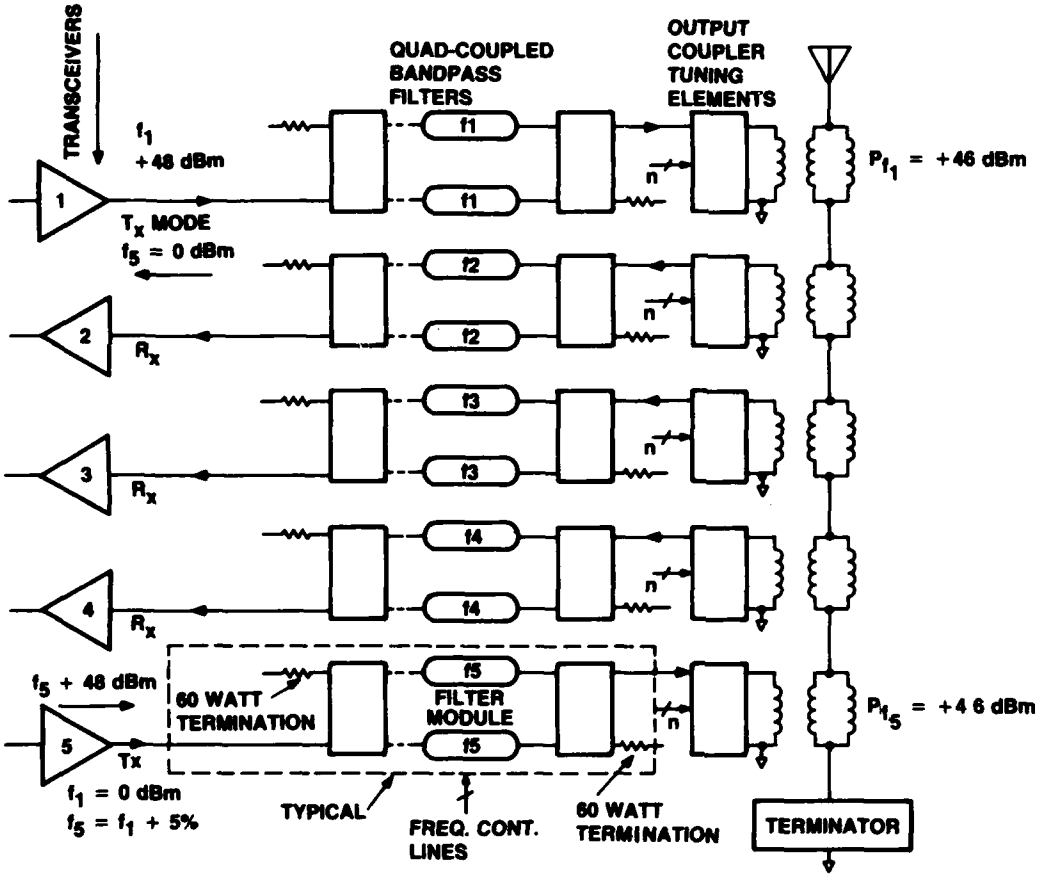

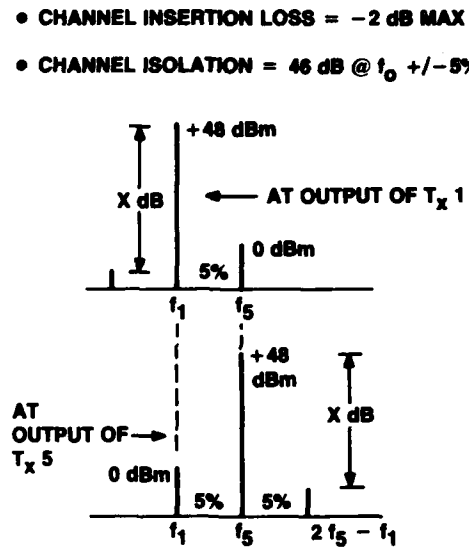

Figure 3-3. IMD Analysis

3.5 ANTENNA STUDY

Results of the load pulling study caused concern over the workability of the FHMUX concept. This concern was removed upon selection of an RF configuration which was rather insensitive to antenna impedance variation. However, the early concern over the antenna impedance led to detailed study of the antenna proposed for use with the FHMUX. Also, it was learned that operation with other antennas was desired. The antenna study and results are found in Appendix D of the Reference Document.

3.6 ANTENNA COMPENSATION

At the completion of the antenna study, the final channel combining scheme was still unknown, and antenna compensation was an important issue. A study was begun to determine the best means of antenna compensation, and an operational scenario was written. These are contained in Section D-4 through D-10 of Appendix D.

SECTION 4

BIT ERROR RATE PERFORMANCE OF THE FHMUX

4.1 INTRODUCTION

This section deals with the overall (BER) performance of a complete system, i.e., the FHMUX, and an array of SINCGARS transceivers. It is shown that the system BER is not only affected by the FHMUX, but is also affected by the transceiver's characteristics such as receiver selectivity, transmitter noise floor, and the transmit-receive duty cycle.

The FHMUX affects the BER by shutting down a particular channel when the channel falls on or inside the guard band of a higher priority channel. This is termed self-blocking.

A reference system is defined, serving as a basis for comparison for the BER performance of the FHMUX.

Finally, the results of the BER analysis are used to define a practical set of FHMUX system parameters, from which a hardware oriented system design assessment can evolve.

4.2 DERIVATION OF A REFERENCE SYSTEM

Discussion of the (BER) performance of the FHMUX may lead to false conclusions unless the FHMUX performance is compared to a reference system. Such a reference system is shown in Figure 4-1.

As shown, the main transceiver and antenna, TR1, is located in the center of a circle with a 100 meter radius. There are four sets of transceivers and antennas (TR 2, 3, 4, and 5) equally spaced around the circle. Transceiver and antenna TR6 is located at the maximum SINCGARS range from TR1, and TR6 is transmitting to TR1. Transceivers TR2-TR5 are transmitting to units other than TR1 or TR6.

The 100 meter spacing automatically provides the 40 dB isolation discussed in the system specification. Analysis of this system will provide the dB ratio of the desired (TR6) to the undesired (TR2-5) signals, and provide a baseline for the BER analysis of the FHMUX.

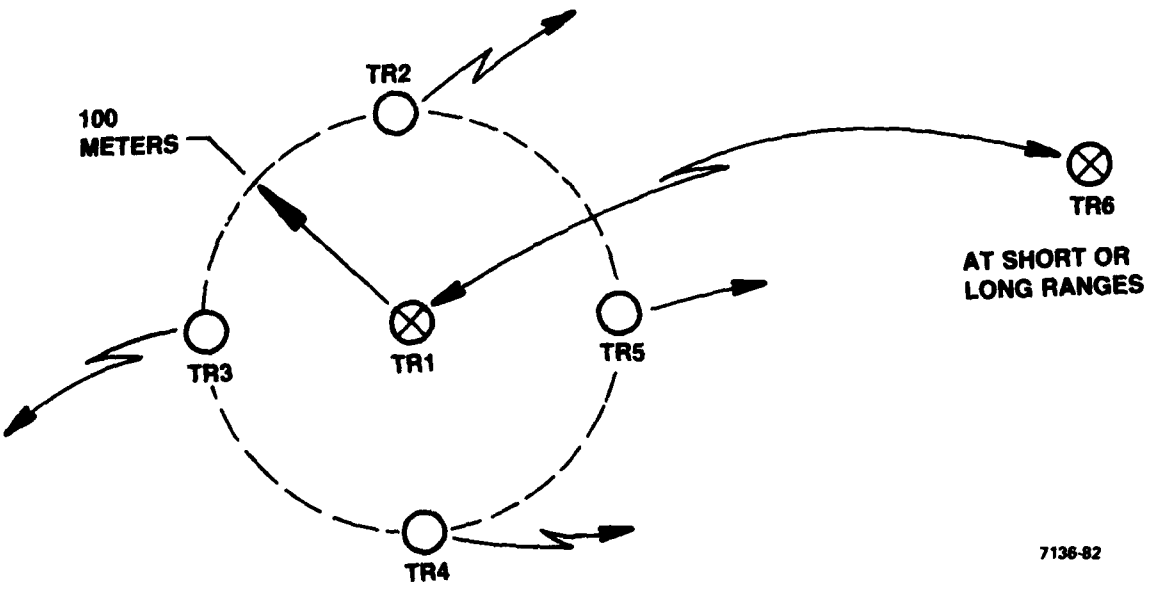

Figure 4-1. Reference System

Path loss calculation for 100 meters, and for SINCGARS short and long ranges are tabulated below in Table 4-1 These are based on use of free space, isotropic radiators, i.e., all antennas are alike.

TABLE 4-1 PATH LOSS DATA

Frequency (MHz)	Path Loss, at 100 meters (dB)	SINCGARS Short Range (dB)	SINCGARS Long Range (dB)
30	-42	-124	-144
88	-52	-133	-155

By subtracting the 100 meter path loss shown in Table 4-1 from the short and long range path losses, the ratio of undesired to desired signal level (S2/SD), can be found. These are listed in Table 4-2.

TABLE 4-2 RATIO OF UNDESIRED TO DESIRED SIGNALS

Frequency (MHz)	SINCGARS Short Range (dB)	SINCGARS Long Range (dB)
30	82	102
80	81	103

An initial observation is that frequency effects only account for a one dB variation, thus are considered insignificant.

An extrapolated plot of the SINCGARS specified frequency offset performance is plotted in Figure 4-2, along with the data from Table

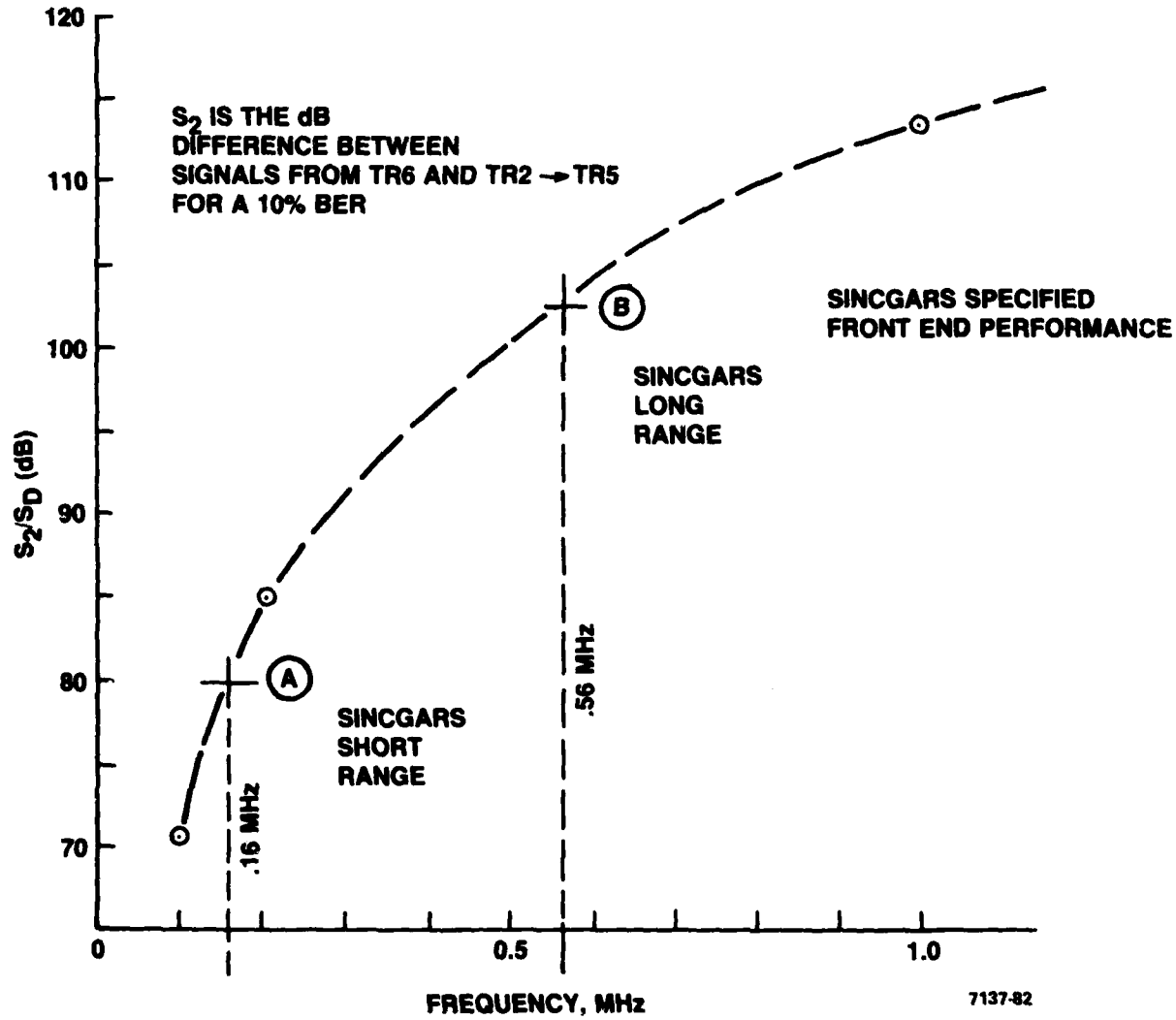

Figure 4-2. Frequency Spacing vs. Acceptable S_2/S_D Ratio

TABLE 4-3 MINIMUM SPACING VS. FREQUENCY

Frequency (MHz)	Minimum Spacing (Percent of Center Frequency)	
	Short Range	Long Range
30	.53	1.87
80	.20	0.70

4-2 (Points A and B). In terms of SINCGARS present bandwidth, the minimum frequency spacings are tabulated in Table 4-3.

Thus, at short range, the four transceivers can transmit within .53% of TR1 at the low end of the band, and to within 0.2% at the high end of the band. Also, at long range, the four transceivers can transmit to within 1.87% at the low end, and 0.7% at the high end.

4.3 FHMUX SELF BLOCKING

In the operation of the FHMUX, if two transceivers frequency hop to the same, or nearly the same frequency, one or both channels can be blocked, thus impairing or preventing operation.

Blockage can be caused by several mechanisms: broadband transmitter noise, and/or transmitter RF power desensitizing the transceiver receiver front end. Intermodulation problems can also cause channel blockage.

When two or more transceivers frequency hop to the same or nearly the same frequency, the FHMUX will automatically shut down one or more of its channels, according to some priority scheme. The rationale for this action is that the more important channel must be kept open, and this is preferred to having both channels desensitized. When the FHMUX channel is shut down, the action is called self blocking and the BER of the self blocked channel will increase to some degree.

Section 4.3.1 describes the model of the multiplexer used to perform blockage calculations. Section 4.3.2 describes the model of

the four-port coupler which is the fundamental iterative unit of the multiplexer. Section 4.4 covers the bit error rate simulation model which was used to estimate multiplexer performance.

4.3.1 An FHMUX Model

Figure 4-3 illustrates a simplified five-channel FHMUX. As shown, each transceiver is numbered and paired with a correspondingly numbered four-port coupler; the transceiver and the coupler are frequency hopped to the same frequency at the same time. The timing of the frequency hops between transceivers may or may not be synchronized, but the transceiver-FHMUX channel similarly numbered pairs must be synchronous to each other. There are two priority approaches, fixed and rotating.

Figure 4-3 shows a possible fixed priority channel arrangement. Each FHMUX channel (1-5), is assigned a different priority (A-E), with A as the highest priority, B next highest, etc. With the grouping shown, Channel 3 can never be self blocked, Channel 4 can only be self blocked by Channel 3 when these two channels are too close to each other's frequencies, and so on.

The concept of the revolving priority scheme is also shown in Figure 4-3, The FHMUX channels are assigned priorities in a revolving manner as shown. The "direction of rotation" and the order of priorities on the channels is arbitrary. As shown, initially Channel 1 has priority A, Channel 2 has priority E, etc. As the wheel rotates (clockwise for this example), Channel 1 will be assigned priority B, Channel 2 will have priority A, Channel 3 will have priority E, and so on. Following sections will help to define the effect of FHMUX self blocking on channel BER.

Returning to the fixed priority system as shown in Figure 4-3, Transceiver 3 has the highest priority; when in the transmit mode it can block any or all of the transceivers from receiving any remote transmitter, or from transmitting to any remote receiver, if the RF frequencies of concern are too close. Transceiver 4 has the second highest priority; when in the transmit mode it can cause self blocking

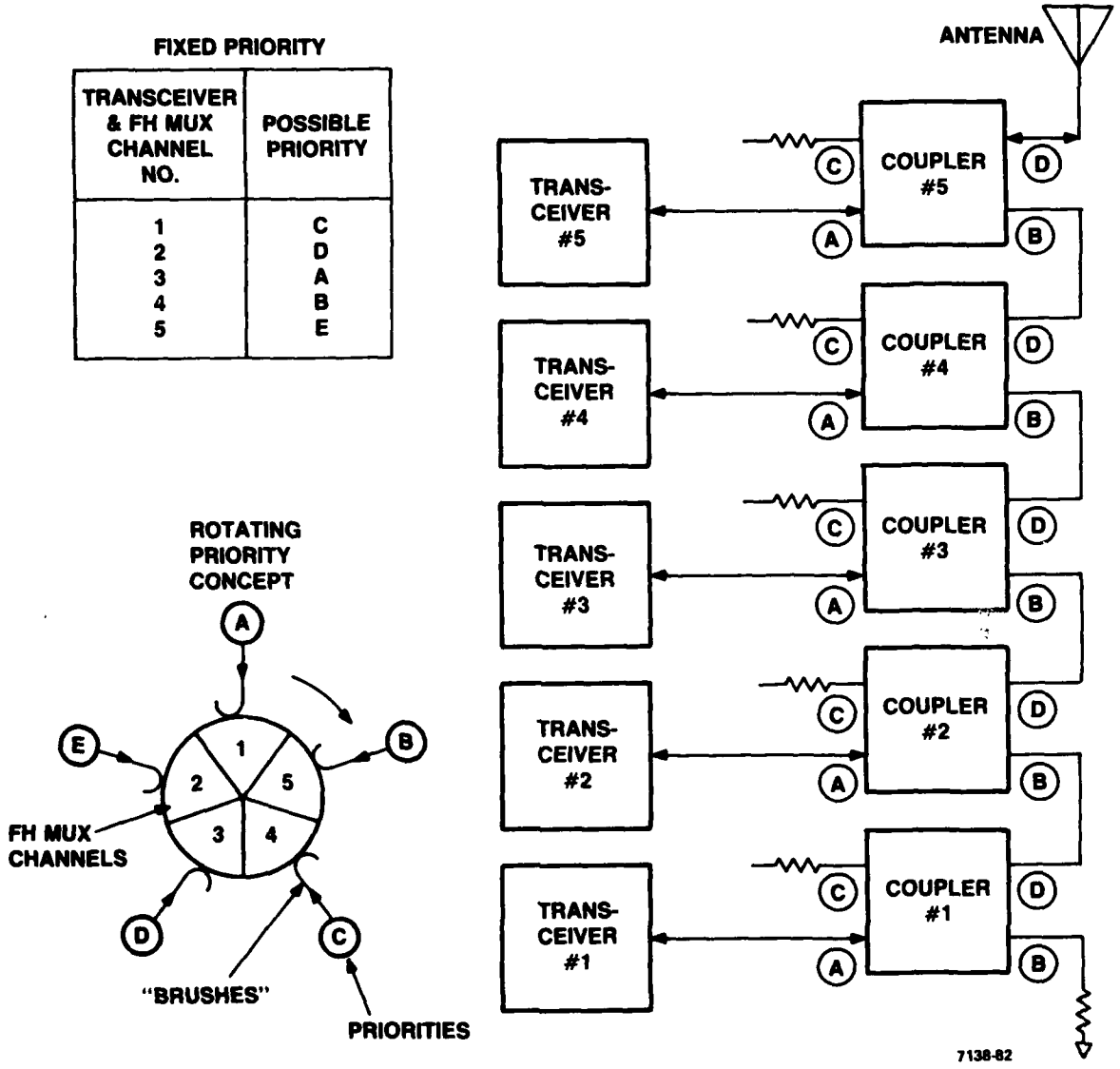

Figure 4-3. Frequency Hopping Multiplexer For a Five-Transceiver System

of Channels 1,2, and 5, and can only be blocked by Channel 3. As shown, the lowest priority is assigned to Channel 5. Thus, Channel 5 can be blocked from receiving or transmitting by any of the other channels, if the frequencies of interest are too close. Subsequent sections will discuss the effects of the transceivers transmit/receive duty cycles on these two priority schemes.

The following observations show that time synchronization of the frequency hops is not required for either priority scheme. In a non-synchronized system, the blocked condition can last for some partial or full hop duration, but does not exceed a hop duration. In a synchronized system, the blocked condition will last for exactly one hop duration.

Self blockage will occur when two or more transceivers hop to the same, or nearly the same frequency. "Nearly the same," means that the frequencies of interest are within the -40 dB bandwidth of the highest priority channels four-port coupler tuning circuit. If self blocking were not to occur, an active transmitter could deliver sufficient RF carrier power and/or broadband noise to desensitize a receiver. If the receiver is completely desensitized for the time duration of the blockage, the transceiver data decisions (in a digital data mode), are randomly in error. That is, the resulting BER is 0.5 for the duration of the desensitization period.

It is important to understand that desensitization of a higher priority channel is prevented by inducing self blockage upon a lower priority channel. The increase in BER caused by this FHMUX self blockage is inflicted only on the lower priority channel or channels. If the average probability of self blockage is known, then the average BER is one half the probability of self blockage, provided that the blocked receiver makes no bit errors when not blocked, and incurs a bit error rate of one half when blocked.

4.3.2 Four-Port Coupler Model

Figure 4-4 shows a typical FHMUX four-port coupler in detail. A mathematical analysis of these 90^{o} hybrid coupled filters is given in a later section.

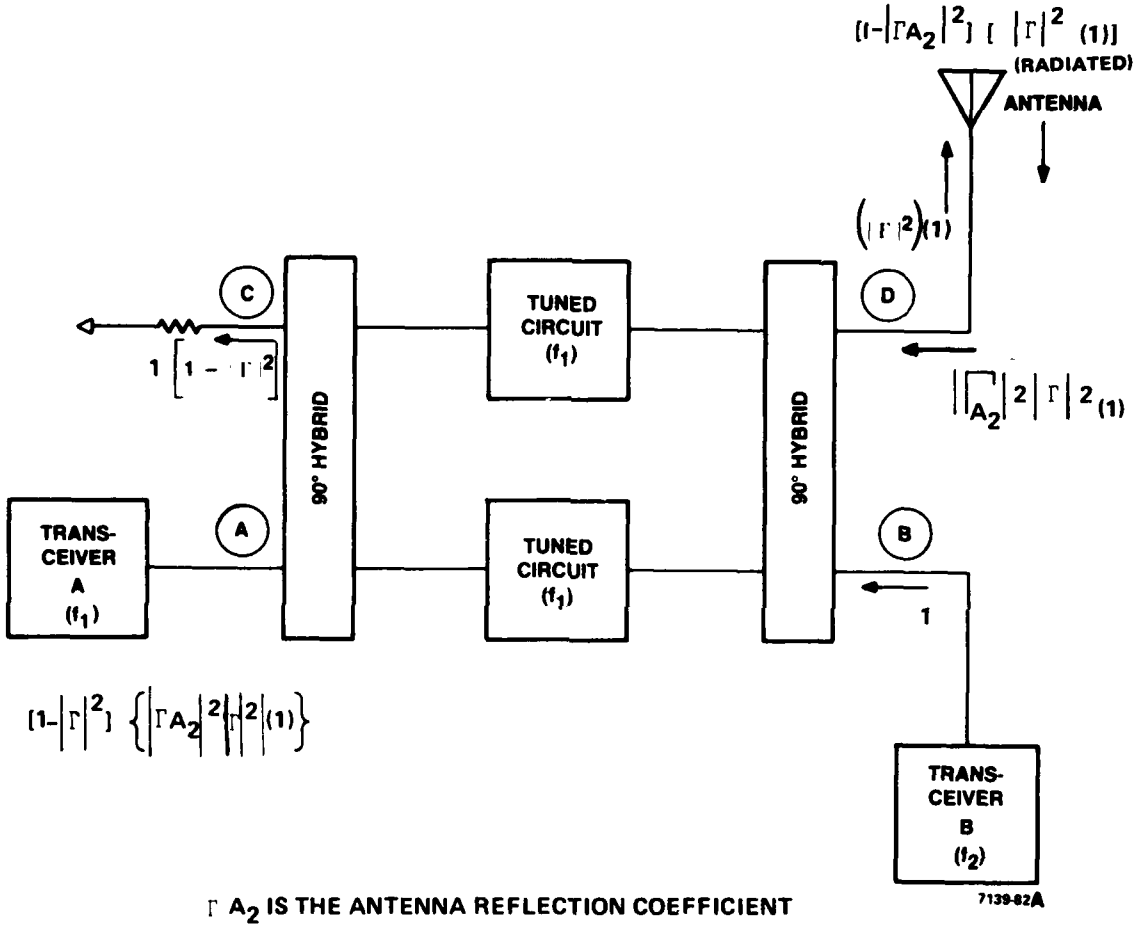

Γ A_2 IS THE ANTENNA REFLECTION COEFFICIENT AT FREQUENCY f_2

Γ IS REFLECTION COEFFICIENT OF THE f_1 TUNED CIRCUIT AT THE f_2 FREQUENCY

Figure 4-4. Four-Port Coupler

The letter designations used on the four coupler ports follow those used in Figure 4-3.

As shown, the transceiver connected to Port B is in the transmit mode, and delivers unit RF power at frequency f_2 into Port B. When the 90° hybrids and the tuned circuits tuned to f_1 are ideally balanced, $|\Gamma|^2$ of the power incident upon Port B is available to the antenna at Port D. The factor Γ is the reflection coefficient of the circuits tuned to f_1 at the f_2 frequency. Since the tuned circuits are not tuned to the Port B RF frequency of f_2, the reflection coefficient Γ is very high, and most of the Port B signal f_2 is indeed coupled to the antenna. This action is fully described in Section 5.6 of this report. Also, the quantity $(1 - |\Gamma|^2)$ is absorbed into the resistive termination at Port C. A benefit of these 90° hybrid coupled circuits is that this $(1 - |\Gamma|^2)$ power is almost completely absorbed by the Port C termination, and not allowed to feed back into the Port A transceiver tuned to f_1.

The previous analysis assumes that the antenna circuit presents a perfect impedance match to Port D. However, the antenna will usually present some mismatch to Port D, resulting in some value of reflection coefficient. Figure 4-4 shows a simple two-channel FHMUX, with the tuned circuits tuned to f_1, and the transceiver tuned to f_2 delivering unit power at f_2 to Port B. The reflection coefficient of the antenna circuit at frequency f_1 will be different than that of frequency f_2. For this discussion, we are concerned with the antenna reflection coefficient at frequency f_2, defined now as ΓA_2. Because of ΓA_2, RF power at frequency f_2 is reflected from the antenna, back into Port D, and some of this power will exit Port A and enter Transceiver A (which is still tuned to f_1). As noted, the reflection coefficient of the f_1 filters (at the f_2 frequency), is Γ.

The amount of unit power from the transceiver at f_2 which is coupled to the antenna, and then reflected back to Port D, and then coupled further to Port A is defined below.

Unit RF Power

$$\text{Out of Port A} = |\Gamma A_2|^2 \cdot |\Gamma|^2 \cdot (1 - |\Gamma|^2) \qquad \text{(A)}$$

The antenna specified for use with the FHMUX (refer to Appendix D of the Reference Document) has a maximum specified reflection coefficient of 0.25, which corresponds to a return loss of 6 dB. Thus, if ΓA_2 is 0.25, the f_2 power reflected back to Port D from the antenna, is 6 dB below the f_2 power incident upon the antenna. Referring now to Equation A, the factor

$$(1 - |\Gamma|^2) \qquad \text{(B)}$$

now represents the proportion of incident f_2 power which will pass through the f_1 tuned filters. In a working FHMUX system the frequency f2 will be such that the term (Equation B) above results in an attenuation of no less than 40 dB for the Transceiver B f_2 signal. Therefore, the B to A worst case coupling is a result of the antenna mismatch (ΓA_2), and has a design value of 6 + 40, or 46 dB. As noted, $(1 - |\Gamma|^2)$ of the f_2 power incident upon Port B is dissipated in the Port C resistive termination, and this value is held to about -40 dB below the f_2 power incident on Port B. There is at least 25 dB isolation between Ports A and C because of the directivity of the 90° hybrid. Thus, the only remaining B to A coupling path is from Port B to Port C to Port A, and it has a value of at least -(40+25) dB. Thus the worst case B to A couping path is caused by the antenna mismatch.

As discussed in a later section, a SINCGARS receiver connected to Port A will be desensitized if a SINCGARS transmitter operating into Port B does not have its signal level reduced by at least 46 dB when it reaches Port A (is within the -40 dB bandwidth criterion; that is, with less than 46 dB of isolation between Port B and Port A).

The condition of the transceiver at B in transmit, and the transceiver at A in receive, is the worst case regarding degradation of transceiver performance due to the multiplexer. Alternate sources of degradation are less severe because they occur less often. The

coupling from Port A to Port B is zero with ideally balanced 90° hybrids and filters. Thus the transceiver at f_1 (when transmitting), will not disable a receiving transceiver connected to Port B.

The worst case or most probable condition occurs when B transmits within the -40 dB coupler bandwidth and desensitizes reception at A. This event exhibits a higher probability of occurrence than other sources of performance degradation. For example, the transmitter power from B is dissipated in the terminating resistor at C when f_2 is within the -3 dB bandwidth of f_1. Being within the -3 dB bandwidth has a lower probability of occurrence than being within the -40 dB bandwidth. Hence the latter can be treated as worst case or most probable degradation.

As further amplification on probability occurrence, consider the hypothetical perfectly balanced multiplexer system. All of the power output from Transceiver A is delivered to the antenna, and all of the power received by and outputted from the antenna due to a remote transmitter on Transceiver A's frequency is delivered to Transceiver A. Regarding Transceiver B, the transmit power delivered to the antenna, and the receive power from the antenna is attenuated by the factor $|\Gamma|^2$, due to the multiplexer. The attenuation due to $|\Gamma|^2$, is only significant if Transceiver B is operating within the -3 dB bandwidth of the coupler tuning circuit ($|\Gamma|^2$ is then less than -3 dB). This -3 dB bandwidth is narrower than the -40 dB bandwidth, thus the probability of operating within the -3 dB bandwidth is much lower and therefore less restrictive on system operation.

4.4 THE BER MODEL

In order to assess FHMUX performance, an operating system was simulated using a computer program. The simulated system consisted of a multiplexer with five transceivers. The transceivers are capable of 25 KHz channelization and operate over the 30-88 MHz frequency range. Each transceiver operates in an independent radio net. Thus, each transceiver hops independently, and may occasionally hop to the same, or nearly the same RF frequency as one or more of the other transceivers.

When the model is exercised, certain parameters (described below), must be inputted to the model. The time period over which the model is exercised can be set to any value. For the results reported here, the exercise duration was set at 20,000 random hop frequencies.

The probability of co-occupying the same or nearly the same frequency (the average blockage rate) is calculated as the number of times that the blockage event occurs divided by 20,000, which is the total number of events in the exercise.

A detailed explanation and justification of the computer simulation is given in Appendix G.

Table 4-4 illustrates the results for some simulated conditions. The lefthand column expresses the -40 dB bandwidth at various percentages of the tuning circuit frequency. This is one of the parameters of the model. Although multiplexer performance in terms of reduced blockage improves as this bandwidth is narrowed, implementation of the real-life hardware equivalent becomes successively more difficult with narrower bandwidth.

The tabulated results are for the fixed priority system defined earlier. The top row of the table lists the transceiver number or user number. The tabulated entries are the probability (expressed as a fraction) that the indicated transceiver is blocked by another transmitter co-occupying a frequency within the indicated -40 dB bandwidth.

In the fixed priority system, Transceiver 1 is never self-blocked, so the entries in that column are zero. For Transceiver 2 at a coupler bandwidth of +/-5%, there is a probability of 10.07% of Transceiver 2 being blocked (but only by Transceiver 1) on any frequency hop.

For the indicated probabilities to apply, several events must occur simultaneously:

- The indicated transceiver is receiving a sensitivity level signal from a distant transceiver transmitting in its own net
- Other FHMUX collocated transceivers with lower transceiver numbers (higher priority) are simultaneously transmitting in their own nets

TABLE 4-4. AVERAGE BLOCKAGE RATE (EXPRESSED AS A FRACTION) VS. 40 dB PERCENTAGE (OF USER OPERATING FREQUENCY) BANDWIDTHS. EXPRESSED UNDER WORST CASE FIXED PRIORITY CONDITIONS

-40 dB BW (percent))	User Number 1	User Number 2	User Number 3	User Number 4	User Number 5
± 5	0	0.10070	0.18895	0.26705	0.33660
± 2.5	0	0.04960	0.09655	0.14170	0.18500
± 1	0	0.02015	0.03865	0.05810	0.07805
± 0.5	0	0.00965	0.01930	0.02955	0.03900
Probability		D^2	D^3	D^4	D^5

If these events are treated probabilistically then the entries in the bottom row of the table apply. For those entries, it is assumed that there is a duty cycle, D (probability of a transceiver being in the transmit mode) that has the same value for all transceivers. For user number 5, for example, the indicated blockage rate applies when a remote transceiver in its net is transmitting and local transceivers 1 to 4 are simultaneously transmitting. This requires five transceivers (four in the FHMUX, plus the remote transceiver) to be on the air simul-
taneously. If all of these active transmitters are independently operating, with probability D, then the joint event has a probability of D^5. For example: if the average transmitter duty cycle is 10%, then the average blockage rates tabulated for user 5 occur with a probability of 10^{-5}. That is, user 5 is rarely blocked with the indicated blockage rate.

To expand on this thought, Table 4-5 reformulates the average blockage rates for user number 5 only. For the tabulated entries, a fixed priority system applies with the the indicated number of other collocated transmitters on the air at the same time that Transceiver 5 is receiving a signal from a distant transceiver. The average blockage rates are tabulated along with the indicated probability of occurrence. For a duty cycle of 0.1, the probabilities are calculated.

- The highest blockage rate occurs with low probability
- The lowest blockage rate (zero with no other collocated transceivers on the air) occurs with approximately a 7% probability, or on 7% of those occasions that the distant transceiver is transmitting.

As indicated in a previous section, these average blockage rates can be converted to an average BER if some further assumptions are made:

- When a transceiver is self blocked, it suffers complete blockage, and makes random bit decisions
- When the transceiver is not self blocked, the received signal to noise ratio is sufficiently high to enable a BER which is zero.

TABLE 4-5. AVERAGE BLOCKAGE RATE FOR USER NUMBER 5 WITH INDICATED NUMBER OF ACTIVE TRANSMITTERS (EXPRESSED AS A FRACTION) VS. 40 dB PERCENTAGE (OF USER OPERATING FREQUENCY) BANDWIDTHS. EXPRESSED UNDER WORST CASE FIXED PRIORITY CONDITIONS

-40 dB Bandwidth (Percent)	No Other Transmitters	1 Other Transmitter	2 Other Transmitters	3 Other Transmitters	4 Other Transmitters
+/-5	0	0.10070	0.18895	0.26705	0.33660
+/-4.25	0	0.08560	0.16061	0.22699	0.28611
+/-2.5	0	0.04960	0.09655	0.14170	0.18500
+/-1	0	0.02015	0.03865	0.05810	0.07805
+/-0.5	0	0.00965	0.01930	0.02955	0.03900
Probability	$D\ (1-D)^4$	$4\ D^2\ (1-D)^3$	$6\ D^3\ (1-D)^2$	$4\ D^4\ (1-D)$	D^5
Probability At D = 0.1	$6.6X10^{-2}$	$2.9\ (10^{-2})$	$4.86X10^{-3}$	$3.6\ (10^{-4})$	10^{-5}

When the above items occur, the average BER is one half of the average blockage rate.

As a point of reference, the SINCGARS RFP stipulates a bound of 10% BER as the acceptable threshold of performance for digitized voice operation. For the FHMUX, an average blockage rate of 20% (corresponding to an average BER of 10%), would then be viewed as a performance threshold.

A final view of the average blockage rate problem is provided in Table 4-6, for a rotating priority scheme. The tabulated entries are in terms of average rate of blockage, as previously discussed. For the tabulated entries under the column heading 5, a target FHMUX transceiver is receiving a signal from a distant transmitter, with four other FHMUX collocated transceivers transmitting. In the column labeled 4, the target transceiver is still receiving a signal from a distant transceiver, with three other FHMUX collocated transceivers transmitting. In the column labeled 1, only the distant transmitter is transmitting, and no local FHMUX transceivers are transmitting, hence there is no self blockage.

The data from Tables 4-5 and 4-6 are plotted in Figures 4-5 and 4-6. Figure 4-7 shows the percent probability of zero to four transmitters being energized (in a five-channel FHMUX) as a function of transmit duty cycle (DU).

Figures 4-5, 4-6, and 4-7 are to be used together to complete the BER analysis in that the blockage rate vs. bandwidth curves are probablistic in themselves. For example, Figure 4-7 shows that the probability of three transceivers transmitting is highest when the duty cycle is 0.8, and this probability is about 32%. The curves shown in Figure 4-7 are based on the probability equations given in Tables 4-5 and 4-6. They assume that at least one of the FHMUX channels is in the receive state. Also, some of the remaining channels may be in the transmit state with a probability of $(1-D)^n$, where D is the transmit duty cycle, and n is the number of channels in the transmit state (n cannot exceed 4). All duty cycles are assumed

TABLE 4-6. AVERAGE RATE OF BLOCKAGE (EXPRESSED AS A FRACTION) VS. 40 dB PERCENTAGE (OF USER OPERATING FREQUENCY) BANDWIDTHS. EXPRESSED UNDER WORST CASE ROTATING PRIORITY CONDITIONS.

NUMBER OF ACTIVE TRANSMITTERS					
40 dB BW Percent	1	2	3	4	5
± 5	0	0.050350	0.09655	0.139175	0.17866
± 2.5	0	0.024800	0.04872	0.071962	0.09457
± 1	0	0.010075	0.01960	0.029225	0.03899
± 0.5	0	0.004825	0.00965	0.014625	0.01950
Probability	$D(1-D)^1$	$4\ D^2(1-D)^3$	$6\ D^3(1-D)^2$	$4\ D^4(1-D)$	D^5
Probability At D = 0.1	$6.6X10^{-2}$	$2.9X10^{-2}$	$4.86X10^{-3}$	$3.6X10^{-4}$	10^{-5}

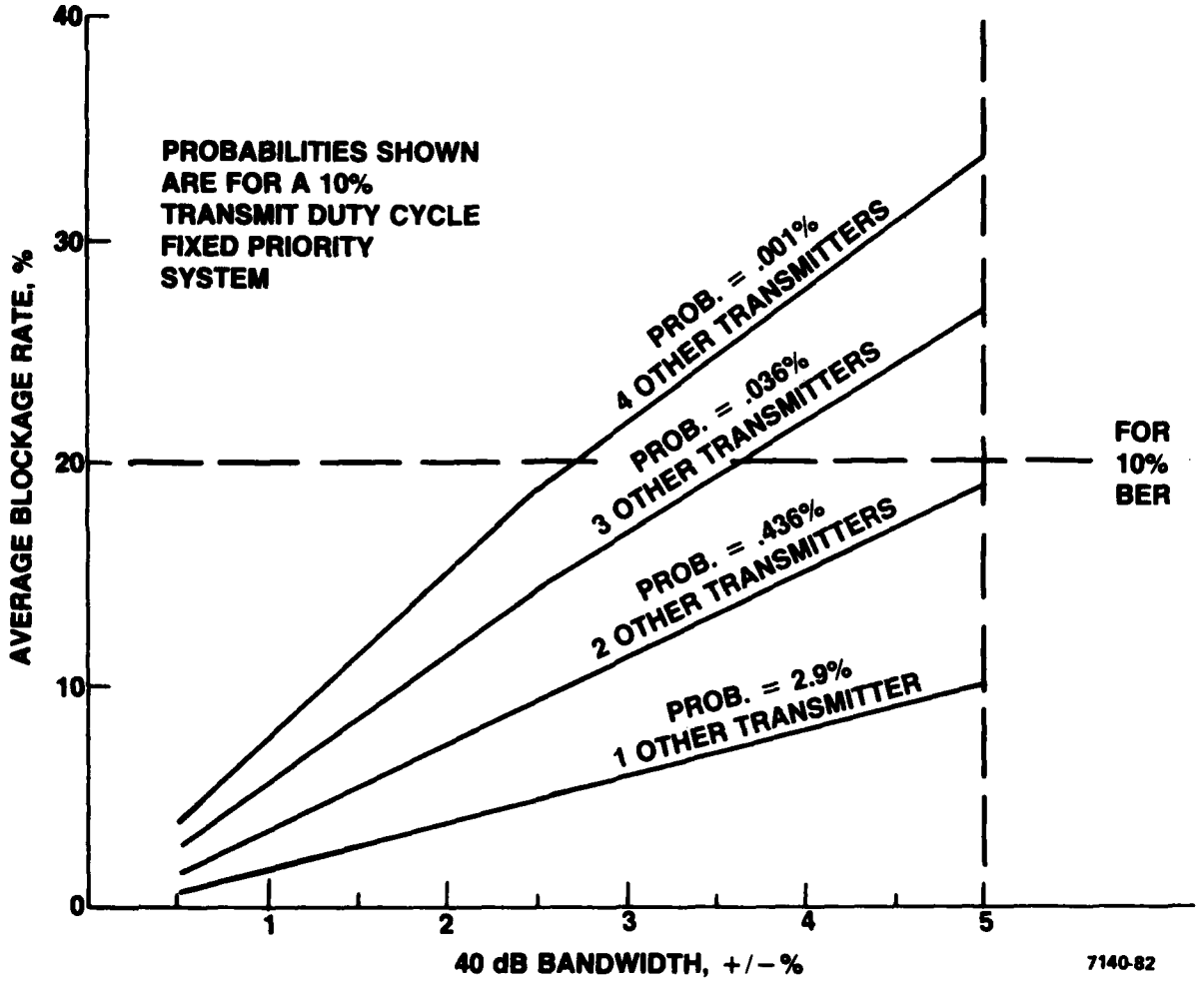

Figure 4-5. Average Blockage Rate for User #5 with the Indicated Number of Transmitters on the Air, Fixed Priority

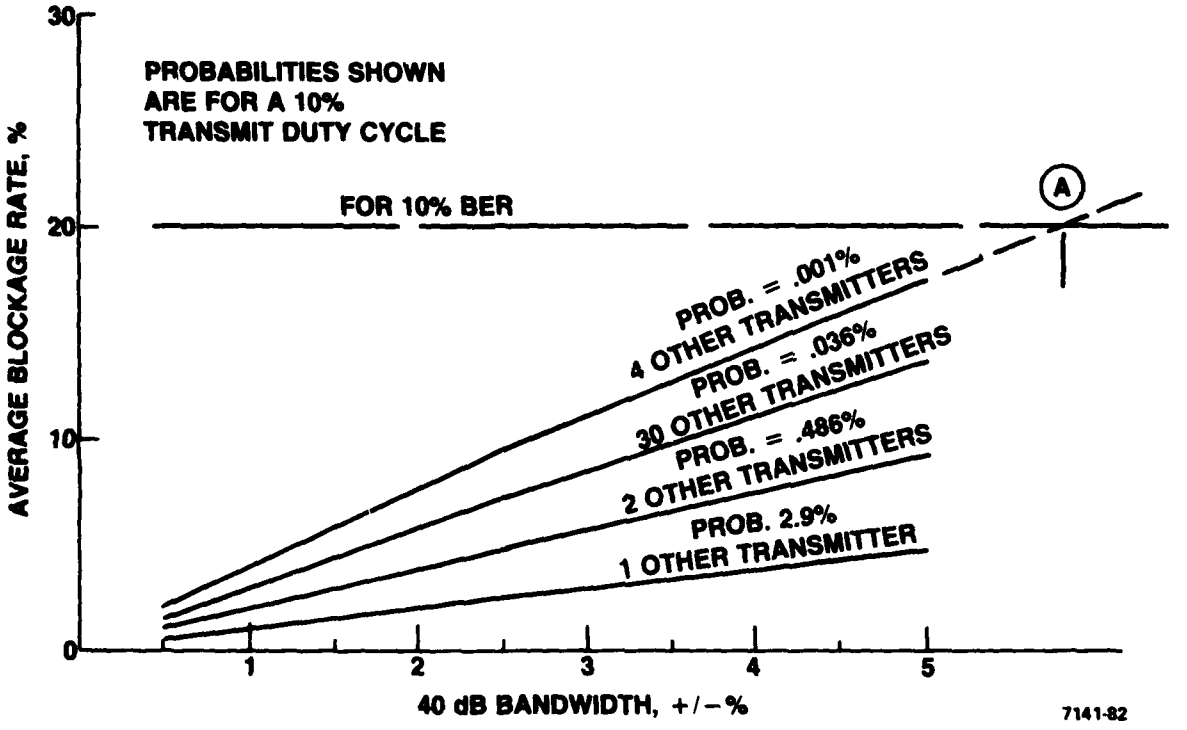

Figure 4-6. Average Blockage Rate vs. 40 dB Bandwidth, Rotating Priority, Worse Case

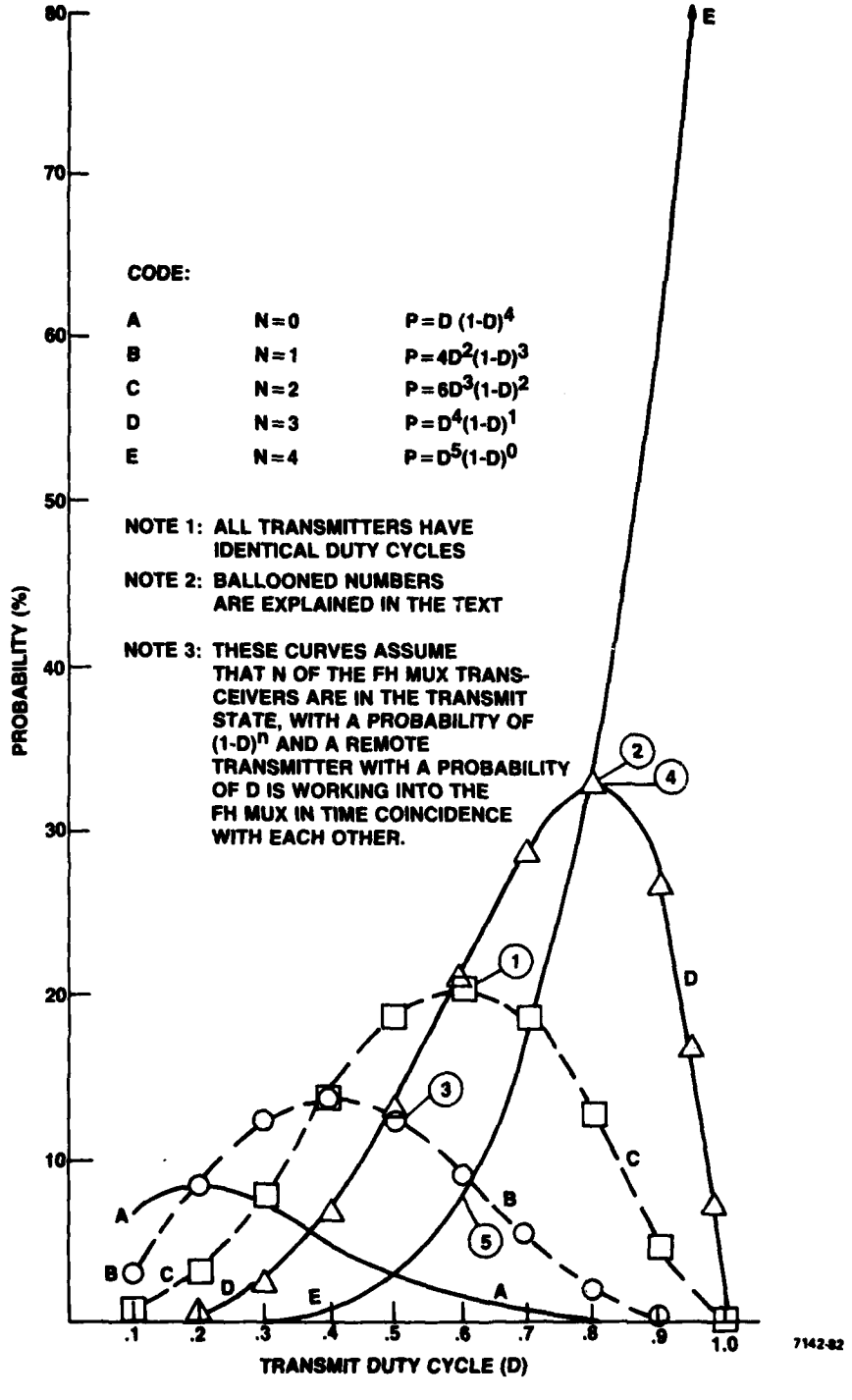

Figure 4-7. Transmitter Duty Cycle vs. Probability That N of Five Transmitters is Active in a 5 Channel FHMUX in Time Coincidence with a Remote Transmitter

to be equal. These FHMUX transmit channels are assumed to be time-coincident with a remote transmitter which is operating into the FHMUX channel which is in the receive state. The duty cycle of this remote transmitter is assumed to be the same as the FHMUX channels in the transmit mode.

Figure 4-6 shows that a revolving priority system is relatively insensitive to these probabalistic effects. Point A shows that a revolving priority system with four transmitters on line will have BER of 10% with a guard band of about +/- 5.8% (Point A), even if the probability of the event is 100%. The revolving priority system is clearly superior to the fixed priority system in this regard.

When the fixed priority system is considered, Figure 4-5 is of interest. As shown, the curves for three and four transmitters on line cross the 10% BER limit line inside the +/- 5% bandwidth abscissa. The probablistic effects shown in Table 4-7 are derived from Figure 4-7, and are highlighted as points 1,2,3,4, and 5 on Figure 4-7.

TABLE 4-7. PROBABALISTIC EFFECTS, FIXED PRIORITY SYSTEM

Number of On Line Transmitters	Maximum Bandwidth for 10% BER	Highest Probability of this Event	Figure 4.7 Reference Points
2	+/- 5%	20%, at DU = 0.6	1
3	+/- 3.75%	32.7%, at DU = 0.8	2
3	+/- 3.75%	14%, at DU = 0.5	3
4	+/- 2.75%	32.7%, at DU = 0.8	4
4	+/- 2.75%	7.2%, at DU = 0.6	5

Table 4-7 and Figure 4-5 imply that a fixed priority system would have some chance of success if the average transmit duty cycle is 0.4 or less. It seems prudent to compare the two priority systems to the reference system on a separate basis. This is done in Tables 4-8 and 4-9.

4.5 THE BER MODEL VS. THE REFERENCE SYSTEM

The reference system described in Section 4.2 and Table 4-3 describes close-in frequency operation of five transceivers, all separated by 100 meters. The BER of this system is degraded by strong undesired signals in adjacent channels. This degradation occurs when the undesired signal is 5.1 dB below the desired signal, in the IF bandwidth. Thus, at 80 MHz, one of these four transceivers can transmit at a frequency as close as 0.7% of the frequency of TR1, and TR1 will be able to maintain a BER of 10% when tuned to the frequency of TR6.

The FHMUX "guard bandwidths" described in Table 4-8 and 4-9 are based on the laws of probability, namely the effect on BER when the FHMUX system "self blocks" a given channel because of its close frequency proximity to another channel with an active transmitter.

Therefore, the reference system has a 30 MHz, 10% BER "guard band" of no less than +/- 1.87%, and at 80 MHz, of no less than +/- 0.7%. The fixed priority FHMUX guard band (five-channel) is probabalistic as shown. The revolving priority FHMUX (five-channel) has a 10% BER guard band of no more than +/- 5.8%.

The Second Quarterly Report defines an FHMUX system electronic guard band of +/-2%. This more recent Final Report uses a refined computer program which more realistically defines the self blockage rate. Thus, an electronic guard band of +/-5% will provide a satisfactory BER when a revolving priority system is used.

TABLE 4-8. REQUIRED GUARD BANDWIDTH FOR 10% BER, FOUR TRANSCEIVERS TRANSMITTING, FIXED PRIORITY

FREQUENCY (MHz)	REQUIRED GUARD BANDWIDTH (%) FOR 10% BER, 4 TRANSCEIVERS TRANSMITTING			
	Reference System Long Range, (From Table 4-3) No Less Than	Fixed Priority FHMUX System (from Figures 4-5 4-7,) and Table 4-7.		
30 80	+/- 1.87% DU = 1 +/- 0.7%			Probability, of 4 Transceivers Transmitting %
		No More Than	DU	
		+/- 2.75%	0.4	1.024
		+/- 2.75%	0.5	3.125
		+/- 2.75%	0.6	7.78
		+/- 2.75%	0.7	16.8
		+/- 2.75%	0.8	32.8
		+/- 2.75%	0.9	54.0
		+/- 2.75%	1.0	100.0

TABLE 4-9. REQUIRED GUARD BANDWIDTH (%) FOR 10% BER, WITH FOUR TRANSCEIVERS TRANSMITTING, ROTATING PRIORITY

Frequency (MHz)	REQUIRED GUARD BANDWIDTH (%) FOR 10% BER, WITH 4 TRANSCEIVERS TRANSMITTING	
	Reference System, Long Range (From Table 4-3) No Less Than	Rotating Priority FHMUX System. (From Figure 4-6) No More Than
30	+/- 1.87% DU = 1	+/- 5.8%, DU = 1
80	+/- 0.7%	

4.6 COMBINED EFFECTS

There are at least three factors which must be considered in the selection of the guard bandwidth:

- BER vs. the probability of FHMUX self blocking
- BER vs. the effect of strong undesired, coherent signals in the IF bandwidth
- BER vs. the effect of strong undesired non-coherent signals in the IF bandwidth (transmitter broadband noise)

The effect of the factors described above is shown in Figure 4-8 for a five-channel FHMUX with a 10% BER guard bandwidth of +/-5%. The RF filter circuit has a 40 dB bandwidth of +/-5 %.

Figure 4-8 shows how close (in frequency) a receive channel in the FHMUX can be tuned to an FHMUX transmitting channel before a BER of 10% occurs. A typical transmitter output power of 60 watts is chosen.

Curve A is a plot of the extrapolated broadband noise floor of a 60 watt transmitter driven by a 200 mW power VCO, and is normalized to a 20 KHz IF bandwidth. This data was derived from the GTE Multimode Radio Program and was obtained at an RF carrier frequency of 50 MHz.

Curve B shows how the FHMUX filters will reduce noise power. Curve C is a plot of the maximum allowable signal power in the SINCGARS receiver IF passband at sensitivity (estimated at -113 dBm) to maintain a 10% BER. Curve C is derived as shown in Table 4-10.

S2 is the adjacent channel signal power, and SD is the desired signal power. The allowable undesired power in dBm is the difference between -113 dBm and S2/SD.

Curve D shows the actual RF power level reduction of Fo caused by the bandpass characteristics of the FHMUX. It is the level of the RF power that would be incident upon the front end of one of the FHMUX transceivers (in the receive mode), tuned to a frequency close to Fo.

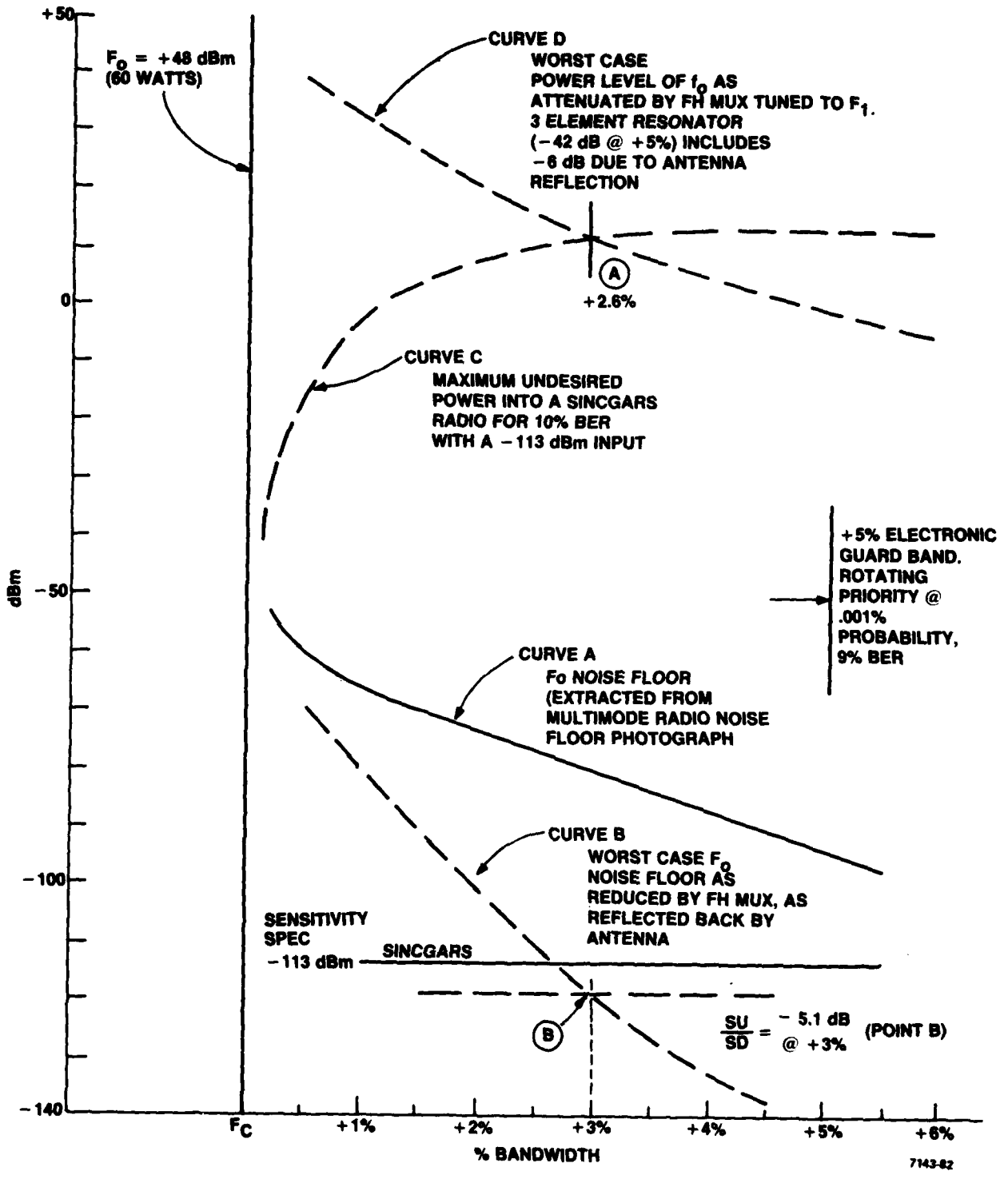

Figure 4-8. Combined Effects, Scaled to 80 MHz

TABLE 4-10. DERIVATION OF CURVE C

Offset (KHz)	Percent Away From From Fo, At 80MHz S2/SD	SINCGARS Spec. (dB above -113 dBm) (dBm)	Allowable Desired Power (dBm)
25	0.031235	35	-78
50	0.0625	63	-50
100	0.125	71	-42
200	0.250	85	-28
1000	1.25	113	0
5000	6.25	125	+12

Thus, the format shown in Figure 4-8 clearly depicts these combined effects and can be used to define the latest FHMUX baseline system.

4.7 DESCRIPTION OF THE BASELINE SYSTEM

Curves B and D of Figure 4-8 are derived from the filter frequency response shown in Table 4-11.

TABLE 4-11. RESPONSE OF A SYSTEM WITH A -40 DB BANDWIDTH OF +/-5%

+/- % Away From Fo	dB
.5	-2.91
1.0	-9.03
1.5	-15.4
2.0	-21.0
2.5	-25.8
3.0	-30.0
3.5	-33.7
4.0	-36.9
4.5	-39.8
5.0	-42.4

This response can be achieved by cascading three single pole bandpass filters, each having a loaded Q of 50. These filters are described in a later section. As shown in Table 4-11, this response gives a 40 dB bandwidth of about +/-5%, and meets the requirements of Figure 4-8.

The intersection of Curves C and D (Figure 4-8) occurs at +/-2.6% of Fo, and is identified as Point A. This is the difference frequency at which a strong, coherent off channel signal will cause the BER to degrade to 10%.

The intersection of the SINCGARS sensitivity level, and Curve B occurs at +/-3% of Fo, and is identified as Point B. This is the difference frequency at which a strong non-coherent off channel signal (broadband transmitter noise) will lie about 5.1 dB below a sensitivity level signal. This will cause the BER to degrade to 10%.

Curve C is scaled to 80 MHz. The other curves are valid at all other frequencies. However, a clear picture of 30 MHz operation is shown in Figure 4-9.

The intersection of Curves C and D in Figure 4-9 is at +/- 4.25% of Fo, for a system scaled at 30 MHz. This is still within the +/- 5% electronic guard band.

The Second Quarterly Report derives the concept of FHMUX "self blocking," and introduces the concept of an electronic, or digital guard band which could vary the self blocking effect as desired. This early work recommends a +/- 2 to 3% digital guardband which necessitates a very narrowband, lossy RF system. The recent work described above eases this problem. The digital guard band can be as much as +/- 5.8%, and is subject to beneficial probabalistic effects.

It has been shown that the FHMUX cannot achieve equivalent performance to the reference system. However, this is really an unfair comparison, in that the reference system has a built in 40 dB frequency insensitive attenuator. The FHMUX is required to use RF filters of finite bandwidth in order to achieve the required channel isolation.

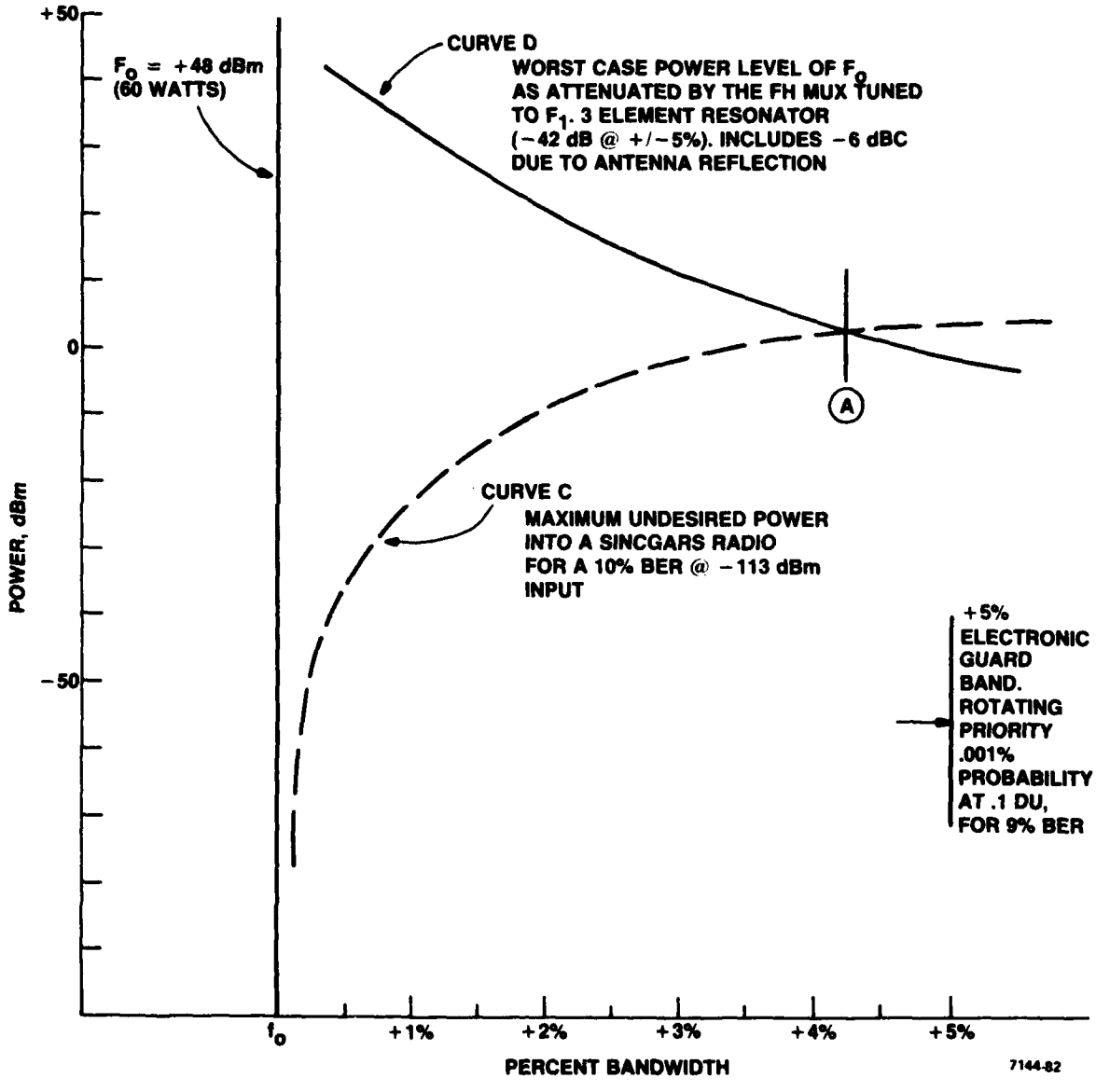

Figure 4-9. Combined Effects, Scaled to 30 MHz

It has been shown that the FHMUX is superior to the reference system in that the FHMUX provides two way suppression of back IMD products, whereas the reference system only provides one way suppression.

The effects of strong near channel signals from active FHMUX transmitters on a FHMUX receiver channel are just as probablistic as the effect on the digital guard band of these strong signals. If no transmitters are active, the guard band can be reduced to a few channel spaces.

The achievable RF 40 dB bandwidth is of prime importance; as well as the selection of the digital guard band, it is under the control of the FHMUX designers. The SINCGARS transceiver receiver selectivity and transmitter broadband noise floor are not. It is probable that FHMUX self blocking will not be a major problem area. A digital guard band of approximately +/- 5%, a revolving priority scheme, and a 40 dB RF bandwidth of +/- 5% are recommended for the FHMUX final system configuration.

4.8 MODEL ERRORS

The derivation of the reference system assumes that one of the five collocated transceivers is in the transmit mode at the same instant in time that a sensitivity level signal arrives from a transceiver at a distance much greater than 100 meters, and is received by the fifth collocated transceiver.

This is a valid starting point for the study and serves as a resonable point of comparison.

An early source of error was the lack of probability data regarding the transmit duty cycle. This work is included in this report.

The extrapolated transmitter noise floor may be another source of error. The data was obtained from a GTE Engineering Model, as described. The exact noise floor of the SINCGARS radios is unknown to GTE at this time. It is hoped that the SINCGARS transmitter noise

floor is lower than the model shown. The noise area of concern is the close in noise associated with the synthesizer FM noise.

As shown, Fo is assumed to be 60 watts. If another power level is to be used, the curves of Figure 4-8 and 4-9 can easily be readjusted. This also holds true for the receiver front end and transmitter noise floor data.

Early work, (Appendix C, Reference Document) shows concern over the effect of antenna VSWR on resonator tuning. A later section of this report will discuss how this concern is eliminated.

The duty cycle analysis shown in Figure 4-7 is based on all transceivers having identical transmit duty cycles. This is really an unlikely event, but the extension of the study to account for different duty cycles will probably over complicate the analysis.

SECTION 5

EVALUATION OF HARDWARE CONFIGURATION

5.1 INTRODUCTION

This section describes and justifies the baseline Rf design of the FHMUX, based on the results of the system study and BER analysis. The selection of a quad-coupled channel combiner, and the benefits of this scheme are described. Justification for the use of helical resonators, and the design of the bandpass filters is discussed. Finally, an estimate of the size and power consumption of the FHMUX is given.

5.2 AN ADDITIONAL COMBINING SCHEME

The Second Quarterly Report discusses combining of the resonators via a series connection of output windings. A disadvantage of this circuit is the need for an additional circuit, the terminator. The terminator is actually an L-C impedance matching network. It is fixed tuned, and will utilize low loss components. The terminator compensates for the parasitic elements of the output coupling loops and the connecting transmission line. A combining scheme which does not require the terminator has been used in the television broadcast industry for many years at microwave frequencies.

Figure 5-1 shows how this combiner utilizes quadrature couplers to sum three MUX channels to a single antenna. The technique is not limited to three channels.

As shown, three transceivers, AA in Tx at frequency f_1, BB in Rx at frequency f_2, and CC in Tx at frequency f_3, are connected to the apppropriate quad coupler ports in similar circuits. Each of the quad coupler pairs contains an identical set of narrow band, tuneable band pass filters. These filters are tuned to the same RF frequency as the associated transceiver.

Transceiver AA is in Tx at f_1, and its signal is passed by the two quad coupled filters, and combined in output Coupler A. The

- INTERIOR FILTER PAIRS ARE IDENTICALLY TUNED, HENCE, COUPLERS ARE MATCHED AT ALL FREQUENCIES.

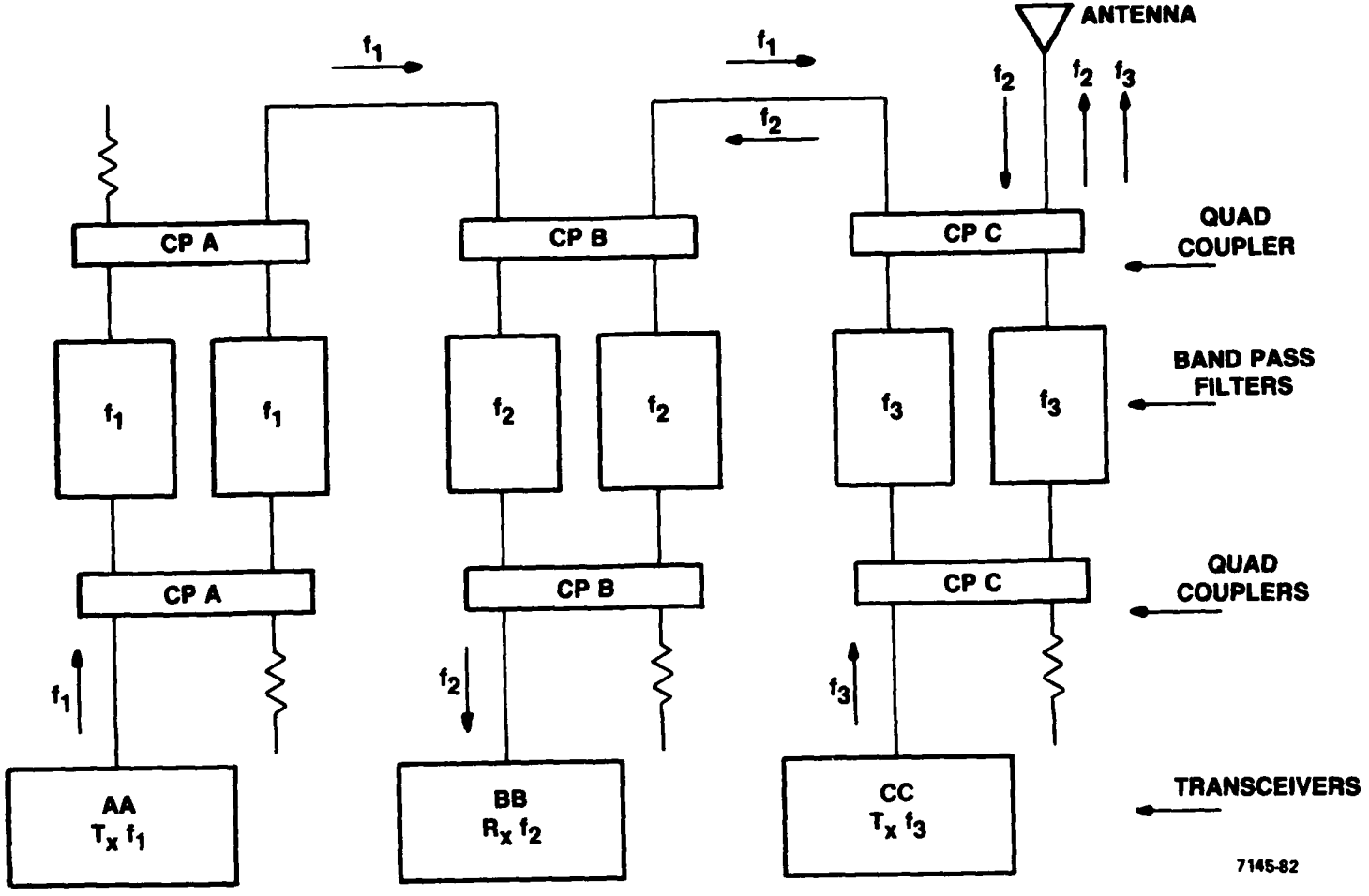

Figure 5-1. RF Combining Scheme

signal propagates down the 50 ohm interconnecting line to Coupler B, where it is divided and falls incident on each of the bandpass filters tuned to f_2. These filters each present a high VSWR to the f_1 signal. Thus the f_1 signal is reflected from the filters, and is recombined by the quad couplers, as shown. The port of Coupler B at which the f_1 signal now appears would be terminated by a 50 ohm load in a conventional circuit. However, the recombined f_1 signal proceeds to Coupler C where the same circuit action occurs, and f_1 is routed to the antenna.

The output of Transceiver CC reaches the antenna in similar fashion. Since the other two banks of filters (tuned to f_1 and f2) are identically tuned within their respective quad coupler pairs, Coupler C will see a matched load.

Transceiver BB is in the receive mode, and operating at f_2. When an f_2 signal is received at the antenna, it propagates to Coupler C, divides and is reflected from the two f_3 filters. It is recombined by Coupler C, and routed to Coupler B and then to the two bandpass filters which are tuned to f_2. The f_2 signal thus is routed to Transceiver BB as desired. Coupler A presents an excellent impedance match to Coupler B because the two f_1 filter sections are identically tuned.

The original channel combining scheme discussed in the GTE FHMUX proposal, and in the FHMUX First Quarterly Report contained a terminator circuit. This circuit was a broadband impedance matching network. It was similiar in function to that used in the TD1288 equipment, and merely serves to provide more efficient power transfer from the channels to the antenna. This circuitry is complex because of the wide bandwidth requirements of the FHMUX. The advantages of the RF combining scheme shown in Figure 5-1 is that a terminator circuit is not needed, as all ports are properly loaded with 50 ohm impedances, and antenna tuning is not required. A disadvantage is the need for additional bandpass filters.

5.3 LOAD PULLING

An early load pulling study (Appendix C of the Reference Docu-

ment) caused concern over the detuning effects of the antenna impedance upon the bandpass filters. The analysis shown below describes how the quad-coupled combiner eliminates the need to compensate for the antenna impedance.

5.4 QUAD COMBINER ANALYSIS

This section addresses the requirement or nonrequirement for a 30-88 MHz electronically tunable antenna matching network which would be employed at the output of the FHMUX. The impedance of the antenna and its 80 foot cable combination are such that its locus vs. frequency virtually fills a 3.0:1 VSWR circle as plotted on a Smith Chart. Thus, the antenna matching network (if required) must be tunable, self-calibrating and fast switching. This unit would be far more complicated than the rest of the FHMUX. As will be shown, an antenna matching network is not required if the appropriate design approach is applied to the FHMUX.

The technical requirement contains the following specification:

"Impedance. The nominal load impedance for the multiplexer shall be 50 ohms real. Specified performance shall be maintained to a VSWR of 3:1."

There is no reference to a requirement or specification for an antenna matching network in the referenced document. Therefore, if the FHMUX can meet all specifications when subject to a load VSWR of 3:1 without the use of an antenna matching network, this network is not required or desired. In other words, the need for an antenna matching network is only subject to whether or not the FHMUX specifications are achievable when it operates into an arbitrary load having a maximum VSWR of 3:1 over the 30-88 MHz frequency band. Thus, we will analyze the operation of the FHMUX into an arbitrary load.

The cascaded networks for analysis (the FHMUX and the antenna system) are depicted by the block diagram of Figure 5-4. A scattering matrix analysis is an excellent methodology to determine the effects of interface conditions on the overall performance of the cascaded networks.

Before proceeding further, a brief review of S parameters is presented in Figure 5-2 and 5-3.

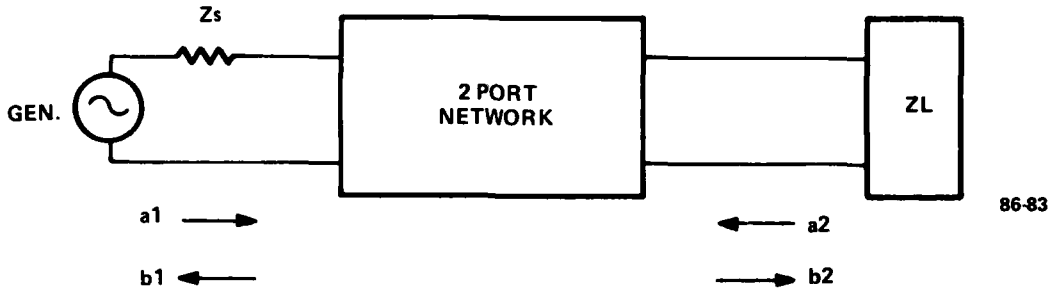

Figure 5-2. General Two-Port Block Diagram

As opposed to the more conventional parameter sets which relate total voltages and total currents at the network ports, S-parameters relate traveling waves (Figure 5-2). The incident voltage waves, a_1 and a_2, are the independent variables, and the reflected voltage waves, b_1 and b_2, are the dependent variables. The network is assumed to be embedded in a transmission line system of known characteristic impedance which shall be designated Z_o. The S-parameters are then measured with Z_o terminations on each of the ports of the network. Under these conditions, S_{11} and S_{22}, the input and output reflection coefficients, and S_{21} and S_{12}, the forward and reverse transmission coefficients, can be measured (Figure 5-4).

$$S11 = \frac{b_1}{a_1}\Bigg|_{a_2 = 0} \qquad S12 = \frac{b_1}{a_2}\Bigg|_{a_1 = 0}$$

$$S21 = \frac{b_2}{a_1}\Bigg|_{a_2 = 0} \qquad S22 = \frac{b_2}{a_2}\Bigg|_{a_1 = 0}$$

Figure 5-3. S Parameter Definitions

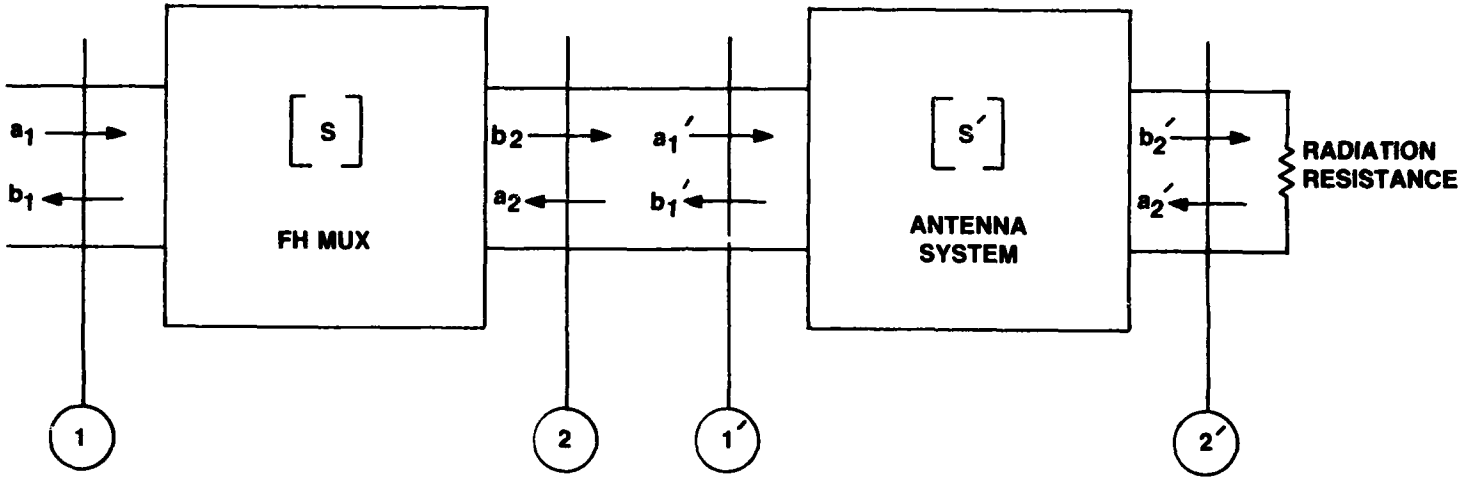

NOTE: THE RADIATION RESISTANCE IS THE ONLY RADIATING ELEMENT IN THE ANTENNA SYSTEM. ALL OF THE INCIDENT COMPONENT b_2' IS ABSORBED AND RADIATED BY THE ANTENNA RADIATION RESISTANCE. THUS $a_2' = 0$. THE ANTENNA SYSTEM IS MADE UP OF COAXIAL CABLE, CONNECTORS, AND IMPEDANCE MATCHING DEVICES. SEE TEXT.

7146-82

Figure 5-4 · Block Diagram for Analysis of Interface Conditions Between FHMUX and Antenna System

S_{11} is then equal to b_1/a_1 with $a_2 = 0$ or no incident wave on Port 2. This is accomplished by terminating the output of the two-port in an impedance equal to Z_0.

Summary:

S_{11} = input reflection coefficient with the output matched

S_{12} = forward transmission coefficient with the output matched
This is the gain or attenuation of the network

S_{22} = output reflection coefficient with the input matched

S_{12} = reverse transmission coefficient with the input matched

S-parameters are determined with resistive terminations. This obviates the difficulties involved in obtaining the broadband open and short circuit conditions required for the H, Y, and Z-parameters.

Parasitic oscillations in active devices are minimized when these devices are terminated in resistive loads.

Equipment is available for determining S-parameters since only incident and reflected voltages need to be measured.

The general scattering matrix equations for the two networks of Figure 5-4 are:

$$[S]\ \vec{a} = \vec{b} \tag{1}$$

$$[S']\ \vec{a}' = \vec{b}' \tag{2}$$

Where the unprimed and primed quantities refer to the FHMUX and antenna system, respectively. The interface conditions from Figure 5-4 are given by:

$$a_2 = b'_1 \tag{3}$$

$$a'_1 = b_2 \tag{4}$$

$$\text{and} \quad a'_2 = 0 \tag{5}$$

Where the a's and b's represent the various incident and reflected voltage wave components.

The antenna system is made up of: the connecting RF cables and connectors, any impedance matching devices such as baluns and transformers, and the radiation resistance of the antenna. The only radiating component of this system is the antenna radiation resistance. The incident wave component b_2 is completely absorbed and hence radiated by this antenna radiation resistance. The reflected wave component a_2 is thus zero by definition.

If the antenna system is perfectly matched to the FHMUX, it is possible for the reflected wave component of the entire antenna system b_1 to be zero. However, the broadband requirements of the antenna system, and the wide range of required impedance transformations place rigorous demands on the antenna system impedance matching circuitry. The radiation resistance is defined as a pure resistance, but it is seldom very close in value to the characteristic impedance of the circuit. Also, a large reactive component is present in the antenna itself. This reactive component is a part of the antenna system.

The antenna system performs three functions:

- It connects the antenna to the FHMUX
- It cancels the reactive component (when needed) of the antenna
- It transforms the impedance level of the antenna resistive component (radiation resistance) to the level of the system characteristic impedance for maximum power transfer.

Substitution of equations 3-5 into equations 1 and 2 yields:

$$\begin{bmatrix} S_{11} & S_{12} \\ S_{21} & S_{22} \end{bmatrix} \begin{bmatrix} a_1 \\ b_1' \end{bmatrix} = \begin{bmatrix} b_1 \\ b_2 \end{bmatrix} \tag{6}$$

$$\begin{bmatrix} S_{11}' & S_{12}' \\ S_{21}' & S_{22}' \end{bmatrix} \begin{bmatrix} b_2 \\ 0 \end{bmatrix} = \begin{bmatrix} b_1' \\ b_2' \end{bmatrix} \tag{7}$$

Note that we have passive reciprocal networks; hence

$$S_{12} = S_{21} \text{ and } S_{12}' = S_{21}'$$

From Figure 5-4, the net insertion loss is

$$L = 20 \log \left| \frac{b_2'}{a_1} \right| \quad \text{dB} \tag{8}$$

where the ratio can be determined by solving the 4 simultaneous equations defined by matrix equations 6 and 7; i.e.,

$$\frac{b_2'}{a_1} = \frac{S_{21} S_{21}'}{1 - S_{22} S_{11}'} \tag{9}$$

Combining equations 8 and 9 we get the net insertion loss in dB:

$$L = 20 \log |S_{21}| + 20 \log |S_{21}'| - 20 \log |1 - S_{22} S_{11}'| \qquad (10)$$

Equation 10 shows that the net insertion loss of the FHMUX - antenna system combination is affected by the term ($1 - S_{22} S_{11}'$). S_{22} is the output reflection coefficient of the FHMUX, and S_{11}' is the input reflection coefficient of the antenna system.

If either S_{22} or S_{11}' is equal to zero, the net insertion loss of the cascaded networks S and S' will be simply the sum of the two individual insertion losses of the network as measured under matched terminal conditions. Equation 9 will then be modified to:

$$\frac{b_2'}{a_1} = \frac{S_{21} S_{21}'}{1} \qquad (9A)$$

and equation 10 will be modified to:

$$\text{Loss (dB)} = 20 \log |S_{21}| + 20 \log |S_{21}'| \qquad (10A)$$

It is unlikely that S_{21}' will be zero, as stated earlier. However, if the FHMUX can be structured such that S_{22} is always zero, then equation 10A can be realized. This means that the antenna system input impedance variations can never affect the FHMUX's contribution (S_{21}) to the net response of the system. In other words, the antenna system cannot detune the FHMUX when the output reflection coefficient of the FHMUX (S_{22}) is equal to zero.

Thus the effects of antenna mismatch on the FHMUX bandpass filters can be eliminated by the implementation of circuitry that will provide the conditions $S_{22} = 0$ at in-band and out-of-band frequencies. The solution is to use quadrature hybrid-coupled tuneable filters at the output of the FHMUX. This approach was recommended as a means to cascade the tuneable resonators, but the output resonators of the

original FHMUX circuitry were not hybrid-coupled at that time because of the reactive series type combiner proposed at that time. Since then, a different combining scheme has been recommended, where all of the resonators are hybrid-coupled. The evaluation of this scheme under antenna mismatch conditions is described below.

A typical hybrid-coupled circuit is shown in Figure 5-5. It is well known that if the two filters present reflection coefficients of $\Gamma 1'$ and $\Gamma 2'$ respectively to the quadrature ports of these hybrids (Ports 1 and 2), the effective input reflection coefficient at Port 3 is:

$$\Gamma IN = \frac{1}{2} \left(\Gamma 1' - \Gamma 2' \right) \tag{11}$$

The derivation of equation (11) is now given.

A 4 port linear network can be defined using S parameters.

$$\begin{bmatrix} S_{11} & S_{12} & S_{13} & S_{14} \\ S_{21} & S_{22} & S_{23} & S_{24} \\ S_{31} & S_{32} & S_{33} & S_{34} \\ S_{41} & S_{42} & S_{43} & S_{44} \end{bmatrix} \begin{bmatrix} a_1 \\ a_2 \\ a_3 \\ a_4 \end{bmatrix} = \begin{bmatrix} b_1 \\ b_2 \\ b_3 \\ b_4 \end{bmatrix} \tag{12}$$

The "a" vectors represent incident waves, and the "b" vectors represent reflected waves. A hybrid coupler is shown in Figure 5-6.

An excellent discussion on "S" parameters is given in Microwave Circuits by J. L. Altman, published by D. Van, Nostrand Co., pp. 40-71. As shown in Figure 5-6, the "a" vectors point into the junction, and the "b" vectors point away from the junction. As an introductory step, consider a simple two-port system.

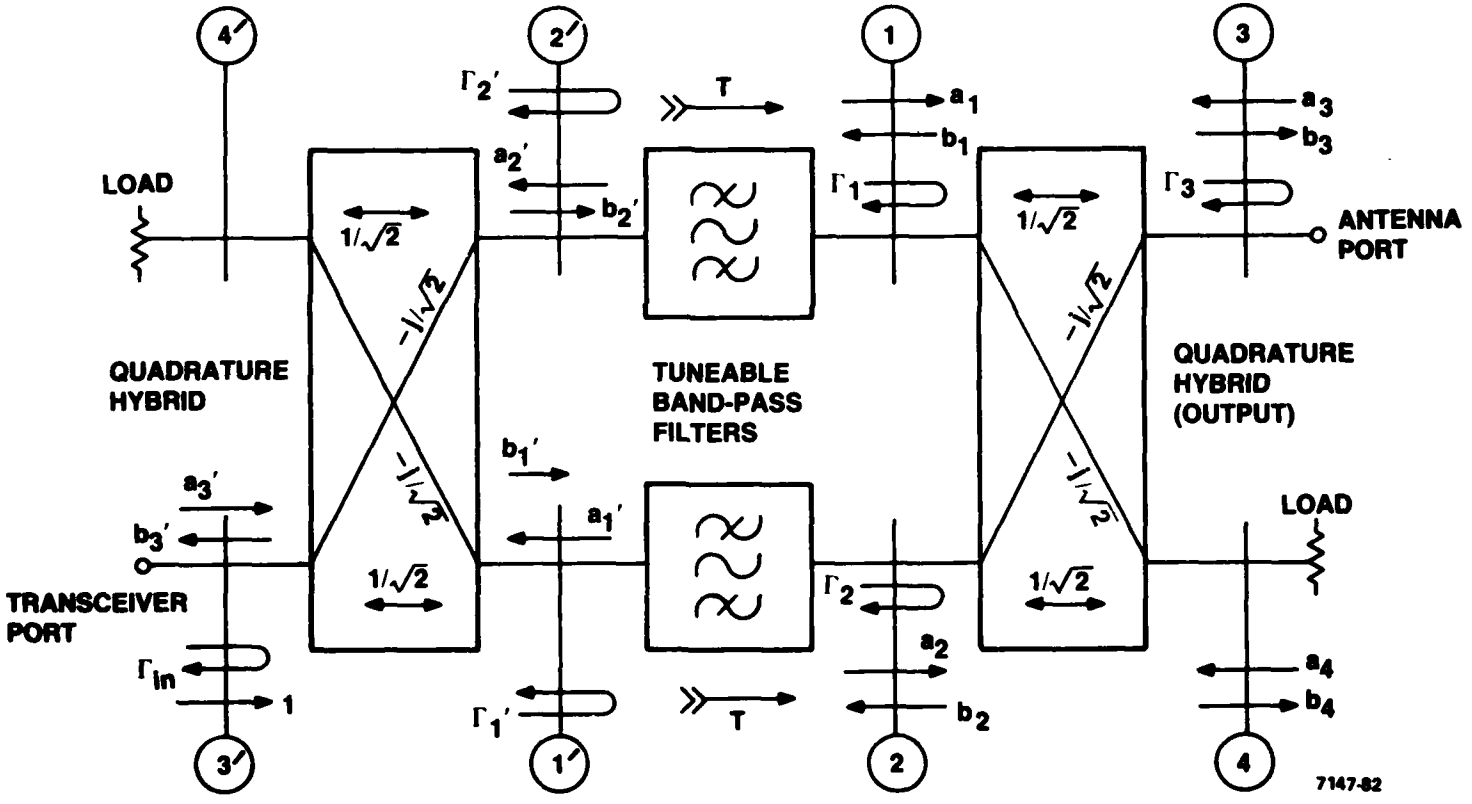

Figure 5-5. Block Diagram for Hybrid-Coupled Band-Pass Filters

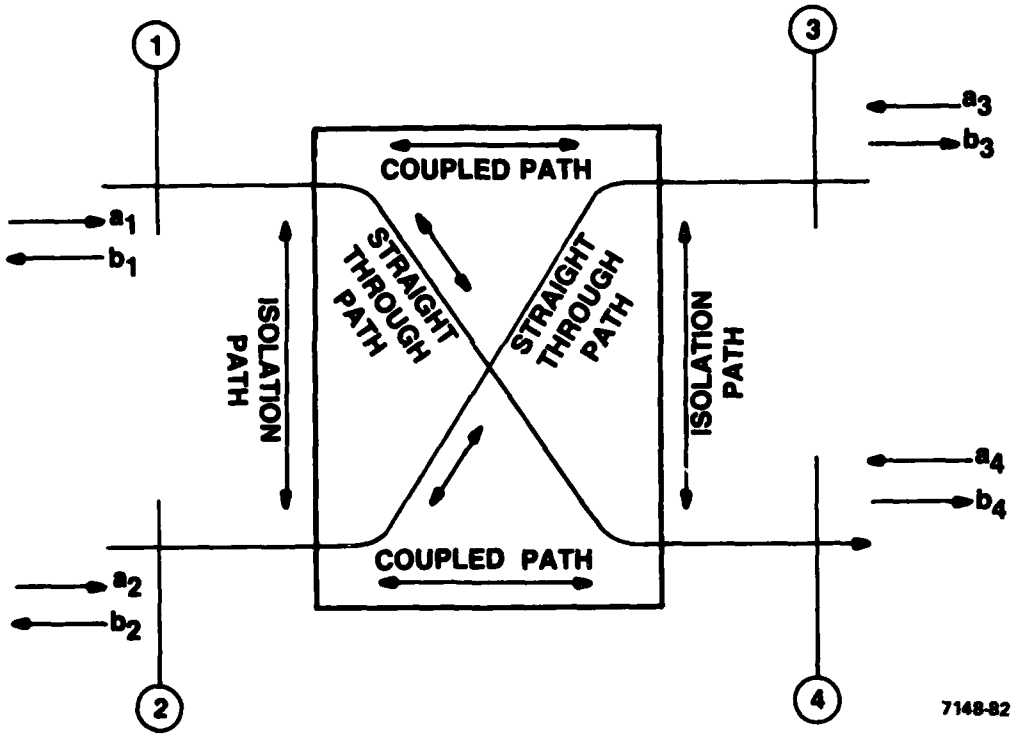

Figure 5-6. Hybrid Coupler

$$\left[\left[S \right] \vec{a} = \vec{b} \right] \tag{13}$$

$$\begin{bmatrix} S_{11} & S_{12} \\ S_{21} & S_{22} \end{bmatrix} \begin{bmatrix} a_1 \\ a_2 \end{bmatrix} = \begin{bmatrix} b_1 \\ b_2 \end{bmatrix} \tag{14}$$

By expansion,

$$\begin{aligned} S_{11}\, a_1 + S_{12}\, a_2 &= b_1 \\ S_{21}\, a_1 + S_{22}\, a_2 &= b_2 \end{aligned} \tag{15}$$

By definition,

$$S_{11} = \left. \frac{b_1}{a_1} \right| a_2 = 0 \tag{16}$$

And

$$S_{12} = \left. \frac{b_1}{a_2} \right| a_1 = 0 \tag{17}$$

The S matrix is represented by "i" number of rows and "j" number of columns.

Transmission coefficients exist where $i \neq j$, and reflection coefficients exist where $i = j$. All ports are to be terminated with matched (50 ohm) loads.

Thus, equation 16 defines the Port 1 reflection coefficient, and equation 17 describes the transmission coefficient of a signal passing to Port 1 from Port 2.

The scattering matrix for an ideal quadrature coupler is based on the following definitions:

- All ports are matched (VSWR = 1.0:1, reflection coefficient (Γ) = 0).

Therefore

$$S_{11} = S_{22} = S_{33} = S_{44} = 0 \qquad (18)$$

Also, infinite directivity exists between Ports 1 and 2, and between Ports 3 and 4. Thus these transmission coefficients are zero.

$$S_{21} = S_{12} = S_{34} = S_{43} = 0 \qquad (19)$$

The coupled port (20) and the straight through transmission coefficients (22) are given on page 778 of Microwave Filter, Impedance - Matching Networks, and Coupling Structures, by G. Matthaei, L. Young, and E.M.T. Jones, published by Artech House Books.

$$S_{13} = S_{31} = S_{24} = S_{42} \qquad \text{(Coupled Ports)}$$

$$= \frac{jc \sin\theta}{\sqrt{1 - c^2 \cos\theta + j \sin\theta}} \qquad (20)$$

where $\theta = \frac{f}{fo} \cdot 90^\circ = 90^\circ$

$C = \frac{1}{\sqrt{2}}$

} AT MIDBAND

Thus: $$S_{13} = S_{31} = S_{24} = S_{42} = \frac{1}{\sqrt{2}} \quad (21)$$

The straight through path is also derived from page 778 of the reference given above:

$$S_{14} = S_{41} = S_{23} = S_{32} \text{ (straight through path)}$$

$$= \frac{\sqrt{1 - c^2}}{\sqrt{1 - c^2 \cos\theta + j \sin\theta}} \quad (22)$$

Where $\theta = \frac{f}{f_o} \cdot 90^\circ = 90^\circ$ AT MIDBAND

$C = \frac{1}{\sqrt{2}}$

Thus $$S_{14} = S_{41} = S_{23} = S_{32} = \frac{-j}{\sqrt{2}} \quad (23)$$

Now, by using equations 18-23, the scattering matrix of an ideal quadrature coupler can be written.

$$[S]_{HYBRID} = \begin{bmatrix} 0 & 0 & 1\angle\sqrt{2} & -j\angle\sqrt{2} \\ 0 & 0 & -j\angle\sqrt{2} & 1\angle\sqrt{2} \\ 1\angle\sqrt{2} & -j\angle\sqrt{2} & 0 & 0 \\ -j\angle\sqrt{2} & 1\angle\sqrt{2} & 0 & 0 \end{bmatrix} \tag{24}$$

Simplifying,

$$[S]_{HYBRID} = \frac{1}{\sqrt{2}} \begin{bmatrix} 0 & 0 & 1 & -j \\ 0 & 0 & -j & 1 \\ 1 & -j & 0 & 0 \\ -j & 1 & 0 & 0 \end{bmatrix} \tag{25}$$

The complete system, including the hybrid coupler, and its external terminations is shown in Figure 5-7.

As shown, Port 4 is terminated with a 50 ohm resistor, Port 3 is the input port, and the problem is to derive the input reflection coefficient Γ in when Ports 1 and 2 are terminated in impedances having reflection coefficients $\Gamma 1'$ and $\Gamma 2'$.
In other words, we are deriving

$$\Gamma \text{ IN} = \frac{b_3}{a_3}$$

where the input incident signal a_3 is set equal to 1. The scattering matrix for this system is:

$$\frac{1}{\sqrt{2}} \begin{bmatrix} 0 & 0 & 1 & -j \\ 0 & 0 & -j & 1 \\ 1 & -j & 0 & 0 \\ -j & 1 & 0 & 0 \end{bmatrix} \begin{bmatrix} a_1 \\ a_2 \\ a_3 \\ a_4 \end{bmatrix} = \begin{bmatrix} b_1 \\ b_2 \\ b_3 \\ b_4 \end{bmatrix} \tag{26}$$

The a matrix is derived from Figure 5-7.

$$a_1 = \Gamma 1' \, b_1 \tag{27}$$

$$a_2 = \Gamma 2' \, b_2 \tag{28}$$

$$a_3 = 1 \tag{29}$$

$$a_4 = 0 \tag{30}$$

(Port 4 is terminated with 50 ohms).

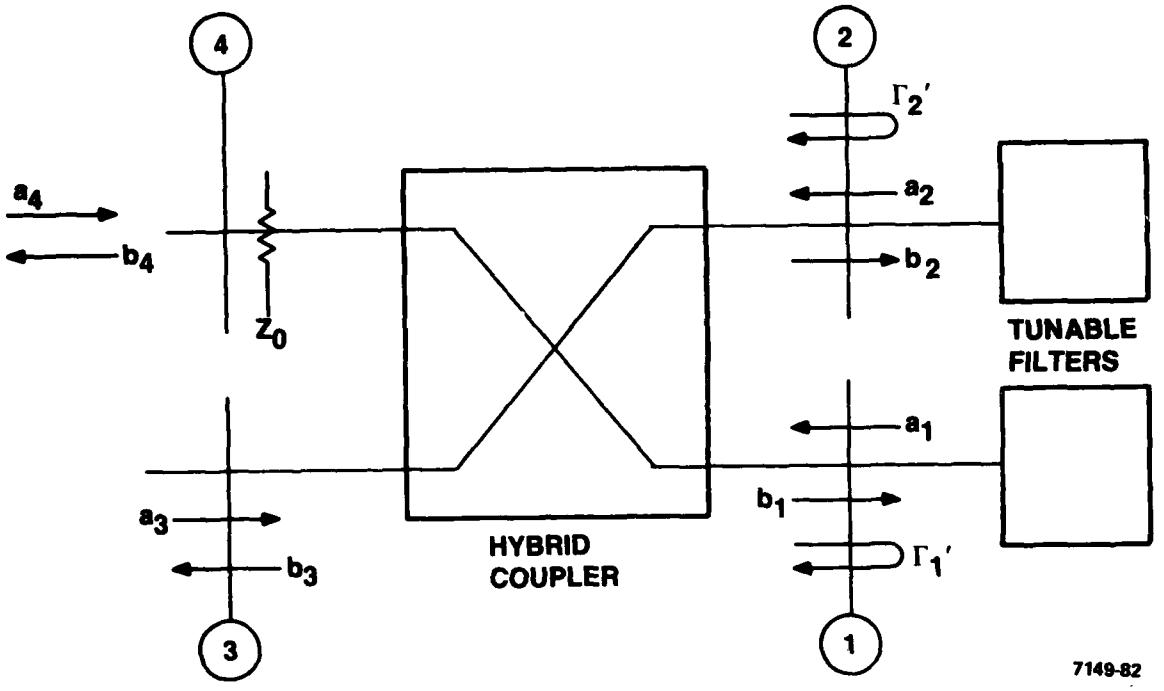

Figure 5-7. Hybrid Coupler System

The system is now completely defined.

$$\frac{1}{\sqrt{2}}\begin{bmatrix} 0 & 0 & 1 & -j \\ 0 & 0 & -j & 1 \\ 1 & -j & 0 & 0 \\ -j & 1 & 0 & 0 \end{bmatrix} \begin{bmatrix} \Gamma 1' & b_1 \\ \Gamma 2' & b_2 \\ 1 & \\ 0 & \end{bmatrix} = \begin{bmatrix} b_1 \\ b_2 \\ b_3 \\ b_4 \end{bmatrix} \tag{31}$$

Now, by expansion:

$$\frac{1}{\sqrt{2}} = b_1 \tag{32}$$

$$\frac{-j}{\sqrt{2}} = b_2 \tag{33}$$

$$\frac{\Gamma 1' \; b_1}{\sqrt{2}} - \frac{j\Gamma 2' \; b_2}{\sqrt{2}} = b_3 \tag{34}$$

$$\frac{-j\Gamma 1' \; b_1}{\sqrt{2}} + \frac{\Gamma 2' \; b_2}{\sqrt{2}} = b_4 \tag{35}$$

We now substitute equations 32 and 33 into 34

$$\frac{\Gamma 1'}{\sqrt{2}\cdot\sqrt{2}} - \left(\frac{j\Gamma 2'}{\sqrt{2}} \cdot \frac{-j}{\sqrt{2}}\right) = b_3 \tag{36}$$

Finally,

$$\Gamma \text{ IN} = \frac{b_3}{a_3} = \frac{b_3}{1} = \frac{\Gamma 1' - \Gamma 2'}{2} \tag{37}$$

Thus, the input reflection coefficient is derived. Equation 37 shows that if $\Gamma 1'$ and $\Gamma 2'$ are equal, or even very close to each other, the input reflection coefficient is zero, or very close to zero.

The following numerical example shows the powerful VSWR reducing mechanism inherent in the hybrid coupled circuit, as described in equation 11.

Let the tuneable bandpass filters of Figure 5-4 have the following impedances when each is tuned to a given FHMUX channel (Z_o =50 ohms):

Filter 1	Filter 2
27 + j30	25 + j33
VSWR = 2.69	VSWR = 3.04
$\Gamma 1' = .457 \angle 106.2$	$\Gamma 2' = .505 \angle 103.4$

The values of Γ are obtained from:

$$\Gamma = \frac{Z_r - Z_o}{Z_r + Z_o} \tag{38}$$

Where Z_r is the complex load, and Z_o is the system characteristic impedance.

Rewriting equation 11,

$$\Gamma_{IN} = \frac{1}{2} [.457 \angle 106.2^\circ - .505 \angle 103.4^\circ] \tag{39}$$

By converting the above polar coordinates to a rectangular form,

$$\Gamma_{IN} = \frac{1}{2}\,[(.54046 + j.5996) - (.50000 + j.6599)] \tag{40}$$

and then rearranging,

$$\Gamma_{IN} = \frac{1}{2}\,[(.54046 - .5000) + (j.5966 - j.6599)] \tag{41}$$

$$\Gamma_{IN} = \frac{1}{2}\,[.04046 - j.0603] \tag{42}$$

Now, converting back to polar form:

$$\Gamma_{IN} = \frac{1}{2}\,[.0726 \angle -56.139] \tag{43}$$

$$\Gamma_{IN} = .0363 \angle -28.07^{\circ}$$

Or, in rectangular form

$$Z_{in} = 1.0656 - j.0365 \qquad \text{(Normalized)} \tag{44}$$

Finally, the input impedance is:

$$Z_{in} = 53.28 - j\,1.825 \tag{45}$$

The input reflection coefficient is 0.0363, corresponding to a VSWR of 1.075:1.

Thus, hybrid coupler action has lowered the effective filter VSWRS of 2.69 and 3.04, to a value of 1.075:1. If the filter impedances were exactly equal, the reflection coefficient would have been zero, and VSWR would be 1.0:1.

Thus, as long as the filters are tuned fairly close to each other, the hybrid coupled circuit will behave as a well matched building block at all frequencies. The S parameter matrix of a hybrid circuit can be given:

$$[S]_{\substack{\text{HYBRID}\\\text{COUPLED}\\\text{CIRCUIT}}} = \begin{bmatrix} S_{11}'' & S_{21}'' \\ S_{21}'' & S_{22}'' \end{bmatrix} \tag{46}$$

If the filters are alike, then

$$[S]_{\substack{\text{HYBRID}\\\text{COUPLED}\\\text{CIRCUIT}}} = \begin{bmatrix} 0 & S_{21}'' \\ S_{21}'' & 0 \end{bmatrix} \tag{47}$$

and the S_{22} criterion is achieved, by virtue of the circuit symmetry. S_{21} is essentially the response of the filters, plus any dissipative loss and phase shift introduced by the quadrature hybrids.

In summary, the use of hybrid coupled filters allows one to establish the desired frequency response of the FHMUX independant of the antenna, even when the antenna is mismatched.

However, the filters are not isolated (nor detuned) from the antenna mismatch. The filters cannot be "isolated" from the antenna, because the quadrature hybrid is a reciprocal device. This point is now to be examined closely.

The next section will derive the reflection coefficients presented to the bandpass filters as a result of the antenna mismatch.

The scattering matrix for an ideal quadrature coupler has been derived, and is shown in equation 25. It will now be used in an analysis of the output hybrid coupler.

The vector describing the input waves to this output hybrid is now derived. This is the A matrix and is determined by the vectors pointing into the ports of the output coupler. Refer to Figure 5-5.

The a_1 incident voltage for Port 1 of the output coupler is now derived

$a_1 = b_2' T$, where T is the filter transmission coefficient. Also,

$$b_2' = a_3'\left(\frac{-j}{\sqrt{2}}\right)$$

where a_3' is the RF signal into Port 3 of the input coupler, and $\frac{-j}{\sqrt{2}}$ is the coupler straight through transmission coefficient (Equation 22)

Thus $a_1 = a_3' \frac{-j}{\sqrt{2}}$

Setting $a_3' = 1$,

$$a_1 = \frac{-jT}{2} \tag{48}$$

The a_2 incident voltage for Port 2 of the output coupler is derived below.

$a_2 = b_1' T$, where T is the filter transmission coefficient.

$b_1' = \frac{a3'T}{\sqrt{2}}$ $\frac{T}{\sqrt{2}}$ where a_3' is the RF signal into Port 3 of the input coupler, and $\frac{1}{\sqrt{2}}$ is the input coupler coupled arm transmission coefficient(20). Again, $a_3' = 1$, and

$$a_2 = \frac{T}{\sqrt{2}} \tag{49}$$

Now, $a_3 = \Gamma_3 \; b_3$ (50)

where Γ_3 is the antenna reflection coefficient, and, $a_4 = 0$, because Port 4 is properly terminated in 50 ohms.

Thus, the A vector is defined, and listed below.

$$\vec{a} = \begin{bmatrix} a_1 \\ a_2 \\ a_3 \\ a_4 \end{bmatrix} = \begin{bmatrix} \frac{-jT}{\sqrt{2}} \\ \frac{T}{\sqrt{2}} \\ \Gamma_3 \; b_3 \\ 0 \end{bmatrix} \tag{51}$$

Therefore, the scattering matrix equation for the output quadrature hybrid is:

$$\frac{1}{\sqrt{2}} a = \begin{bmatrix} 0 & 0 & 1 & -j \\ 0 & 0 & -j & 1 \\ 1 & -j & 0 & 0 \\ -j & 1 & 0 & 0 \end{bmatrix} \begin{bmatrix} \frac{-jT}{\sqrt{2}} \\ \frac{T}{\sqrt{2}} \\ \Gamma_3 \; b_3 \\ 0 \end{bmatrix} = \begin{bmatrix} b_1 \\ b_2 \\ b_3 \\ b_4 \end{bmatrix} \tag{52}$$

Expanding equation 50 yields

$$\frac{1}{\sqrt{2}}\,\Gamma_3\,b_3 = b_1 \tag{53}$$

$$\frac{-j}{\sqrt{2}}\,\Gamma_3\,b_3 = b_2 \tag{54}$$

$$\frac{1}{\sqrt{2}}\left[\frac{-jT}{\sqrt{2}} - \frac{jT}{\sqrt{2}}\right] = b_3$$

$$0 = b_4 \tag{54A}$$

$$\frac{1}{\sqrt{2}}\left[\frac{-2jT}{\sqrt{2}}\right] = b_3,\ -jT = b_3 \tag{55}$$

Now, using equations 51-55, we can calculate the reflection coefficients presented to the bandpass filters of Figure 5-5.

$$\Gamma_1 = \frac{b_1}{a_1} = \frac{\frac{\Gamma_3 b_3}{\sqrt{2}}}{\frac{-jT}{\sqrt{2}}}$$

$$\Gamma_1 = \frac{b_1}{a_1} = \frac{\frac{1}{\sqrt{2}}\,\Gamma_3 b_3}{\frac{-j}{\sqrt{2}}\,T}$$

Substituting equation 55 for the b_3 term,

$$\Gamma_1 = \frac{b_1}{a_1} = \frac{\frac{-j\,T\Gamma_3}{\sqrt{2}}}{\frac{-j\,T}{\sqrt{2}}} = \Gamma_3 \tag{56}$$

And

$$\Gamma_2 = \frac{b_2}{a_2} = \frac{\frac{-j\Gamma_3 b_3}{\sqrt{2}}}{\frac{T}{\sqrt{2}}}$$

Since $b_3 = -jT$,

$$\Gamma_2 = \frac{b_2}{a_2} = \frac{\frac{-j\Gamma_3(-jT)}{\sqrt{2}}}{\frac{T}{\sqrt{2}}} = -\Gamma_3 \qquad (57)$$

The analysis shows that both filters "see" the antenna mismatch 3, and therefore the RF voltages across these filters are affected accordingly. However, the filters are <u>not</u> detuned or pulled by the antenna, as shown by equation 9, because re-reflections at the filters are dissipated, and are not returned to the antenna.

In other words, the filters of the hybrid coupled FHMUX will "see" initial reflections from the mismatched antenna, but there will be no multiple reflections, and therefore no interaction between the antenna and the FHMUX.

5.5 LABORATORY VERIFICATION

A simple laboratory experiment was performed to verify the previous analysis. The circuit is shown in Figure 5-8. The components used, and 50 ohm impedance level resulted in a relatively low loaded Q of 10. The insertion loss was 2.8 dB at 54 MHz, hence the unloaded Q of the filters was only 36.3.

When load impedances corresponding to a VSWR of 3:1 were used, the impedance of the input hybrid was measured. Since the insertion loss was 2.8 dB, the VSWR measured at the input port was expected to be lower than 3:1. The calculated value of this lower VSWR is 1.71:1.

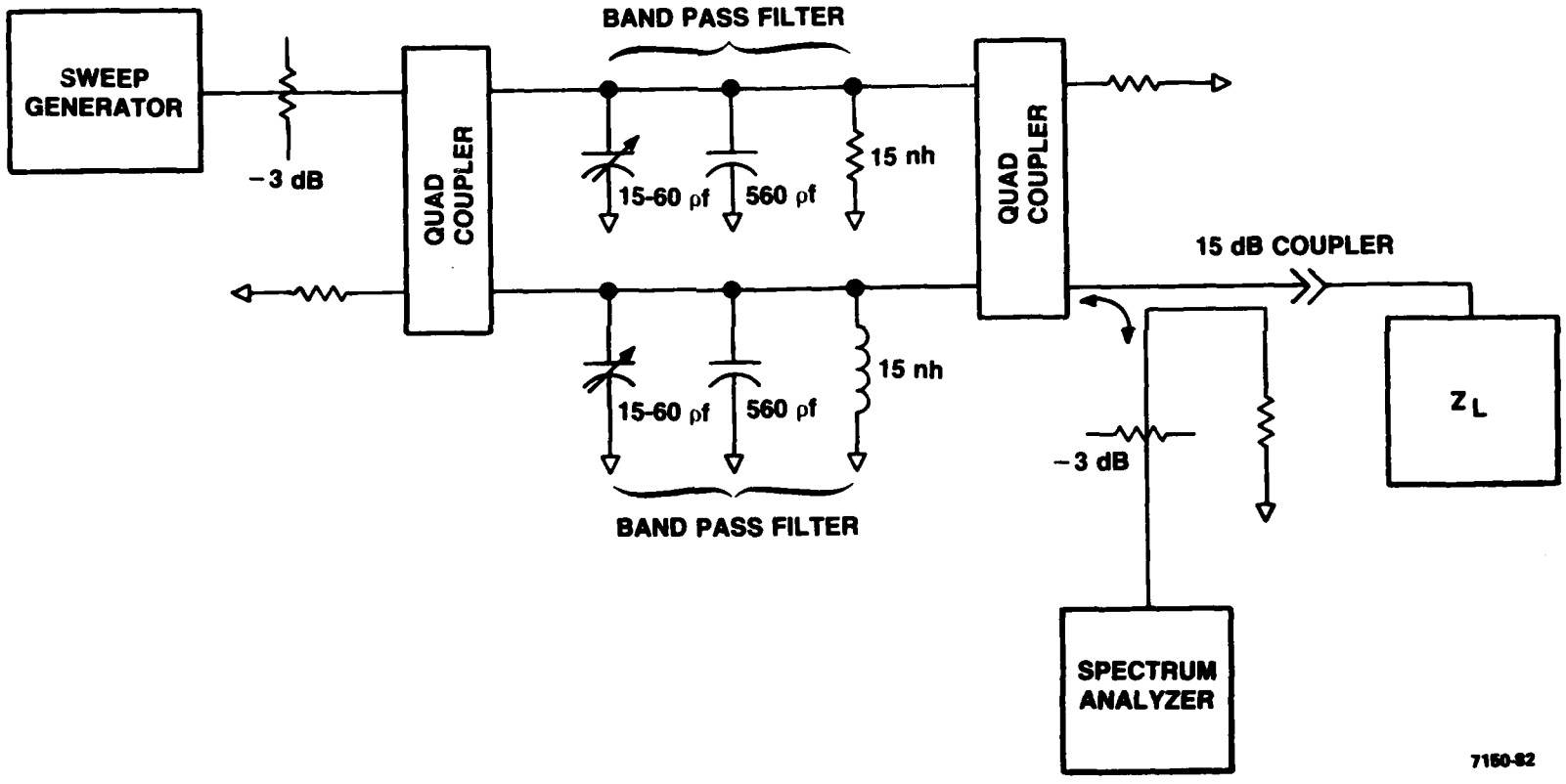

Figure 5-8. Test Circuit

This calculated value was verified, indicating that the load impedance is indeed "handed off" to the input port, but is modified by the insertion loss and phase shift of the circuit.

The load pulling effect was investigated by connecting various loads to the output port of the filter, and observing the swept output response via the directional coupler and the spectrum analyzer. Six loads were used, 50 + j0, 16 + j0, 150 + j0, short and open circuits, and 75-j 58 ohms. The various loads all had a small effect on the swept response.

Upon completion of the above, the input port was terminated with a 50 +j0 load, and the impedance looking back into the output port was measured at 54 MHz, and found to have a magnitude of 58 ohms instead of the anticipated 50 ohms. Even though the filter elements were synchronously tuned to 50 MHz by the variable capacitors, differences between the inductors, etc. were such that the reflection coefficients of each filter were not identical. The analysis showed that near identical reflection coefficients are needed to obtain the desired immunity from load variations. However, the performance obtained throughly verified the theory.

A photograph of the spectrum analyzer display is shown in Figure 5-9. Extreme load variations are shown, namely an open and a short circuit. The small differences in the center frequency and the shape of the skirts between these two loads is indeed encouraging.

A word on the construction and operation of the individual band pass filters used above, and those to be used in the FHMUX is in order. The filter used in the experiment was not a high Q precisely built circuit; the inductors were certainly not exactly alike, and the entire assembly was tuned manually by viewing the spectrum analyzer. As such, the output impedance was not very close to 50 ohms.

Conversely, the intended nature of the FHMUX filter construction is of a precise nature. The helical resonators will be closely fixtured. The physical size of the resonators will be such that close tolerances can be achieved without high tooling costs. The above,

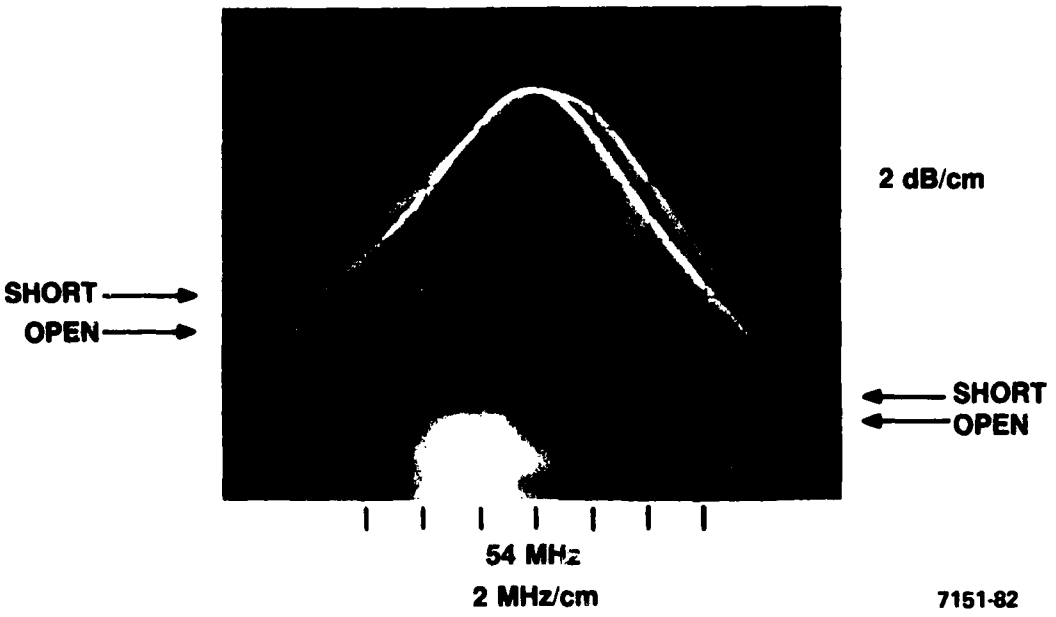

Figure 5-9. Comparison of Short and Open Circuit Swept Response

plus the precise tuning afforded by the shunt capacitive bus, and the resulting digital input code, makes possible a mating of nearly identical band pass filters inside a given pair of quad couplers. Each band pass filter will be individually calibrated, and have its own digital tuning calibration code stored in a PROM attached to the assembly.

With the above construction and tuning techniques the analytical requirement of a 50 ohm output impedance can be met, and thus load pulling will not be a problem.

5.6 POWER COMBINING PROPERTIES

Section 5.2 describes how the quad-coupled filters can be used to combine the channels. This technique is advantageous in that a true building block approach is possible. Therefore, the same resonator design can be used in the output combiner, or cascaded in the individual combiners. This section deals with the requirements for efficient power combining when using the quad coupled technique.

A summary of quadrature hybrid equations is given in Figure 5-10. For ease of understanding, the same nomenclature as in the preceeding derivations is used. Figure 5-10 shows the FHMUX Channel A output. Note that Port 4 of the Channel A output coupler is connected to Port 3 of the Channel B output coupler.

Equation 4 has been derived, and the effect on the bandpass filters by the antenna VSWR has also been analyzed. This section is concerned with the power combining properties of the quadrature coupled resonators when connected together as in Figure 5-10. A mathematical analysis will follow a description of the circuit action.

Assume that Channel B is in the transmit state, at frequency f_2. Channel A can be in either receive or transmit, and the two bandpass filters are tuned to frequency f_1. Guard band limitations are setup so that the filter response of the Channel A filters are down by at least 14 dB for a Channel B signal. The bandpass filters are thus highly reflective to this Channel B signal. Thus the Channel B signal is incident to Port 4 of the Channel A output coupler; it divides

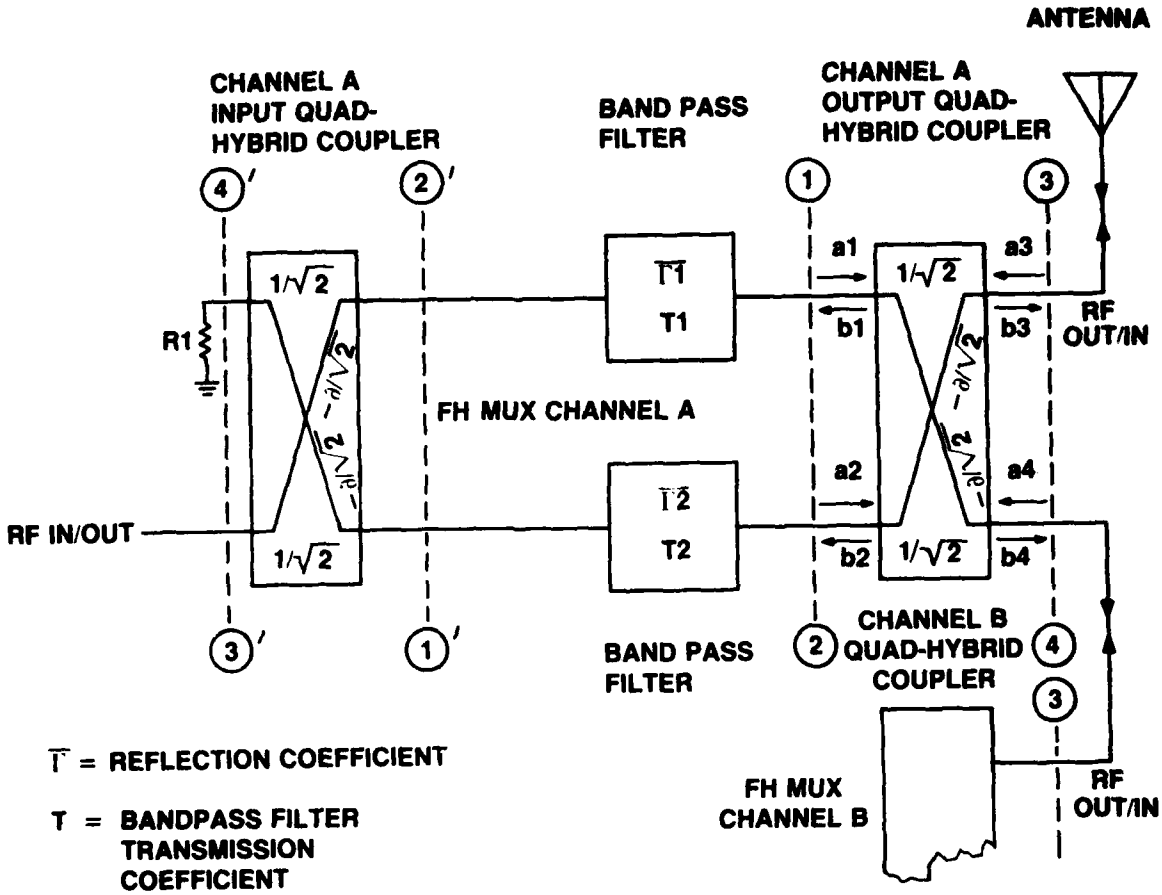

$\overline{\Gamma}$ = REFLECTION COEFFICIENT

T = BANDPASS FILTER TRANSMISSION COEFFICIENT

EQUATION 1:

RF POWER OUT AS PORT 3 DUE TO RF POWER IN AT PORT 3′ = $\dfrac{\text{PORT 3′ POWER IN } (\overline{\Gamma 1} + \overline{\Gamma 2})^2}{4}$

EQUATION 2:

POWER INTO R1 DUE TO RF POWER IN AT PORT 3′ = $\dfrac{\text{PORT 3′ POWER IN } (\overline{\Gamma 1} + \overline{\Gamma 2})^2}{4}$

EQUATION 3:

POWER INTO PORT 3 OF CHANNEL B OUTPUT COUPLER DUE TO POWER INTO PORT 3′ = $\dfrac{\text{PORT 3′ POWER IN } (T2 - T1)^2}{4}$

EQUATION 4:

PORT 3′ INPUT REFLECTION COEFFICIENT = $\overline{\Gamma}_{IN} = \frac{1}{2}(\overline{\Gamma 1} - \Gamma 2)$

7152-82

Figure 5-10. Quadrature Hybrid Relationships

equally, and its components are incident upon the bandpass filters. Since the filters are highly reflective to the Channel B signal, they are cast back to the Channel A output coupler, recombined, and then routed to the antenna via Port 3 of the Channel A output coupler. Therefore it is desirable for the Channel A filters to be very reflective as far as the other channel frequencies are concerned.

The combining loss on a per channel basis is thus defined as the power ratio of the Channel 2 output at Port 3 of the Channel A output coupler, to the Channel 2 signal incident on Port 4 of the Channel A output coupler. A thorough discussion of normalized waves and the scattering matrix is given on pages 40-45 of Altmans' text on "Microwave Cicuits."

$$\text{Power out of Port 3 of Channel A to antenna} = \frac{1}{2} |b_3|^2 \tag{58}$$

$$\text{Power into Port 4 of Channel A from Channel B} = \frac{1}{2} |a_4|^2 \tag{59}$$

Therefore, the combining loss can be defined as:

$$\frac{\frac{1}{2} |b_3|^2}{\frac{1}{2} |a_4|^2} = \frac{|b_3|^2}{|a_4|^2} \tag{60}$$

The quadrature hybrid scattering matrix (Equation 24) can again be used. The A matrix will now be defined.

$$a_1 = b_1 \Gamma_1 \tag{61}$$

$$a_2 = b_2 \Gamma_2 \tag{62}$$

$$a_3 = 0 \tag{63}$$

$$a_4 = 1 \qquad \text{(input)} \tag{64}$$

Therefore

$$A = \begin{bmatrix} b_1 \Gamma_1 \\ b_2 \Gamma_2 \\ 0 \\ 1 \end{bmatrix} \tag{65}$$

And, the system scattering matrix is:

$$\frac{1}{\sqrt{2}} \begin{bmatrix} 0 & 0 & 1 & -j \\ 0 & 0 & -j & 1 \\ 1 & -j & 0 & 0 \\ -j & 1 & 0 & 0 \end{bmatrix} \begin{bmatrix} b_1 \Gamma_1 \\ b_2 \Gamma_2 \\ 0 \\ 1 \end{bmatrix} = \begin{matrix} b_1 \\ b_2 \\ b_3 \\ b_4 \end{matrix} \tag{66}$$

By expanding,

$$b_1 = \frac{-j}{\sqrt{2}} \tag{67}$$

$$b_2 = \frac{1}{\sqrt{2}} \tag{68}$$

$$b_3 = \frac{b_1 \Gamma_1}{\sqrt{2}} - \frac{jb_2 \Gamma_2}{\sqrt{2}} \tag{69}$$

$$b_4 = \frac{-jb_1 \Gamma_1}{\sqrt{2}} + \frac{b_2 \Gamma_2}{\sqrt{2}} \tag{70}$$

Now, substitute equations 67 and 68 into 69.

$$b_3 = \frac{-j \Gamma_1}{2} - \frac{j \Gamma_2}{2}$$

$$b_3 = \frac{-j}{2} (\Gamma_1 + \Gamma_2) \tag{71}$$

Using Equation 60, we have:

$$\frac{\text{Power Out of Port 3}}{\text{Power Into Port 4}} = \left| \frac{b_3}{a_4} \right|^2 = \frac{\left| \frac{-j}{2} (\Gamma_1 + \Gamma_2) \right|^2}{|1|^2}$$

$$\frac{\text{Power Out of Port 3}}{\text{Power Into Port 4}} = \frac{1}{4} (\Gamma_1 + \Gamma_2)^2 \tag{72}$$

Equation 71 is the same as Equation 2 of Figure 5-10, thus showing the symmetry of the hybrid coupler.

Altmans text "Microwave Circuits", pages 12-16, derives the following expression relating incident and transmitted power, and reflection coefficient:

$$\text{Power transmitted} = \text{Power incident } (1 - |\Gamma|^2). \tag{73}$$

This derivation is found between pages 12 and 16.

As discussed earlier, the bandpass filters are detuned to a Channel B signal. Equation 72 can be used to calculate the reflection coefficient of the filters, given the power ratio. Since the filters are identically tuned, their reflection coefficients will be equal. Since the skirt attenuation of the filter elements is known, the combining loss of the RF path from Port 4 to Port 3 of the Channel A output hybrid can be computed.

Let -X= filter skirt attenuation, in dB

$$dB = -X = 10 \log \frac{Pt}{Pi} \tag{74}$$

Where Pt is the transmitted power and Pi is the incident power.

$$\frac{Pt}{Pi} = 10^{\frac{-X}{10}} \tag{75}$$

Now, substituting from equation 72

$$\frac{Pt}{Pi} = (1|-|\Gamma|^2) = 10^{\frac{-X}{10}}$$

$$\text{and} \quad |\Gamma|^2 = 1 - 10^{\frac{-X}{10}} \tag{76}$$

Equation 76 is substituted in equation 72 to obtain the desired combining loss.

The combining loss

$$\frac{P3}{P4} = \frac{1}{4}\left(\Gamma_1 + \Gamma_2\right)^2$$

$$= \frac{1}{4}\left(\sqrt{1 - 10^{\frac{-x}{10}}} + \sqrt{1 - 10^{\frac{-x}{10}}}\right)^2$$

$$= \frac{1}{4}\left(2\sqrt{1 - 10^{\frac{-x}{10}}}\right)^2$$

$$= \frac{4}{4}\left(1 - 10^{\frac{-x}{10}}\right)$$

$$dB = 10 \log \left(1 - 10^{\frac{-x}{10}}\right) \qquad (77)$$

The results of equation 77 have been plotted and are shown in Figure 5-11.

The system study specified three cascaded bandpass filters, each having a loaded Q of 50. Now, at +/-5%, each of these filters will have an insertion loss of 14 dB. This corresponds to point A of Figure 5-11, which shows a combining loss of -.176 dB. Thus, the actual combining loss will be .176 dB plus the dissipative loss of the hybrid itself.

5.7 FILTER INTERACTION

The system study which discussed the FHMUX BER performance, showed the need for a narrow RF bandwidth. It appears that the -40 dB bandwidth of the FHMUX must be about +/-5%. This can be accomplished by 3 cascaded helical resonators, each with a loaded Q of 50. This cascaded arrangement results in a 3 dB bandwidth of only +/-0.51%. In order to maintain a low insertion loss, it is essential that the

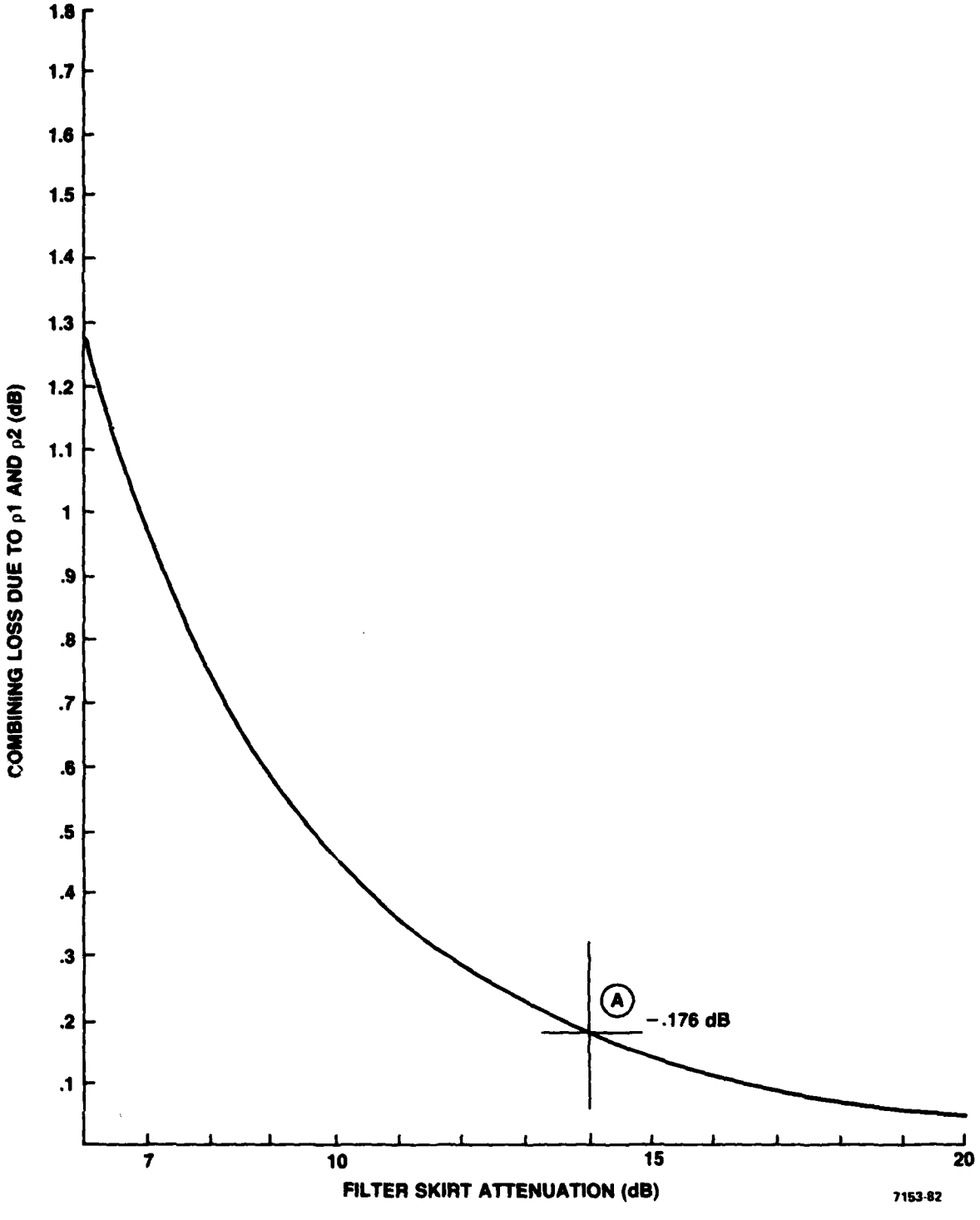

Figure 5-11. Combining Loss Due to Filter p1 and p2 vs. Filter Skirt Attenuation

filters do not interact with each other. Forms of interaction can be caused by unfavorable VSWR, undesired coupling of RF fields, and possible grounding effects.

Undesired coupling of the high voltage RF fields can be reduced greatly by shielding and the use of helical resonators. The means of connecting the resonators together to reduce adverse loading is also critical.

Figure 5-12 shows two methods of obtaining the desired selectivity. Part A of Figure 5-12 shows a standard means of obtaining a two resonator response. Of concern is the means of coupling between Sections A and B of the two cascaded resonators. This is usually implemented by a carefully designed iris (I), which is cut into the common wall between the two resonator cavities.

Assuming power flow from left to right as shown, power reflected from the load is coupled back through the output quad coupler, and re-reflected from the resonator circuits to the quad coupler termination R. Thus, power is not reflected from the quad back to the load, but the load VSWR is seen by each of the resonator sections inside the quad pair, and its magnitude is tempered only by the insertion loss of the quad coupler itself. The iris is designed to efficiently couple energy from resonator Section A, to Section B. The effect of a poor impedance match on the output section will thus detune both resonator sections, and will increase insertion loss and deform the shape of the filter skirts.

Part B of Figure 5-12 shows how the filter interaction problem can be greatly reduced, but at the expense of an additional pair of quad couplers. The actio[illegible] quad coupler Q3 presents an excellent impedance match to the output of the input filter section. Also, any VSWR effects present at the input are not handed on to the output section. As long as the individual resonators inside the quad pairs are tuned reasonably close to each other, the cascaded sections are independent of each other.

This circuit presents an attractive means to cascade additional resonator sections in order to improve FHMUX selectivity.

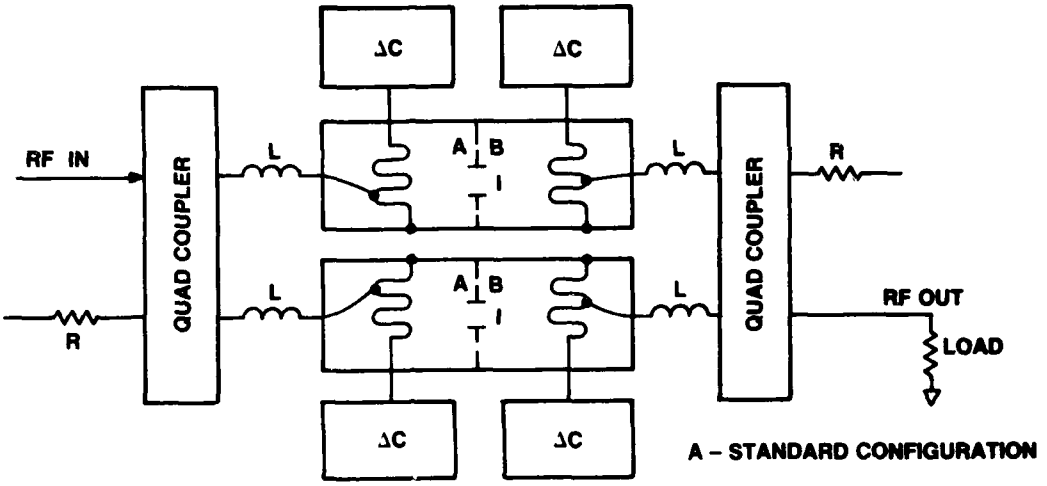

A – STANDARD CONFIGURATION

B – REDUCED LOADING EFFECT.

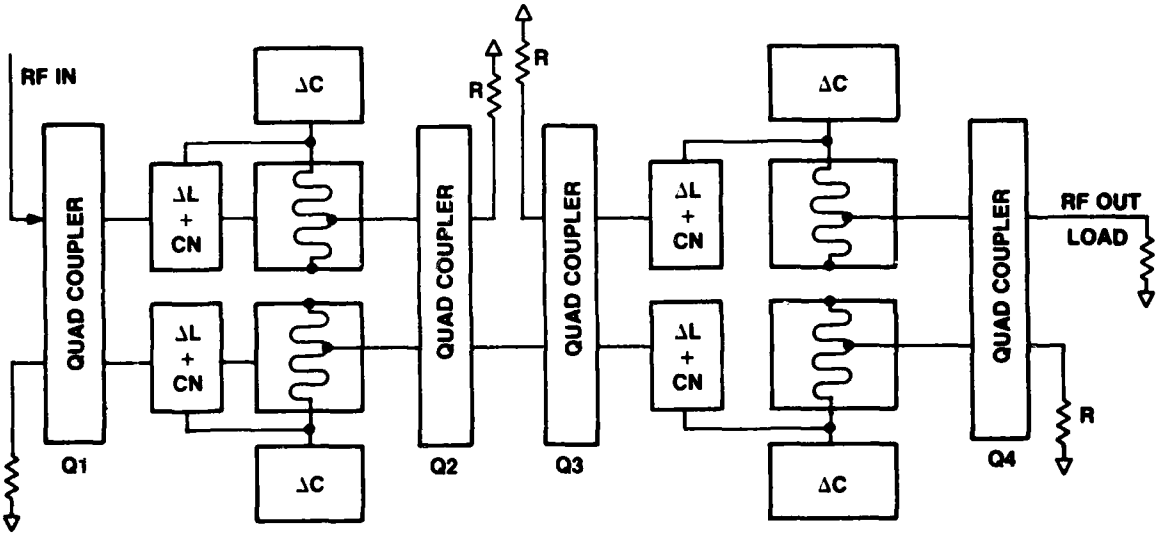

NOTE: "CN" MEANS WIDE BAND, FIXED TUNED COMPENSATING NETWORK

7164-82

Figure 5-12. Means of Connection

5.8 HIGH Q RESONATOR STUDY

The Second Quarterly Report recommended the use of helical resonators instead of lumped L-C circuits. A separate study has since verified this selection. Alternate high Q resonators have been studied, and the results are shown in Appendix E.

5.8.1 Introduction

The system study recommended a 40 dB bandwidth of +/-5%. Achievement of a -2 dB insertion loss at the center frequency of any given channel is the design goal. If three filter sections are cascaded, with each quad coupler having nominal -0.1 dB combining loss and a resonator loss of about -0.5 dB, the -2.0 dB design goal figure may be feasible. However, the combining loss described in the previous section must also be taken into account. Namely, an off tuned filter may have a combining loss of 0.18 dB. This effect is shown in Figure 5-13. Thus, the insertion loss of any given channel can vary from -2.1 to -3.2, depending on its closeness to the antenna.

As shown, an RF signal leaving Port 9 will pass through channels D, C, B, and A before reaching the antenna, and incur a 0.18 dB combining loss in each channel, plus an additional 0.1 quad coupler loss in each channel.

5.8.2 Bounding The Problem

The insertion loss of a resonant circuit is set by the ratio of unloaded to loaded Q as noted below, and is shown in Figure 5-14.

$$\text{Loss (dB)} = 20 \text{ Log} \quad \frac{(Qu/Ql)}{Qu/Ql-1} \tag{78}$$

Thus, achievement of a 0.5 dB insertion loss will require a ratio of Qu to Ql of at least 18. This means that the unloaded Q of the resonator (including the switchable capacitors) must equal or exceed 900.

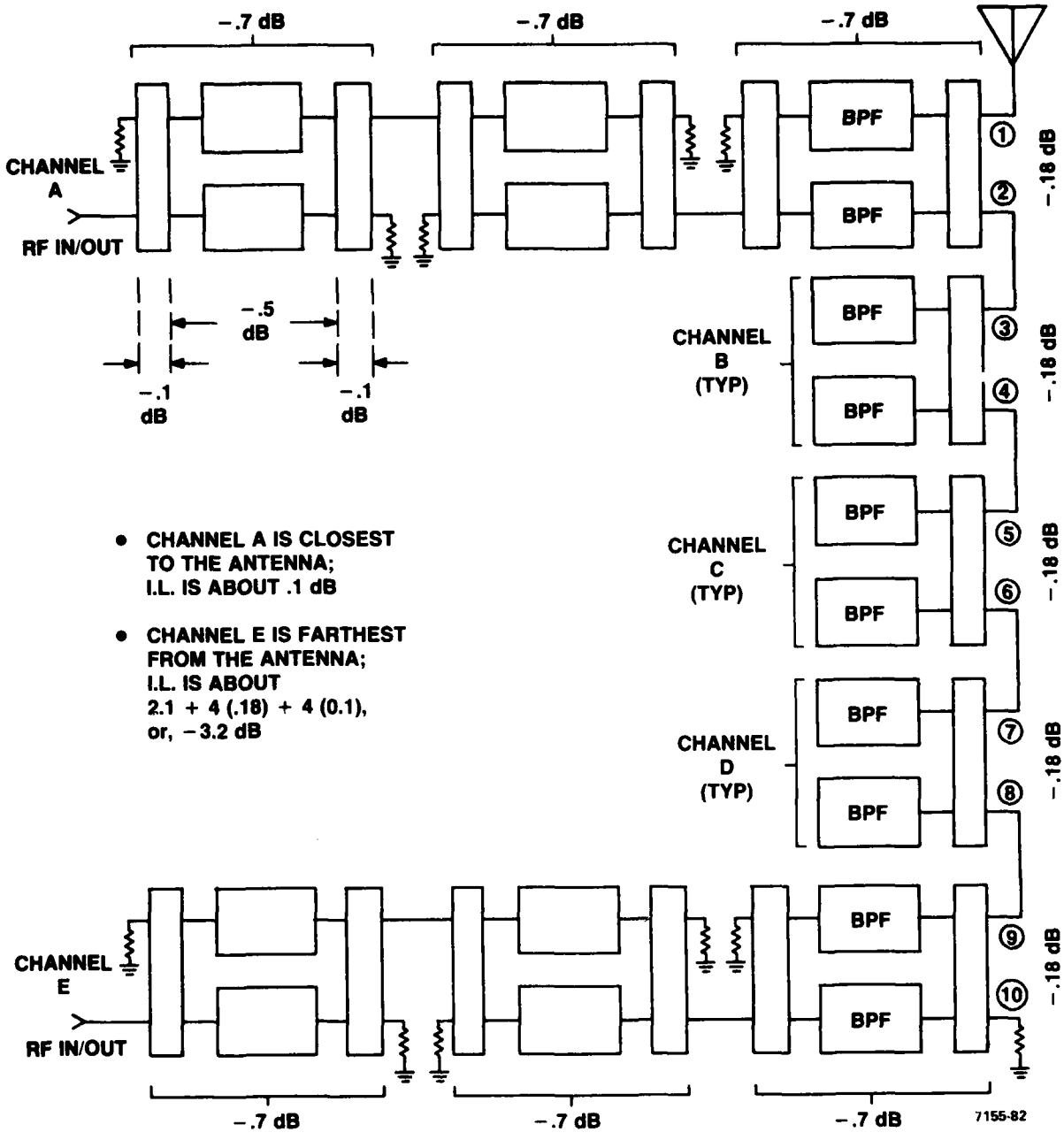

Figure 5-13. Loss Analysis

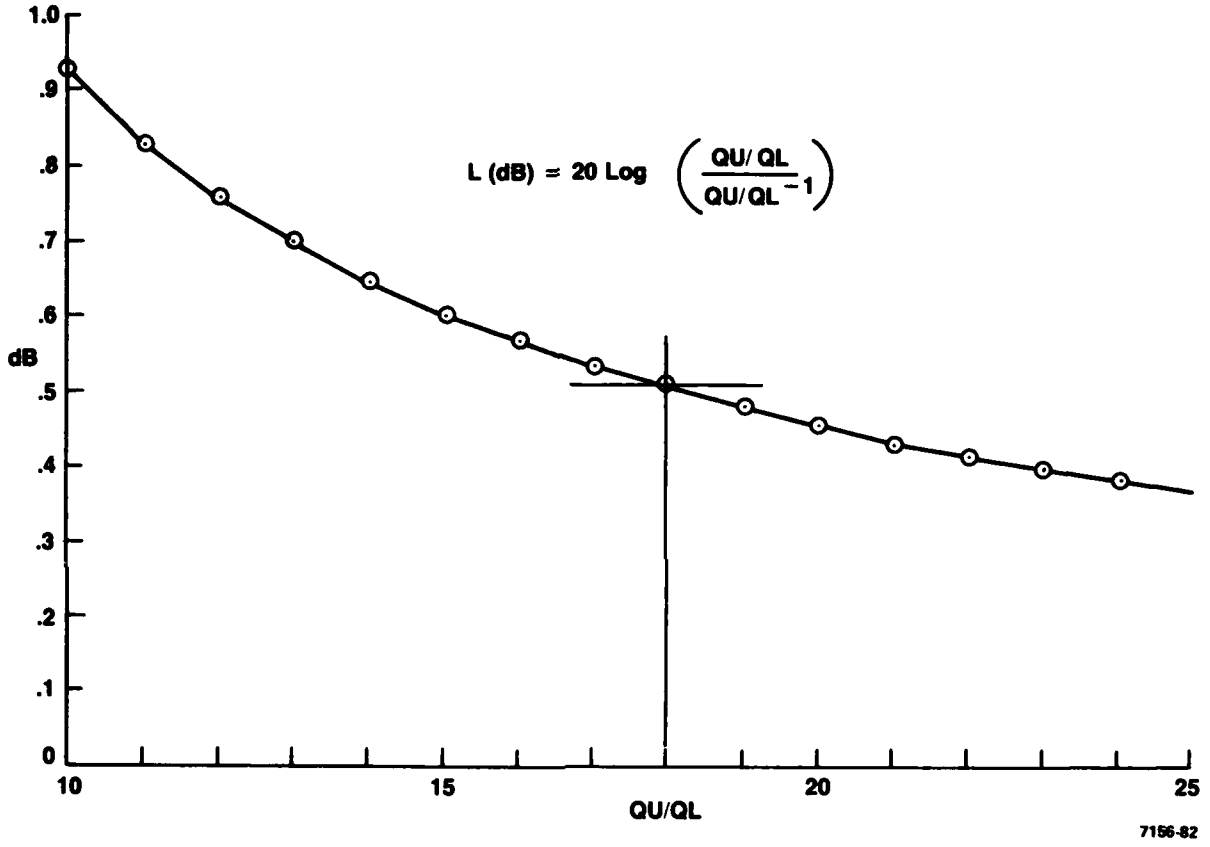

Figure 5-14. Insertion Losss in dB vs QU/QL

A basic model of the resonator is shown in Figure 5-15, along with equations 79 and 80. Equation 79 shows that the resonator unloaded Q is the parallel combination of the inductor and capacitor Q. Thus, the resonator unloaded Q will always be lower than the lesser of the two. Usually, the Q of the capacitor is much higher than that of the inductor, but with use of the switched capacitive shunt reactive bus, this is no longer true.

Helical resonator design is predicated on the desired Q and self resonant frequency. The physical size of the resonator is a result of these two parameters. This value of Q exists only at the self-resonant frequency, and is lower at other frequencies. At the self resonant frequency, the resonator model approaches that of a quarter wave transmission line with a short circuit termination. Also, as the frequency is lowered, the effective inductance decreases. At frequencies close to self resonance, the value of inductance is high, and the amount of capacity needed to resonate the filter is small.

The Q of the helical resonator is proportional to the square root of the frequency, hence the lowest Q is obtained at 30 MHz. The general design procedure is to select a helical resonator self resonant frequency that is about 10% higher than the highest in band frequency, along with the desired Q at this same frequency. The higher the desired Q, the larger the size of the resonator, as shown below.

Desired fo	100 MHz
Desired Q	3000
Width = Length	5 Inches
Height	8 Inches
Turns	3.2

The Q at the low end of the band will be less than at fo, and must be taken into account.

As noted, an insertion loss of 0.5 dB requires an unloaded to loaded Q ratio of about 18. Thus a filter circuit with a loaded Q of 50, and an insertion loss of -.5 dB will require an unloaded Q of

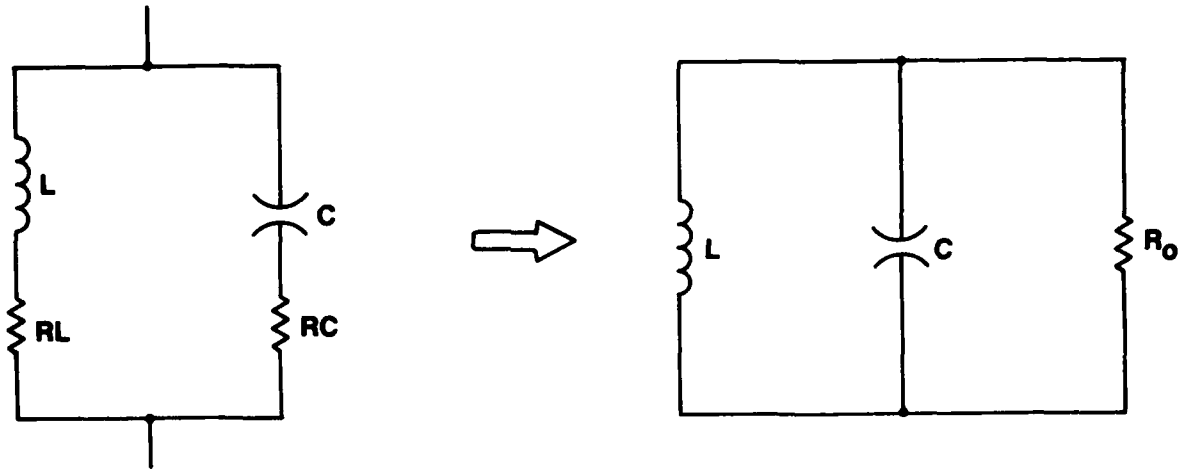

$$Q_{IND} = \frac{WL}{RL}$$

$$Q_{CAP} = \frac{1}{WCRC}$$

R_0 = PARALLEL EQUIVALENT RESISTANCE

$$Q_U = \frac{Q_L\, Q_C}{Q_L + Q_C} \qquad (79)$$

$$\frac{1}{Q_L} = \left.\frac{\Delta f}{f_o}\right|_{-3\,dB} = \left[\frac{1}{Q_U} + \frac{1}{Q_U} \cdot \frac{L}{CRR_o}\right] \qquad (80)$$

WHERE $R = R_L + R_C$

FOR A HELICAL RESONATOR,

$Q = 60\, D\sqrt{f}$

D = SIDE DIM. IN INCHES

F = MHz

7157-82

Figure 5-15. Resonator Model

about 900. Also, the filter unloaded Q is the parallel combination of the inductor and capacitance Q's. Figure 5-16 illustrates this point. Point A shown that if Q1 is 2400 at the lowest frequency of interest, the capacitor must have a Q of about 1400 if the insertion loss is to be 0.5 dB.

A search for a high quality transmitting capacitor indicates that the ATC 100E series has the highest Q. The Q is specified to be greater than 10,000 at 1 MHz. It is estimated that the Q will be about 3500 at 88 MHz. Thus, the parameters of size, Q, and insertion loss have been assembled such that the problem is adequately bounded.

5.9 COMPUTER AIDED DESIGN AND ANALYSIS

5.9.1 Helical Resonator

The design procedure for helical resonators is well-documented, but most references present cluttered nomographs as a design aid. A calculator program was written to enable easy computation of the resonator physical dimensions, and its characteristic impedance. The program also computes the required value of resonating capacitance, effective inductance, and unloaded Q at frequencies other than the self resonant frequency. A sample printout, and a plotted graph are shown in Table 5-1 and Figure 5-17.

The helical resonator is actually a shorted transmission line, and is self resonant at a frequency where its electrical length is close to a quarter wavelength.

Now, as the frequency is lowered, the impedance remains inductive, and varies as shown:

$$x = j\, Z\emptyset \tan \left[\frac{f}{fo} \cdot 84.6 \right]$$

Thus, as the frequency is lowered, the reactance changes. When this reactance is divided by the radians per second, it is seen that the actual "inductance" is not constant.

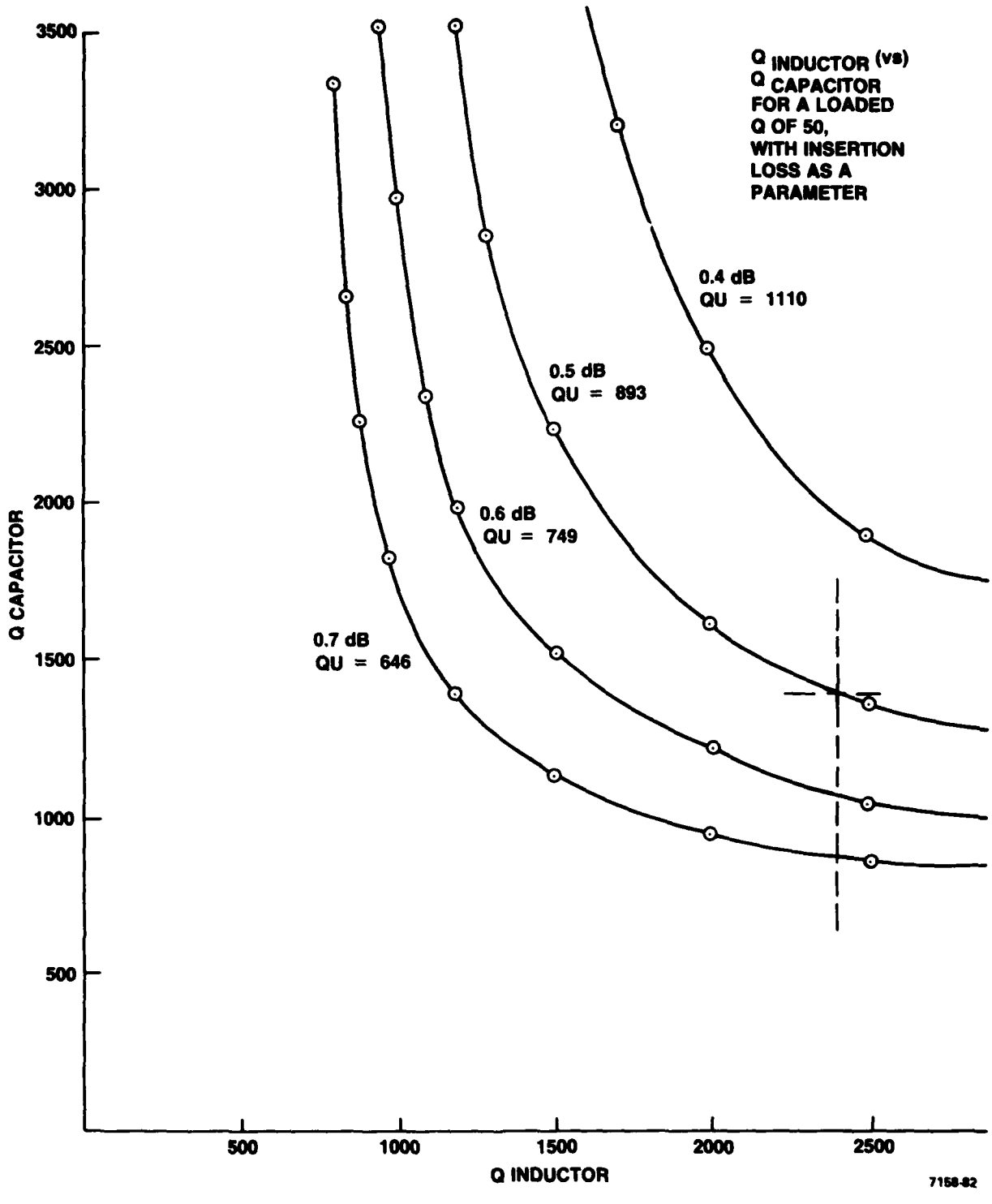

Figure 5-16. Q Inductor vs. Q Capacitor For a Loaded Q of 50, with Insertion Loss as Parameter

TABLE 5-1. HELICAL RESONATOR DESIGN

3500.	QU
94.	FMHZ
6.016623937	S,IN
2.829041133	N
144.1042827	Zo
3.970971798	D,IN
9.626598298	H,IN
50.	FMHZ
2.2088857 01	C,PF
4.5869818-01	L,UH
2.552637 03	QU
5.5 01	FMHZ
1.7150605 01	C,PF
4.8824233-01	L,UH
2.6772287 03	QU
6. 01	FMHZ
1.3373745 01	C,PF
5.261199-01	L,UH
2.7962741 03	QU
6.5 01	FMHZ
1.0412361 01	C,PF
5.757903-01	L,UH
2.9104544 03	QU
70.0	FMHZ
8.0391676 00	C,PF
6.4303276-01	L,UH
3.0203212 03	QU
7.5 01	FMHZ
6.0996694 00	C,PF
7.3826358-01	L,UH
3.1263295 03	QU
8. 01	FMHZ
4.4856904 00	C,PF
8.8232989-01	L,UH
3.2288592 03	QU
8.5 01	FMHZ
3.1194502 00	C,PF
1.1238914 00	L,UH
3.3282319 03	QU
8.8 01	FMHZ
2.3941334 00	C,PF
1.3662387 00	L,UH
3.3864561 03	QU

QU = RESONATOR UNLOADED Q
FMHZ = FREQUENCY IN MEGACYCLES
S = RESONATOR WIDTH AND DEPTH IN INCHES
N = NUMBER OF TURNS
Zo = RESONATOR CHARACTERISTIC IMPEDANCE IN OHMS
D,IN = DIAMETER OF HELIX, IN INCHES
H,IN = HEIGHT OF RESONATOR IN INCHES
C,PF = CAPACITANCE IN PICOFARADS
L,UH = INDUCTANCE IN MICROHENRIES

7159-82

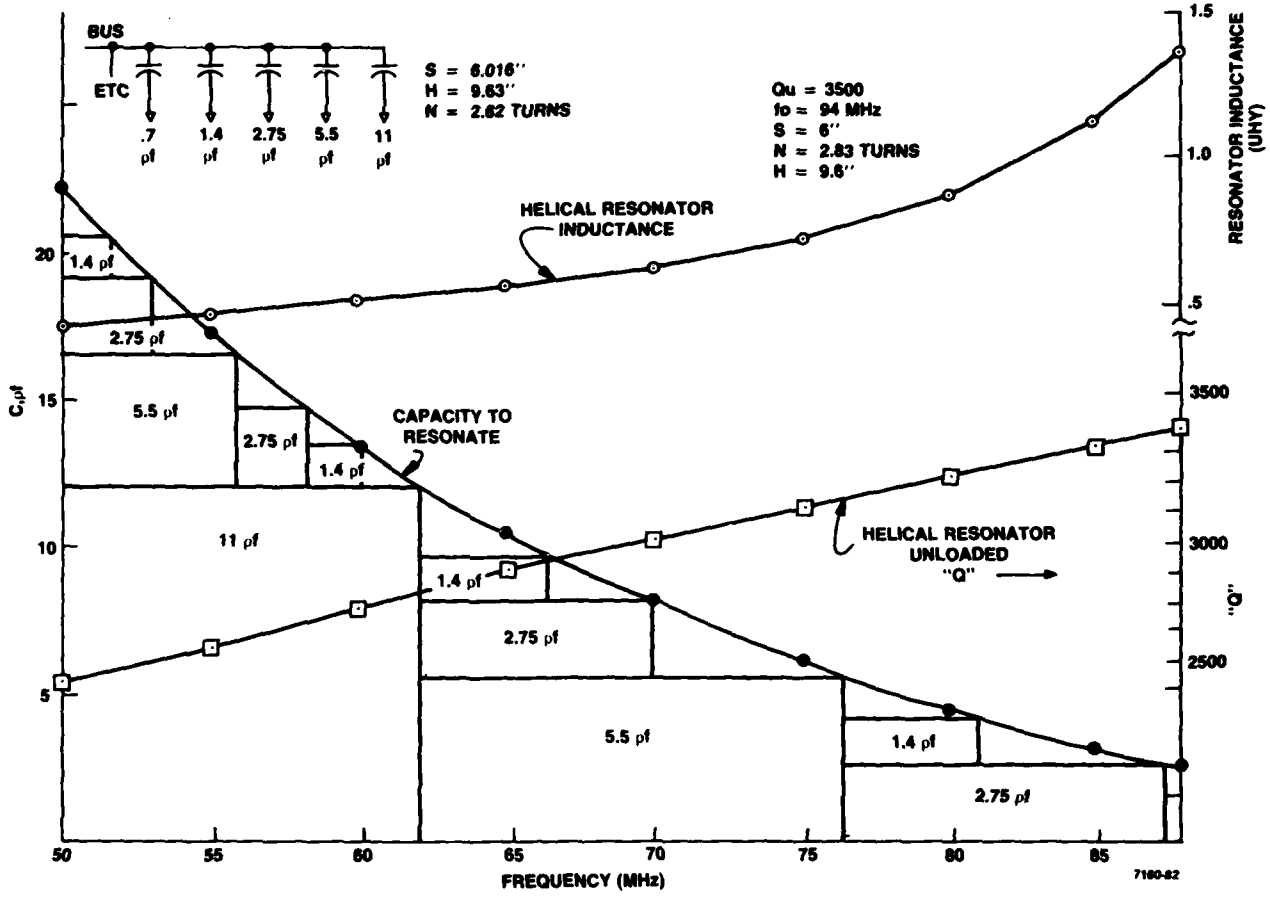

Figure 5-17. Resonator Design Aid High Band Resonator

Table 5-1 shows that a self resonant Q of 3500 is necessary to obtain a helical resonator Q of 2552 at 30 MHz. This is the basis for point A in Figure 5-16. Figure 5-17 also shows the frequency increments over which certain capacitive elements are active in the shunt binary capacitive bus.

The calculator printout shown in Table 5-1 begins with the selection of the resonator unloaded Q (3500) at the self resonant frequency (94 MHz). With this data, the program then calculates the resonator physical parameters such as width, height, and number of turns. It also calculates the resonator characteristic impedance. This is the design section of the program.

The analysis section computes the effective inductance and unloaded Q of the resonator at a given frequency, and the value of capacity needed to provide resonance at that frequency. The entry at 88 MHz shows that 2.39 pF is needed to provide resonance. Thus, the shunt capacitive bus cannot present more than 2.39 pF with all capacitors switched into the "off" state at 88 MHz. This is a key design parameter for the shunt capacitive bus.

5.9.2 Shunt Capacitance Binary Bus Discussion

The binary capacitance bus is the vehicle chosen to tune the helical resonator. This circuit possesses advantages characteristic of digital structures. It can be instantly tuned to a desired state without slewing. The use of solid state switching devices enables its use for fast frequency hopping applications. In this way, extreme frequency agility can be achieved because any reactance value is only removed by one configuration period from any other reactance value.

Previous work reported in the Third Quarterly Report is contained in Appendix F. This initial model was unsuccessful, but still useful in that the problem areas were quickly identified.

A simplified schematic of a shunt binary reactive bus is shown in Figure 5-18. The actual values of the capacitors are modeled in a binary manner, as shown.

A limiting factor in achieving a resonator unloaded Q of about 900 is the PIN Diode. Extensive computer modeling leads to the conclusion that some form of band splitting is necessary. Also, the "on/off" capacitance ratio is not nearly ideal for the smaller capacitors in the bus.

A preliminary PIN diode specification was prepared and sent out to 15 PIN diode vendors. A few vendors were optimistic regarding the achievement of this performance, however it is now realized that this specification was not rigorous enough.

A recent IEEE MTT Publication (May, 1979) "Microwave Semiconductor Control Devices" by Mr. R.V. Garver, states the following:

"A second area of interest is the speed and power limitations of P-I-N diode control devices. This art has progressed little in the last 10 years and remains short of the theoretical limit without explanation. The technology suffers with poor and conflicting definitions for switching speed, certain theoretical areas have been consistantly handled incorrectly, and no one has yet taken a good look at the experimental performance of the P-I-N diode junction in switching transition."

This respected author then describes a possible FET configuration which will in theory surpass the PIN Diode as an RF switching element. In general, he proposes a GaAs depletion mode FET. Such a device is not yet available, but the above article is at least a start.

The above reference spurred a literature search describing development of an FET RF switch. Nothing was found. The author of the reference, Mr. R.V. Garver, was contacted at the Harry Diamond Laboratory, and provided the following comments:

- There is insufficient dollar interest at this time to entice the semiconductor industry to build such an FET
- PIN Diodes, despite their failings, will continue to be the major RF switching element for approximately the next five years

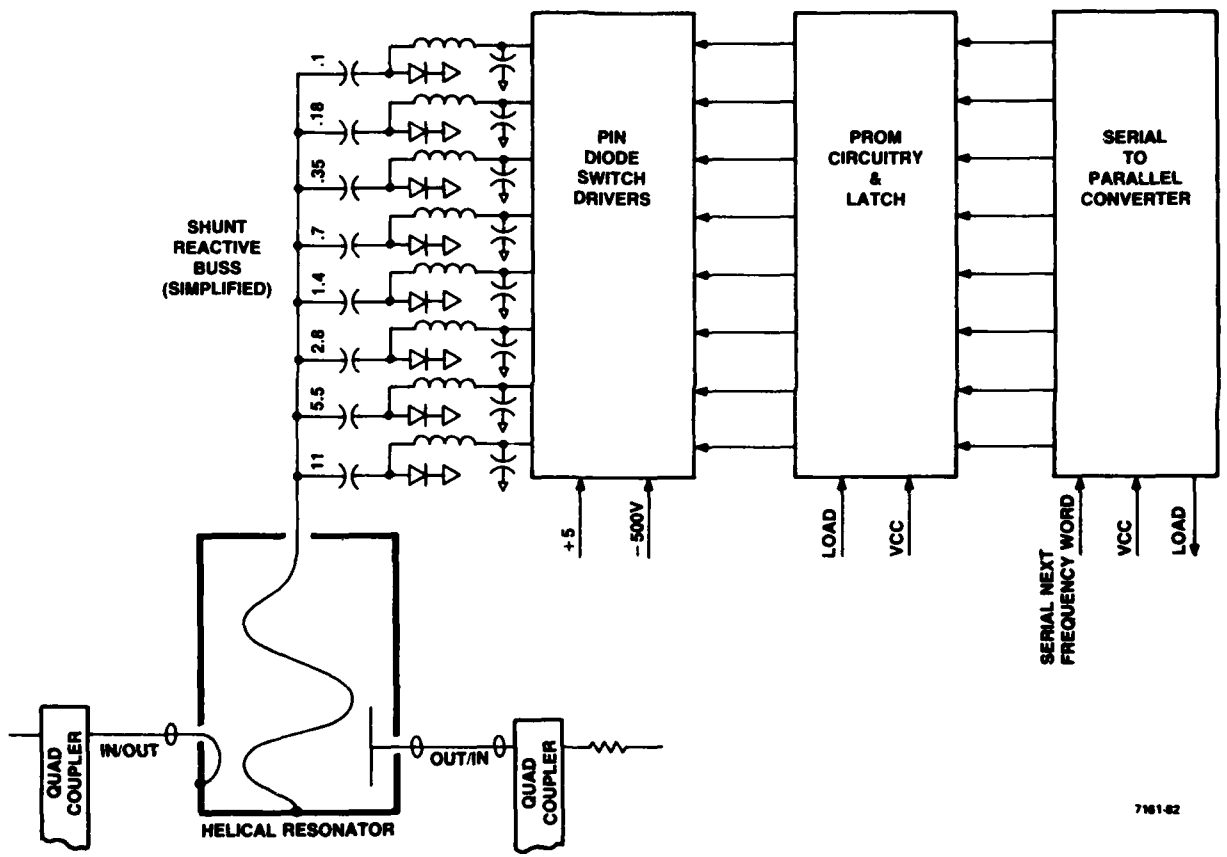

Figure 5-18. Frequency Hoppable Band Pass Filter

- Those who are using FET's select available devices and try them emperically in circuits
- In general, the all glass construction used in Unitrode PIN Diodes gives the highest off resistance available. An Rp of 1 Megohm, and Cp of 1-5 pF is achievable.

The main problem areas of the binary bus described in Appendix F are:

- The wide frequency range necessitated relatively large values of capacity in the bus. These large values were only switched in at the low end of the band (30-50 MHz). Thus at higher frequencies, the off impedance of the PIN Diode in series with these larger capacitor values, destroyed the Q of the resonator
- Tuning accuracy was impaired by the poor "on/off" ratio of the small capacitor elements
- At that time, a +/-2%, 40 dB bandwidth system was contemplated, thus a loaded Q of 113 was needed.

5.9.3 Resonator Design Decisions

It was decided to paper-design a bandpass filter with the following features:

- The frequency range is 50-88 MHz
- The helical resonator self resonant frequency (f_0) will be set at 105 MHz, thus enabling the bus to tune the resonator at 88 MHz. The bus described in Figure 5-17 has a minimum capacity of about 4.5 pF at 88 MHz, and a resonator with an f_0 of 105 Mhz will require 4.6 pF at 88 MHz.
- The three highest value capacitors will use two PIN Diodes in series to raise the Rp
- The diode parameters are assumed to be: Rp = 1 MEG, Cp = 2 pF, and Rs = 0.1 ohms.

Table 5-2 shows the basic design and analysis of the resonator described above. The design procedure and parameter nomenclature are the same as shown in Table 5-1.

A schematic diagram of the resonator design given in Table 5-2, and the required shunt capacitive bus is shown in Figure 5-19. Note that each of the three branches with the highest value of capacity (3, 4, and 12 pF) have two PIN Diodes in series to increase the "off" impedance.

A rigorous analysis of Figure 5-19 was performed at three frequencies. These frequencies, and associated parameters are given in Table 5-2. Case one is at 53 MHz, case two at 70 MHz, and case three is at 87 MHz.

A brief description of the calculator program used for this analysis is given in Figure 5-20, along with an explanation of the abbreviations.

Figure 5-19 shows a total of eight branches in the shunt capacitive bus. For accurate tuning, the correct PIN Diode switching arrangement must be known for every desired frequency. As noted, the circuit of Figure 5-19 is to be analysed at three frequencies. As a first step each branch of the bus must be analyzed in both PIN Diode states. The diode parameters associated with these states are shown in Figure 5-19. Upon completion of this diode "on/off' analysis, the diode switching arrangement can be determined by simply summing the branch capacitors to obtain the correct value of total bus capacity. These values are obtained from Table 5-2.

The "on/off' analysis for 53, 70, and 87 MHz is shown in Tables 5-3, 5-4, and 5-5. These figures serve as a "shopping list" of capacitive values to structure the bus.

The actual filter analysis is shown in Table 5-6, 5-7, and 5-8. The diode states for each branch are shown in the figures. The printout shows the Q of each branch: hence problem situations can be easily recognized.

TABLE 5-2. HELICAL RESONATOR DESIGN AND ANALYSIS

DESIGN DATA		MHZ	ANALYSIS DATA	
3500.	QU	70	1.1079101 01	C,PF
105.	FMHZ		4.6659456 01	C,PF
5.692750426	S,IN		4.6659456-01	L,UH
2.676754486	N		2.857738 03	QU
136.3471816	ZO			
3.757215281	D,IN	65	1.3843877 01	C,PF
9.108400681	H,IN		4.3306771-01	L,UH
			2.7537853 03	QU
MHZ ANALYSIS DATA				
		60	1.7307346 01	C,PF
88 4.5925085 00	C,PF		4.0654374-01	L,UH
7.1223768-01	L,UH		2.6457513 03	QU
3.204164 03	QU			
		55	2.1737396 01	C,PF
87 4.857635 00	C,PF		3.852187-01	L,UH
6.8898282-01	L,UH		2.533114 03	QU
3.1859065 03	QU			
		54	2.2771943 01	C,PF
86 5.1311259 00	C,PF		3.814632-01	L,UH
6.6746836-01	L,UH		2.0599801 03	QU
3.1675437	QU			
		53	2.3864897 01	C,PF
85 5.413399 00	C,PF		3.778583-01	L,UH
6.4763808-01	L,UH		2.4866309 03	QU
3.1490739 03	QU			
		52	2.502081 01	C,PF
80 6.9729345 00	C,PF		3.7439687-01	L,UH
5.6760303-01	L,UH		2.4630604 03	QU
3.0550505 03	QU			
		51	2.6244687 01	C,PF
75 8.8311464 00	C,PF		3.7107228-01	L,UH
5.0991837-01	L,UH		2.4392622 03	QU
2.9580399 03	QU			
		50	2.7542037 01	C,PF
			3.6787833-01	L,UH
			2.4152295 03	QU

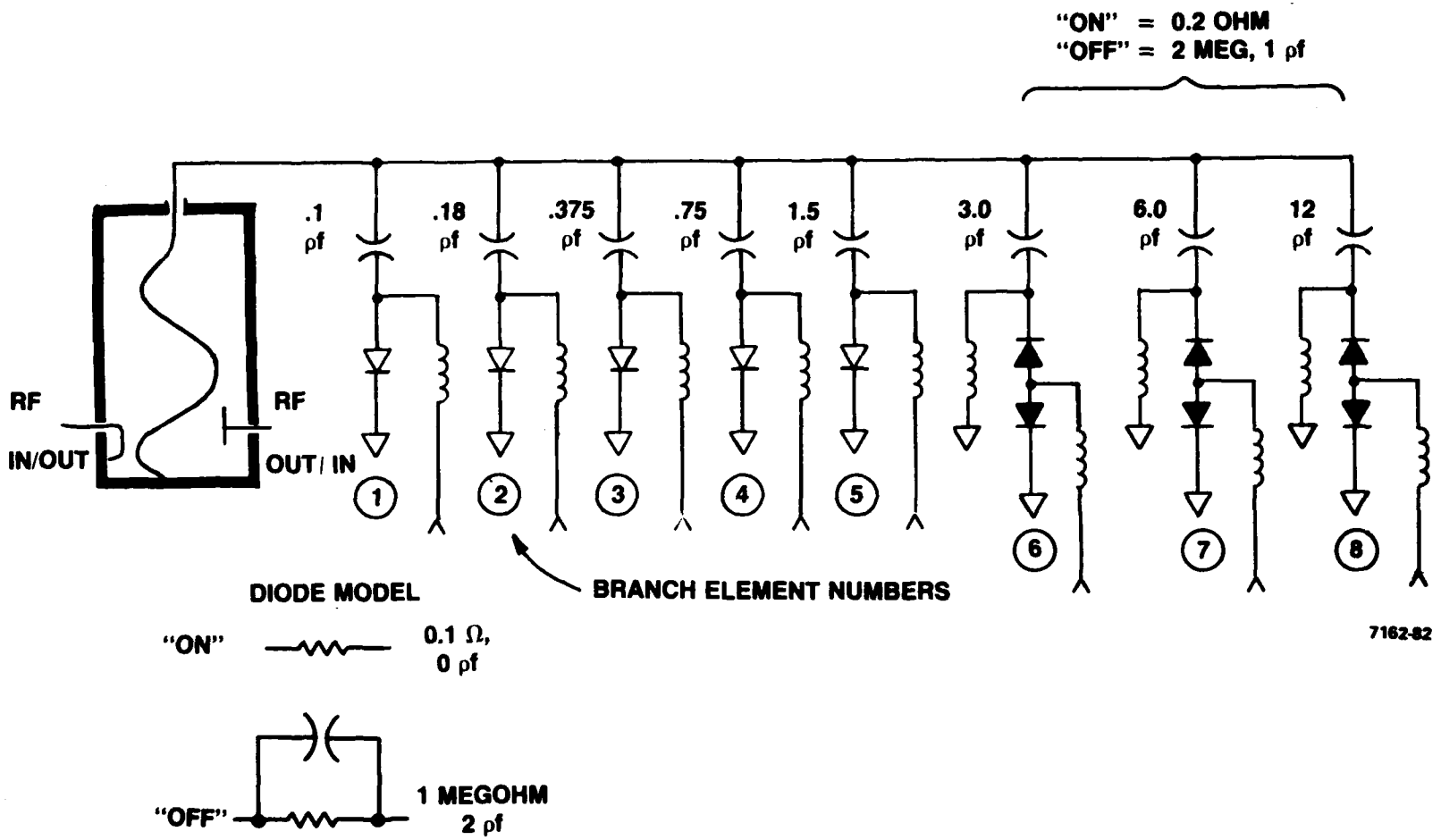

Figure 5-19. Schematic, 50-88 MHz Frequency Hoppable Band Pass Filter

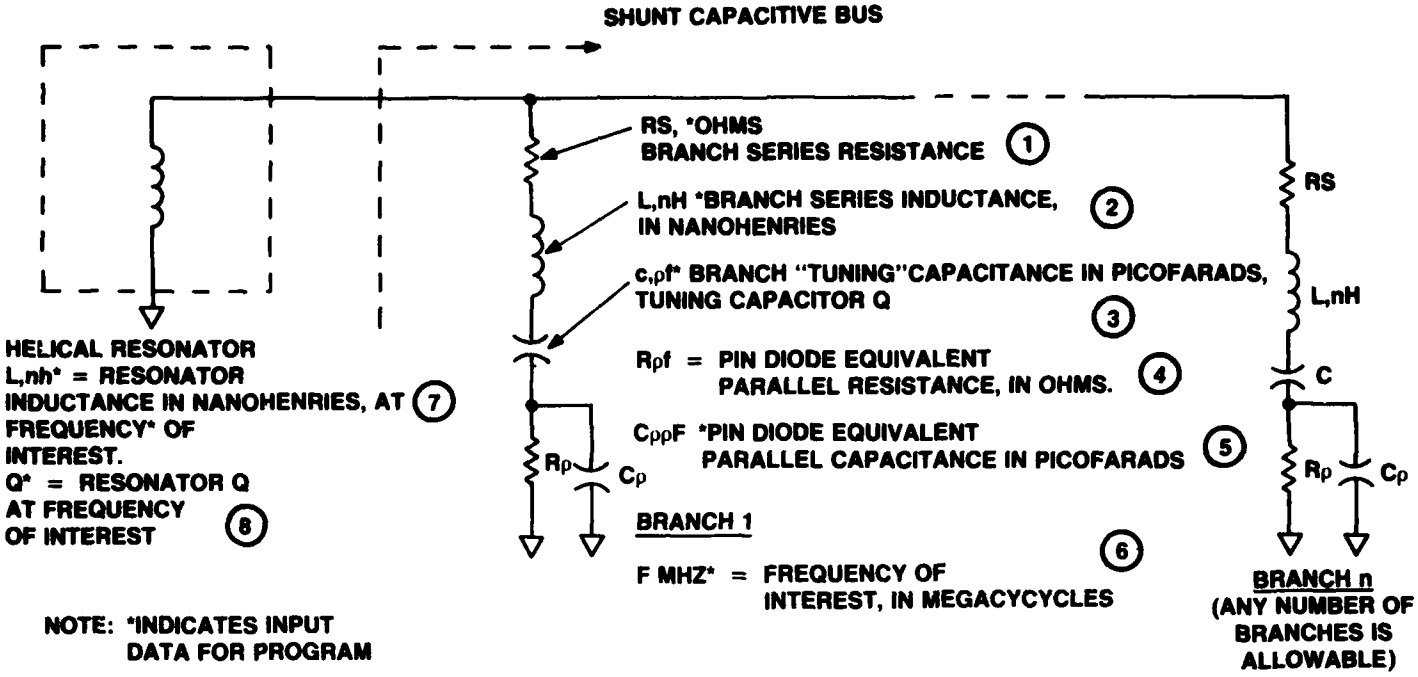

NOTE: *INDICATES INPUT DATA FOR PROGRAM

TO RUN PROGRAM:

- INPUT ITEMS (1) THROUGH (6).
- PROGRAM WILL CALCULATE BRANCH ADMITTANCE AND STORE IT. PROGRAM WILL PRINT EQUIVALENT CAPACITY AND Q OF THE BRANCH.
- INPUT DATA FOR AS MANY BRANCHES AS NEEDED. PROGRAM WILL SUM ALL ADMITTANCES AND WILL PRINT CAPACITANCE AND Q OF EACH BRANCH.
- PROGRAM WILL CALCULATE AND PRINT TOTAL BUS CAPACITANCE AND Q.
- INPUT ITEMS (7) AND (8).
- PROGRAM WILL CALCULATE AND PRINT ACTUAL RESONANT FREQUENCY IN MEGACYCLES, AND Q OF ENTIRE CIRCUIT.

7163-82

Figure 5-20. Explanation of Calculator Program

TABLE 5-3. ON/OFF VALUES AT 53 MHz

DIODE STATE	BRANCH ANALYSIS		DIODE STATE	BRANCH ANALYSIS	
	0.	RS		0. 00	RS
	0.075	L,NH		7.5-02	
	1.-01	C,PF		1.-01	C,PF
	3.5 03	Q	OFF	3.5 03	Q
ON	1.-01	RP		1. 06	RP
	0. 00	CPPF		2. 00	CPPF
	5.3 01	FHMZ		53.	FHMZ
	1.0000008-01	C,PF		9.5240447-02	C,PF
	3.4596735 03	Q		2.9108361 03	Q
	1.-01	C,PF		1.8-01	C,PF
ON	3.5 03	Q		3.5 03	Q
	1.8000027-01	C,PF	OFF	1. 06	RP
	3.4280753 03	Q		2. 00	CPPF
				1.6514469-01	C,PF
	3.75-01	C,PF		2.5907442 03	Q
	3.5 03	Q			
ON	3.7500117-01	C,PF		3.75-01	C,PF
	3.3534198 03	Q		3.5 03	Q
				1. 06	RP
	7.5-01	C,PF		2. 00	CPPF
ON	3.5 03	Q		3.1581534-01	C,PF
	7.5000468-01	C,PF		2.0943458 03	Q
	3.2186228 03	Q			
				7.5-01	C,PF
	1.5 00	C,PF		3.5 03	Q
	3.5 03	Q	OFF	1. 06	RP
ON	1.5000187 00	C,PF		2. 00	CPPF
	2.9791182 03	Q		5.4553171-01	C,PF
				1.6208534 03	Q
	3. 00	C,PF			
	3.5 03	Q		1.5 00	C,PF
ON	2.-01	RP		3.5 03	Q
	0. 00	CPPF	OFF	1. 06	RP
	3.0000749 00	C,PF		2. 00	CPPF
	2.0595978 03	Q		8.5733342-01	C,PF
				1.2402583 03	Q
	6. 00	C,PF			
	3.5 03	Q		3. 00	C,PF
ON	2.-01	RP		3.5 03	Q
	0. 00	CPPF		2. 06	RP
	6.0002994 00	C,PF	OFF	1. 00	CPPF
	1.4590892 03	Q		7.50056831-01	C,PF
				8.3599512 02	Q
	1.2 01	C,PF			
	3.5 03	Q		6. 00	C,PF
ON	2.-01	RP	OFF	3.5 03	Q
	0. 00	CPPF		2. 06	RP
	1.2001198 01	C,PF		1. 00	CPPF
	9.2162182 02	Q		8.5788522-01	C,PF
				7.5394409 02	Q
TOTAL CAPACITY PF					
	2.3906595 01	C,PF		1.2 01	C,PF
	1.2246866 03	Q	OFF	3.5 03	Q
				2. 06	RP
				1. 00	CPPF
				9.2393795-01	C,PF
				7.1099355 02	Q
			TOTAL CAPACITY PF	4.5114565 00	C,PF
			Q OF BUS	9.7856866 02	Q

94-83

TABLE 5-4. ON/OFF VALUES AT 70 MHZ

DIODE STATE	BRANCH ANALYSIS		DIODE STATE	BRANCH ANALYSIS	
	0.	RS		0. 00	
	0.075	L,NH		7.5 02	L,NH
	1.-01	C,PF		1.-01	C,PF
	3.5 03	Q		3.5 03	Q
ON	1. 01	RP	OFF	1. 06	RP
	0. 00	CPPF		2. 00	CPPF
	7. 01	FMHZ		7. 01	FMHZ
	1.0000015-01	C,PF		9.5240499-02	C,PF
	3.4463335 03	Q		3.0656298 03	Q
	1.8-01	C,PF		1.8-01	C,PF
	3.5 03	Q		3.5 03	Q
ON	1.8000047-01	C,PF		1. 06	RP
	3.4056249 03	Q	OFF	2. 00	CPPF
				1.6514484-01	C,PF
	3.75-01	C,PF		2.8096927 03	Q
ON	3.5 03	Q			
	3.7500204-01	C,PF		3.75-01	C,PF
	3.3089651 03	Q		3.5 03	Q
			OFF	1. 06	RP
	7.5-01	C,PF		2. 00	CPPF
	3.5 03	Q		3.1581591-01	C,PF
ON	7.5000816-01	C,PF		2.3812069 03	Q
	3.137703 03	Q			
				7.5-01	C,PF
	1.5 00	C,PF		3.5 03	Q
	3.5 03	Q	OFF	1. 06	RP
ON	1.5000326 00	C,PF		2. 00	CPPF
	2.8433697 03	Q		5.4553341-01	C,PF
				1.9319978 03	Q
	3. 00	C,PF			
	3.5 03	Q		1.5 00	C,PF
ON	2.-01	RP		3.5 03	Q
	0. 00	CPPF	OFF	1. 06	RP
	3.0001306 00	C,PF		2. 00	CPPF
	1.8193992 03	Q		8.5733762-01	C,PF
				1.5381432 03	Q
	6.00	C,PF			
	3.5 03	Q		3. 00	C,PF
ON	2.-01	RP		3.5 03	Q
	0. 00	CPPF		2. 06	RP
	6.0005223 00	C,PF	OFF	1. 00	CPPF
	1.2291465 03	Q		7.5052126-01	C,PF
				1.083373 03	Q
	1.2 01	C,PF			
	3.5 03	Q		6.00 00	C,PF
ON	2.-01	RP		3.5 03	Q
	0. 00	CPPF	OFF	2. 06	RP
	1.200209 01	C,PF		1. 00	CPPF
	7.4542145 02	Q		8.5788907-01	C,PF
				9.8602864 02	Q
TOTAL CAPACITY PF	2.3907782 01	C,PF		1.2 01	C,PF
				3.5 03	Q
			OFF	2. 06	RP
BUS Q	1.0133131 09	Q		1. 00	CPPF
				9.2394241-01	C,PF
				9.3435513 02	Q
			TOTAL CAPACITY PF	4.5114747 00	C,PF
			BUS Q	1.2483555 03	Q

92-83

TABLE 5-5. ON/OFF VALUES AT 87 MHz

DIODE STATE	BRANCH ANALYSIS		DIODE STATE	BRANCH ANALYSIS	
	0.			6.2575358 02	Q
	0.057				
	1.-01	C,PF		0. 00	RS
ON	3.5 03	Q		7.5-02	L,NH
	1.-01	RP		1.-01	C,PH
	0. 00	CPPF	OFF	3.5 03	Q
	8.7 01	FMHZ		1. 06	RP
	1.00000022-01	C,PF		2.	CPPF
	3.4342864 03	Q		8.7 01	
				9.5240569-02	C,PF
	1.8-01	C,PF		3.1682682 03	Q
ON	3.5 03	Q			
	1.8000073-01	C,PF		1.8-01	C,PF
	3.3834656 03	Q		3.5 03	Q
				1. 06	RP
	3.75-01	C,PF	OFF	2. 00	CPPF
	3.5 03	Q		1.6514505-01	C,PF
ON	3.7500315-01	C,PF		2.9621976 03	Q
	3.2656713 03	Q			
				3.75-01	C,PF
	7.5-01	C,PF		3.5 03	Q
	3.5 03	Q		1. 06	RP
ON	7.5001261-01	C,PF	OFF	2. 00	CPFF
	3.0607476 03	Q		3.1581667-01	C,PF
				2.5979833 03	Q
	1.5 00	C,PF			
ON	3.5 03	Q		7.5-01	C,PF
	1.5000504 00	C,PF		3.5 03	Q
	2.7194441 03	Q	OFF	1. 06	RP
				2. 00	CPPF
	3.00	C,PF		5.4553569-01	C,PF
	3.5 03	Q		2.1878493 03	Q
ON	2.-01	RP			
	2. 00	CPFF		1.5 00	C,PF
	3.0002015 00	C,RF		3.5 03	Q
	1.6293604 03	Q		1. 06	RP
			OFF	2. 00	CPPF
	6.00	C,PF		8.573432e-01	C,PF
	3.5 03	Q		1.8017685 03	Q
ON	0.2	RP			
	0.	CPPF		3. 00	C,PF
	6.0008069 00	C,PF		3.5 03	Q
	1.0617904 03	Q	OFF	2. 06	
				1. 00	CPPF
	1.2 01	C,PF		7.5057545-01	C,PF
ON	3.5 03	Q		1.3216136 03	Q
	2.-01	RP			
	0. 00	CPPF		6. 00	C,PF
	1.2003228 01	C,PF		3.5 03	Q
			OFF	2. 06	RP
				1. 00	CPPF
				8.5789455-01	C,PF
				1.2136122 03	Q
TOTAL CAPACITY PF				1.2 01	C,PF
	2.3909298 01	C,PF		3.5 03	Q
			OFF	2. 06	RP
				1. 00	CPPF
Q OF BUS	8.6412665 02	Q		9.2394877-01	C,PF
				1.1554934 03	Q
		TOTAL CAPACITY PF		4.5114999 00	C,PF
		Q OF BUS		1.5003391 03	Q

95-83

TABLE 5-6. FILTER ANALYSIS AT 53 MHz

BRANCH	DIODE	BRANCH ANALYSIS	FREQUENCY ERROR ANALYSIS
		00 .0 RS	Single Resonator
		7.5-02 L,NH	Desired Fo = 53.000 MHz
		1.-01 C,PF	
		3.5 03 Q	1. N
1	OFF	1. 06 RP	50. Q1
		2. 00 CPPF	52.958924 N
		5.3 01 FMHZ	53. F
		9.5240447-02 C,PF	-.0260482907 Q1
		2.9108361 03 Q	
			-.026dB Loss Per Resonator
		1.8-01 C,PF	Due to Frequency Error
		3.5 03 Q	
2	ON	1.-01 RP	
		0. 00 CPPF	
		1.8000027-01 C,PF	Loss Analysis Based on
	3.4280753 03	Q Ratio of	Unloaded To Loaded Q.
		3.75-01 C,PF	
		3.5 03 Q	$\frac{QU}{QL} = \frac{820}{50} = 16.4$
3	ON	1.-01 RP	
		0. 00 CPPF	
		3.7500117-01 C,PF	dB = 20 Log $\frac{QU/QL}{QU/QL-1}$ + Tuning Loss
		3.3534198 03 Q	
		7.5-01 C,PF	= 20 Log $\frac{16.4}{16.4-1}$ + .026
		3.5 03 Q	
4	ON	1.-01 RP	
		0. 00 CPPF	= 0.55 + .026
		7.5000468-01 C,PF	
		2.21862228 03 Q	= 0.576 dB Per Filter
		1.5 00 C,PF	
		3.5 03 Q	
5	ON	1.-01 RP	
		0. 00 CPPF	
		1.5000187 00 C,PF	
		2.9791182 03 Q	
		3. 00 C,PF	
		3.5 03 Q	
6	ON	2.-01 RP	
		0. 00 CPPF	
		3.0000749 00 C,PF	
		2.0595978 03 Q	
		6. 00 C,PF	
		3.5 03 Q	
7	ON	2.-01 RP	
		0. 00 CPPF	
		6.0002994 00 C,PF	
		1.4590892 03 Q	
		1.2 01 C,PF	
		3.5 03 Q	
		2.-01 RP	
		0. 00 CPPF	
		1.2001198 01 C,PF	
		9.21162182 02 Q	
TOTAL CAPACITY, PF		2.3901835 01 C,PF	
BUS Q		1.2242036 03 Q	
RESONATOR INDUCTANCE (nH), AND Q AT 53 MHz		3.7786 02 L,NH 2.487 03 Q	
ACTUAL FILTER RESONANT FREQUENCY AND UNLOADED Q.		5.2958924 01 FMHZ 8.2037922 02 Q	

93-83

TABLE 5-7. FILTER ANALYSIS AT 70 MHz

BRANCH NUMBER	DIODE STATE	BRANCH ANALYSIS	FREQUENCY ERROR ANALYSIS
		0. RS	SINGLE RESONATOR,
		0.075 L,NH	DESIRED FO =
		1.-01 C,PF	70.000 MHz
		3.5 03 Q	
1	ON	1.-01 RP	1. N
		0. 00 CPPF	50. Q1
		7. 01 FMHZ	71.631853 FC
		1.0000015-01 C,PF	70. F
		3.4469335 03 Q	-7.916758412 DB
		1.8-01 C,PF	-7.92 dB LOSS PER RESONATOR
		3.5 03 Q	DUE TO FREQUENCY ERROR.
2	ON	1.-01 RP	(CORRECTABLE)
		0. 00 CPPF	
		1.8000047-01 C,PF	
		3.4056249 03 Q	LOSS ANALYSIS BASED ON
			RATIO OF UNLOADED TO LOADED
		3.75-01 C,PF	Q.
		3.5 03 Q	
3	ON	1.-01 RP	$\frac{QU}{QL} = \frac{942}{50} = 18.84$
		0. 00 CPPF	
		3.7500204-01 C,PF	
		7.3089651 03 Q	$dB = 20 \text{ Log } \frac{QU/QL}{QU/QL-1}$ + TUNING LOSS
		7.5-01 C,PF	
		3.5 03 Q	$= 20 \text{ LOG } \frac{18.84}{18.84 - 1} + 7.92$
		1.-01 RP	
4	ON	0. 00 CPPF	
		7.5000816-01 C,PF	= 0.473 = 7.92
		3.137703 03 Q	
			dB = 8.39 dB PER FILTER
		1.5 00 C,PF	
		3.5 03 Q	
		1.-01 RP	COMMENT: THE 7.92 dB
5	ON	0. 00 CPPF	TUNING LOSS IS CORRECTABLE
		1.5000326 00 C,PF	
		2.8433697 03 Q	
		3. 00 C,PF	
		3.5 03 Q	
		2. 06 RP	
6	OFF	1. 00 CPPF	
		7.5057126-01 C,PF	
		1.083373 03 Q	
		6. 00 C,PF	
		3.5 03 Q	
		2.-01 RP	
7	ON	0. 00 CPPF	
		6.0005223 00 C,PF	
		11.2291465 03 Q	
		1.2 01 C,PF	
		3.5 03 Q	
8	OFF	2. 06	
		1. 00 CPPF	
		9.2394241-01 C,PF	
		9.3435513 02 Q	
TOTAL CAPACITY PF		1.0580079 01 C,PF	
BUS Q		1.4059336 03 Q	
RESONATOR INDUCTANCE (nH), AND Q AT 70MHz		4.66594 01 L,NH 2.858 03 Q	
ACTUAL FILTER RESONANT FREQUENCY		7.1631853 01 FMHZ	
UNLOADED Q		9.4235946 02 Q	

90-83

TABLE 5-8. FILTER ANALYSIS AT 87 MHz

BRANCH NUMBER	DIODE STATE	BRANCH ANALYSIS		FREQUENCY ERROR ANALYSIS
		0. 00	RS	Single Resonator,
		7.5-02	L,NH	Desired Fo = 87,000 MHz
		1.-01	C,PF	
		3.5 03	Q	1. N
1	ON	1.-01	RP	50. Q1
		0. 00	CPPF	87.568593 FC
		8.7 01	FMHZ	87.
		1.0000022-01	C,PF	-1.527790969 DB
		3.4342864 03	Q	
				-1.53 dB Loss Per Resonator
		1.8-01	C,PF	Due to Frequency Error
2	ON	3.5 03	Q	(Correctable)
		1.-01	RP	
		0. 00	CPPF	
		1.8000073-01	C,PF	LOSS ANALYSIS BASED ON
	3.3834656 03		Q RATIO	UNLOADED TO LOADED Q.
		3.75 01	C,PF	$\frac{QU}{QL} = \frac{1066}{50} = 21.32$
		3.5 03	Q	
3	ON	1.-01	RP	
		0. 00	CPPF	$dB = 20 \text{ Log } \frac{QU/QL}{QU/QL-1} + \text{Tuning}$
		3.7500315-01	C,PF	
		3.2656713 03	Q	
				$dB = 20 \text{ Log } \frac{21.32}{21.32} + 1.53$
		7.5-01	C,PF	
		3.5 03	Q	
		1.-01	RP	dB = .417 + 1.53
4	ON	0. 00	CPPF	
		7.5001261-01	C,PF	= 1.94 dB Per Filter
		3.0607476 03	Q	
		1.5 00	C,PF	Comment: The 1.53 dB Tuning
		3.5 03	Q	Loss is Correctable.
		1. 06	RP	
5	OFF	2. 00	CPPF	
		8.5734326-01	C,PF	
		1.8017685 03	Q	
		3. 00	C,PF	
		3.5 03	Q	
6	OFF	2. 06	RP	
		1. 00	CPPF	
		7.5057545-01	C,PF	
		1.3216136 03	Q	
		6. 00	C,PF	
		3.5 03	Q	
7	OFF	2. 06	RP	
		1. 00	CPPF	
		8.5789455-01	C,PF	
		1.2136122 03	Q	
		1.2 01	C,PF	
		3.5 03	Q	
8	OFF	2. 06	RP	
		1. 00	CPPF	
		9.2394877-01	C,PF	
		1.1554934 03	Q	
TOTAL CAPACITY PF		4.7947785 00	C,PF	
BUS Q		1.602288 03	Q	
RESONATOR INDUCTANCE (nHY), and Q at 87 MHz		6.8893 02	L,NH	
		3.186 03	Q	
Actual Filter Resonant Frequency, and Unloaded Q		8.7568593 01	FMHZ	
		1.06612 03	Q	

91-83

5.9.4 Results And Conclusions

- The band splitting technique, and the circuit modeling described above result in a workable resonator as far as the Q is concerned. Only three frequencies were analyzed, but in general, the Q can be expected to vary from 800 to 1000, resulting in acceptable insertion losses
- An accuracy problem exists, and is apparent in Table 5-7, where the filter is detuned by 163 KHz, and the insertion loss is -8.4 dB. This is correctable by adding additional sections to the bus. These extra sections will have small capacitors, to enable better resolution, and will not significantly lower the Q, because the values of capacity are small. Accuracy will probably emerge as the main implementation problem of the FHMUX
- The development of a PIN Diode with the low "on" and high "off impedances may or may not be compatible with the FHMUX distortion requirement. Some PIN Diode distortion reduction techniques are:
  - The PIN Diode should have a wide I region, and a long carrier lifetime
  - The diode should be forward biased to as high a current, and reverse biased at the highest voltage as possible.

Distortion produced in the PIN Diode circuit can be reduced further by adding another PIN Diode in series with the first. This increases the effective I region of the diode. In addition, the diodes are connected in a back to back orientation which causes an additional decrease in distortion due to cancellation of the distortion currents. An updated PIN Diode specification is shown in Table 5-9.

- A funded PIN Diode program will probably be needed, preferably during development of the Advanced Engineering Model.

TABLE 5-9. PIN DIODE SPECIFICATION

. Frequency	30-88 MHz
. Input RF Power	100 Watts, C.W.*
. Temperature	-55 to +85 (Est.)
. IMD Products	-120 dBc Max.
. Harmonic Distortion	-120 dBc Max.
. Size	N/A
. Forward Current	200 ma
. Reverse Voltage	100
. Parallel Resistance	1 M
. Power Dissipation	TBD
. Series Resistance	0.1 ohms Max.
. Diode Capacitance	2 pf
. Effective Minority Carrier Lifetime	TDB
. Switching Speed	10-20 Microseconds
. "Hot" Switching is not Required.	

* .16 Duty Cycle for High Power RF, Foward Bias May Have 1.0 Duty Cycle.

5.10 PACKAGING CONCEPT

5.10.1 Mechanical Concept

The use of quad-coupled filters, and the combining scheme described, makes possible a true-building block approach for the FHMUX.

Each building block bandpass filter (BPF) is composed of two quadrature couplers, two identical tuneable resonators, terminating resistors, and a set of PROMS and PIN Diode drivers. The system is easily expandable to almost any desired number of channels. Complicated matching networks are not required to combine channels, and all Rf impedances are 50 ohms.

The tuning of each BPF is accomplished by a shunt capacitive bus, where the various capacitive values are weighted in a binary manner. Each capacitive element will be switched in or out of the bus with a PIN Diode. The high degree of capacitive resolution required, and tolerance variations of all of the components require some means of calibration. Also, it is necessary that each BPF present identical impedances to the quadrature couplers. This difficulty is overcome by individually programming the capacitive bus of each BPF with a PROM. Thus each BPF will have its component variations calibrated out at each frequency, and thus present an identical impedance to the quad coupler.

A preliminary sketch of the quad coupled BPF assembly is shown in Figure 5-21. The quad couplers are presently available from Merrimac, namely the QHF-3-.060G, which is 5 " X 5 " X .215" in size.

An estimated volumetric breakdown of the BPF is given.

	Cu. in. each	Extension
Resonators (2)	360	720
Coupler Assy's (2)	144	288
Prom Assy (2)	72	144
Cap. Buss (2)	72	144
		1296 in^3

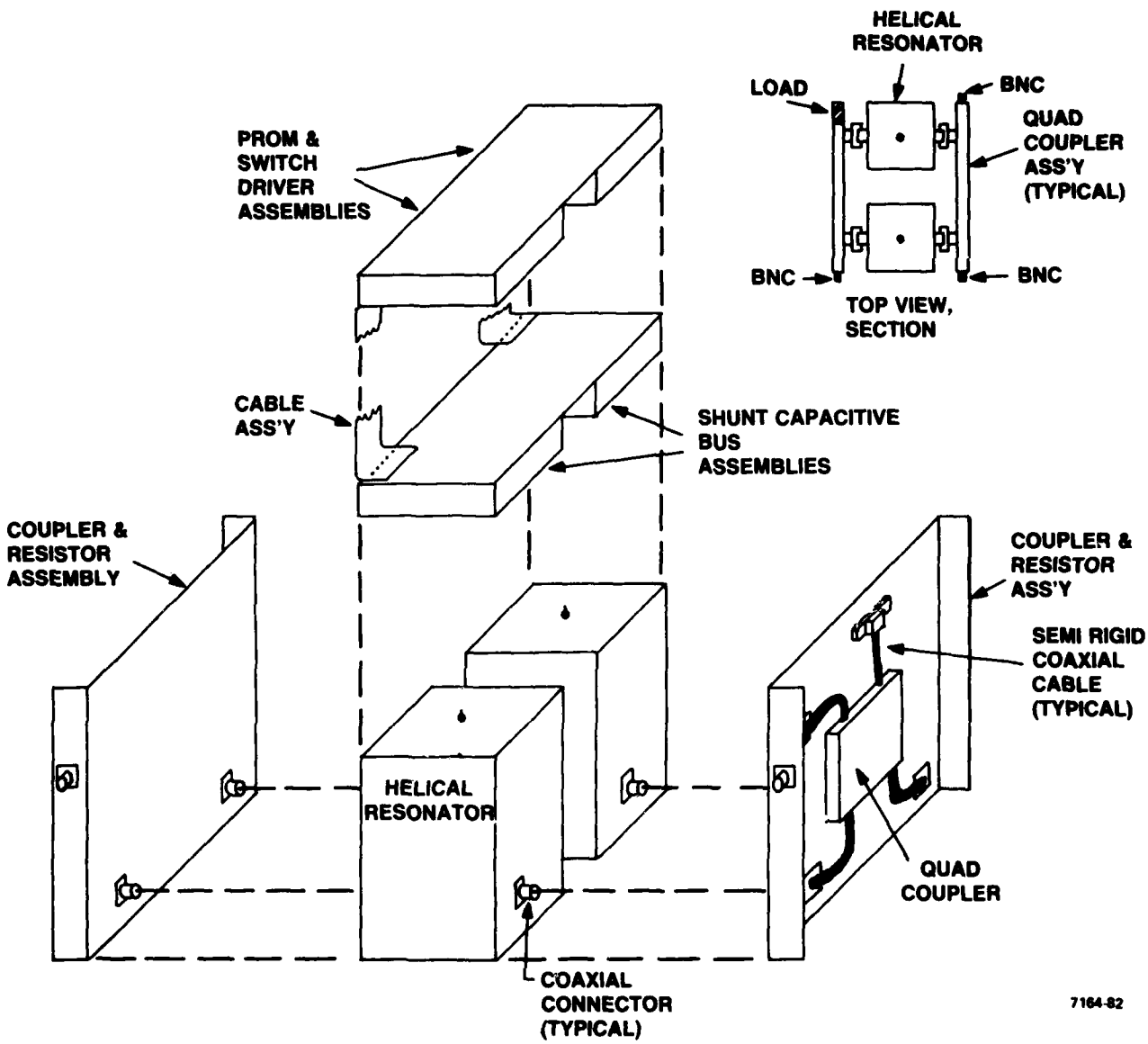

Figure 5-21. Preliminary Mechanical Concept

The volume required for one quad-coupled BPF is 1296 cubic inches, or, 0.75 cubic feet.

A five-channel FHMUX, with band splitting will require 30 BPF assemblies, and use 22.5 cubic feet.

Also required are:

Microprocessor Assy's	1 cubic foot, est.
Power Supply Ass'y	2 cubic feet, est.

Thus a first cut size estimate for a five channel FHMUX is about 26 cubic feet, or a box about 3 ft X 3 ft X 3 ft.

5.10.2 Power Consumption

The PIN Diodes will require a large amount of dc power. The preliminary PIN Diode spec called for an Rs of 0.1 ohms at about 200 ma. It may be necessary to raise the current even higher to obtain this low Rs. However, an Rs of 0.1 ohms is not really needed for all elements of the bus. The smaller value elements can tolerate a higher Rs and still maintain a respectable Q.

An estimated current budget for an individual bus is given in Table 5-10. These currents will probably be derived from a high efficiency switching regulator which delivers a nominal 5.0 volts for the logic and the PIN Diode switch drivers.

TABLE 5-10. POWER CONSUMPTION

Capacitive Element (pF)	Tolerable RS at 88 MHz	Estimated Forward Current (ma)
0.1	2.5	5
0.18	1.5	10
0.375	1.0	20
0.75	.50	50
1.5	.25	100
3	.1	400
6	.1	400
12	.1	700
		1685

It is unlikely that at any given time, all diodes in a bus are "on." An estimated average value might be 800 ma. Thus each quad coupled filter assembly would draw an estimated 1600 ma of current from a 5 volt regulator.

A five channel FHMUX with band switched resonators will have 30 BPF assemblies. However, only 20 of these have to be powered up at any one time. Thus, the average 5 volt current needed is:

$$\begin{aligned} I_{avg} &= 20 \times 1.6 \\ &= 32 \text{ amperes} \end{aligned}$$

It is estimated that the logic assembly will require about 4 amperes. If the 5 volt switching regulator is 75% efficient, then the required dc input power is:

$$\begin{aligned} P_{dc} &= \frac{(32 + 4) \times 5}{.75} \\ &= 240 \text{ watts, average} \end{aligned}$$

A high voltage bias supply is also required, but current drain will be minimized. This supply is estimated to be 500 volts dc, at a current of about 0.50 amperes, and is operating at 65% efficiency.

The dc input power for this supply is:

$$\begin{aligned} P &= \frac{500 \times .05}{.65} \\ &= 38.5 \text{ watts average} \end{aligned}$$

Thus the average power drain of the FHMUX is about 280 watts of dc power.

SECTION 6

CONCLUSIONS AND RECOMMENDATIONS

6.1 COMMENT

- The systems study has shown that an acceptable BER is obtained with a +/-5% guard band, for a five channel FHMUX
- This guard band is compatible with a +/-5%, -40 dB RF bandwidth, in regard to user transceiver adjacent channel selectivity and transmitter noise floor
- Band splitting is necessary to achieve the RF selectivity described above. The PIN Diodes are the limiting component
- The conclusion of this design assessment is that the FHMUX is feasible, and that hardware development is a logical next step
- A PIN development effort is a desirable addition to an advanced engineering model program.

6.2 FINAL CONFIGURATION

The need to split the operating bandwidth of each channel has increased the complexity of the FHMUX. Each of the five transceiver channels now has two sub-channels; 30 to 49.975 and 50 to 87.975 MHz. At any one time however, only one of the sub-channels of a given channel is in use. The means of efficiently combining the ten sub-channels to a single antenna was investigated.

A fundamental difference exists between multiplexing and power combining. Efficient power combining requires nearly identical phase and amplitude relationships between the signals being combined. Differences between the signals are dissipated in the power combiner load resistor. This is true of all types of combiners.

Multiplexing usually involves the combining of signals having different frequency and power characteristics. None of the ten sub-channels will ever have the necessary phase and voltage similarity to use power combining techniques in an efficient manner. The use of

frequency selective devices is still the most efficient way to structure the FHMUX.

The full band FHMUX is shown in Figure 6-1. This is the final circuit configuration, and allows each transceiver to hop the full 30-88 MHz band.

- Each transceiver is connected to a PIN Diode SPDT band switch, which routes the RF signal to the correct high or low band sub channel. This switch will add approximately 0.25 dB to the insertion loss. Thus, the sub channel insertion loss will be about 2.3 to 2.7 dB
- The quad-coupled combining technique has been extended to easily accomodate the five extra sub channels. However, the combining losses of the sub channels farthest from the antenna are now higher. For example, the combining loss of the Channel E low band path will be:

$$dB = (.18 + .1)\ (n-1)$$
$$= (.28) \times 9$$
$$dB = 2.52$$

This is in addition to the actual channel insertion loss of 2.3 to 2.7 dB, or 4.8 to 5.2 dB.

- This configuration will satisfy the original goals of the specification except for the insertion loss requirement. About two thirds of the channels will have a higher than specified insertion loss
- About 27 cubic feet are required, and power consumption will be about 250 to 300 watts.

6.3 ALTERNATE CONFIGURATION

The building block approach described earlier, and shown in Figure 6-1 is extremely flexible and hence easily adaptable to alternate configurations. The need to split the frequency band increases the complexity of the FHMUX by a factor of two, and results

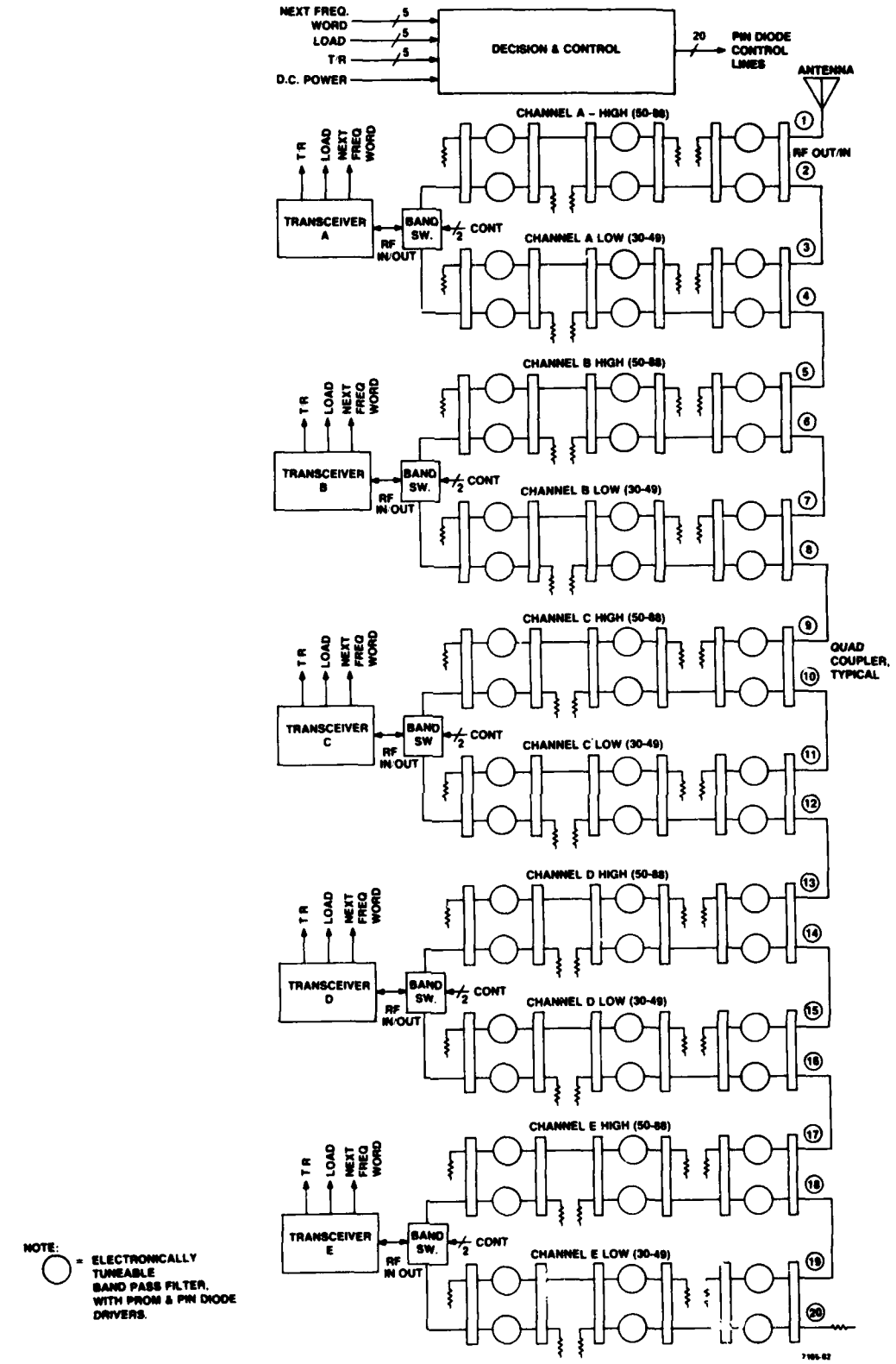

Figure 6-1. Five Channel FHMUX

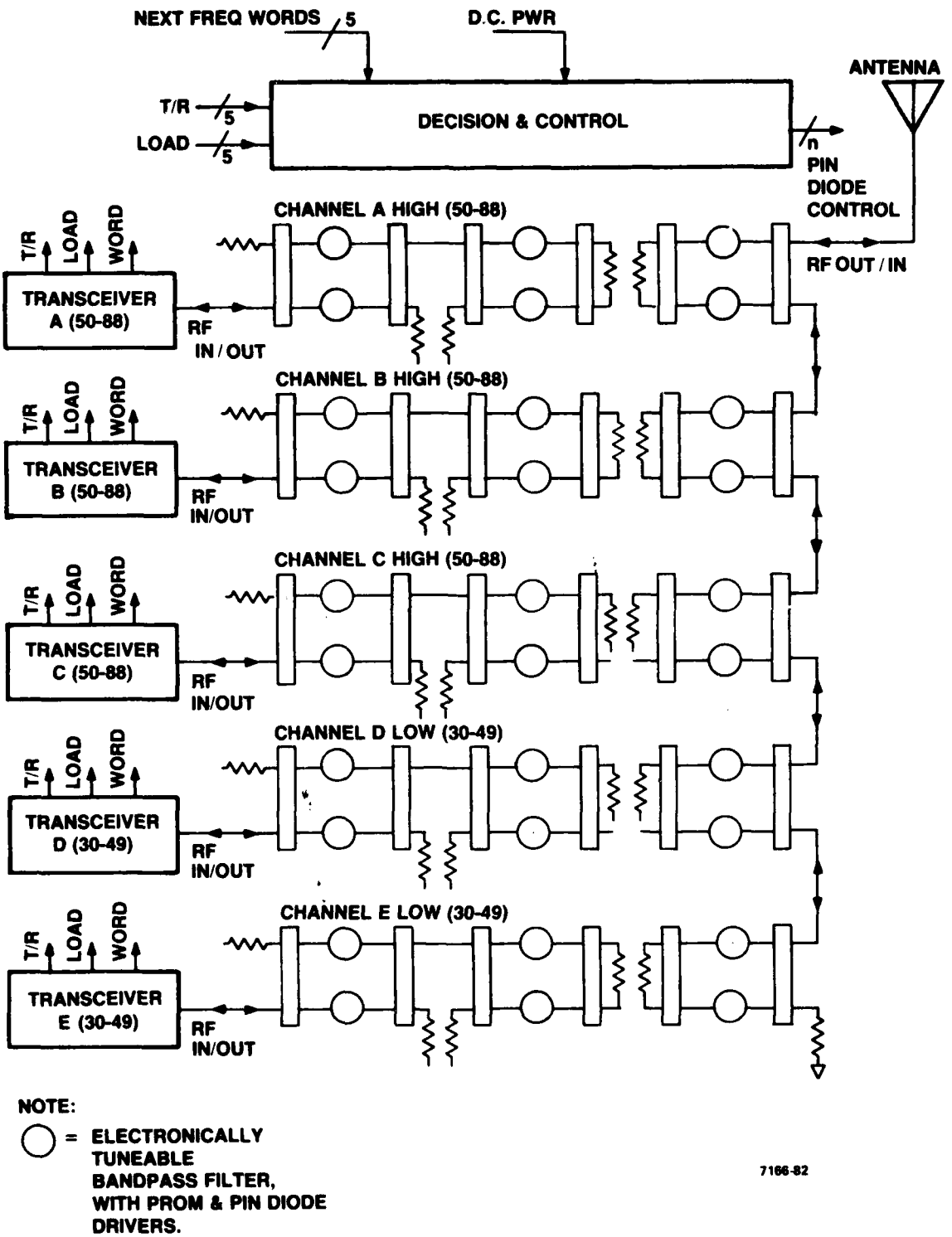

Figure 6-2. Five Channel FHMUX Alternate Configuration

in combining losses which may be unacceptable. A simplified configuration is shown in Figure 6-2. This version is predicated on reducing the hopping bandwidth of each transceiver to either 30-50, or 50-88 MHz. Figure 6-2 shows three highband channels, but many combinations exist. The FHMUX decision and control function can be programmed to accept either band of frequencies for any channel.

Insertion loss and combining losses would be lower with this configuration. The size would be about 30" X 30" X 30", and power consumption less than 200 watts.

SECTION 7

BIBLIOGRAPHY

7.1 REFERENCED DOCUMENTS

- "Microwave Circuits" by J.L. Altman: D. Van Nostrand Co.
- "Microwave Filter, Impedance-Matching Networks, and Coupling Structures" by G. Mathaei, L. Young, and E.M.T. Jones,: Artach House Books.

7.2 JAMMING - FREQUENCY HOPPING - SPREAD SPECTRUM

- Asynchronous Frequency Hopping Format. Aasterud. National Telecommunications Conference, 1974. pp. 976-984.
- A/J Performance of Spread-Spectrums FSK and DPSK. Houston. Transactions-Aerospace and Electronic Systems. July 1975. p. 677.
- FSK Signal Detection Transactions - Communications May 1975. pp. 543-546.
- CW in Band Intererence Effect on M-ary FSK Frequency Hopped Communications Houston. National Telecommunications Conference, 1978. 43 1/1-4.
- Hybrid Frequency hop/direct sequency and frequency hop/time hop systems. El-HAKEEN National Telecommunications Conference, 1978. 35.5/1-5.
- Interference with AM and FM Voice Communications FARBER Electro-Magnetic Conference Symposium EMC-5 1978, pp. 282-287.
- Jamming Susceptablity of Binary Non-Coherent FSK, Frequency Hopping Systems with Partial Band Jamming. PETTIT. South Eastern Conference 1978. pp. 51-54.
- Mutiple Access Communication Hopping Patterns SARWATE. Communications, International Conference ICC 1978. 7.4/1.3.

- Multiple Users Employing Same Spread Spectrum Techniques In Multiple User Environment. CO-Channel Interference. MUSA. Transactions--Communications. Vol. 26 No. 10. Oct. 1978. pp. 1405-1413.
- Interleaving, frequency hopping, and Spread Spectrum for finite messages under jamming. Transactions: Aerospace and Electronic Systems 1977. July. p. 464.
- Tactical Communications, Application of new Technologies. Jain. Transactions: Aerospace and Electronic Systems. 1977 Nov. p. 729.
- Error Correction Coding and Data Modulation, effect on system Performance. Batson. National Telecommunications Conference 1976. 32.5/1-5.
- Interference Effects of Pseudo-Random Frequency Hopping Signals on AM and FM Receivers. Cohen. Transactions: Aerospace and Electronic Systems T-AES 1971. March pp. 279-283.
- Frequency Hopping Radios Outwit "Smart" Jammers Microwaves, Nov. 1979.
- Bit Error Probabilities Relate to Data - Link S/N Microwaves, Nov. 1978.

7.3 DEVICES

- Microwave Semi Control Devices R. V. Garver. IEEE MTT-27 May 1979.

7.4 FERRITE CIRCULATORS

- An annotated Bibiography of Microwave Circulators and Isolators: 1968-1975 R. H. Knerr IEEE - MTT - 23 Oct. 1975.
- Understanding Coaxial Circulators and Isolators B. S. Sekhow, R. G. Sanders, and C. Nugent Microwave Systems News June 1979.

- Take Two Steps Toward Better *Circulator Design* M. Dydyk. Microwaves March 1979
- Lumped Element Circulators Y. Konishi, IEEE Trans. on Magnetics Mag-11 Sept. 1975
- Broadband VHF/UHF Circulators with Tailored Filter Characteristics I. M. Alexander, F.M. Aiken IEEE *Transactions on Magnetics* Sept. 1975
- Octave Coverage Lumped Element Circulator (Switched) IEEE GMTT Microwave Symposium pp 84-85 June 1973
- Analysis of Broadband Circulators with External Tuning Elements. IEEE MTT March 1968
- Planar Circulators for Wide Band Design Myoski IEEE Trans. MTT #28 3 March 1980

7.5 ACTIVE CIRCULATORS

- An Op Amp Circulator Atija. IEEE Trans., Circuits and Systems Vol CAS-22 June 1975
- Active Circulators - the Realization of Circulators Using Transistors S. Tanaka, N. Shimomura, and K. Ontake Proc. IEEE March 1965

7.6 DISTORTION

- A Study of Non Linearities and Inter-Modulation Characteristics of 3 port Distributed Circulators You-Sun Wu, W. H. Ku, and J. Erickson IEEE Trans. MTT-24 February 1976
- Intermodulation Interference in Mobile Multiple Transmission Communications Systems Operating at High Frequencies (3 -30 MHz) Proc. IEEE Vol. 120, No. 11 November 1973
- A Brief Survey of Intermodulation Due to Microwave Transmission Components. F. Matos, IEEE Trans. on Electromagnetic Compatibility February 1977

. Intermodulation Product Generation by Electron Tunneling. C. D. Bono. Proc. IEEE Vol 67, No 12. December 1979.

7.7 CIRCUITS

. If Back Intermodulation is a Problem. D. H. Lohrmann, Electronic Design 23, November 1971.

. Electronically Tuneable Filters Isolate High Power Transmitters, J. C. DeLeon, Microwaves December 1976.

. Design Techniques Using Helical Resonators M. Cohen, Microwave Journal May 1965.

. The Electrical Tuning of Helical Resonators G. A. Vander Haagen, Microwave Journal August 1967.

. Helical Resonator Design Chart, Electronics August 1960.

. Coaxial Resonators with Helical Inner Conductor. W. Macalphine, R. O Schildknecht Proc. IRE, Vol. 47, No. 12 December 1959.

7.8 MISCELLANEOUS

. A High Isolation RF Switch, E. Fong, RF Design, Sept/Oct. 1980.

. Broadband Reflectometers at High Frequencies R. T. Adams and A. Horvath Electrical Communications, June 1955, Pg. 118-125.

. PIN Diode Switches, Speed (vs) Power R. V. Garver, Microwave Journal, Feb. 1978.

. The Resonant Mode Pin Switch R. J. Chaffin, Microwave Journal, Dec. 1980.

. The RF Capacitor Handbook ATC, June 1972.

. Large Area Varactor Diode for Electrically Tunable, High Power UHF Filter G. Swartz, D. Kern, P. Robinson IEEE Trans, on Electron Devices Vol. Ed-27, No. 11 November 1980.

- A Broadband Optoelectronic Microwave Switch E. Harra and R. MacDonald IEEE Trans. on MTT, Vol. MTT-28, No. 6, June, 1980.
- Group Delay Distortion of Filter Reflected Signals M. Jamil Ahmed, Microwave Journal, June, 1976.
- Low Noise "Circulator-Coupled" Amplifier for Unattended Small Earth Terminals IEEE Proc., Vol. 127, Pt.H, No. 4, August 1980.
- A Five Channel (2KW-PEP), 2 to 30 MHz Distribution System H. Murray, N.R.L. AD-773-476, Dec. 1973.
- High Accuracy RF Amplitude Comparator A. Sokal, IEEE Journal of Solid State Circuits Vol. SC-12, No. 6, December 1977.
- Miniaturization of Wideband VHF Filters by Using Spiral Inductors O. Inui and J. Nagai, Proc. of the IEEE Vol. 67, No. 1, Jan. 1979.
- Solid State Radio Engineering — Wiley
  Krauss, Bostian, Rabb
- Microwave Diode Control Devices — Artech House
  Robert V. Garver
- Networks, Lines, Fields — Prentice Hall
  John D. Ryder
- Handbook of Filter Synthesis — Wiley
  A. I. Zverev
- The Electrical Tuning of Helical Resonators. — The Microwave Journal, August, 1967
  G. A. Vander Haagen
- The Harmonics Produced by A PIN Diode In a Microwave Switching Application. — IEEE-MTT Vol MTT-15 March 1967
  H. Mott and D. M. McQuiddy
- Intermodulaton Producs Generated by A PIN Diode Switch. — Proc. IEEE Vol. 56

R. L. Sicotte & R. N. Assaly	pp 74-75 Jan., 1968
. Intermodulation Product and Switching Noise Amplitudes of A Pin Diode Switch In the UHF Band.	IEEE-MTT Vol. MIT-18 pp 48-50 Jan. 1970
. Recent Advances In Binary Programmed Electronically Tunable Bandpass Filters of the "FLAUTO" Type Arthur Karp & William B. Weir	IEEE MW Sym. 1975 pp 167-169
. Further Advances In High Power Electronically Tuned Resonators Arthur Karp	IEEE MW Sym. 1977
. PIN Diode Designers Handbook & Catalog	Unitrode Corp.
. Communications System Transmission Losses	Motorola Application Note
. Power DMOS for High Frequency Switching Applications	IEEE T - Electron Devices Feb., 1980
. A 6 Volt MOSFET Design for Low On Resistance Temple, Love, And Grey	IEEE T - ELECTRONIC Devices Feb., 1980
. Dual gate Ga As Switches Vorhaus, Fabian, Paul, Jajimer	IEEE T - ELECTRONIC Devices Feb., 1981
. Field - Effect and Bipolar Power Transistor Physics Adolph Bilcher	Academic Press 1981

. Analysis Improvement of Intermodulation Distortion in Ga As Power Fets J. A. Higgins, R. L. Kuvis	IEEE T-MTT, Jan., 1980
. A Generalized Multiplexer Theory J. David Rhodes, R. Levy	IEEE T-MTT, Feb., 1979
. Microwave Power Combining Techniques Kenneth Russell	IEEE T-MTT, May, 1979
. A Directional Coupler with Very Flat Coupling Gordon P. Riblet	IEEE T-MTT Feb., 1978
. Correction to the Above	IEEE T-MTT Sept., 1978, Page 691

APPENDIX E

RESONATOR STUDY

E.1 *INTRODUCTION*

The Frequency-Hopping Multiplexer (FHMUX) requires electronically-tunable High Q Resonators for its filters. These Resonators must meet the following requirements:

Tuning Range: 30-88 MHz in 25 KHz steps
Insertion Loss at Resonance: $\geq$ 0.5 dB
Rejection at $\pm$ 4% of Center Frequency: $\geq$ 13.3 dB

To accomplish this, some form of electronically-tunable, distributed-element resonator must be used, since lumped L-C circuits cannot provide high enough Q.

The following equations give the relationships between insertion loss or rejection (insertion loss off-resonance), and Qu (unloaded Q), Q_L (loaded Q), and Q_E (external Q):

I.L. = Insertion Loss

$$\text{I.L. at Resonance} = 20 \text{ Log } \left[\frac{Qa}{Qu} + 1\right] \quad \text{dB}$$

$$\text{or} \quad 20 \text{ Log } \left[\frac{Qu}{Qu-QL}\right] \quad \text{dB}$$

$$\text{I.L. at any Frequency} = 10 \text{ Log } \left[Q_E^2 \left(\frac{1}{QL^2} + \xi^2\right)\right] \quad \text{dB}$$

$$\text{Where:} \quad \xi = \frac{W}{W_o} - \frac{W_o}{W}$$

Q_e = Doubly-Loaded External Q

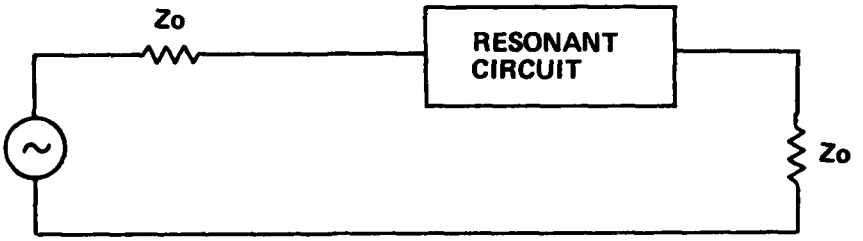

Figure E-1. Series Resonant Bandpass Filter

$$\text{I.L. At Resonance} = 20 \text{ Log } \left[\frac{1}{1 - \frac{QL}{Qu}} \right] \quad \text{dB}$$

$$\text{I.L. at any Frequency} = 10 \text{ Log } \frac{1 + (QL\ \xi)^2}{(1 - \frac{QL}{Qu})^2} \text{ dB}$$

$$\text{Where: } \xi = \frac{W}{W_o} - \frac{W_o}{W}$$

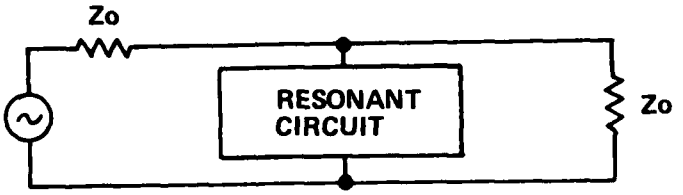

Figure E-2. Parallel Resonant Bandpass Filter

From the preceeding equations, both Q_U and QL or Q_E must be high to provide both low I.L. at resonance and high-rejection off-resonance.

Three types of resonators were investigated for the FHMUX application: the Flauto-C Resonator, the Helical Resonator, and the Shortened-Line Coaxial Resonator. The Flauto-C Resonator is a half-wave coaxial resonator which employs shunt capacitors placed at certain points along its transmission line. These capacitors act to increase the line's electrical half-wave length and decrease the resonant frequency. On the other hand, the Helical Resonator is a

coiled quarter-wave-length coaxial resonator, and it can be tuned with a variable shunt capacitor at its open-circuited end. Finally, the Shortened-Line Resonator is a half-wave length coaxial resonator that uses PIN Diodes to change the electrical length of the transmission line. When a PIN Diode (placed between two points along the transmission line) is turned on, it supposedly shorts-out a section of the transmission line, thereby decreasing the line's electrical length and increasing the resonant frequency.

E.2 FLAUTO-C RESONATOR MODEL

The Flauto-C was modeled as shown below, so that analysis and optimization could be performed using the "COMPACT" microwave computer-aided design program.

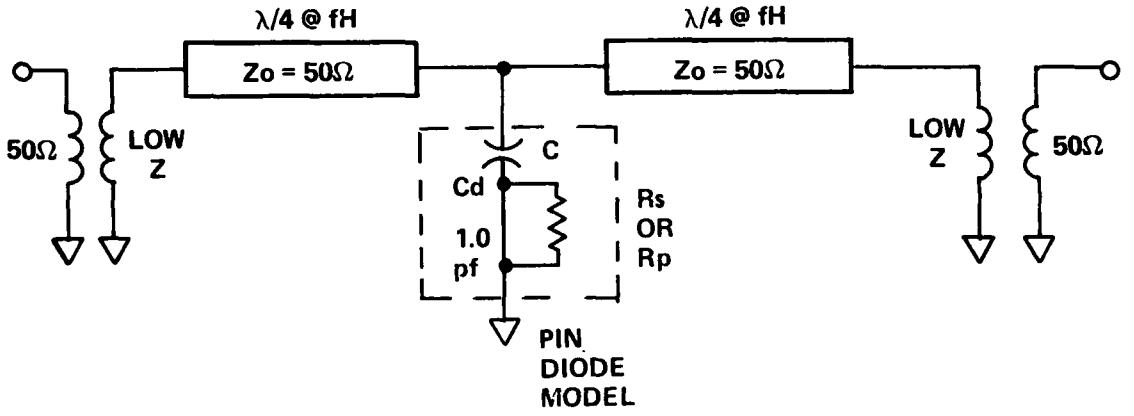

Figure E-3. Flauto-C Resonator Model

The ideal transformers in the model represent the input and output coupling that is usually provided by loops inside a cavity that contains the transmission line. Moreover, the transformers provide approximate short circuits at both ends of the transmission lines, thereby making the line a half-wavelength resonator. Also, the transformer impedance ratios help determine the Q_e (external Q) and Q_L (loaded Q); and therefore help define the resonator's rejection and in-band insertion loss.

The tuning capacitor at the center, C, can be switched in or out by the PIN Diode, which is represented by R_s when "on", and R_p and C_p when "off". This capacitor has the greatest tuning effect when placed at the center of the line where the voltage standing wave is the greatest. However, the placement of this capacitor (and additional tuning capacitors) at other points along the line is sometimes used.

The equations for the resonant frequencies shown below were derived for a single-capacitor Flauto:

$$\text{Diode "on":} \quad 0 = \frac{Zo}{2} \text{ Tan } \frac{\omega_o \ell}{v} - \frac{1}{\omega o C}$$

$$\text{Diode "off":} \quad 0 = \frac{Zo}{2} \text{ Tan } \frac{\omega_o \ell}{v} - \frac{R_p^2 \omega_o^2 C_1 C_2 + R_p^2 \omega_o^2 C_2 + 1}{(\omega_o C_1)(R_p^2 \omega_o^2 C_2^2 + 1)}$$

The preceeding equations are transcendental, and therefore an equation for ω_o cannot be shown in closed form. Consequently, C and f_H (the frequency for which each transmission line section equals 90^o) were chosen through the use of "COMPACT" computer analysis and optimization.

The elements respesenting the PIN Diode (C_d and R_s or R_p) were either chosen to give the desired resonator performance specifications (insertion loss and rejection) or they were taken from available PIN Diode specifications. However, C_d (the diode "off" capacitance) was fixed at 1PF, which is a typical value for high-quality, high-frequency PIN Diodes.

E.3 HELICAL RESONATOR MODEL

The Helical Resonator was modeled as shown below:

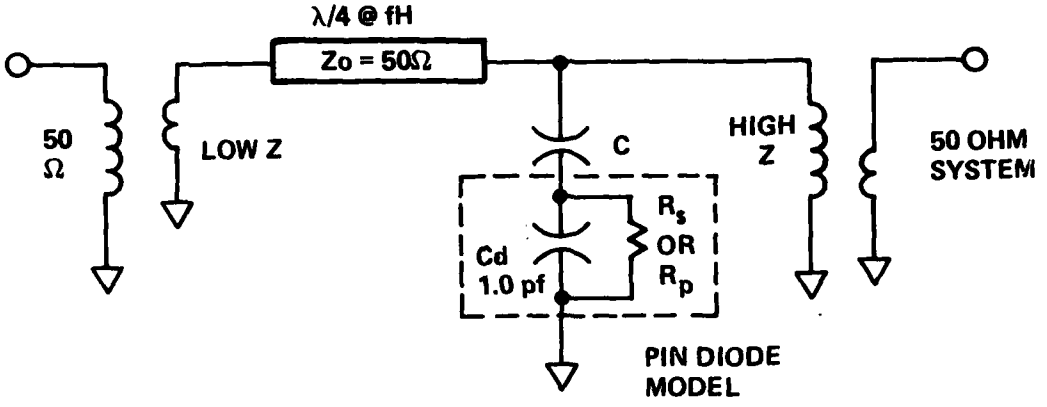

Figure E-4. Helical Resonator Model

This circuit represents a quarter-wave coaxial resonator with an approximate short circuit on the left end and an approximate open-circuit on the right end. The coupling used here has two separate ports (two ports were necessary for "COMPACT" computer modeling), whereas Helical Resonators are sometimes used as single-port devices. Also, most of the reasoning for this model is the same as for the Flauto-C Resonator Model. A Flauto-C Resonator can be looked at as two identical Helical Resonators connected back to back.

E.4 SHORTENED-LINE RESONATOR MODEL

The Shortened-Line Resonator was modeled on "COMPACT" as shown below:

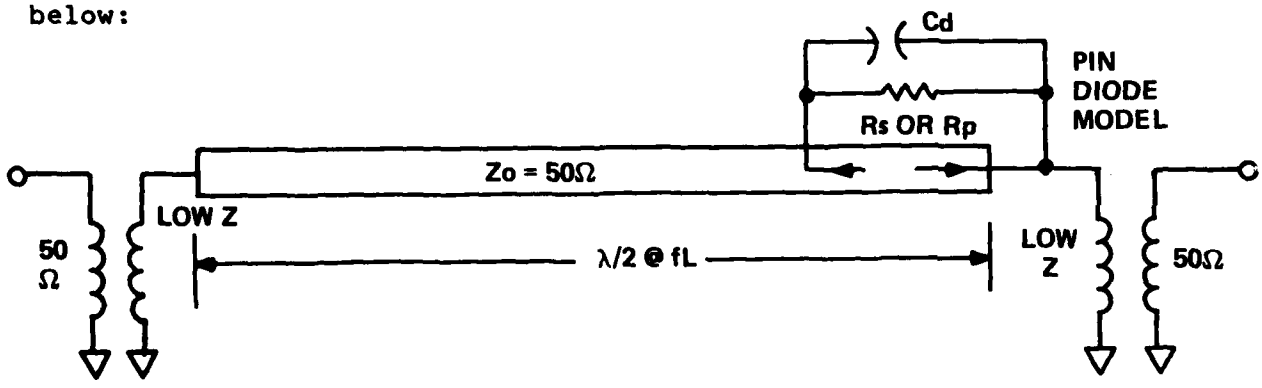

Figure E-5. Shortened Line Resonator

In addition, an odd-even mode analysis was performed on the diode and the shorted section of transmission line. These results are shown below:

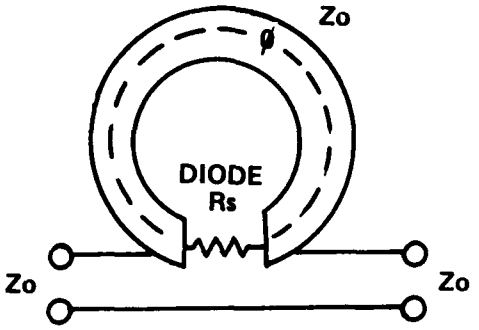

Where:
ø = Electrical Length of Shorted Section of Transmission Line

$$G = \frac{1}{R_s}, \quad Y_o = \frac{1}{Z_o}, \quad \bar{G} = \frac{G}{Y_o}$$

$$S_{12} = S_{21} = \frac{2\bar{G} - j\left(\cot\frac{\theta}{2} + \tan\frac{\theta}{2}\right)}{2(\bar{G}+1) + j\left[\left(\tan\frac{\theta}{2}\right)(2G+1) - \cot\frac{\theta}{2}\right]}$$

$$S_{11} = S_{22} = \frac{-j2G\tan\frac{\theta}{2}}{2(\bar{G}+1) + j\left[\left(\tan\frac{\theta}{2}\right)(2\bar{G}+1) - \cot\frac{\theta}{2}\right]}$$

Figure E-6. Odd-Even Mode Model For Shortened Line Resonator

There are two problems with the Shortened-Line Resonator. As can be seen from the Shortened-Line analysis (which was confirmed by "COMPACT" analysis), the section of transmission line is not simply shorted-out by the PIN Diode. Therefore, the resonator electrical length is not as short as originally expected. Also, the total resonator length would be longer than the Flauto-C, since the length is chosen for the lowest (not the highest) frequency of interest.

E.5 FLAUTO-C RESULTS

Several "COMPACT" computer runs were made using the Flauto-C model. Some of these results appear at the end of this appendix, and most of thse figures show the diagram of the model, the program and the results.

Figures E-7 and E-8 show a Flauto-C Resonator that is tuned to 59 MHz with the diode "on" and 88 MHz with the diode "off". The diode "on" and "off" resistances were selected to give 0.5 dB of insertion loss at resonance and about 13-14 dB of rejection at $\pm$ 4% off resonance. For example, shown at the bottom of Figure E-7, are the S_{21} values in dB (insertion losses) for the corresponding frequencies.

The R_s shown in Figure E-7 that is required to meet the insertion loss and rejection specifications with the diode "on" is 0.074 ohms. This R_s value is not presently obtainable with the PIN Diodes on the market. Therefore, "COMPACT" runs were also made with Unitrode UM6200 (a low-R_s PIN Diode) specifications. The Specifications were taken for heavily biased conditions: "on" at about 0.5 amp. (R_s = 0.15 ohms), and "off" at about 200 volts (R_p = 500K ohm).

Figures E-9 and E-10 show the runs with the UM6200 diode. Only the insertion loss in the "on" state (resonant at 59 MHz) failed to meet the insertion loss specification; this specification was missed by about 0.5 dB. However, these runs (Figures E-7, E-8, E-9, and E-10 were made for single-diode, single-tuning-capacitor resonators with only two resonance points.

It was also determined if the Flauto-C could be tuned over the 30-88 MHz frequency range. Figures E-11 and E-12 show that with a large value of switched shunt capacitance, the resonator frequency can be varied from 30-88 MHz.

Another problem considered was tuning the Flauto in 25 KHz increments. For Example, tuning using a Binary Tuning Signal was accomplished by Arthur Karp at the Stanford Research Institute. However the percentage bandwidth was small (12%) when compared with the 30-88 MHz (98%) frequency range required for this study. Consequently, Karp's Filter was loaded with small capacitance values,

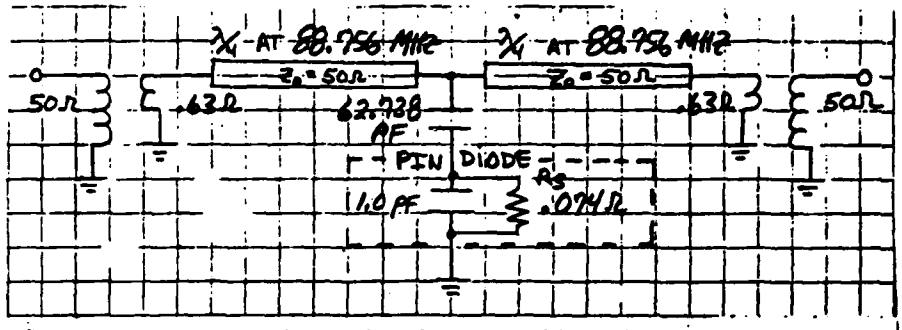

Meets insertion loss specification

```
L FLTOR.DATA
 FLTOR.DATA
00010 TRF AA IM 50 -.63
00020 TRL BB SE 50 90 88.756
00030 CAS AA BB
00040 PRC CC PA -.074 1
00050 CAP DD PA 62.738
00060 SER CC DD
00070 CAS AA CC
00080 TRL EE SE 50 90 88.756
00090 CAS AA EE
00100 TRF FF IM -.63 50
00110 CAS AA FF
00120 PRI AA S1 50
00130 END
00140 50 56.64 59 61.36 68
00150 END
00160 .001
00170 0 0 10 -13.3
00180 END
READY
COMPACT FLTOR
COMPACT MICROWAVE ANALYSIS PROGRAM (VERSION 2.3) 6/12/76

ANAL(1),SENS(2),OPT(3),SWEEP(4),MAP(5)
 WRITE 1,2,3,4,5 OR 13(1&3);
?
1
                    POLAR S-PARAMETERS IN   50.0 OHM SYSTEM

   F          S11                S21                S12                S22          S21
  in MHZ  (MAGN<ANGL)  (  MAGN<ANGL)  (  MAGN<ANGL)  (MAGN<ANGL)   IN DB

    50.0 (1.00<  -2) (  0.06< -92) (0.064< -92) (1.00<  -2) -23.81
fo -4% 56.6 (0.97< -11) (  0.21<-102) (0.215<-102) (0.97< -11) -13.37
fo  59.0 (0.06<   1) (  0.94<-179) (0.944<-179) (0.06<   1)  -0.50
fo +4% 61.4 (0.98<  12) (  0.20< 103) (0.202< 103) (0.98<  12) -13.90
    68.0 (1.00<   3) (  0.05<  93) (0.051<  93) (1.00<   3) -25.91
```

Figure E-7. Schematic and Computer Printout, Flauto-C Resonator Tuned at 59 MHz

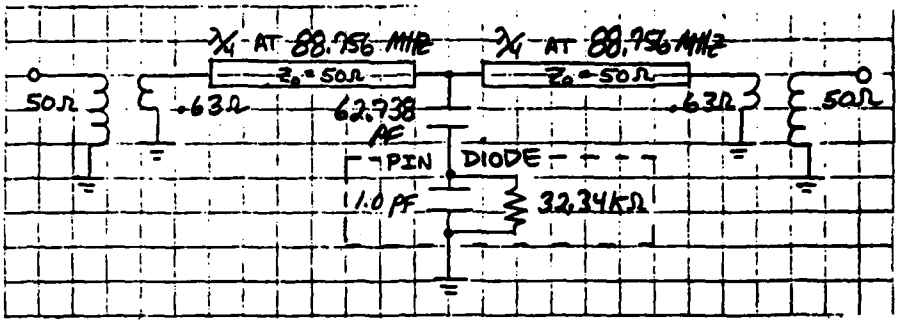

Meets Insertion Loss Specification

```
L FLTOR.DATA

 FLTOR.DATA
00010 TRF AA IM 50 .63
00020 TRL BB SE 50 90 88.756
00030 CAS AA BB
00040 PRC CC PA -32340 1
00050 CAP DD PA 62.738
00060 SER CC DD
00070 CAS AA CC
00080 TRL EE SE 50 90 88.756
00090 CAS AA EE
00100 TRF FF IM .63 50
00110 CAS AA FF
00120 PRI AA S1 50
00130 END
00140 80 84.48 88 91.52 95
00150 END
00160 .001
00170 0 0 10 -.5
00180 END
READY
COMPACT FLTOR
COMPACT MICROWAVE ANALYSIS PROGRAM (VERSION 2.3) 6/12/76

ANAL(1),SENS(2),OPT(3),SWEEP(4),MAP(5)
 WRITE 1,2,3,4,5 OR 13(183):
?
1
                    POLAR S-PARAMETERS IN   50.0 OHM SYSTEM

    F          S11              S21              S12              S22          S21
   MHZ   (MAGN<ANGL)  ( MAGN<ANGL)  ( MAGN<ANGL)  (MAGN<ANGL)    DB

   80.0 (1.00<  -4) ( 0.09< -95) (0.089< -95) (1.00<  -4) -20.99
   84.5 (0.98< -11) ( 0.20<-101) (0.197<-101) (0.98< -11) -14.11
   88.0 (0.06<   3) ( 0.94< 179) (0.944< 179) (0.06<   3) -0.50
   91.5 (0.98<  11) ( 0.20< 101) (0.196< 101) (0.98<  11) -14.14
   95.0 (0.99<   5) ( 0.10<  95) (0.101<  95) (0.99<   5) -19.91
```

Figure E-8. Schematic and Computer Printout, Flauto-C Resonator Tuned to 88 MHz

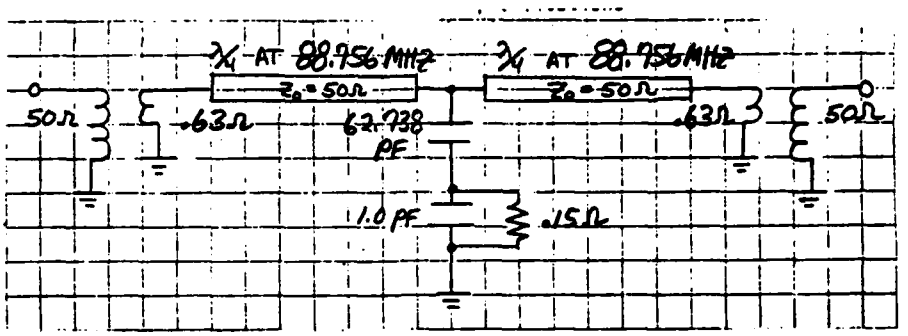

With Unitrode UM6200 Pin Diode parameters

```
L FLTOR.DATA
 FLTOR.DATA
00010 TRF AA IM 50 -.63
00020 TRL BB SE 50 90 88.756
00030 CAS AA BB
00040 PRC CC PA .15 1
00050 CAP DD PA 62.738
00060 SER CC DD
00070 CAS AA CC
00080 TRL EE SE 50 90 88.756
00090 CAS AA EE
00100 TRF FF IM -.63 50
00110 CAS AA FF
00120 PRI AA S1 50
00130 END
00140 50 56.64 59 61.36 68
00150 END
00160 .001
00170 0 0 10 -13.3
00180 END
READY
COMPACT FLTOR
COMPACT MICROWAVE ANALYSIS PROGRAM (VERSION 2.3) 6/12/76

ANAL(1),SENS(2),OPT(3),SWEEP(4),MAP(5)
 WRITE 1,2,3,4,5 OR 13(1&3):
?
1
                POLAR S-PARAMETERS IN  50.0 OHM SYSTEM

  F        S11            S21            S12            S22          S21
 MHZ  (MAGN<ANGL) ( MAGN<ANGL) ( MAGN<ANGL) (MAGN<ANGL)    DB

 50.0 (1.00<  -2) ( 0.06< -92) (0.044< -92) (1.00<  -2) -23.81
 56.6 (0.97< -11) ( 0.21<-102) (0.214<-102) (0.97< -11) -13.39
 59.0 (0.11<   1) ( 0.89<-179) (0.893<-179) (0.11<   1)  -0.99
 61.4 (0.97<  12) ( 0.20< 103) (0.201< 103) (0.97<  12) -13.92
 68.0 (1.00<   3) ( 0.05<  93) (0.051<  93) (1.00<   3) -25.91
```

Figure E-9. Schematic and Computer Printout, Flauto-C Resonator Tuned to 59 MHz

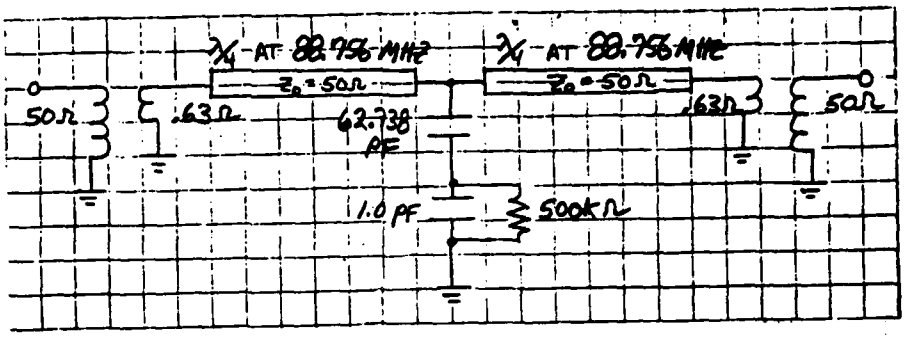

With Unitrode UM6200 Pin Diode parameters

```
L FLTOR.DATA
 FLTOR.DATA
00010 TRF AA IM 50 -.63
00020 TRL BB SE 50 90 88.756
00030 CAS AA BB
00040 PRC CC PA 500000 1
00050 CAP DD PA 62.738
00060 SER CC DD
00070 CAS AA CC
00080 TRL EE SE 50 90 88.756
00090 CAS AA EE
00100 TRF FF IM -.63 50
00110 CAS AA FF
00120 PRI AA S1 50
00130 END
00140 80 84.48 88 91.52 95
00150 END
00160 .001
00170 0 0 10 -13.3
00180 END
READY
COMPACT FLTOR
COMPACT MICROWAVE ANALYSIS PROGRAM (VERSION 2.3) 6/12/76

ANAL(1),SENS(2),OPT(3),SWEEP(4),MAP(5)
 WRITE 1,2,3,4,5 OR 13(1&3):
?
1
                    POLAR S-PARAMETERS IN  50.0 OHM SYSTEM

   F          S11             S21             S12             S22          S21
  MHZ   (MAGN<ANGL)  ( MAGN<ANGL)  ( MAGN<ANGL)  (MAGN<ANGL)    DB

  80.0  (1.00<  -4)  ( 0.09< -94)  (0.089< -94)  (1.00<  -4)  -20.98
  84.5  (0.98< -11)  ( 0.20<-101)  (0.197<-101)  (0.98< -11)  -14.09
  88.0  (0.01<  48)  ( 1.00< 179)  (0.996< 179)  (0.01<  48)   -0.03
  91.5  (0.98<  11)  ( 0.20< 101)  (0.197< 101)  (0.98<  11)  -14.12
  95.0  (0.99<   5)  ( 0.10<  95)  (0.101<  95)  (0.99<   5)  -19.90
```

Figure E-10. Schematic and Computer Printout, Flauto-C Resonator Tuned to 88 MHz

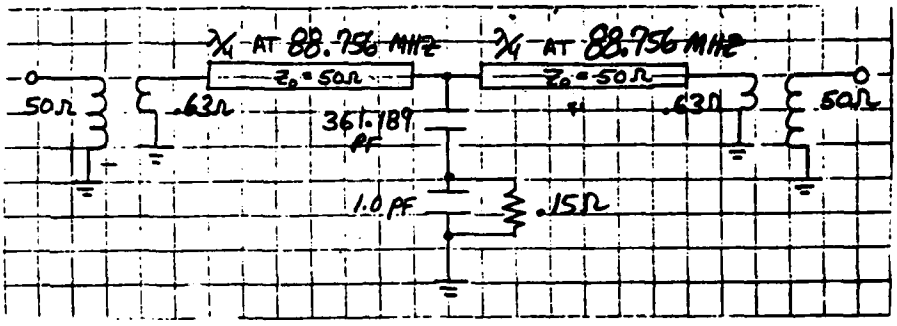

— With Unitrode UM6200 Pin Diode parameters

```
L FLTOR.DATA
 FLTOR.DATA
00010 TRF AA IM 50 .63
00020 TRL BB SE 50 90 88.756
00030 CAS AA BB
00040 PRC CC PA -.15 1
00050 CAP DD PA 361.189
00060 SER CC DD
00070 CAS AA CC
00080 TRL EE SE 50 90 88.756
00090 CAS AA EE
00100 TRF FF IM .63 50
00110 CAS AA FF
00120 PRI AA S1 50
00130 END
00140 28 28.8 30 31.2 32
00150 END
00160 .001
00170 0 0 10 -.5
00180 END
READY
COMPACT FLTOR
COMPACT MICROWAVE ANALYSIS PROGRAM (VERSION 2.3) 6/12/76

ANAL(1),SENS(2),OPT(3),SWEEP(4),MAP(5)
 WRITE 1,2,3,4,5 OR 13(1&3):
?
1
                    POLAR S-PARAMETERS IN   50.0 OHM SYSTEM

  F        S11              S21              S12              S22          S21
  MHZ   (MAGN<ANGL)    ( MAGN<ANGL)     ( MAGN<ANGL)     (MAGN<ANGL)     DB

  28.0 (0.97<  -9)  ( 0.21<-102)  (0.206<-102)  (0.97<  -9) -13.71
  28.8 (0.92< -15)  ( 0.31<-111)  (0.313<-111)  (0.92< -15) -10.08
  30.0 (0.26<  -1)  ( 0.74<-177)  (0.739<-177)  (0.26<  -1)  -2.63
  31.2 (0.92<  18)  ( 0.28< 115)  (0.284< 115)  (0.92<  18) -10.93
  32.0 (0.97<  12)  ( 0.17< 106)  (0.174< 106)  (0.97<  12) -15.18
```

Figure E-11. Schematic and Computer Printout, Flauto-C Resonator Tuned to 30 MHz

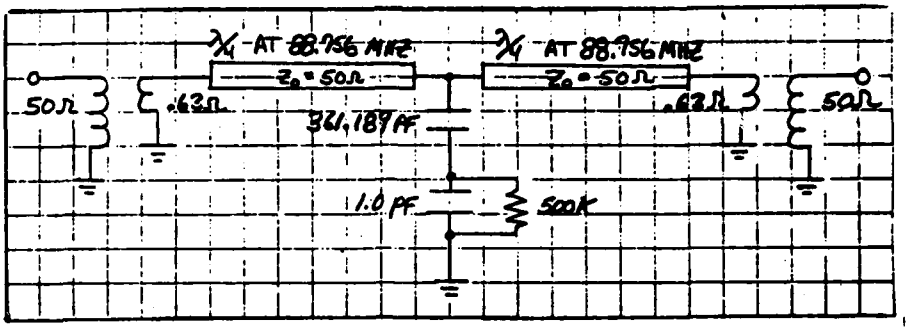

With Unitrode UM6200 Pin Diode Parameters

```
L FLTOR.DATA
 FLTOR.DATA
00010 TRF AA IM 50 .63
00020 TRL BB SE 50 90 88.756
00030 CAS AA BB
00040 PRC CC PA -500000 1
00050 CAP DD PA 361.189
00060 SER CC DD
00070 CAS AA CC
00080 TRL EE SE 50 90 88.756
00090 CAS AA EE
00100 TRF FF IM .63 50
00110 CAS AA FF
00120 PRI AA S1 50
00130 END
00140 80 84.48 88 91.52 95
00150 END
00160 .001
00170 0 0 10 .5
00180 END
READY
COMPACT FLTOR
COMPACT MICROWAVE ANALYSIS PROGRAM (VERSION 2.3) 6/12/76

ANAL(1),SENS(2),OPT(3),SWEEP(4),MAP(5)
 WRITE 1,2,3,4,5 OR 13(1&3);
?
1
                    POLAR S-PARAMETERS IN   50.0 OHM SYSTEM

   F          S11              S21              S12              S22          S21
  MHZ   (MAGN<ANGL)  ( MAGN<ANGL)  ( MAGN<ANGL)  (MAGN<ANGL)    DB

  80.0 (1.00<  -4) ( 0.09< -94) (0.089< -94) (1.00<  -4) -20.97
  84.5 (0.98< -11) ( 0.20<-101) (0.198<-101) (0.98< -11) -14.07
  88.0 (0.02<  76) ( 1.00< 178) (0.996< 178) (0.02<  76)  -0.04
  91.5 (0.98<  11) ( 0.20< 101) (0.196< 101) (0.98<  11) -14.14
  95.0 (0.99<   5) ( 0.10<  95) (0.101<  95) (0.99<   5) -19.91
```

Figure E-12. Schematic and Computer Printout, Flauto-C Resonator Tuned to 88 MHz. (30 MHz with Diode "ON")

and therefore he was able to maintain a similar half-wave standing wave pattern along the resonator throughout the tuning range. Thus, his assumptions on the effect of each tuning capacitance followed a simple formula. Also if the tuning capacitors have small values, front to back symmetry of the resonator need not be maintained, but with larger values (such as those in Figures E-13 and E-14), this symmetry must be maintained in order to provide for low insertion loss at resonance.

A standard half-wave coaxial resonator has a second passband that appears at the second harmonic; this problem was investigated for the Flauto Filter. Figure E-15 shows that with the resonator tuned to 44 MHz, no second passband appears. This is due to the large value of tuning capacitance (146.603 pF) that is used.

E.6 HELICAL RESONATOR RESULTS

"COMPACT" runs were made for a Helical Resonator (with $\pm$ 2%, 13.3 dB bandwidth). Two of these runs are shown in Figures E-16 and E-17. As can be seen from Figure E-16, a low R_s is also required for this resonator. However, the Helical Resonator is about half the size of the Flauto-C, and seems to present no apparent disadvantages for the frequency range considered (30-88 MHz), when compared to the Flauto-C. Also the Helical Resonator would have to be tuned with a capacitance bus as would the Flauto-C for this large frequency range required.

E.7 CONCLUSIONS

It appears that the Helical Resonator with the capacitance bus is the best method available to attempt to meet the resonator requirements. On the other hand, no PIN Diodes for the capacitance bus are available to meet the R_s (on resistance) necessary for low insertion loss at resonance and high-rejection off-resonance.

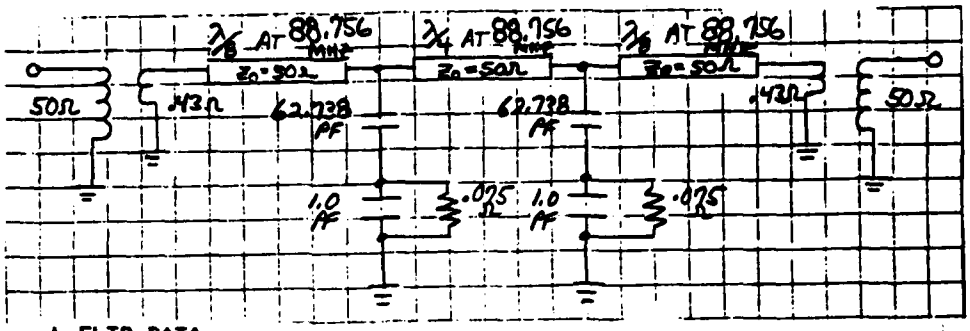


```
L FLTO.DATA          Meets insertion loss specification
 FLTO.DATA
00010 TRF AA IM 50 -.43
00020 TRL BB SE 50 45 88.756
00030 CAS AA BB
00040 CAP CC PA 62.738
00050 PRC DD PA -.075 1
00060 SER CC DD
00070 CAS AA CC
00080 TRL EE SE 50 90 88.756
00090 CAS AA EE
00100 CAP FF PA 62.738
00110 PRC GG PA -.075 1
00120 SER FF GG
00130 CAS AA FF
00140 TRL HH SE 50 45 88.756
00150 CAS AA HH
00160 TRF II IM -.43 50
00170 CAS AA II
00180 PRI AA S1 50
00190 END
00195 56.64 61.36
00200 59
00210 END
00220 .1
00230 0 0 10 -13.3
00235 0 0 10 -.5
00240 END
READY
COMPACT FLTO
COMPACT MICROWAVE ANALYSIS PROGRAM (VERSION 2.3) 6/12/76

ANAL(1),SENS(2),OPT(3),SWEEP(4),MAP(5)
 WRITE 1,2,3,4,5 OR 13(183):
?
1
                    POLAR S-PARAMETERS IN   50.0 OHM SYSTEM

   F         S11              S21              S12              S22          S21
  MHZ   (MAGN<ANGL)  ( MAGN<ANGL)  ( MAGN<ANGL)  (MAGN<ANGL)    DB

  56.6 (0.97<  -12) ( 0.21<-102) (0.211<-102) (0.97<  -12) -13.51
  61.4 (0.97<   12) ( 0.22< 103) (0.216< 103) (0.97<   12) -13.30
  59.0 (0.06<    0) ( 0.94< 179) (0.945< 179) (0.06<    0)  -0.50
```

Figure E-13. Schematic and Computer Printout, Flauto-C Resonator with 2 Tuning Capacitors. Tuned to 59 MHz.

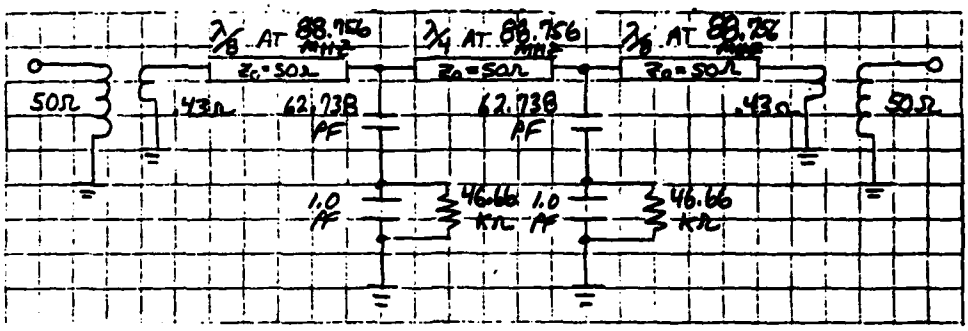


```
L FLTO.DATA          Meets insertion loss specification
 FLTO.DATA
00010 TRF AA IM 50 .43
00020 TRL BB SE 50 45 88.756
00030 CAS AA BB
00040 CAP CC PA 62.738
00050 PRC DD PA -46660 1
00060 SER CC DD
00070 CAS AA CC
00080 TRL EE SE 50 90 88.756
00090 CAS AA EE
00100 CAP FF PA 62.738
00110 PRC GG PA -46660 1
00120 SER FF GG
00130 CAS AA FF
00140 TRL HH SE 50 45 88.756
00150 CAS AA HH
00160 TRF II IM .43 50
00170 CAS AA II
00180 PRI AA S1 50
00190 END
00195 84.48 88 91.52
00210 END
00220 .1
00235 0 0 10 -.5
00240 END
READY
COMPACT FLTO
COMPACT MICROWAVE ANALYSIS PROGRAM (VERSION 2.3) 6/12/76

ANAL(1),SENS(2),OPT(3),SWEEP(4),MAP(5)
 WRITE 1,2,3,4,5 OR 13(1&3);
?
1
                    POLAR S-PARAMETERS IN   50.0 OHM SYSTEM

   F          S11              S21              S12              S22          S21
   MHZ   (MAGN<ANGL)   ( MAGN<ANGL)   ( MAGN<ANGL)   (MAGN<ANGL)    DB

   84.5 (0.99<  -7) ( 0.14< -98) (0.138< -98) (0.99<  -7) -17.21
   88.0 (0.06<  14) ( 0.94< 179) (0.944< 179) (0.06<  14)  -0.50
   91.5 (0.99<   7) ( 0.14<  98) (0.137<  98) (0.99<   7) -17.24
```

Figure E-14. Schematic and Computer Printout, Flauto-C Resonator with 2 Tuning Capacitors, Tuned to 88 MHz

```
FLTOR.DATA
00010 TRF AA IM 50 .63
00020 TRL BB SE 50 90 88.756
00030 CAS AA BB
00040 PRC CC PA .15 1
00050 CAP DD PA 146.603 PF
00060 SER CC DD
00070 CAS AA CC
00080 TRL EE SE 50 90 88.756
00090 CAS AA EE
00100 TRF FF IM .63 50
00110 CAS AA FF
00120 PRI AA S1 50
00130 END
00140 40 94 2
00150 END
00160 .001
00170 10 0 0
00180 END
READY
COMPACT FLTOR
COMPACT MICRO

ANAL(1),SENS(
 WRITE 1,2,3,
?
1
```

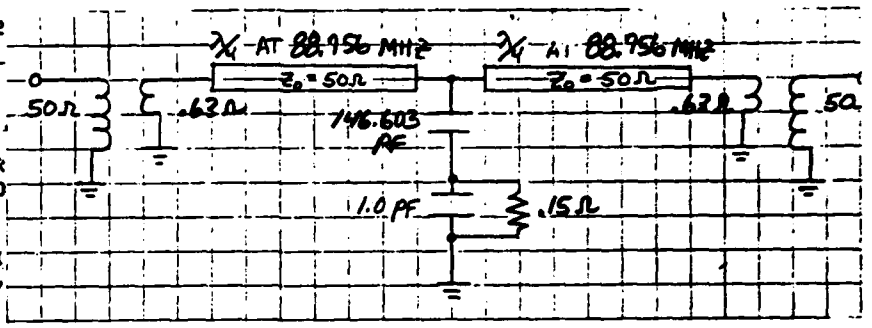

POLAR S-PARAMETERS IN 50.0 OHM SYSTEM

F MHZ	S11 (MAGN<ANGL)	S21 (MAGN<ANGL)	S12 (MAGN<ANGL)	S22 (MAGN<ANGL)	S21 DB
40.0	(0.99< -5)	(0.12< -96)	(0.119< -96)	(0.99< -5)	-18.46
42.0	(0.97< -11)	(0.22<-103)	(0.220<-103)	(0.97< -11)	-13.15
44.0	(0.19< 0)	(0.81<-178)	(0.806<-178)	(0.19< 0)	-1.88
46.0	(0.97< 12)	(0.20< 106)	(0.200< 106)	(0.97< 12)	-13.98
48.0	(0.99< 6)	(0.10< 98)	(0.098< 98)	(0.99< 6)	-20.17
50.0	(1.00< 4)	(0.06< 96)	(0.063< 96)	(1.00< 4)	-24.02
52.0	(1.00< 3)	(0.05< 94)	(0.045< 94)	(1.00< 3)	-26.84
54.0	(1.00< 3)	(0.04< 94)	(0.035< 94)	(1.00< 3)	-29.08
56.0	(1.00< 2)	(0.03< 93)	(0.028< 93)	(1.00< 2)	-30.95
58.0	(1.00< 2)	(0.02< 93)	(0.024< 93)	(1.00< 2)	-32.56
60.0	(1.00< 1)	(0.02< 92)	(0.020< 92)	(1.00< 1)	-33.96
62.0	(1.00< 1)	(0.02< 92)	(0.017< 92)	(1.00< 1)	-35.20
64.0	(1.00< 1)	(0.02< 92)	(0.015< 92)	(1.00< 1)	-36.32
66.0	(1.00< 1)	(0.01< 92)	(0.014< 92)	(1.00< 1)	-37.32
68.0	(1.00< 1)	(0.01< 91)	(0.012< 91)	(1.00< 1)	-38.24
70.0	(1.00< 1)	(0.01< 91)	(0.011< 91)	(1.00< 1)	-39.07
72.0	(1.00< 1)	(0.01< 91)	(0.010< 91)	(1.00< 1)	-39.84
74.0	(1.00< 0)	(0.01< 91)	(0.009< 91)	(1.00< 0)	-40.54
76.0	(1.00< 0)	(0.01< 91)	(0.009< 91)	(1.00< 0)	-41.19
78.0	(1.00< 0)	(0.01< 91)	(0.008< 91)	(1.00< 0)	-41.78
80.0	(1.00< 0)	(0.01< 91)	(0.008< 91)	(1.00< 0)	-42.32
82.0	(1.00< 0)	(0.01< 91)	(0.007< 91)	(1.00< 0)	-42.82
84.0	(1.00< 0)	(0.01< 91)	(0.007< 91)	(1.00< 0)	-43.27
86.0	(1.00< 0)	(0.01< 91)	(0.007< 91)	(1.00< 0)	-43.69
88.0	(1.00< 0)	(0.01< 91)	(0.006< 91)	(1.00< 0)	-44.07
90.0	(1.00< 0)	(0.01< 91)	(0.006< 91)	(1.00< 0)	-44.41
92.0	(1.00< 0)	(0.01< 90)	(0.006< 90)	(1.00< 0)	-44.72
94.0	(1.00< 0)	(0.01< 90)	(0.006< 90)	(1.00< 0)	-44.99

Figure E-15. Schematic and Computer Printout, Flauto-C Resonator Showing Absence of Second Passband

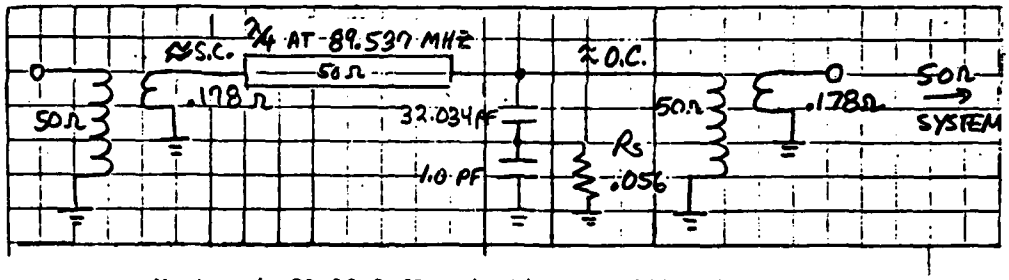

Meets +/- 2% 13.3 dB rejection specification

```
L FLT03.DATA
 FLT03.DATA
00010 TRF AA IM 50 .178
00020 TRL BB SE 50 90 89.537
00030 CAS AA BB
00040 CAP CC PA 32.034
00050 PRC DD PA -.056 1
00060 SER CC DD
00070 CAS AA CC
00080 TRF EE IM 50 .178
00090 CAS AA EE
00100 PRI AA S1 50
00110 END
00115 57.8 59 60.2
00130 END
00140 .0001
00145 0 0 10 -13.3
00150 0 0 10 -.5
00155 0 0 10 -13.3
00160 END
READY
COMPACT FLT03
COMPACT MICROWAVE ANALYSIS PROGRAM (VERSION 2.3) 6/12/76

ANAL(1),SENS(2),OPT(3),SWEEP(4),MAP(5)
 WRITE 1,2,3,4,5 OR 13(183):
?
1
                    POLAR S-PARAMETERS IN  50.0 OHM SYSTEM

   F          S11             S21             S12             S22          S21
  MHZ   (MAGN<ANGL)  ( MAGN<ANGL)  ( MAGN<ANGL)  (MAGN<ANGL)   DB

   57.8 (0.98< -13) ( 0.20< -12) (0.200< -12) (0.98< 170) -13.97
   59.0 (0.10<-178) ( 0.94< -89) (0.944< -89) (0.19< 179)  -0.50
   60.2 (0.98<  13) ( 0.20<-167) (0.199<-167) (0.98<-170) -14.02
```

Figure E-16. Schematic and Computer Printout, Helical Resonator Tuned to 59 MHz

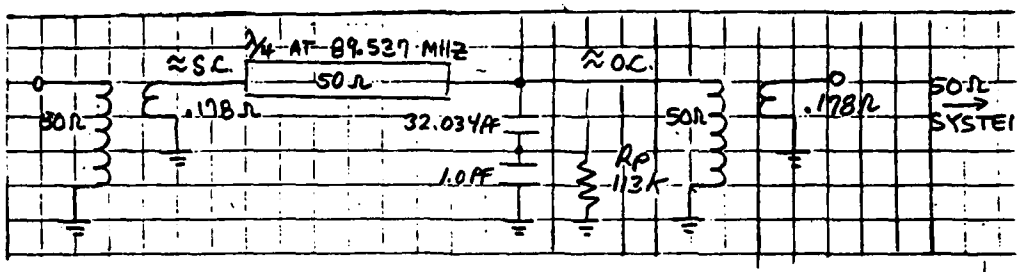

Meets +/- 2%, 13.3dB rejection specification.

```
L FLT03.DATA
 FLT03.DATA
00010 TRF AA IM 50 .178
00020 TRL BB SE 50 90 89.537
00030 CAS AA BB
00040 CAP CC PA 32.034
00050 PRC DD PA -113000 1
00060 SER CC DD
00070 CAS AA CC
00080 TRF EE IM 50 .178
00090 CAS AA EE
00100 PRI AA S1 50
00110 END
00115 86.2
00120 88
00125 89.8
00130 END
00140 .0001
00145 0 0 10 -13.3
00150 0 0 10 -.5
00155 0 0 10 -13.3
00160 END
READY
COMPACT FLT03
COMPACT MICROWAVE ANALYSIS PROGRAM (VERSION 2.3) 6/12/76

...AL(1),SENS(2),OPT(3),SWEEP(4),MAP(5)
 WRITE 1,2,3,4,5 OR 13(1&3):
?
1
                    POLAR S-PARAMETERS IN   50.0 OHM SYSTEM

   F          S11              S21              S12              S22          S21
   MHZ   (MAGN<ANGL)  ( MAGN<ANGL)  ( MAGN<ANGL)  (MAGN<ANGL)    DB

   86.2 (0.97< -12)  ( 0.21< -13)  (0.214< -13)  (0.97< 167)  -13.41
   88.0 (0.07< -36)  ( 0.94< -87)  (0.944< -87)  (0.07< 143)   -0.50
   89.8 (0.97<  12)  ( 0.22<-166)  (0.218<-166)  (0.97<-167)  -13.24
```

Figure E-17. Schematic and Computer Printout, Helical Resonator Tuned to 88 MHz

E.8 REFERENCES

1. A. Karp and W. Weir

   "Electronically Tunable High-Power Filter for Interference Reduction in Air Force Communications Systems," DITC Technical Report No. AD748810, Defense Technical Information Center, 1972.

2. A. Karp and L. N. Heynick

   "UHF Electronically Tunable High-Power Filter," RADC Final Technical Report No. RADC-TR-75-220, Rome Air Development Center, 1975.

3. A. Karp

   "Electronically Tunable UHF High-Power Filter, "RADC Final Technical Report No. RADC-TR-77-167, Rome Air Development Center, 1977.

4. G. L. Matthaei, L. Young, E.M.T. Jones

   "Microwave Filters, Impedance-Matching Networks, and Coupling Structures, "McGraw-Hill, N.Y., 1964.

5. "Unitrode PIN Diode Designers' Handbook and Catalog," Unitrode Corporation, 1981.

APPENDIX F

SHUNT CAPACITANCE BINARY BUS DESIGN

F.1 INTRODUCTION

This is a clarified version of work described in the Third Quarterly Report.

A preliminary model of a helical resonator and the shunt capacitive bus is shown in Figure F-1. The 30 and 88 MHz resonator parameters are obtained from Figure 4.5 of the Third Quarterly Report. At 30 MHz, 63.877 pF is needed for resonance, and at 88 MHz, 2.11 pF is needed for resonance. The desired state of the PIN Diode switches, and the on/off diode parameters are also shown.

A description of the calculator program used to analyze the circuit shown in Figure F-1 is given in Figure 5-20 of the main text of this report.

F.2 INITIAL RESULTS

The circuit shown in Figure F-1 was analyzed at 30 MHz. The results are shown in Table F-1.

- A value of 3500 was used for the Q of each of the tuning capacitors, and each branch has a series inductance of 0.075 nH
- The desired capacity was 63.88 pF, the actual array capacitance is 66.01 pF
- Even with a series diode "on" resistance of only 0.2 ohms, the capacitor bus unloaded Q is only 415
- The actual resonant frequency is 29.51 MHz and the final value of the resonator unloaded Q is 331. This error in the resonant frequency can be compensated for as long as it is a known error
- The diode "off" parallel resistance and capacitance are dominant factors regarding the Q of the individual branches

- For a loaded Q of 113, the insertion loss would be -3.63 dB. This resonator is thus unsuitable for the FHMUX.

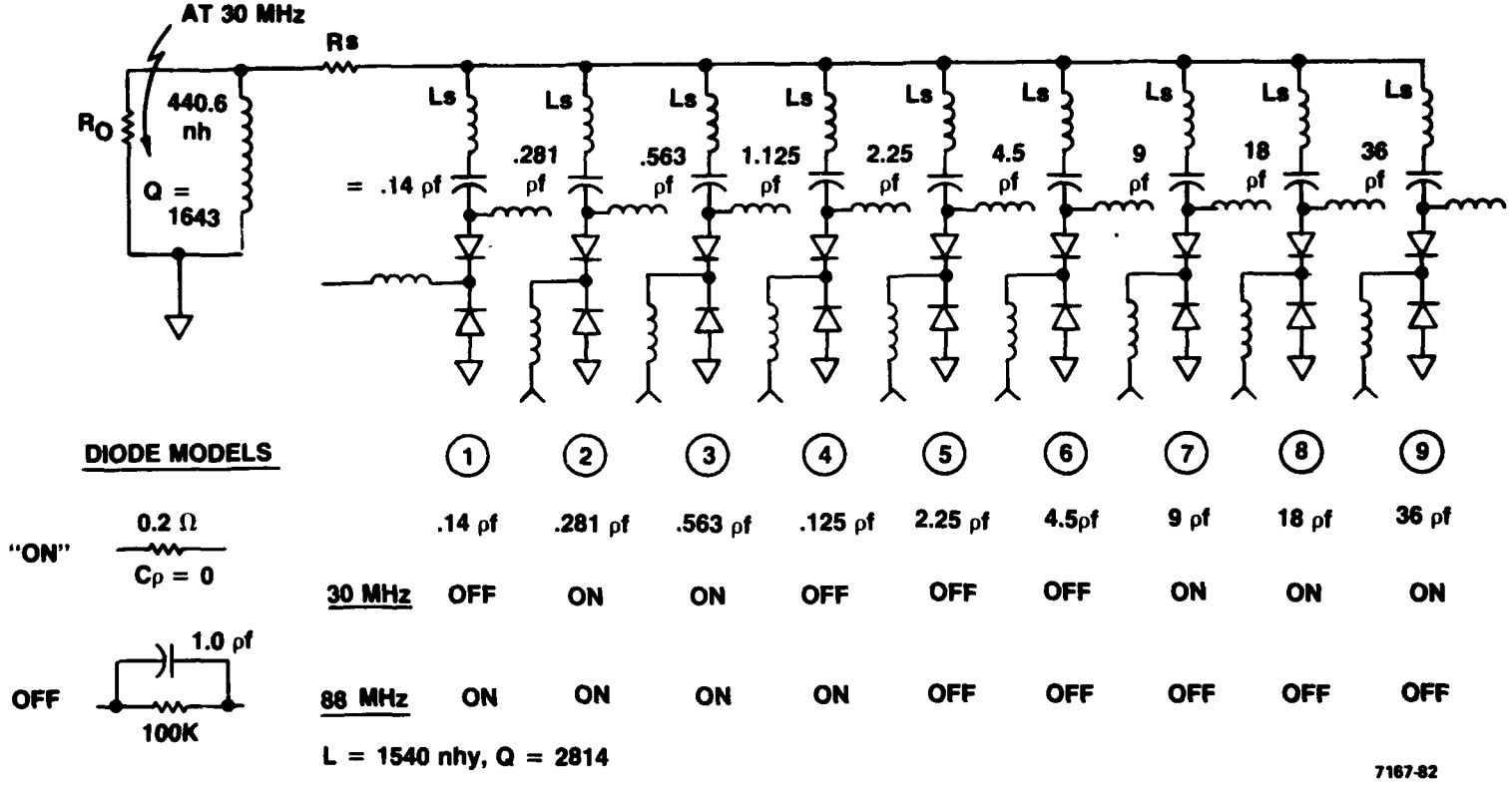

Figure F-1. Preliminary Model Capacitance Bus

TABLE F-1. FILTER ANALYSIS AT 30 MHZ

DIODE STATE	BRANCH ANALYSIS		DIODE STATE	BRANCH ANALYSIS	
	0.	RS		9. 00	C,PF
	0.075	L,NH		3.5 03	Q
	1.4-01	C,PF	OFF	2.-01	RP
OFF	3.5 03	Q		0. 00	CPPF
	1. 05	CPPF		9.0002159 00	C,PF
	3.01	FMHZ		1.5999455 03	Q
	1.2286435-01	C,PF			
	1.4841943 02	Q		1.8 01	C,PF
				3.5 03	Q
	281-01	C,PF		2.-01	RP
	3.5 03	Q	ON	0. 00	CPPF
ON	2.-01	RP		1.8000863 01	C,PF
	0. 00	CPPF		1.0369738 03	C,PF
	2.8100021-01	C,PF			
	3.3748672 03	Q		3.6 01	C,PF
				3.5 03	Q
	5.63-01	C,PF	ON	2.-01	RP
	3.5 03	Q		0. 00	CPPF
	2. -01			3.6003454 01	C,PF
ON	0. 00	CPPF		6.0862793 02	Q
	5.6300084-01	C,PF			
	3.2579727 03	Q	TOTAL CAPACITY (F) AND Q OF BUS		
	1.125 00	C,PF			
	3.5 03	Q	6.6014108 01	C,PF	
	1. 05	RP	4.1479837 02	Q	
OFF	1. 00	CPPF			
	5.3047892-01	C,PF			
	3.5533276 01	Q	RESONATOR INDUCTANCE (nH) AND Q		
	2.25 00	C,PF			
	3.5 03	Q	4.4061 02	L,NH	
	1. 05	RP	1.643 03	Q	
OFF	1. 00	CPFF			
	6.9413373-01	C,PF			
	2.7220808 01	Q	RESONANT FREQUENCY IN MHA, AND OVERALL Q.		
	4.5 00	C,PF			
	3.5 03	Q	2.9510445 01	FMHZ	
	1. 05	RP	3.3118586 02	Q	
OFF	1. 00	CPPF			
	8.2073346-01	C,PF			
	2.3049598 01	Q			

- The helical resonator unloaded Q is not the dominant parameter in the overall filter design for this configuration
- The Q of the capacitive bus is dominant.

When the model shown in Figure F-1 is configured for 88 MHz operation, the required value of capacitance for resonance is only 2.116 pF. The 88 MHz analysis is shown in Table F-2. Again, performance is inadequate. The resonant frequency is well below 88 MHz, and the unloaded Q is only 89.5. As shown, the Q of the branches is very low.

F.3 ANALYSIS OF PROBLEM AREAS

The capacitive Bus Connection Point is one of the main problem areas. At resonance, the parallel resistance of the filter should be very high in order to have a high unloaded Q. Placing the shunt capacitive bus across the "open ended" point of the helical resonator has a drastic effect on the Q of the resonant circuit.

In order to achieve success with the shunt reactive bus as modeled in Figure F-1, the following diode parameters are required:

Ron	<	.1 ohms
Rp	=	10 Meghoms
Cp	=	0.1 pF-2 pF

Clearly, these parameters will not soon be available with PIN Diodes or FETS. It is felt that a special form of Reed relay could approach the needed performance, but careful design would be needed to provide switch plus bounce times compatible with the slow frequency hopping case. The fast frequency hopping case will always require electronic switching.

Table F-3 depicts performance obtained with relay type parameters. The results are better but still below the requirements. The ratio of unloaded to loaded Q is only 8.9, so the insertion loss would be -1.04 dB.

TABLE F-2. FILTER ANALYSIS AT 88 MHz

DIODE STATE	BRANCH ANALYSIS		DIODE STATE	BRANCH ANALYSIS	
	0.	RS		9. 00	C,PF
	0.075	L,NH		3.5 03	Q
	1.4-01	C,PF		1. 05	RP
	3.5 03	Q	OFF	1. 000	CPPF
ON	2.-01	RP		9.0109316-01	C,PF
	0. 00	CPPF		6.1395894 01	Q
	8.8 01	FMHZ			
	1.4000045-01	C,PF		1.8 01	C,PF
	3.320086 03	Q		3.5 03	Q
				1. 05	RP
	2.81-01	C,PF	OFF	1. 00	CPPF
	3.5 03	Q		9.4857975-01	C,PF
ON	2.-01	RP		5.8373632 01	Q
	0. 00	CPPF			
	2.8100181-01	C,PF		3.6 01	C,PF
	3.156608 03	Q		3.5 03	Q
			OFF	1. 05	RP
	5.63-01	C,PF		1. 00	CPPF
	3.5 03	Q		9.7425071-01	C,PF
ON	2.-01	RP		5.6860507 01	Q
	0. 00	CPPF			
	5.6300727-01	C,PF	TOTAL CAPACITY (PF)		
	2.8737482 03	Q	AND Q OF BUS		
	1.125 00	C,PF	6.4446469 00	C,PF	
	3.5 03	Q	9.2445237 01	Q	
ON	2.-01	RP			
	0. 00	CPPF			
	1.125029 00	C,PF	RESONATOR INDUCTANCE		
	2.4382398 03	Q	(nH) AND Q		
	2.25 00	C,PF	1.54 03	L,NH	
	3.5 03	Q	2.814 03	Q	
	1. 05	RP			
OFF	1. 00	CPPF			
	6.9295435-01	C,PF	RESONANT FREQUENCY IN		
	7.9418586 01	Q	MHZ, AND OVERALL Q		
	4.5 00	C,PF	5.0522588 01	FMHZ	
	3.5 00	Q	8.9504834 01	Q	
	1. 05	RP			
OFF	1. 00	CPPF			
	8.1908515-01	C,PF			
	6.7424524 01	Q			

TABLE F-3. FILTER PERFORMANCE WITH LOW CAPACITANCE RELAY PARAMETERS

DIODE STATE	BRANCH ANALYSIS	
	0.	RS
	0.075	L,NH
	1.4-01	C,PF
	3500.	Q
ON	0.2	RP
	0.	CPPF
	8.8 01	FMHZ
	1.4000045-01	C,PF
	3.320086 03	Q
	0.281	C,PF
	3.5 03	Q
ON	2.-01	RP
	0. 00	CPPF
	2.8100181-01	C,PF
	3.1566608 03	Q
	5.63-01	C,PF
	3.5 03	Q
	2.-01	RP
ON	0. 00	CPPF
	5.6300727-01	C,PF
	2.8737482 03	Q
	1.125 00	C,PF
	3.5 03	Q
ON	2.-01	RP
	0. 00	CPPF
	1.125029 00	C,PF
	2.4382398 03	Q
	2.25 00	C,PF
	3.5 03	Q
OFF	1. 07	RP
	1.-01	CPPF
	9.6661506-02	C,PF
	5.7936684 02	Q
	4.5 00	C,PF
	3.5 03	Q
OFF	1. 07	RP
	1.-01	CPPF
	9.8783407-02	C,PF
	5.6894485 02	Q

DIODE STATE	BRANCH ANALYSIS	
	9. 00	C,PF
	3.5 03	Q
OFF	1. 07	RP
	1.-01	CPPF
	9.987968-02	C,PF
	5.6370592 02	Q
	1.8 01	C,PF
	3.5 03	Q
OFF	1.07	RP
	1.-01	CPPF
	1.0043699-01	C,PF
	5.6107942 02	Q
	3.6 01	C,PF
	3.5 03	Q
OFF	1. 07	RP
	1.-01	CPPF
	1.0071799-01	C,PF
	5.5976441 02	Q

TOTAL CAPACITY (PF) AND Q OA BUS

2.6055173 00 C,PF
1.5647869 03 Q

RESONATOR INDUCTANCE (nH) AND Q

1.54 03 L,NH
2.814 03 Q

RESONANT FREQUENCY IN MHZ, AND OVERALL Q

7.9453466 01 FMHZ
1.0056005 03 Q

Relay Parameters

Off Capacitance - 0.1pf
Off Resistance - 10 meg ohms
On Resistance - 0.2 ohms

At 88 MHz:

Reasonable Accuracy
Qu (1000) Moderate

Table F-4 shows the effect of an increased "off" capacity. The parameters remained the same as in Figure 4-10, but the"off" capacity was increased from 0.1 to 2.0 pF. This resulted in much higher unloaded Q (over 5500), but the on/off capacity ratio suffered considerably, and hence tuning accuracy is very poor.

F.4 COMMENT

Recent work by Karp (Reference 9 and 10) showed that a transmission line resonator could be tuned by capacitively tapping the line at several lower impedance points. A loaded Q of 200 was achieved with an insertion loss of about 2 dB, when tuning from 350 to 400 MHz.

In addition, the structure of the shunt reactive bus should be changed. The bus eventually may have three main sections, as noted below.

The three or four shunt elements having the highest value of capacity will probably have to be well isolated from the rest of the bus when they are in the off state.

A better means of Achieving the needed fine grain tuning is needed. In addition, a high Q trimmer capacitor will probably be needed to accommodate manufacturing tolerance variations. This will result in a high resolution section of the bus, probably at a location which is tapped well down from the high impedance "open ended" area.

A third section would contain all other elements of the bus.

TABLE F-4. FILTER PERFORMANCE WITH HIGH CAPACITANCE RELAY PARAMETERS

DIODE STATE	BRANCH ANALYSIS	
	0.	RS
	0.075	L,NF
	1.4-01	C,PF
	3.5 03	Q
ON	2.-01	RP
	0. 00	CPPF
	8.8 01	FMHZ
	1.4000045-010	C,PF
	3.320086 03	Q
	2.81-01	C,PF
	3.5 03	Q
	2.-01	
ON	0. 00	CPPF
	2.8100181-01	C,PF
	3.1566608 03	Q
	5.63-01	C,PF
	3.5 03	Q
	2.-01	RP
ON	0. 00	CPPF
	5.6300727-01	C,PF
	2.8737482 03	Q
	1.125 00	C,PF
	3.5 03	Q
	2.-01	RP
ON	0. 00	CPPF
	1.125029 00	C,PF
	2.4382398 03	Q
	2.25 00	C,PF
	3.5 03	Q
	1. 07	
OFF	2. 00	CPPF
	1.0591295 00	C,PF
	5.484478 03	Q
	4.5 00	C,PF
	3.5 03	Q
OFF	1. 07	RP
	2. 00	CPPF
	1.3851386 00	C,PF
	6.644031 03	Q

DIODE STATE	BRANCH ANALYSIS	
	9.00	C,PF
	3.5 03	Q
	1. 07	RP
OFF	2. 00	CPPF
	1.6370945 00	C,PF
	7.9416984 03	Q
	1.8 01	C,PF
	3.5 03	Q
OFF	1. 07	RP
	2. 00	CPPF
	1.800843 00	C,PF
	9.0966867 03	Q
	3.6 01	C,PF
	3.5 03	Q
OFF	1. 07	RP
	2. 00	CPPF
	1.8957167 00	C,PF
	9.9330953 03	Q

TOTAL CAPACITY (PF)
AND Q OF BUS

9.887002 00 C,PF
5.5387432 03 Q

RESONATOR INDUCTANCE
(nH) AND Q

1.54 03 L,NH
2.814 03 Q

RESONANT FREQUENCY
IN MHZ, AND OVERALL Q

4.0787533 01 FMHZ
1.8659766 03 Q

Relay Parameters

Off Capacitance - 2pf
Off Resistance - 10 meg ohms
On Resistance - 0.2 ohms

At 88 MHz
Higher Qu
Poorer on/off Ratio

APPENDIX G

BLOCKAGE RATE OF THE FHMUX

The purpose of this appendix is:

1. To provide additional detail on the simulation of the blockage rate for the frequency hopping multiplexer.
2. To provide an approximate analytical calculation that corroborates the simulation.
3. To provide a further interpretation of the results to preclude any misunderstanding as to the regime of their applicability.

Figure 4.3 illustrates the system for which blockage rate calculations are to be performed. Five transceivers are connected to the FHMUX. Transceiver Number 1 has highest priority; Number 5, the lowest. Five blockage probabilities are to be calculated as follows:

1. The probability that Transceiver Number 1 is blocked from receiving a signal by a transmission from a higher priority transmitter. (Identically zero since there are no higher priority transmitters).
2. The probability that Transceiver 2 is blocked from receiving a signal by a transmission from a higher priority transmitter. (Number 1 is the only higher priority transmitter).
3. The probability that Transceiver 3 is blocked from receiving a signal by a transmission from a higher priority transmitter. (Either Number 1 or 2).
4. The probability that Transceiver 4 is blocked from receiving a signal by a transmission from a higher priority transmitter. (Either 1, 2, or 3).
5. The probability that Transceiver 5 is blocked from receiving a signal by a transmission from a higher priority transmitter. (Any of the other transceivers).

For the purpose of the calculation, a receiver is blocked when one or more higher priority transceivers are transmitting within the receiver's -40dB bandwidth (reference the receiver's frequency). Each of the five cases listed above was simulated. For each single event of the simulation, a receiver frequency was picked at random; an appropriate number of transmitter frequencies were independently picked at random; the event was defined as a blocked event if any transmit frequency was within the receiver's bandwidth. A large

number of events were exercised (20,000) for each simulation run. The ratio of the blocked events to the total number of events in a run is defined as the probability of being blocked.

The simulation results are summarized in Table 4-4 where the entries of the table under "User Number 1" are to be identified with the first probability listed above; the tabulated entries under "User Number 2" are to be identified with the second probability listed above, etc.

In addition to the simulation results, the blockage probability can be calculated analytically. Note that the blockage probability is equal to 1 minus the probability of not being blocked. That is,

$$P_B = 1 - P_{NB} \tag{1}$$

The probability of not being blocked is the probability that any one of the independently hopping transmitters will not hop within the receiver's -40dB bandwidth. That is,

$$P_B = 1 - (P_{nb})^m \tag{2}$$

where m is the number of transmitters (between 0 and 4) and P_{nb} is the probability that an individual transmitter will not hop within the receiver's -40 dB bandwidth.

In order to get the probability of an individual transmitter not hopping within the receiver's bandwidth, first note that the ratio of the average of the receiver's -40 dB bandwidth to the total hopping bandwidth is,

$$r = \frac{0.1 \quad (f_U + f_L)/2}{f_U - f_L} = 0.1 \frac{(59)}{58} = 0.10172 \tag{3}$$

where r is the bandwidth ratio, the multiplier 0.1 occurs because the -40 dB bandwidth is assumed to span $\pm$ 5% or 0.1 times the receiver's operating frequency, f_U is the upper frequency of the hopping range (80 MHz in the SINCGARS example), f_L is the lower frequency of the hopping range (30 MHz in the SINCGARS example), $(f_U + f_L)/2$ is the average value of the receiver's operating frequency (59 MHz in the

SINCGARS example) and ($f_U - f_L$) is the hopping frequency bandwidth (58 MHz in the SINCGARS example). The ratio r is approximately 10% for the case of a $\pm$ 5% (-40 dB) bandwidth and the SINCGARS frequencies.

When a transmitter in the blockage scenario picks a frequency, approximately 90% of the hopping bandwidth is available in which the receiver is not blocked. That is,

$$P_{nb} = 1 - r = 0.89828$$

where P_{nb} is the probability that a single transmitter will not block the target receiver and r is the receiver's occupied bandwidth expressed as a percentage of the hopping bandwidth.

Then the blockage rate for the receiver is

$$P_B = 1 - (1 - r)^m \tag{4}$$

where r is the receiver occupied bandwidth ratio and m is the number of possible blocking transmitters.

For r small,

$$P_B \approx m\ r \tag{5}$$

Table G-1 summarizes some simulated and calculated results. The simulated results are taken directly from those previously provided in Table 4-4 for the case of a $\pm$ 5% (-40 dB) bandwidth. The analytical results are calculated from equation 4 above. The probabilities P_{B1} to P_{B5} are the blockage probabilities for the first to fifth receiver as defined at the opening of the appendix.

The tabulated entries show simulation and analysis. The latter is likely to have the lesser accuracy since the percent bandwidth occupied by the receiver is approximated as the average value at the center of the band.

Equation 5 indicates for sufficiently small r (the receiver occupied bandwidth ratio), the tabulated entries should be linear in m, the number of interfering transmitters. The linear relation is only somewhat followed in the tabulated entries. For $r \approx 0.1$ as in the table, the approximation is not sufficiently exact.

TABLE G-1. COMPARISON OF BLOCKAGE PROBABILITIES FROM SIMULATED AND ANALYTICAL MODELS

	P_{B1} m = 0	P_{B2} m = 1	P_{B3} m = 2	P_{B4} m = 3	P_{B5} m = 4
SIMULATION RESULTS	0	0.10070	0.18895	0.26705	0.33660
ANALYTICAL RESULTS	0	0.10172	0.19310	0.27518	0.34891

Certain constraints apply to the results discussed in this appendix and in the main test, particularly as presented in Table 4-4.

1. The blockage rate applies to a receiver blocked by one or more higher priority transmitters. Neither the simulation nor the analytical calculation "double count." That is, if a receiver is blocked by more than one transmitter in a single event, this counts as only one blockage.

2. The results of the appendix are only for $\pm$ 5% receiver bandwidth. The main test includes simulations for lesser bandwidths. When the analytical results, calculated from Equation 4 of this appendix, are compared to the simulation results of the main text, there is close agreement.

3. The results of this section and those tabulated in Table 4-4 apply to a fixed priority scheme. The main text treats the rotating priority scheme.

4. The blockage ratio, as tabulated, generally requires the occurrence of a number of simultaneous events, best described statistically. For example P_{B5} applies when four higher priority transmitters are simultaneously transmitting. Further, the receive blockage events are only relevant when the receiver is receiving an active distant transmission.

5. The blockage probabilities discussed herein are testable when prototype hardware is built and tested along with SINCGARS hopping radios.

6. In another use of the FHMUX scenario, there are multiple distant transmitters operating in independent frequency hopping nets with the local transceivers operating on the received signals. Occasionally, nearly the same frequency is used in the independent nets. The receiver operation at the FHMUX is deleteriously affected only when the hop frequencies are within the -3 dB bandwidth of the FHMUX filter (rather than the -40 dB bandwidth as in the transmitter to receiver scenario discussed previously). By appropriate tuning of the FHMUX filters, the received signals can be power split between the affected receivers. Since external atmospheric or man-made noise is also power split, the received signal to noise ratio is not necessarily deleteriously affected. In any case, the blockage rate, defined for this scenario as being within the -3 dB bandwidth, is lower than that for the transmitter-receiver coupling scenario previously described since the -3 dB bandwidth is narrower than the -40 dB bandwidth.

FREQUENCY HOPPING MULTIPLEXER FEASIBILITY MODEL

FINAL REPORT

NOVEMBER 1982

PREPARED FOR
USA CORADCOM
ON CONTRACT
DAAK80-80-C-0588

Systems

Communication Systems Division
GTE Communications Products Corporation
77 "A" Street
Needham Heights, MA 02194
Area Code 617 449-2000
TELEX: 922497

FREQUENCY HOPPING MULTIPLEXER

FEASIBILITY MODEL

FINAL REPORT

NOVEMBER 1982

Prepared For:

USA CORADCOM
Contract No. DAAK80-C-0588

Communication Systems Division
GTE Communications Products Corporation
77 "A" Street
Needham Heights, Mass. 02194

TABLE OF CONTENTS

Section	Title	Page
	ABSTRACT	1
1	INTRODUCTION	3
1.1	Program Description	3
1.2	Report Organization	4
2	JUSTIFICATION FOR RESONATOR DESIGN	5
3	RESONATOR DESIGN	9
3.1	Baseline Design	9
3.2	Coupling Study	12
3.3	Justification of Losses	15
3.4	Resonator Comments	16
4	PIN DIODE EVALUATION AND BIAS CIRCUIT DESIGN	19
4.1	Introduction	19
4.2	PIN Diode Test Circuit	19
4.3	PIN Diode Test Data	22
4.4	Calculation of Diode Parameters	24
5	SHUNT CAPACITIVE BUS DESIGN	27
5.1	Introduction	27
5.2	Tuning Range	27
5.3	Design of Coarse and Medium Range Tuning Sections	30
5.4	Discussion of Problem Areas	42

TABLE OF CONTENTS (Cont.)

Section	Title	Page
6	SYSTEM TESTS	43
6.1	Introduction	43
6.2	Loss Analysis of Quad-Hybrid Couplers	46
6.3	Load Pulling Tests	49
6.3.1	Introduction	49
6.3.2	Load Pulling Test Setup and Procedure	49
6.3.3	Comments, Load Pulling Data	57
6.4	Channel Isolation and Combining Loss	57
6.4.1	Combining Losses	57
6.4.2	Channel Isolation	59
6.4.3	Comments Regarding Systems Data	59
6.4.4	Calibration Data	65
7	CONCLUSIONS AND RECOMMENDATIONS	69
7.1	Conclusions	69
7.2	Comment	69
7.3	Recommendations	70
8	BIBLIOGRAPHY	71
9	APPENDIX A	73
9.1	Vendor Data Sheets	73

LIST OF FIGURES

Figure	Title	Page
3-1	Breadboard Resonator	10
3-2	Two Tap System	14
4-1	PIN Diode Test Circuit	21
5-1	Schematic, 50-88 MHz Frequency Hoppable Bandpass Filter	28
5-2	Distance From Short vs. "Effective Capacity"	31
5-3	Distance From Short vs. "Effective Capacity"	32
5-4	FHMUX Feasibility Model Resonator Design	34
5-5	Mechanical Configuration, 4 Bit Coarse Tuning Section	35
5-6	Mechanical Configuration, 8 Bit Frequency Hoppable Bandpass Filter	36
6-1	Block Diagram, FHMUX Feasibility Model	44
6-2	FHMUX Feasibility Model	45
6-3	Quad-Hybrid Coupler Test Fixtures	47
6-4	Quad-Hybrid Coupler Loss Data	48
6-5	Load Pulling Test Setup	50
6-6	Load Pulling Data Baseline, Zl= 50 ohms	52
6-7	Load Pulling Data: VSWR = 4.0:1, 0 = 0^{o}, 180^{o}	53
6-8	Load Pulling Data: VSWR = 4.0:1, 0 = $+/-45^{o}$	54
6-9	Load Pulling Data: VSWR = 4.0:1, 0 = $+/-90^{o}$	55
6-10	Load Pulling Data: VSWR = 4.0:1, 0 = $+/-135^{o}$	56
6-11	Combining Loss Data	58
6-12	System Data	60
6-13	System Data	61
6-14	System Data	62

LIST OF FIGURES (Cont.)

Figure	Title	Page
6-15	System Data	63
6-16	Switch Identification	66
9-1	ATC 100 Chip Capacitor Data Sheet	74
9-2	ATC 175 Ultra High Q Capacitor Data Sheet	75
9-3	Microwave Associates 4P506 PIN Diode Data Sheet	76
9-4	Unitrode UM6200 Series PIN Diode Data Sheet	77
9-5	Unitrode UM6200 Series PIN Diode Data Sheet (Cont.)	78
9-6	Unitrode UM6200 Series PIN Diode Data Sheet (Cont.)	79
9-7	Unitrode UM7200 Series PIN Diode Data Sheet	80
9-8	Unitrode UM7200 Series PIN Diode Data Sheet (Cont.)	81
9-9	Unitrode UM7200 Series PIN Diode Data Sheet (Cont.)	82

LIST OF TABLES

Table	Title	Page
2-1	Helical Resonator Design	5
3-1	Resonator Baseline Data	11
3-2	Comparison of Tapping Methods	13
3-3	Loss Justification	16
4-1	PIN Diode Specification	20
4-2	PIN Diode Evaluation Data	23
4-3	PIN Diode Parameters as Calculated From Measured Data	24
5-1	Required Capacitance vs. Desired Resonant Frequency	33
5-2	Data Sets	38
5-3	3 Bit Shunt Capacitive Bus Data	39
5-4	Performance Data, Breadboard 8 Bit Capacitive Bus	41
6-1	Channel 1 Calibration and Insertion Loss Data	67
6-2	Channel 2 Calibration and Insertion Loss Data	68

ABSTRACT

This GTE Sylvania Final Report completes a successful program to prove the design concept and demonstrate equipment feasibility for a VHF Frequency Hopping Multiplexer (FHMUX). This is a continuation of the FHMUX Design Assessment Program, which develops and explains an approach to permit the operation of up to five frequency hopping transceivers, in the 30-88 MHz frequency range, with a common wideband antenna.

The results of the program are positive. The FHMUX will perform as required and also enhance certain transceiver performance parameters such as broadband transmitter noise rejection, more constant transmitter loading, and increased receiver selectivity. These positive results should encourage the design and development of an FHMUX advanced engineering model.

SECTION 1

INTRODUCTION

1.1 PROGRAM DESCRIPTION

This Final Report describes the design and evaluation of a frequency hoppable multiplexer (FHMUX) feasibility model to operate in the 50-88 MHz range. The FHMUX Design Assessment Final Report discusses the need to divide the 30-88 MHz frequency range into two segments; 30 to approximately 50 MHz, and 50-88 MHz. The upper frequency range was selected for the FHMUX feasibility model because the most severe RF switching problem, circuit stray capacitance, has the greatest tuning effect at the high frequency range.

The brassboard feasibility model consists of two filter couplers, and adequately demonstrates the feasibility of the GTE Sylvania FHMUX concept. This model shall serve as a performance baseline for future refinements and improvements.

The FHMUX system designed herein consists of frequency agile bandpass filters combined with quadrature couplers to produce filter couplers. These individual filter couplers are then multiplexed together to provide two channels of FHMUX operation.

A breadboard resonator was designed, built, and tested, and the RF signal input/output coupling structures were optimized. Initial filter tuning was accomplished with high Q chip capacitors.

Electronically tuneable capacitive busses were then designed and built using the best available PIN Diodes, and were installed in the resonators in place of all of the fixed values of capacitance. This provided an electronically switchable mode for the bandpass filters.

After the resonator and PIN Diode switched capacitive bus designs were finished, two complete electrically tuneable filter-coupler assemblies were fabricated and tested. They were then combined to form the two channel FHMUX feasibility model.

The model was evaluated for insertion loss, channel isolation, and load pulling. Channel isolation under load VSWR conditions was better than expected. Intermodulation distortion and harmonic generation observations at a 0.1 watt level were also performed.

1.2 REPORT ORGANIZATION

This is a hardware oriented report, and the theoretical justification for this work is contained in the FHMUX Design Assessment Final Report, and not contained herein. This Feasibility Model Final Report is organized as shown below:

Section 2	Justification for Resonator Design
Section 3	Resonator Design
Section 4	PIN Diode Evaluation and Circuit Design
Section 5	Shunt Capacitive Bus Design
Section 6	System Tests
Section 7	Conclusions and Recommendations
Section 8	Bibliography
Section 9	Appendix A

SECTION 2

JUSTIFICATION FOR RESONATOR DESIGN

The FHMUX Design Assessment effort recommended the use of helical resonators. The only other suitable inductive element is the standard transmission type quarter wave resonator.

When the feasibility study began, the helical resonator design was addressed in detail. It was decided to set the frequency range of the model at 56-88 MHz, a bandwidth of 45.6%. The low band would thus cover 30-56 MHz, a bandwidth of 63%. The differences in percent bandwidth were made to compensate for possible problem areas in the design of the shunt capacitive bus.

A first helical resonator design was performed, and the results are shown in Table 2-1. The design equations which were used are contained in Handbook of Filter Synthesis, by A. Zverev, Pages 499-502.

TABLE 2-1. HELICAL RESONATOR DESIGN (ROUND)

Desired unloaded Q	3000
Self Resonant Frequency	110 MHz
Minimum Diameter	5.72 Inches
Assigned Diameter	6.0 Inches
Diameter of Helix	3.3 Inches
Length of Helix	4.95 Inches
Turns Per Inch	.584
Number of Turns	2.88
Height of Resonator	7.95 Inches
Diameter of Wire	0.856 Inches
Characteristic Impedance	148.5 OHMS
Unloaded Q	3146
Capacity Needed to Resonate at 88 MHz	5.00 pF
Volume	225 Cubic Inches

A review of the design parameters showed that the helix wire diameter was required to be 0.856 inches. A mandrel with a diameter of 2.44 inches would have to be machined, and the helix wound on it. The need for extensive precision machining (especially if changes were needed), and the difficulty in soldering and fixturing such heavy wire, would seriously compromise the design flexibility and increase fabrication costs.

Further, a review of Table 2-1 shows that only 5.0 pF of capacity in the shunt bus would resonate the filter at 88 MHz. This value of 5.0 pF would have to include all stray capacitances in the circuit. This is another limitation of the helical resonator.

Therefore a more flexible, less critical form of resonator was needed, if the feasibility model was to accomplish its goals. Since physical size was not of importance at this time, a transmission line quarter wave resonator design was started.

The design equations for the quarter wave resonator were found on Pages 191 and 192 of Radio Engineers Handbook, First Edition, by Dr. Frederick E. Terman.

Most quarter wave resonators are designed to have a characteristic impedance of 75 ohms. This results in the minimum attenuation per foot. The derivation of this is given in Microwave Filters, Impedance Matching Networks, and Coupling Structures, by G. Mathaei, L. Young, and E.M.T. Jones, Pages 165-166, published by Artech House.

Expensive machining was not necessary for this type of resonator, and it was quickly discovered that a four inch diameter outer conductor, and a one inch diameter inner conductor would give a 75 ohm characteristic impedance. These parts were readily available (standard plumbing items), and the self resonant frequency could be easily changed by merely changing the length of the inner conductor.

The reactance of the quarter wave resonator is given on page 192 of Radio Engineers Handbook as:

$$Xs = j\ Zo \tan (2\pi\ \ell/\lambda) \qquad (1)$$

Where Zo is the characteristic impedance in ohms, ℓ is the resonator length, and λ is the wavelength of the self resonant frequency.

This is essentially the same expression as that used for a helical resonator. A quarter wave resonator with a characteristic impedance of 75 ohms will have about half as much inductive reactance as the helical resonator described in Table 2-1, which has a characteristic impedance of 148 ohms. This means that about 10 pF of capacity (instead of 5) will resonate the filter at 88 MHz. This eases the design of the capacitive bus.

Thus, the quarter wave resonator was chosen for use in the feasibility model.

SECTION 3

RESONATOR DESIGN

3.1 BASELINE DESIGN

As noted, the quarter wave resonator was selected for use in the feasibility model. Two sections of hard drawn copper pipe were used for the breadboard resonator, and the basic means of construction is shown in Figure 3-1.

The inner diameter of the four inch section was measured and found to be 3.960 inches, and the outer diameter of the one inch section was found to be 1.124 inches. The characteristic impedance of a concentric transmission line is given by this equation:

$$Zo = \frac{138}{\sqrt{\varepsilon}} \log D/d \qquad (2)$$

Where ε is the dielectric constant, D is the inside dimension of the outer conductor, and d is the outside dimension of the inner conductor.

The impedance of the breadboard resonator is thus calculated to be 75.48 ohms, which is very close to the desired minimum loss value mentioned earlier.

Since the desired self resonant frequency was 110 MHz, the length of the inner conductor was set to be a quarter wavelength at 110 MHz. This length was calculated to be 26.84 inches, using the equation.

$$\lambda = 300/f \qquad (3)$$

Where λ is the wavelength in meters, and f is the frequency in megacycles.

The inner pipe sits down in an endcap which is about 0.1 inches thick, so the actual pipe length was set to be 26.75 inches.

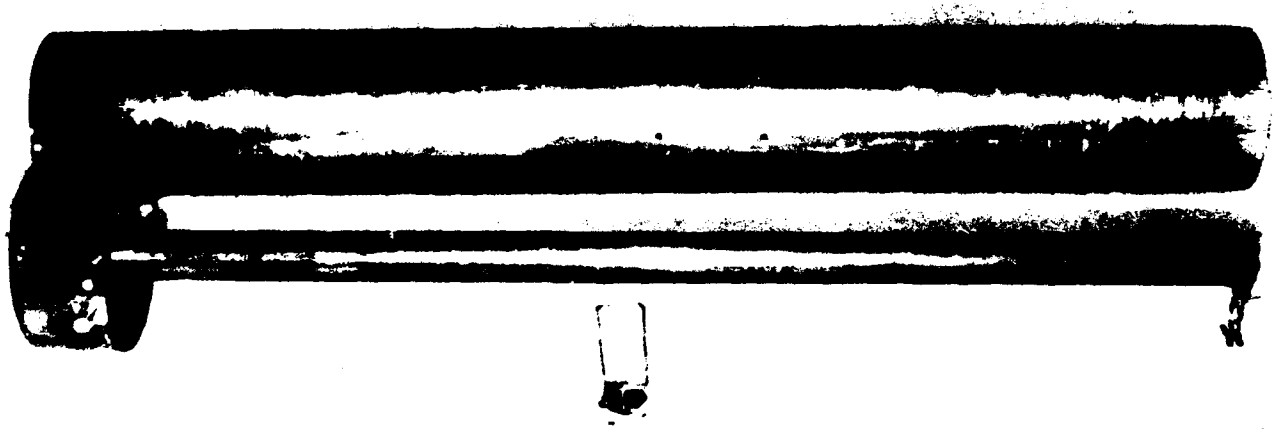

82-263F
9742-82

Figure 3-1. Breadboard Resonator

The unloaded Q of this resonator is calculated using equation 69 on page 192 of Radio Designers Handbook.

$$Q = 0.0839 \sqrt{f}\ bH \qquad (4)$$

Where f is in Hz
b = 3.96 inches
h = 0.98 (Figure 53)

thus, $Q = 3415$

The resonator was assembled, and relatively small input and output coupling loops were installed and aligned for minimum insertion loss at the self resonant frequency.

Baseline data was taken with no capacitive resonating elements in order to characterize the resonator alone. This data is summarized in Table 3-1.

TABLE 3-1. RESONATOR BASELINE DATA

Self Resonant Frequency	108.166 MHz
Insertion Loss	-0.376 dB
Loaded Q	116.31

The unloaded Q of the resonator can be obtained from the measured data and compared with the previously calculated value of 3415. The insertion loss of a resonant circuit is given by the ratio of unloaded to loaded Q, as shown in the FHMUX Design Assessment Final Report.

$$L = 20 \log \frac{Qu/QL}{Qu/QL - 1} \quad (5)$$

Where Qu is the unloaded Q, and Q_L is the loaded Q and L is insertion loss in dB.

Solving for Qu, we have:

$$Qu = \frac{10^{L/20}}{10^{L/20} - 1)} \quad (QL) \quad (6)$$

Using the measured values of insertion loss and loaded Q, the unloaded Q of the resonator at the self resonance frequency is calculated to be 2745. This is 19.6% lower than the calculated value of 3415. Construction details of the resonator which might affect these variations in Q are:

- The resonator is made of solid, hard drawn copper, so the resistivity should be acceptably low
- Silver plating was not used. It was felt that later on, when PIN Diodes were used in the resonator, the degradation in Q would be completely set by these diodes, whether plating was used or not
- Finger stock made of beryllium copper was used to guarantee good connection between the four inch tube and the large end cap
- Common 60/40 solder was used. Later models used silver bearing solder.

It was concluded that this resonator design was a good first effort. The self resonant frequency was within 1.7% of the design value, and the unloaded Q was acceptable.

3.2 COUPLING STUDY

The RF architecture defined by the FHMUX Design Assessment is that of quadrature coupled bandpass filters, used as building blocks.

The quad couplers provide VSWR isolation between the cascaded filter sections. Thus, the bandpass filters are not directly cascaded, and each filter must have its own coaxial 50 ohm input/output ports.

Initial coupling efforts used loops of various sizes for both input and output ports, and in general, both insertion loss (I.L.) and loaded Q varied considerably across the 55-88 MHz frequency range. One of these coupling loops is shown in the foreground of Figure 3-1. A combination of loop and tap coupling was also tried. Finally a two tap system was tried and adopted. The two tap system was not entirely satisfactory, but seemed to be the best available method. A comparision between the loop-tap and two tap systems in given in Table 3-2.

TABLE 3-2. COMPARISON OF TAPPING METHODS

Resonating Element Value	1.125" X 2.25" Loop and Tap (2" From Short)			Two Taps, at Common Point, (1" From the Short).		
	fo (MHz)	I.L. (dB)	Loaded Q	fo (MHz)	I.L. (dB)	Loaded Q
None	108.4	-0.292	72.6			
18 pF (midway down pipe)	83.0	-0.81	71.7			
10 pF on end				82.1	-0.57	85.7
18 pF on end	69.5	-1.22	118.3	69.22	-0.98	111.5
Two 18 pF on end	55.68	-1.6	135.3	-55.15	-1.24	133.2

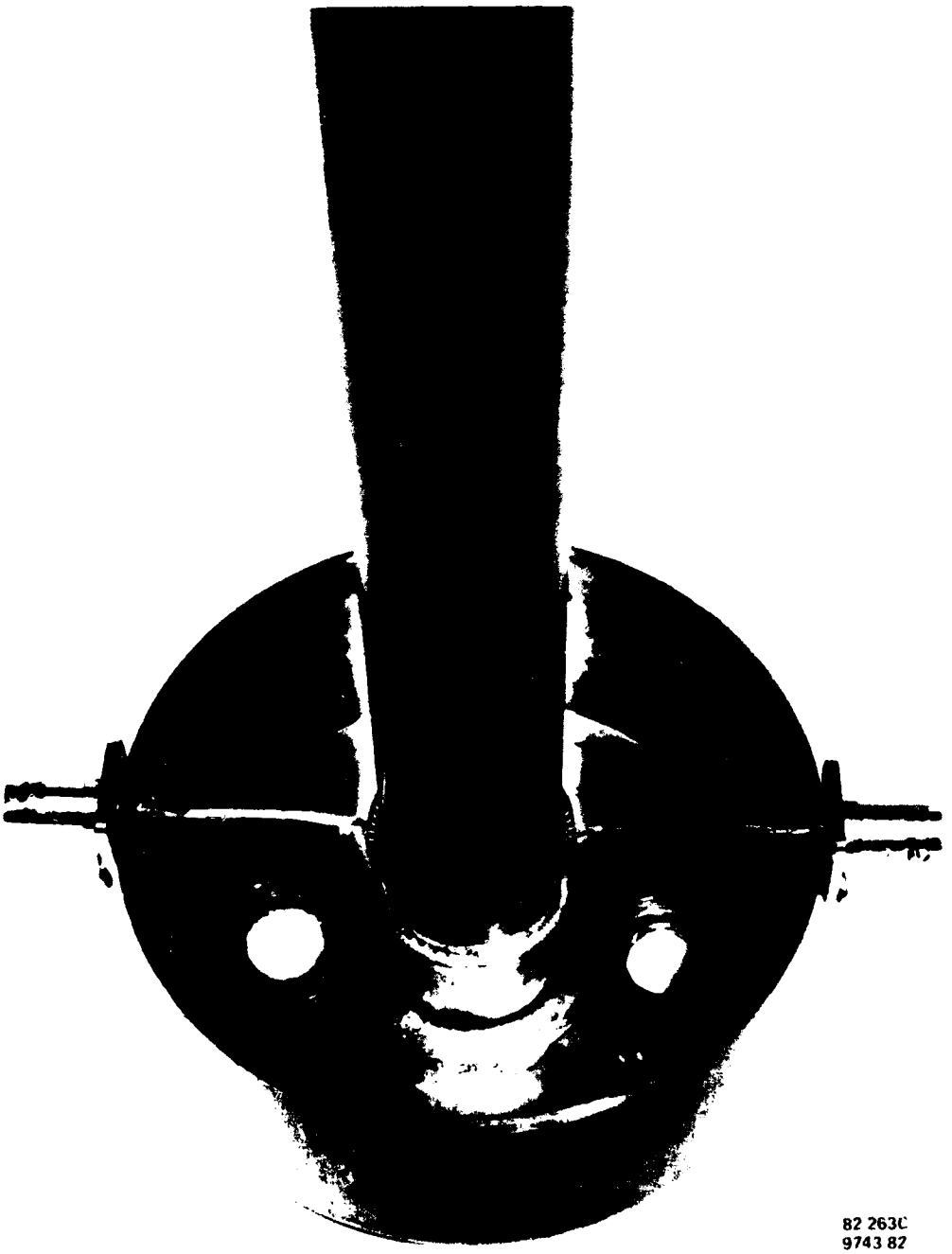

Figure 3-2. Two Tap System

Table 3-2 shows that the two tap system gives lower insertion loss for about the same loaded Q. Figure 3-2 shows the two tap system.

3.3 JUSTIFICATION OF LOSSES

The shunt capacitive bus analysis given in Section 5.9 of the FHMUX Design Assessment Final Report was based on the use of ATC (American Technical Ceramics) 175 style transmitting capacitors. These components were selected for their high voltage and Q characteristic. However, they have been discontinued by the vendor. The ATC 100B series, which has lower Q and voltage ratings (500 volts), were available, and were used for this model. Vendor data for the ATC 100 and ATC 175 capacitors is given in Appendix A.

Before proceeding to the design of the switched capacitive bus and its associated PIN Diode circuitry, an attempt was made to justify the insertion loss measured with the two tap system (Table 3-2). The unloaded Q of the ATC 100B capacitors was extrapolated from the vendors data, and used with the resonator unloaded Q as calculated from Equation 4. If these two values of unloaded Q are known, the unloaded Q of the filter can be computed. The filter unloaded Q is the parallel combination of the resonator and capacitor unloaded Q's.

$$Qu = \frac{Qres \times Qcap}{Qres + Qcap} \qquad (7)$$

Now, since the filter loaded Q had already been measured, the expected filter insertion loss could be calculated by using Equation 5. The results of this comparison are shown in Table 3-3.

TABLE 3-3. LOSS JUSTIFICATION

Resonating Capacitor Value

	10 pF	18 pF	36 pF
Frequency (MHz)	82.1	69.22	55.158
Q Resonator	2950	2709	2428
Q Capacitor	1700	1400	1400
Combined Unloaded Q	1079	923	887
Measured Q_L	85.7	111.5	133.2
Insertion Loss (dB)			
Calculated	0.719	1.12	1.41
Measured	0.57	0.98	1.24
"Error"	0.15	0.14	0.17

Comments regarding Table 3-3:

- The measured values of insertion loss were lower than the calculated values
- The difference between the calculated and measured values of insertion loss is small
- Previous measurements have indicated that the resonator unloaded Q may be 19% lower than the calculated values shown in Table 3-3. However, the unloaded Q of the ATC chip capacitors may well be higher than the vendors data, thus offsetting the effect of the lower resonator Q.

3.4 RESONATOR COMMENTS

- The volume of the quarter wave resonator is 377 cubic inches. The outer conductor extends three inches past the inner conductor to eliminate detuning effects caused by nearby objects. This volume is 49% more than that of the helical resonator. However, this design is extremely cost effective for a feasibility model type of program

- The design of the shunt capacitive bus is eased by the lower characteristic impedance of the quarter wave resonator
- The only advantage offered by the helical resonator is that of reduced volume
- The data presented in Table 3-3 shows that the resonator design is on firm ground.

SECTION 4

PIN DIODE EVALUATION AND BIAS CIRCUIT DESIGN

4.1 INTRODUCTION

The FHMUX Design Assessment Final Report describes how bandpass filters can be instantaneously tuned by the use of a shunt binary bus. This report also describes the nature of the bus and how PIN Diodes are used to switch tuning capacitors in or out of the parallel resonant circuit. An updated PIN Diode specification is also presented. This specification is shown in Table 4-1. It is necessary that the FHMUX be compatible with fixed channel (non frequency hopping) transmitters similar to radio nets operating with VRC-12 equipments. This means that the PIN Diode and its associated bias circuits must be capable of operating at a 100% duty cycle. Thus a stud or flange mounted device will be needed.

One of the goals of this feasibility study is to select the best available PIN Diode for use in the FHMUX feasibility model, and also to determine whether a formal PIN Diode development program is needed.

This section shows that the PIN Diode problem is not as severe as once thought, but that some development work is needed.

4.2 PIN DIODE TEST CIRCUIT

When the specification shown in Table 4-1 was reviewed, several PIN Diode vendors described the difficulty encountered in measuring the very low "on" impedance, and high "off" impedances specified. Also, no common test method seemed to exist between vendors. The following procedure was adopted:

- PIN Diode samples would be evaluated in a common GTE test fixture which would enable direct performance comparison
- Evaluation would begin when a sufficient number of different diodes was available, and be completed without interruption. This would prevent unwanted test fixture variations from occurring

- Samples were requested from many vendors. Diodes from Alpha, Microwave Associates, and Unitrode were evaluated
- This should be a continuing activity, but time and funding constraints have limited the evaluation to 4 different PIN Diodes.

TABLE 4-1. PIN DIODE SPECIFICATION

. Frequency	30-88 MHz
. Input RF Power	100 watts, C.W.
. Temperature	-55 to + 85 (Est.)
. IMD Products	-120 dBc Max.
. Harmonic Distortion	-120 dBc Max.
. Size	N/A
. Forward Current	200 ma
. Duty Cycle	100%, both RF and dc bias
. Reverse Voltage	TBD
. Parallel Resistance	1 Megohm (min.)
. Power Dissipation	TBD
. Series Resistance	0.1 ohms Max.
. Diode Capacitance	2 pF
. Effective Minority Carrier Lifetime	TDB
. Switching Speed	10-20 Microseconds
. "Hot" Switching Is Not Required	

The PIN Diode test circuit is shown in Figure 4-1. The diode under test is soldered into a removeable section which is held in place at the high impedance point (open circuit end) of the resonator by beryllium copper finger stock.

The value of bias choke L1 was measured at 60 MHz and then verified by calculation. At 60 MHz this choke is actually operating close to parallel resonance, and provides a high capacitive reactance above 60 MHz. The "effective" value of L1 is 0.075 pF, and its unloaded Q is about 172. The Q of bypass capacitor C2 is unimportant

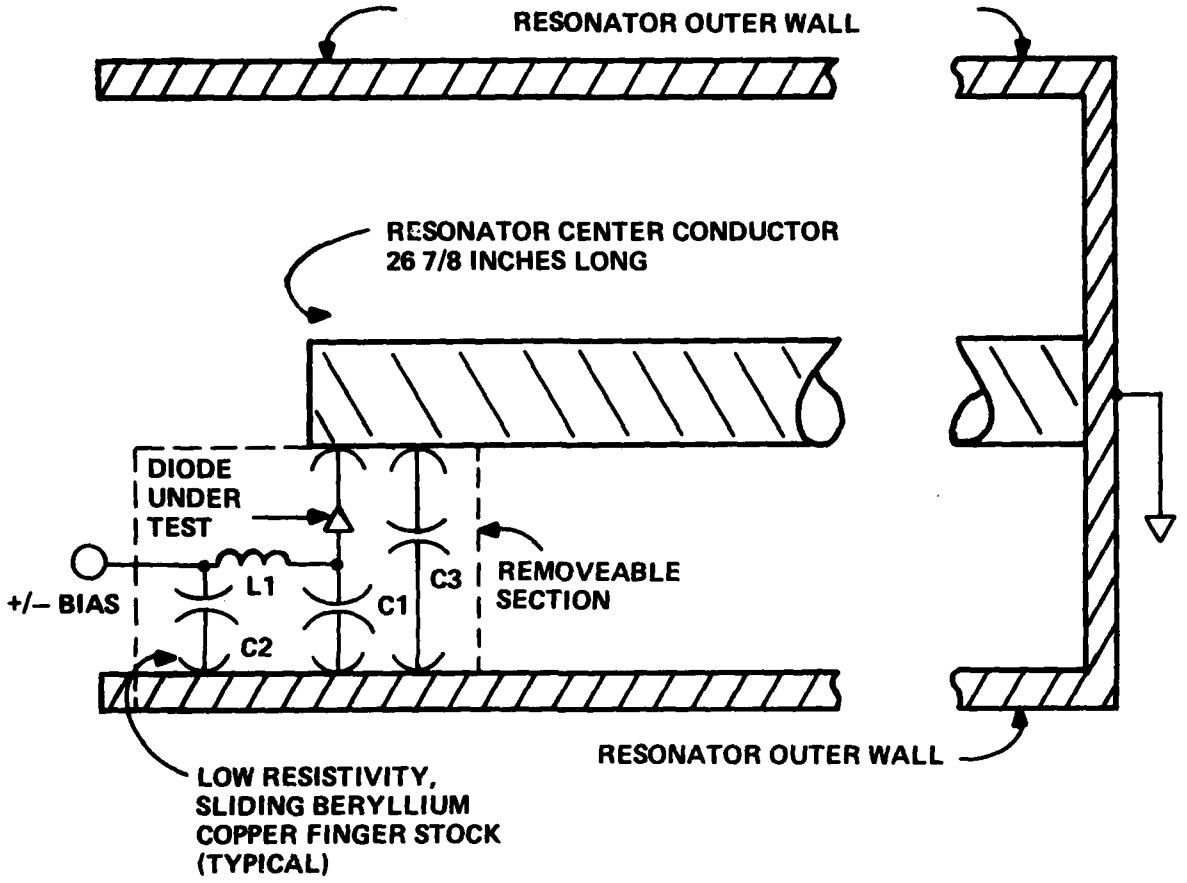

C1 = C3 = 18 pF, ATC 1000B CHIP CAPACITOR

C2 = 1000pF VITRAMON BYPASS CAPACITOR

L1 = 40 TURNS OF #28 AWG ON INDIANA GENERAL F625-Q3 TOROID

12,555-82

Figure 4-1. PIN Diode Test Circuit

because it is not part of the resonant circuit. Capacitors C1 and C3 are ATC 100B styles; their unloaded Q's have been extrapolated from ATC data sheets and found to be close to 1300.

When the test diode is in the "on" state, C1 is in series with the diode, and these two components are then in parallel with C3. When the diode is in the "off" state, the high impedance of the diode effectively isolates C1 from C3.

4.3 PIN DIODE TEST DATA

Baseline data was taken with chip capacitors alone, thus providing a comparison of data with and without the PIN Diode (and bias circuit). The complete data set is shown in Table 4-2.

The baseline data shown in Table 4-2 simulates diode "on" and "off" performance. The "off" condition is obtained with a single 18 pF chip capacitor, and the "on" condition uses two 18 pF capacitors. Thus the resonant frequency for the "on" state is lower than that of the "off" state. The baseline insertion loss in the simulated "on" state is -1.6 dB, and in the simulated "off" state is -1.22 dB. The increased insertion loss in the simulated "on" state is accompanied by a higher loaded Q. This is attributed to the variation in input/output coupling which was discussed in the previous section.

Comments regarding the various PIN Diodes measured are listed below:

- The added attenuation due to the diode and its bias circuit varied from 0.29 to 0.68 dB
- The best diode (and also the most costly) was the Microwave Associates MA4P506-30, but the Unitrode UM6201 ran a very close second, and is considerably less expensive
- These data were obtained at an input level of +10 dBm
- Loaded Q is only slightly affected by addition of the PIN Diode
- Early calculations show that the bias choke accounts for between 0.15 and 0.2 dB of insertion loss all by itself

TABLE 4-2. PIN DIODE EVALUATION DATA

	DIODE "ON"				DIODE "OFF"			
	INSERTION LOSS (dB)	Q_L	fo (MHz)	I_f (ma.)	INSERTION LOSS (dB)	Q_L	fo (MHz)	V_B (VOLTS)
BASELINE								
Two 18 pF chip caps (no diodes)	-1.6	135.3	55.482	-				
One 18 pF chip cap (no diodes)					-1.22	118.3	69.55	
A * 4P506-30 ($27.50 ea.)	-1.89	133.8	55.516	400	-1.33	119.51	68.48	-40
Unitrode UM7201 ($18.60 ea.)	-1.91	131.52	55.500	400	-1.54	121.72	67.237	-100
Unitrode UM6201 ($21.70 ea.)	-1.97	129.5	55.549	400	-1.44	117.7	68.407	-100
ALPHA CBS7201	-2.28	127.8	55.607	400	-1.84	113.3	68.446	-100
(2) UM6201 in Parallel	-1.85	130	55.532	400	-1.48	105	67.314	-100

* Microwave Associates

- Vendor data sheets for the PIN Diodes evaluated are given in Appendix A.

4.4 CALCULATION OF DIODE PARAMETERS

In the "on" state, the PIN diode can be modeled as a small valued, pure resistor. In the "off" state, the model is that of a large resistor in parallel with a small capacitor. Since all other circuit element values are known, the actual diode parameters can be calculated. The results of these calculations are given in Table 4-3.

TABLE 4-3. PIN DIODE PARAMETERS AS CALCULATED FROM MEASURED DATA

DIODE TYPE	Rs (ohms)	Cp (pF)	Rp (ohms)
MA4P506-30	0.086	1.0	2.57 Meg
UM7201	0.0894	2.55	382K
UM6201	0.110	1.06	678K
Alpha CSB7201-03	0.186	1.04	192K
(2) UM6201 in Parallel	0.0813	2.33	362K

Comments on Table 4-3 are:

- The MA4P506-30 meets the PIN Diode specification at low power and the UM6201 comes very close
- This data is very encouraging
- The data is believed to be accurate. An earlier section of this report describes how the unloaded Q of the resonator was measured and found to be about 19% lower than the calculated value. The value of unloaded Q used herein was 15% lower than the calculated value. In addition, the remaining component Q's were either extrapolated from vendor sheets or measured

- The values of series "on" resistance (Rs) were generally lower than vendor data. The "off" state shunt capacity (Cp) data was very close to vendor data. The parallel resistance data (Rp) correlation with vendor data was good
- Future diode evaluation should be performed at much higher power levels, using the existing test bed. The MA4P506-30, and the UM6201 diodes should be baseline types for this effort
- The unloaded Q of the bias choke is a loss factor in the circuit. The bias choke used herein should be improved. The calculation of the diode parameters shown in Table 4-3 takes the bias choke parameters into account.

SECTION 5

SHUNT CAPACITIVE BUS DESIGN

5.1 INTRODUCTION

The FHMUX Design Assessment Final report defined a shunt capacitance bus which enabled frequency hopping operation of a high Q bandpass filter. A schematic diagram of this capacitive bus is shown in Figure 5-1.

This section describes the design activities which lead to the successful implementation of an 8 bit capacitive bus. The topics of interest are:

- Tuning range
- Design of coarse and fine tuning sections
- Test data
- Discussion of problem areas

5.2 TUNING RANGE

The shunt capacitive bus shown in Figure 5-1 has several problem areas. Analysis shows that the PIN Diode specification parameters would work reasonably well as far as insertion loss was concerned. However, the smaller value capacitors would be difficult to implement, and the "on/off" capacitance ratio is at best, poor. As shown, the smallest value of capacitance is 0.1 pF, and the "on/off" ratio of this branch is about 1.0/0.9. This would necessitate the use of many of these sections.

The work of Karp and W. Weir, "Recent Advances in Binary Programmed Electronically Tuneable Bandpass Filters of the 'Flauto Type,'" IEEE Microwave Symposium 1975, pp. 167-169, describes a technique whereby the effectiveness of a tuning capacitor in a high Q resonator could be varied by changing the location of its connection to the resonator center conductor.

This work suggests that the effectiveness of the tuning capacitor is a function of $\sin^2 \theta$ where θ is the electrical length between the capacitor tap point and the shorted end of the resonator.

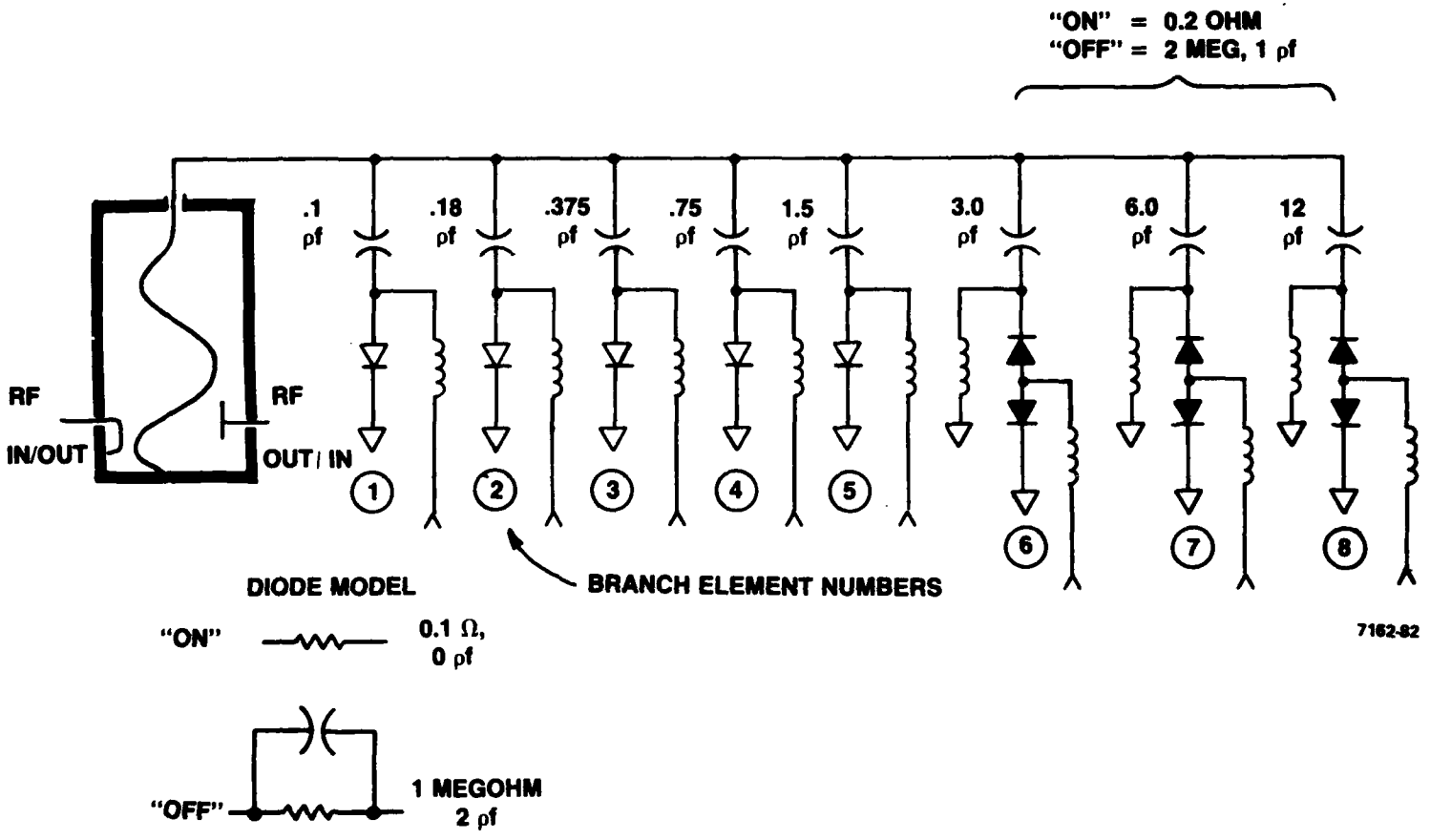

Figure 5-1. Schematic, 50-88 MHz Frequency Hoppable Bandpass Filter

To verify this relationship, a slideable shunt capacitor test fixture was used with various values of ATC 100B chip capacitors. The stray capacitance of this fixture was experimentally determined to 0.46 pF, and this value was added to the measured value of the chip cap itself. Six different values of capacitance were placed at five different locations along the resonator center conductor and changes in the filter resonant frequency were noted. By knowing the resonant frequency, the "effective capacity" can be calculated.

At resonance, $C = \frac{1}{\omega^2 L}$

Where $L = \frac{X_\ell}{\omega}$

Thus $$C = \frac{1}{\frac{\omega^2 X_\ell}{\omega}}$$

$$= \frac{1}{\omega X_\ell}$$

Where C is the capacitance in farads, w is the resonant frequency in radians per second, and X_L is the resonator inductive reactance at this resonant frequency.

From an earlier equation,

$$X_\ell = j\ Zo \tan (90^o\ f/fo)$$

Finally,

$$\text{"Ceff"} = \frac{1}{2\pi\ fo\ [Zo \tan f/fo]} \qquad (8)$$

The six values of capacitance used are: 37.6, 18.04, 9.86, 5.01, 3.2, and 1.88 pF. The relationship between the distance from the

inner conductor short and the resulting effective capacitance is shown in Figures 5-2 and 5-3.

- In general, a linear relationship exists between the distance from the short, and the "effective capacity"
- As the capacitor is moved toward the short, its effectiveness is lowered.

An exact analysis of this data is not straightforward.

- The "effective" capacity varies about as $\sin^2 \theta$, but the value of θ changes with frequency
- The inductive reactance varies as: tangent (90 $^{f}/fo$)
- The resonant frequency varies as the half power of the LC product.

As discussed earlier, the original bus design suffered from a poor capacitive "on/off" ratio with the smaller values of capacitance. This latest data shows that larger values of capacity can be made to appear as smaller values, and still maintain a good "on/off" capacitance ratio. This technique leads to the design of a secondary, separate section of the capacitive bus, which provides a medium and fine tuning capability.

5.3 DESIGN OF COARSE AND MEDIUM RANGE TUNING SECTIONS

The tuneable frequency range of this model was set to be 56-88 MHz, and the self resonant frequency of the quarter wave resonator is 108.166 MHz. The characteristic impedance of the resonator is 75.45 ohms. Thus, equation 1 can be used to determine the value of capacity needed to resonate the bandpass filter at any frequency in the design bandwidth. This data is listed in Table 5-1.

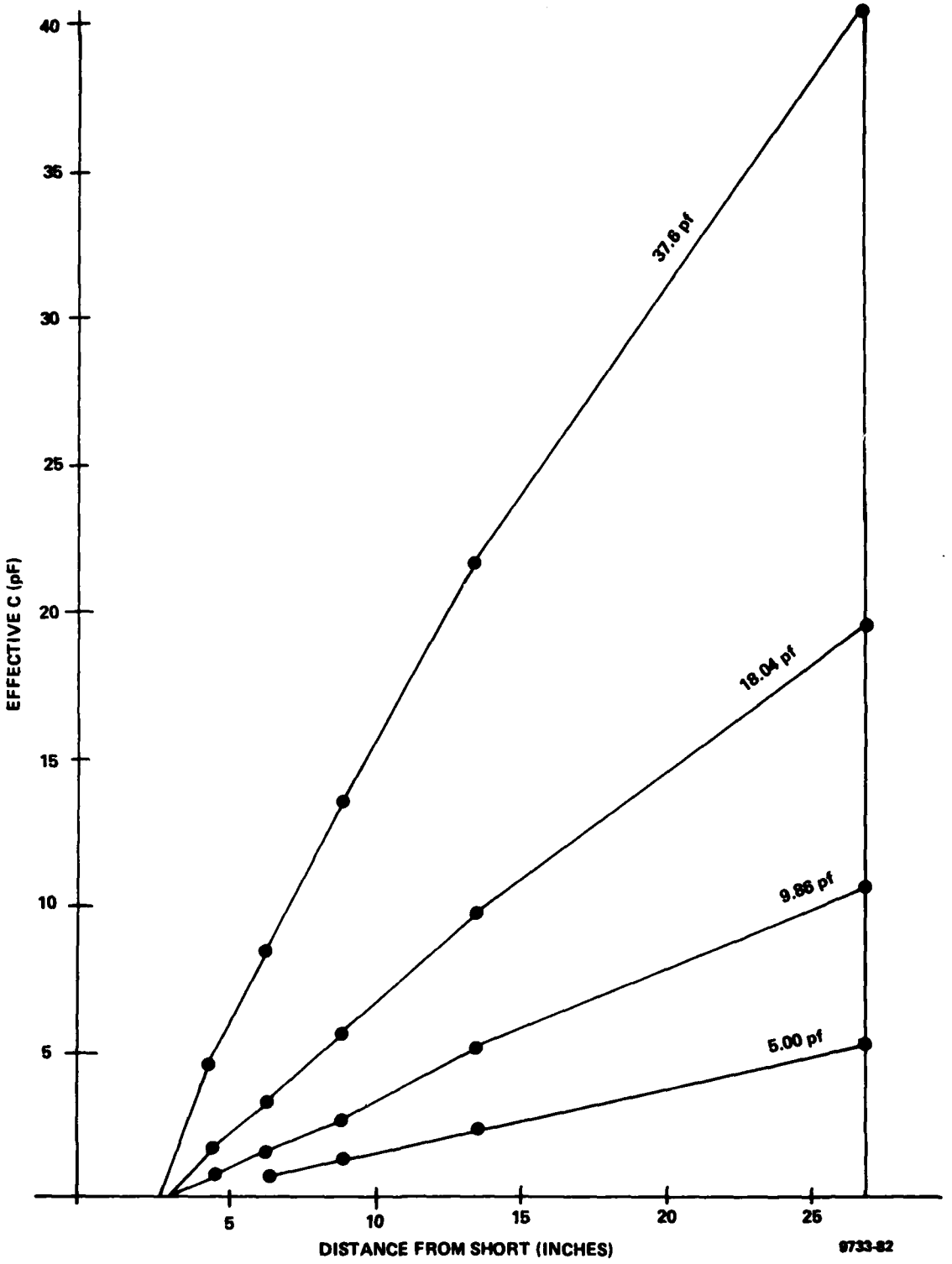

Figure 5-2. Distance From Short vs. "Effective Capacity"

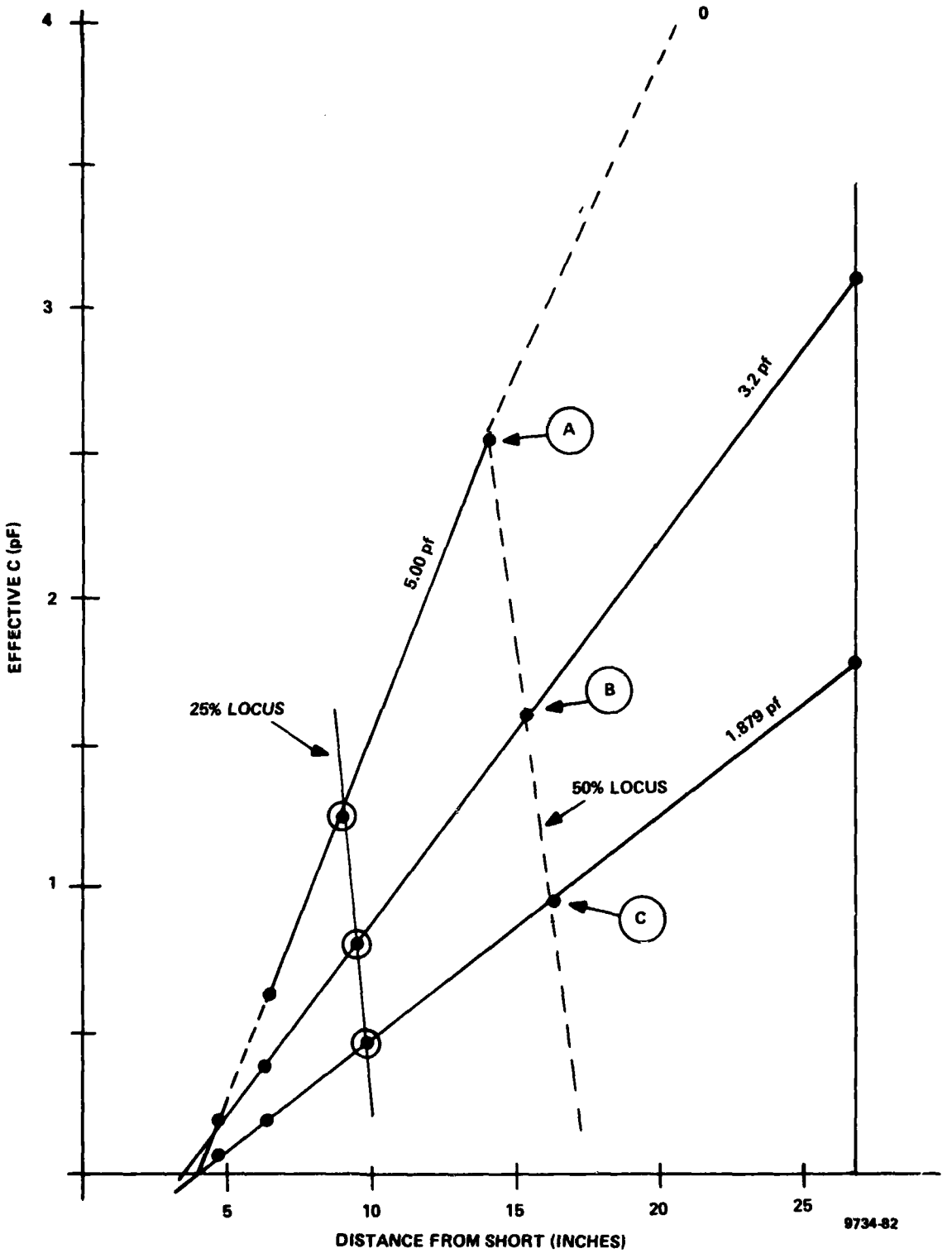

Figure 5-3. Distance From Short vs. "Effective Capacity"

TABLE 5-1. REQUIRED CAPACITANCE VS. DESIRED RESONANT FREQUENCY

DESIRED RESONANT FREQUENCY (MHz)	REQUIRED CAPACITANCE (pF)
55	37.3
60	29.6
65	23.5
70	18.6
75	14.7
80	11.4
85	8.68
88	7.23
90	6.33

The range of capacity needed to tune from 55-88 MHz is thus shown to be 37.3 to 7.23 pF.

A schematic diagram of the final version of the switched binary capacitive bus is shown in Figure 5-4 and the mechanical configuration is shown in Figures 5-5 and 5-6. Figures 5-5 and 5-6 show how beryllium copper finger stock was used to form low resistance, moveable RF assemblies which, with the flexible resonator design, enabled design evaluations and changes to be performed in a timely manner.

A preliminary 4 bit coarse tuning bus was designed using 18.7, 10, 5.6, and 2.7 pF capacitors. This bus was attached to the open end of the center conductor as shown in Figures 5-4 and 5-6. It was quickly discovered that about 3 pF of stray capacity was present. Thus, the design was changed to the values shown in Figure 5-4. The PIN diode bias scheme used for this coarse tuning bus is the same as that used in the PIN diode evaluation study.

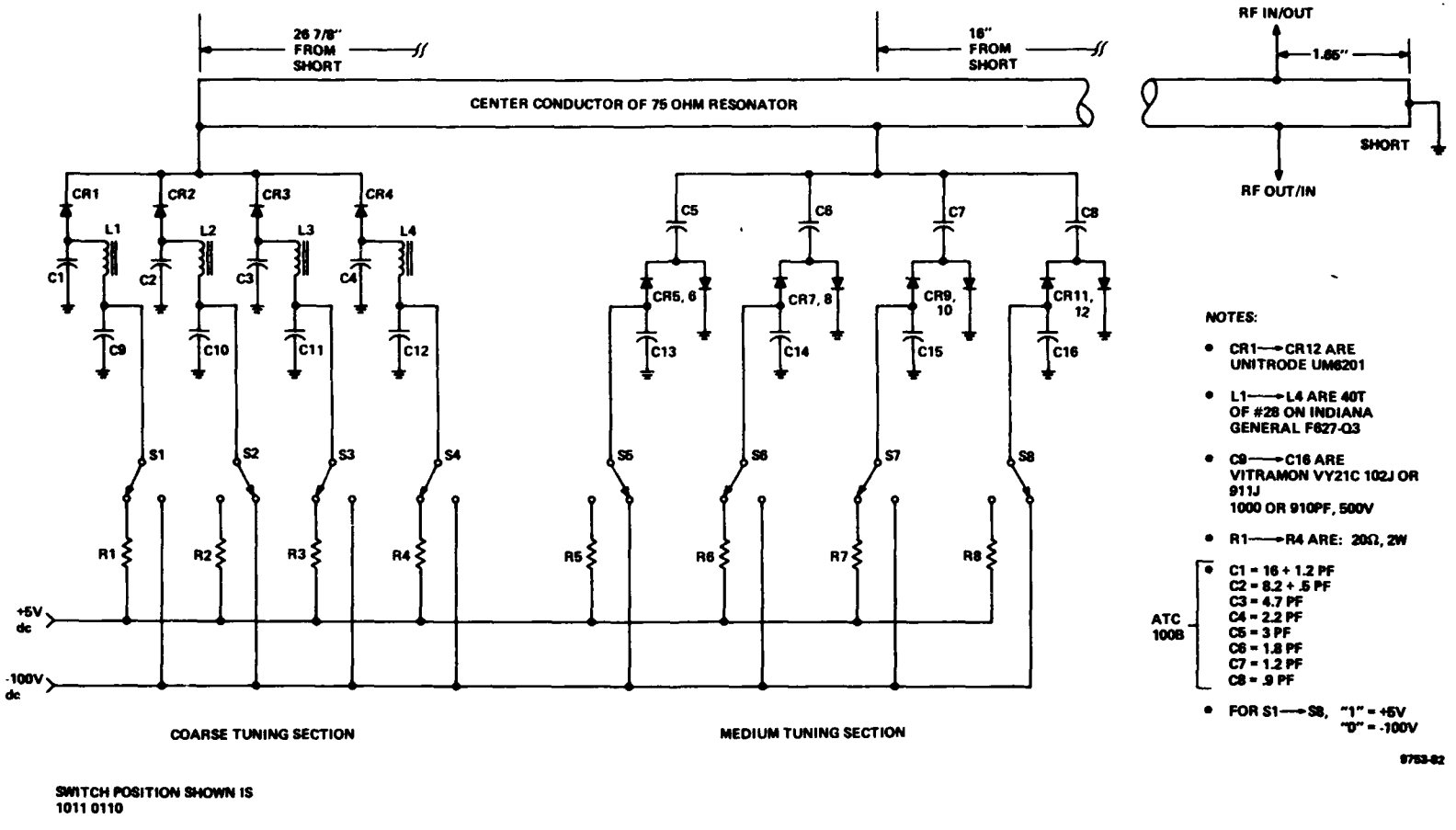

Figure 5-4. FHMUX Feasibility Model Resonator Design

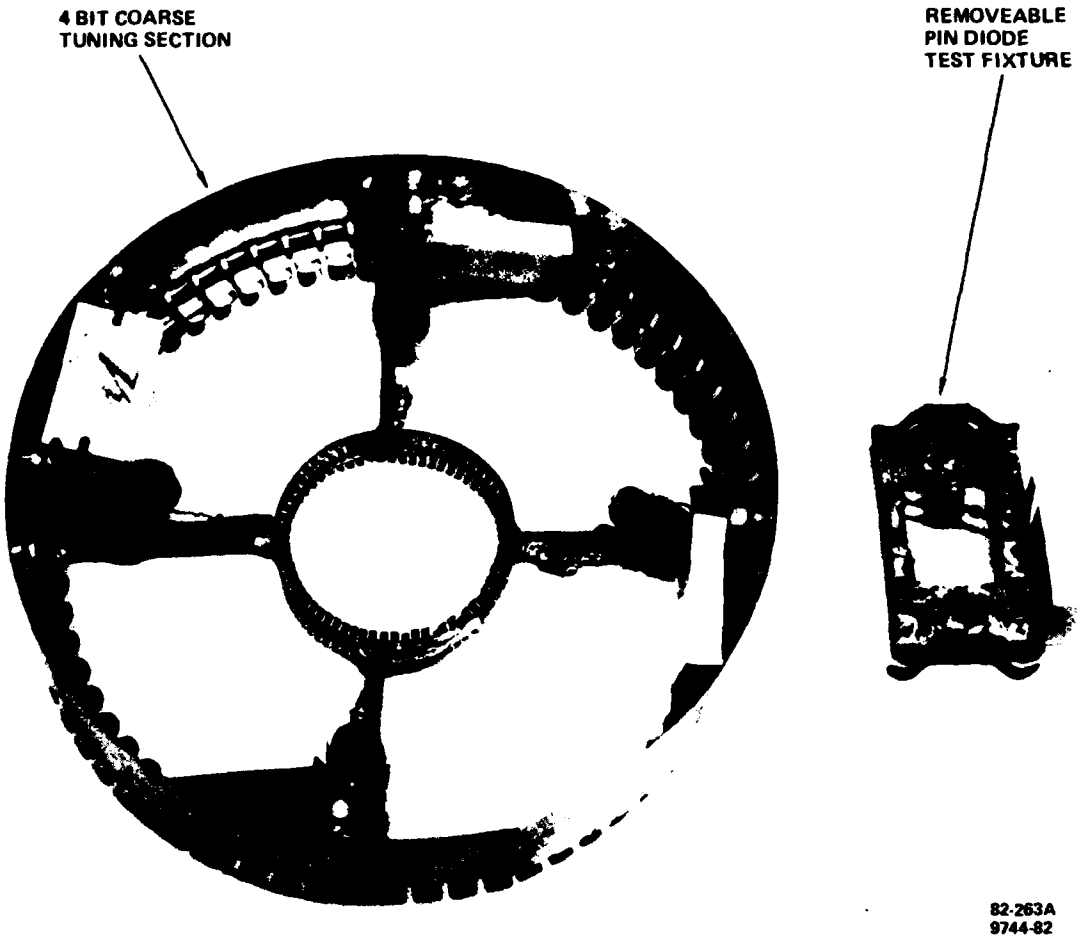

Figure 5-5. Mechanical Configuration, 4 Bit Coarse Tuning Section

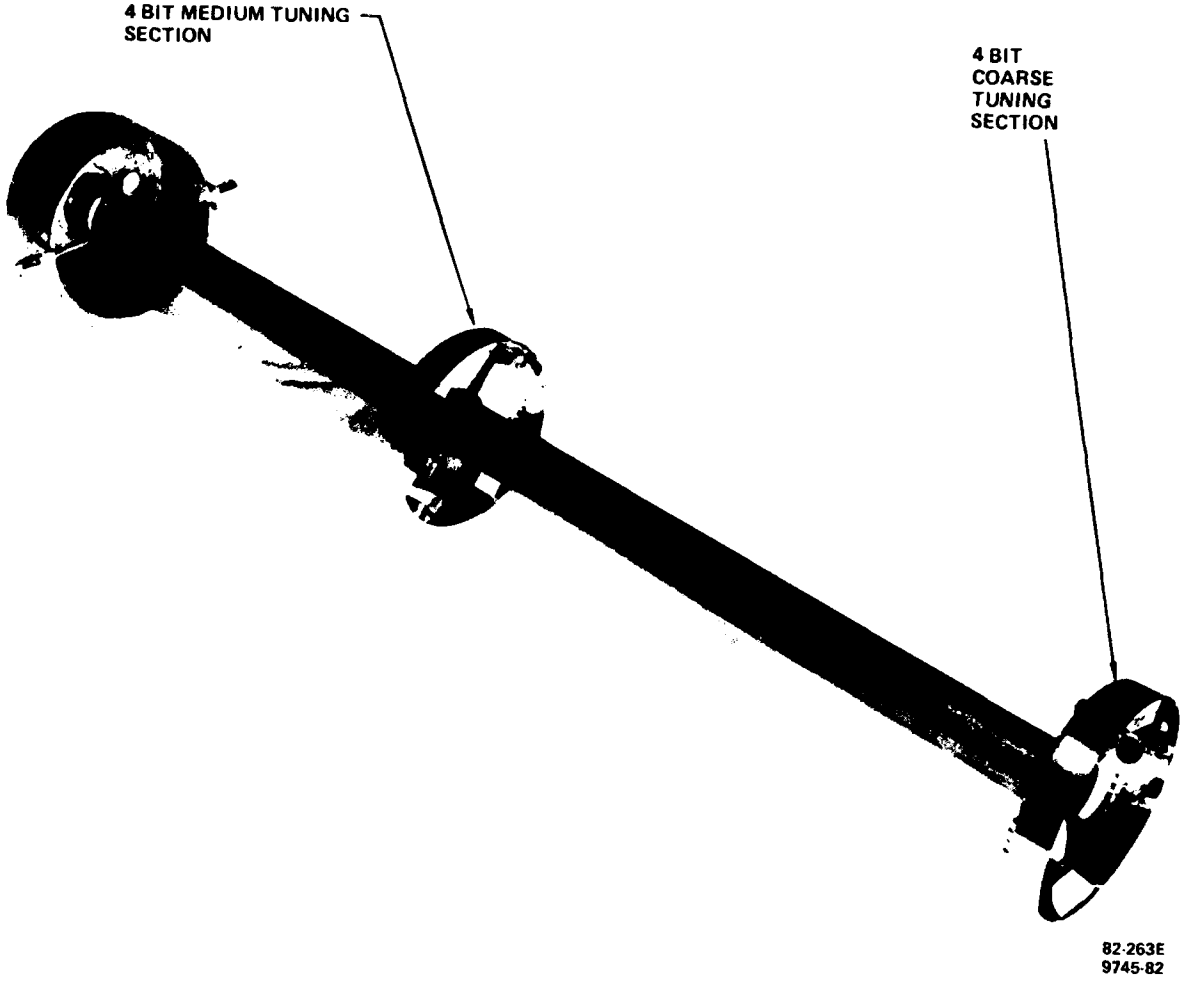

Figure 5-6. Mechanical Configuration, 8 Bit Frequency Hoppable Bandpass Filter (Without Outer Conductor)

The design of the medium range tuning section is not as straightforward as that of the coarse tuning section.

The PIN diode biasing scheme used in the coarse tuning section works well because the value of the tuning capacitors is large enough to present a low impedance compared to the inductive reactance of the bias choke (L1 through L4). When small values of capacity are used, such as 0.9 pF or so, the impedance of the bias chokes is not high enough, and the circuit becomes lossy. The bias circuit shown (for CR5-CR12) is well suited for this purpose, but does not function well for the coarse tuning case.

Two additional factors complicate the design of this bus:

- The bus itself will be located at a lower impedance point along the resonator center conductor
- The desired value of capacitance "change", i.e., the on/off ratio becomes more critical with the small values of capacitance used.

Points A, B, and C shown in Figure 5-3 form a locus of points where the effective capacity approximates 50% of the actual capacity value. The average distance from the short circuit for this locus is about 16 inches, and this distance was selected for the location of the medium range tuning section.

The values selected for C5, C6, C7, and C8 were selected to provide the proper capacitance change, rather than a certain on/off capacitance ratio. The bias circuit used for these capacitors places the diode "off" capacitances in parallel. This parallel combination is then in series with the actual tuning capacitor.

Before construction of the complete 8 bit bus, a preliminary 3 bit bus was evaluated. The bias circuit was the same as used with CR1, CR2, and CR3 of Figure 5-4.

The values of capacity were carefully measured after the capacitors were mounted on the circuit board, and are listed below:

C1 = 18.70 pF

C2 = 10.04 pF

C3 = 5.84 pF

Data was taken using the MA4P506-30 diodes. Three sets of data were taken as noted below in Table 5-2.

TABLE 5-2. DATA SETS

DIGITAL BIT	CAPACITORS IN CIRCUIT	DIODE STATES
001	C3	CR1 Off CR2 Off CR3 On
011	C2, C3	CR1 Off CR2 On CR3 On
111	C1, C2, C3	All Diodes On

In addition, each of the data sets listed in Table 5-2 were divided into 3 subsets:

- Tuning capacitor with RF short circuit simulating the PIN Diode in the "on" state
- Tuning capacitor with RF short, plus bias choke
- Tuning capacitor with bias choke and PIN Diode in ON state
- Where a "zero" bit is called for, the PIN Diode "off" state is simulated by an open circuit.

This data is listed in Table 5-3.

TABLE 5-3. 3 BIT SHUNT CAPACITIVE BUS DATA

DATA SET	DATA SUBSET	INSERTION LOSS (dB)	LOADED Q	RESONANT FREQUENCY (MHz)	△ dB	CAPACITY DATA (pF)	
						MEASURED CAPACITY	"EFFECTIVE CAPACITY"
001	.C3 + Short	-.395	48.6	90.96			5.90
	.C3 + L3 + Short	-.535	51.4	84.44	-.14	5.84	8.94
	.C3 + L3 + CR3 "ON"	-.788	54.7	84.25	-.253		9.04
011	.(C3 + Short) + (C2 + Short)	-1.046	66.1	73.33		15.88	15.91
	.(C3 + L3 + Short) + (C2 + L2 + Short)	-10.34	70.44	71.53	+.012		17.33
	.(C3 + L3 + CR3 ON) + (C2 + L2 + CR2 ON)	-1.273	68.56	70.23	-.227		18.43
111	.(C3 + Short) + (C2 + Short) + (C1 + Short)	-.969	86.21	57.07		34.58	33.85
	.(C3 + L3 + Short) + (C2 + L2 + Short) + (C1 + L1 + Short)	-1.22	87.86	56.212	-.251		35.24
	.(C3 + L3 + CR3 ON) + (C2 + L2 + CR2 ON) + (C1 + L1 + CR1 ON)	-1.63	84.75	55.842	-.41		35.86

The data presented in Table 5-3 was taken with great care, but the results obtained do not yield straightforward results.

- The 011 case shows a decrease in loss and an increase in loaded Q. Probably the bias circuit is close to self resonance at this frequency, and is thus isolated from the rest of the circuit
- When the PIN Diodes were turned on, the loaded Q was only slightly affected
- For the 001 case, the insertion loss increased by about 0.4 dB with the bias choke and the PIN Diode in the circuit (only 1 diode on)
- For the 111 case, the insertion loss increased by about .66 dB when all 3 bias chokes and PIN Diodes were used
- Thus at least for the coarse tuning section, an increase of 0.22 dB might be expected for each energized PIN Diode circuit.

With the above data as a baseline, the complete 8 bit bus was assembled and tested. The first set of data indicated that the resonator tap should be lowered to improve the loaded Q at the high end of the band. Therefore, the 8 bit bus data is not traceable to the 3 bit bus data. The 8 bit bus data is shown in Table 5-4.

TABLE 5-4. PERFORMANCE DATA, BREADBOARD 8 BIT CAPACITIVE BUS

RESONANT FREQUENCY (MHz)	DIGITAL CODE	INSERTION LOSS (dB)	LOADED (Q)
56.000	1 1 1 0 1 1 1 1	-1.91	82.2
58.000	1 1 0 1 0 0 1 1	-2.0	77.23
60.000	1 0 1 1 1 1 1 0	-1.62	75.59
62.000	1 0 1 0 0 1 0 1	-1.61	73.64
64.000	1 0 0 1 0 0 0 1	-1.61	72.24
66.000	1 0 0 0 0 0 0 0	-1.87	65.3918
68.000	0 1 1 0 1 1 1 1	-1.43	62.79
70.000	0 1 1 0 0 0 0 0	-1.32	66.244
72.000	0 1 0 1 0 0 1 1	-1.21	63.77
74.000	0 1 0 0 0 1 1 1	-1.07	59.99
76.000	0 0 1 1 1 1 1 0	-0.832	58.31
78.000	0 0 1 1 0 0 1 0	-0.845	57.50
80.000	0 0 1 0 1 0 0 1	-0.677	54.07
82.000	0 0 1 0 0 0 0 0	-0.744	51.87
84.000	0 0 0 1 1 0 0 1	-0.736	47.22
86.000	0 0 0 1 0 0 0 1	-0.630	47.64
88.000	0 0 0 0 1 0 1 0	-0.410	44.25
91.4023	0 0 0 0 0 0 0 0	-0.421	43.31

Comments on the 8 bit data are:

- The bus was successfully tuned from 56-88 MHz, and the resonant frequency with all diodes "off" was 91.4 MHz
- The bus used MA4P506-30 diodes in the coarse tuning section, and the UM6201 diodes in the medium tuning section

- The loaded Q varied from 82.2 at 56 MHz, to 44.25 at 88 MHz. The design goal was for a minimum loaded Q of 50. This goal could be met by raising the tap point, but then the insertion loss would also increase
- The insertion loss varied from -1.91 dB at 56 MHz to -0.41 dB at 88 MHz. Again, this variance in attenuation is largely due to the change in coupling effectiveness into and out of the resonator as the frequency varied
- The feasibility of the capacitive bus concept was proven. The tuning range and loaded Q were satisfactory. Insertion loss problem areas had been identified as:

    - The PIN Diode
    - The bias choke
    - Variations in coupling

It is to be noted that GTE has been assigned United States Patent 4,095,198. This patent describes an impedance matching network which uses a shunt binary controlled capacitive bus. The patent is dated June 13, 1978, and was developed by Thomas J. Kirby.

5.4 DISCUSSION OF PROBLEM AREAS

- The design goal for the insertion loss of the resonator and bus is 0.5 dB. Some of the causes of the increased loss have been previously listed
- It was noted that the bus could not be tuned to any desired frequency. For example, 71.275 MHz would be desired, but the bus could only tune within 50 KHz of this frequency. A 10 bit bus is probably needed
- The tolerances on the tuning capacitors (C1 to C8) have to be very tight. Some form of high voltage, high Q trimmer capacitor is probably needed.

SECTION 6

SYSTEM TESTS

6.1 INTRODUCTION

Having completed the breadboard design of the resonator and the switched capacitive bus, the complete FHMUX feasibility model was built and successfully tested. A block diagram of the model is shown in Figure 6-1, and a photograph is shown in Figure 6-2.

No attempt was made to reduce the size of this model as the chassis was deliberately made large to provide great flexibility and ease of modification.

The theory of operation of the FHMUX and its load insensitivity features have been derived and explained in the FHMUX Design Assessment Final Report and will not be repeated herein.

As shown in Figure 6-2, the 4 shunt capacitive busses are manually controlled by the four arrays of switches on the front of the unit. The quadrature hybrid couplers are mounted inside the unit along with the PIN Diode current limiting resistors. The interconnections between the quad-hybrid couplers and the resonators are made with matched lengths of coaxial cables.

It has been noted that the Microwave Associates 4P506-30 PIN Diode was the best of the diodes evaluated, and that the Unitrode UM6201 ran a close second. The 4P506-30 diodes cost about $31 a piece, and 48 devices were needed. However a cache of Unitrode UM6201 diodes was discovered in-house, so the feasibility model was built using these diodes.

The theory developed in the Design Assessment Phase was verified; no real surprises were encountered. However, the insertion loss of the 30-90 MHz quad-hybrid couplers was much higher than expected, and one of the units was returned to the vendor for evaluation. The vendor has since verified that this unit is indeed defective. Therefore, some system data was taken with lower loss 30-76 MHz quad-couplers to give more realistic data.

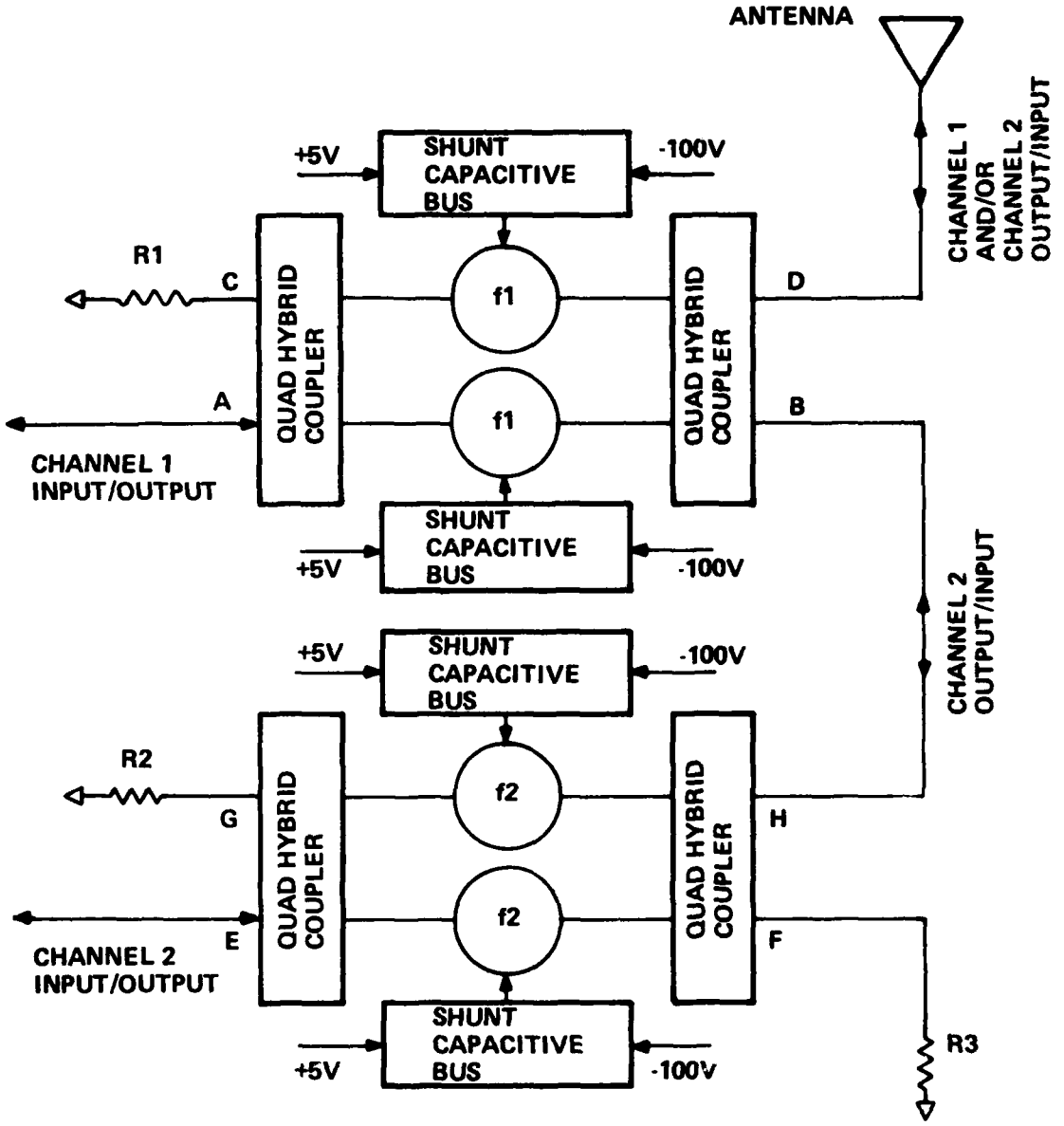

Figure 6-1. Block Diagram, FHMUX Feasibility Model

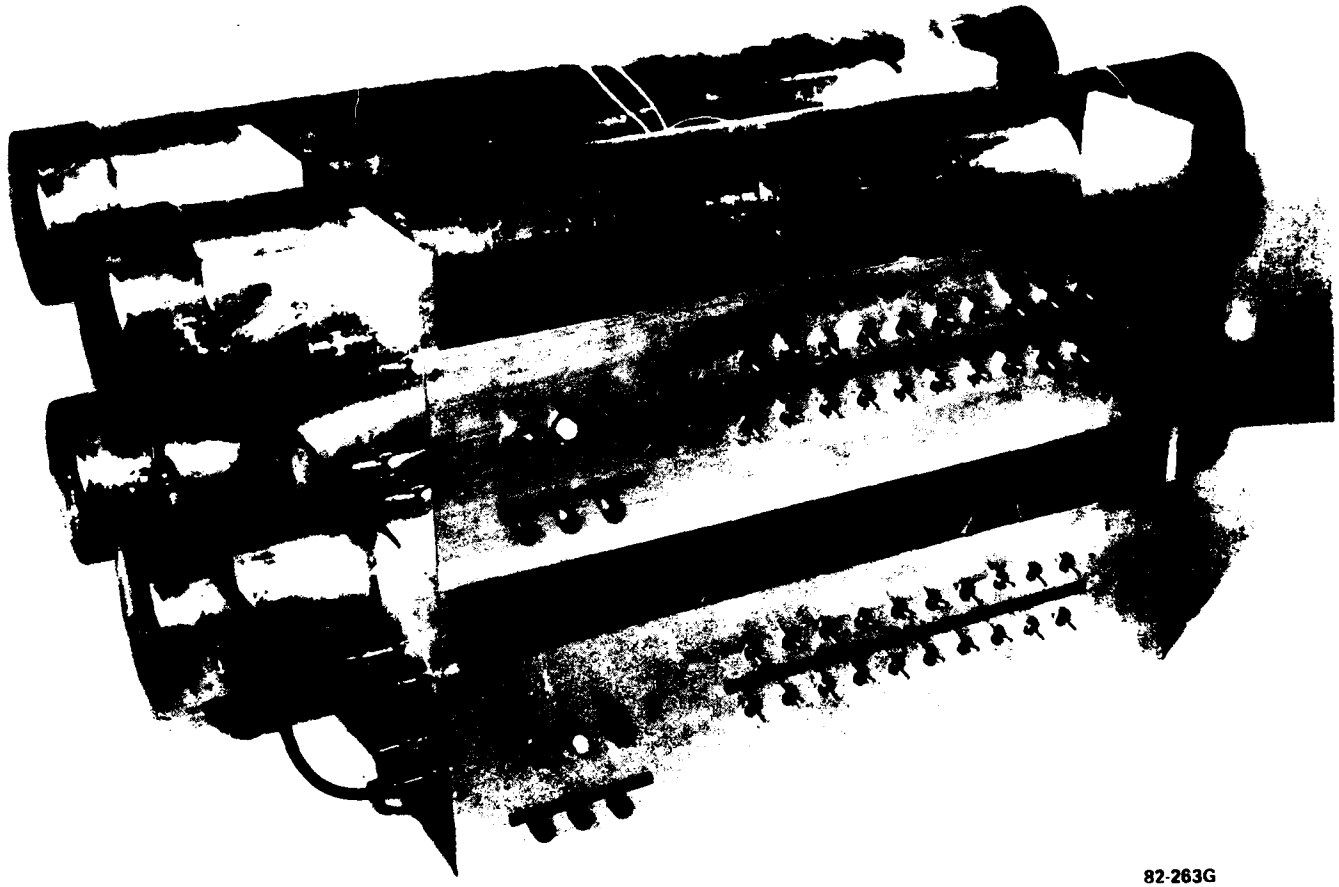

82-263G
9746-82

Figure 6-2. FHMUX Feasibility Model

The following system tests were performed:

- Loss Analysis of Quad-Hybrid Couplers
- Load Pulling
- Channel Isolation
- IMD & Harmonic Isolation Observations.

6.2 LOSS ANALYSIS OF QUAD-HYBRID COUPLERS

Initial baseline testing of the feasibility model showed that the insertion loss of both channels was higher than expected. Further investigation revealed that the insertion loss of the Merrimac QHF-3-.060G quad-hybrid couplers was higher than expected. A test fixture using a spare unit was constructed, and is shown in Figure 6-3, along with a similiar test fixture which uses a more narrow band quad coupler, the QHF-2-.053GC. The larger unit is a 30-90 MHz device, and has extra coupling sections to increase the bandwidth. The smaller unit covers a 30-76 MHz bandwidth.

Swept insertion loss data was taken using a Hewlett Packard 8505A Network Analyzer, and then this data was spot checked with single frequency equipment. The results were the same.

The insertion loss of the quad couplers, as defined by the vendor, is measured at the frequency where each arm of the coupler has identical losses. The insertion loss of the 30-90 MHz coupler is specified at -0.3 dB. Loss data for the two couplers mentioned is shown in Figure 6-4. The 30-76 MHz device data (part B of Figure 6-4) shows an equal power split between the two arms at 72.3 MHz, and the loss in each arm is -3.23 dB. Thus the insertion loss is -0.23 dB. Part C of Figure 6-4 shows that an equal power split for the large, 30-90 MHz coupler occurs at about 69.8 MHz, and that the loss per arm is -3.83 dB. The data taken for part C includes a cable which has an insertion loss of -0.1 dB. Thus, the loss per arm is -3.73 dB, and the insertion loss is -0.73 dB, or about 0.43 dB higher than the 30-76 MHz device.

The wideband 30-90 MHz coupler shows excellent amplitude balance compared to the narrow band 30-76 MHz units.

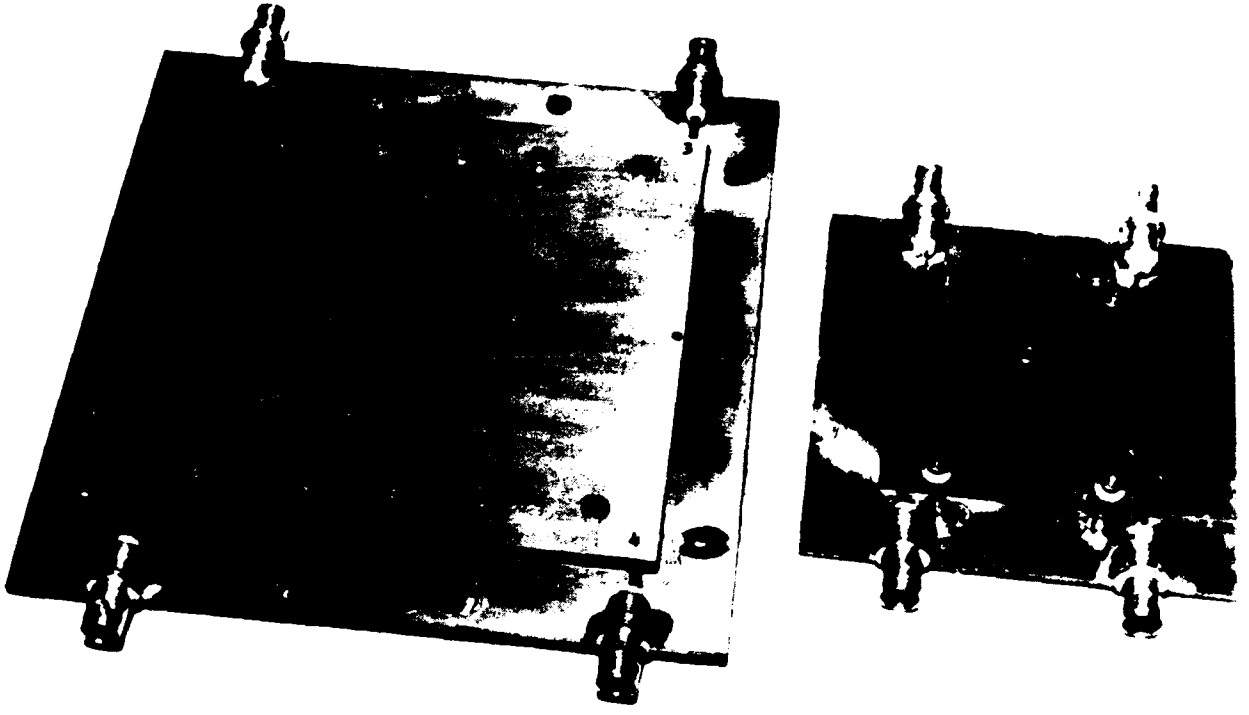

82-263D
9747-82

Figure 6-3. Quad-Hybrid Coupler Test Fixtures

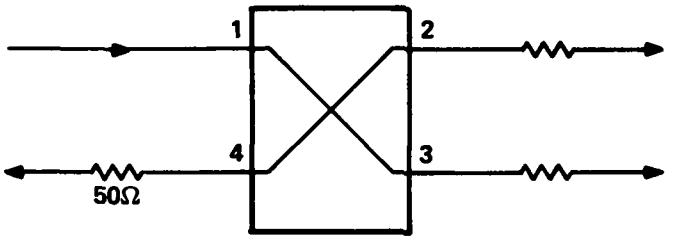

(a) SCHEMATIC, QUAD-HYBRID COUPLER

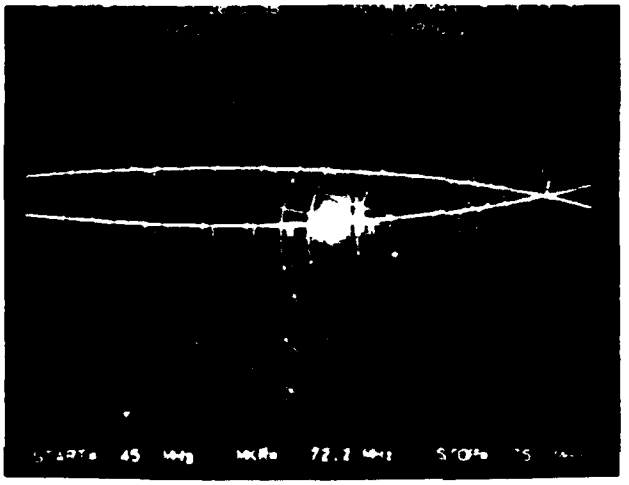

(b) LOSS DATA,

- PATH 1-3, AND PATH 1-2.
- 1 dB/DIVISION
- LOSS AT 72 MHz IS -3.23 dB.
- 30-76 MHz COUPLER

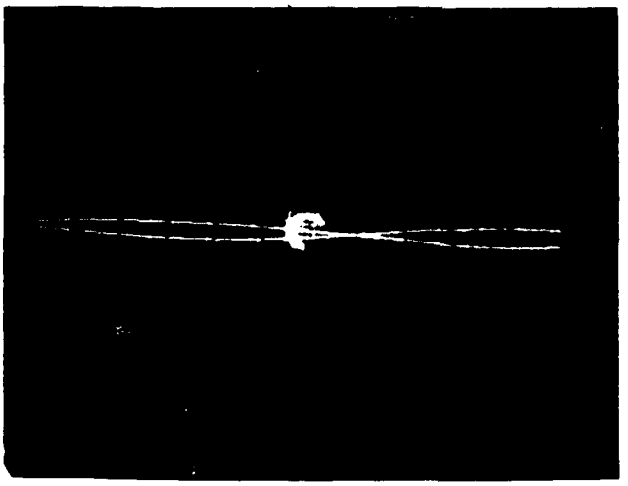

(c) LOSS DATA,

- PATH 1-3, AND PATH 1-2.
- 1 dB/DIVISION
- LOSS AT 70 MHz IS -3.83 dB.
- 30-90 MHz COUPLER

9735-82

Figure 6-4. Quad-Hybrid Coupler Loss Data

As noted, the vendor has recently confirmed this high insertion loss. It was decided to use the narrow band, low loss units for the load pulling tests, and to use units of each style for the channel isolation test, in order to get data at 88 MHz.

6.3 LOAD PULLING TESTS

6.3.1 Introduction

The FHMUX Design Assessment Final Report proved mathematically that the RF architecture of the FHMUX would be insensitive to antenna impedance variations. The proof assumed that the quadrature hybrid couplers were ideal, and that the two bandpass filters were identically tuned so that their reflection coefficients were equal. This section describes the load pulling tests performed, and the successful results obtained.

6.3.2 Load Pulling Test Setup And Procedure

Figure 6-5 shows the test setup used for the load pulling tests. The load VSWR was set up by connecting the reference plane of the load pulling circuit to Port 1 of the network analyzer. The desired load impedance was obtained by adjusting the bias voltage for the correct VSWR, and then rotating this VSWR to the desired phase angle by varying the variable reactive load components which are connected to Port 4 of the quadcoupler. The reference plane and the load pulling circuit were then connected to the output port of Channel 1 of the FHMUX.

The RF output of Channel 1 of the FHMUX was sampled by the directional coupler and routed to Port 2 of the network analyzer.

The antenna intended for use with the FHMUX is specified as having a 3.0:1 VSWR. The load pulling tests were performed with a 4:1 VSWR at various phase angles to provide a more rigorous test.

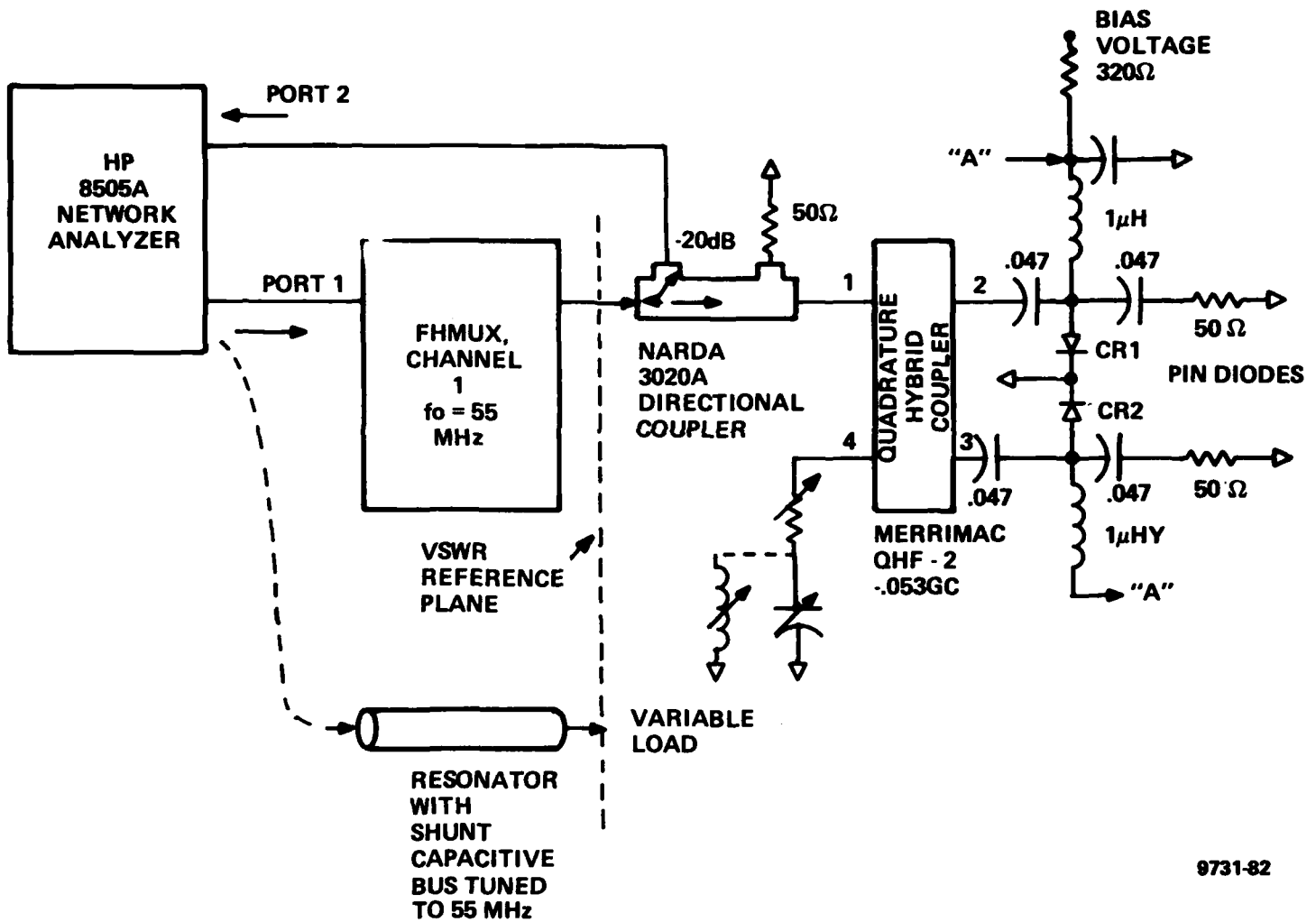

Figure 6-5. Load Pulling Test Setup

Two sets of data were taken:

- Baseline data was taken using a resonator and shunt capacitive bus with no quad-couplers. This data shows what can happen to a narrow band, high Q filter if VSWR isolating techniques are not available
- The second set of data was taken with the complete Channel 1 FHMUX
- Each data set was taken at VSWR phase angles (set at the reference plane) of 0°, $+/-45^{\circ}$, $+/-90^{\circ}$, $+/-135^{\circ}$, and 180°

Figure 6-6 will serve as an introductory piece of data. All data shown is displayed at 2 dB per division. Both amplitude (insertion loss) and impedances are displayed. Figure 6-6 shows only one set of data per photograph, namely input impedance and insertion loss. Each of the remaining photographs show the following:

- Input impedance (circle)
- Load impedance (small arc)
- Insertion loss with 4:1 VSWR

Figure 6-6 (a) shows how rapidly the resonator input impedance changes over the relatively narrow bandwidth of 52-58 MHz. Figure 6-6 (b) shows how well the quad coupler action improves the broad band input VSWR properties of the FHMUX.

The load pulling data is shown in Figures 6-7, 6-8, 6-9, and 6-10. The amplitude traces often change considerably when the 4:1 load is applied. When the amplitude trace shows a decrease in insertion loss as a result of applying a high VSWR, phase addition of the forward and reflected waves is occurring. When the amplitude trace shows an increase in insertion loss, phase cancellation is occurring. The important parameters to observe when the 4:1 VSWR is applied are:

- Changes in input VSWR
- Pulling of the filter center frequency away from the desired value
- Deformation of the shape of the filter skirts.

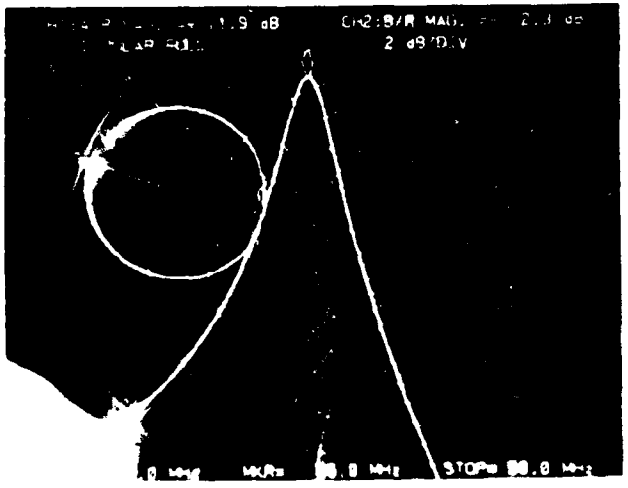

(a) RESONATOR ALONE

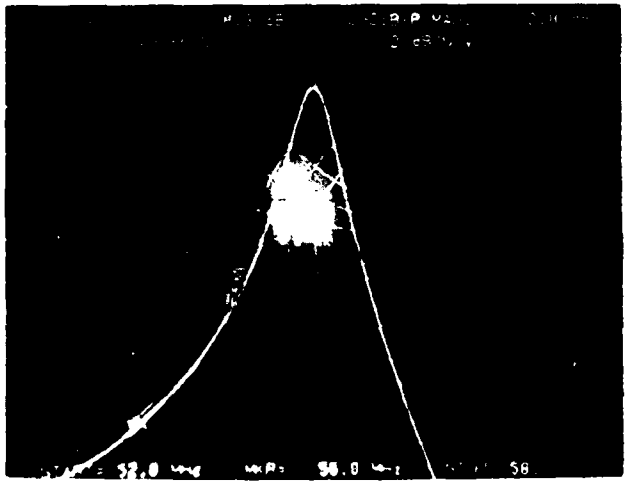

(b) FHMUX CHANNEL 1, LOOKING INTO THE OUTPUT PORT.

9736-82

Figure 6-6. Load Pulling Data Baseline ZL = 50 ohms

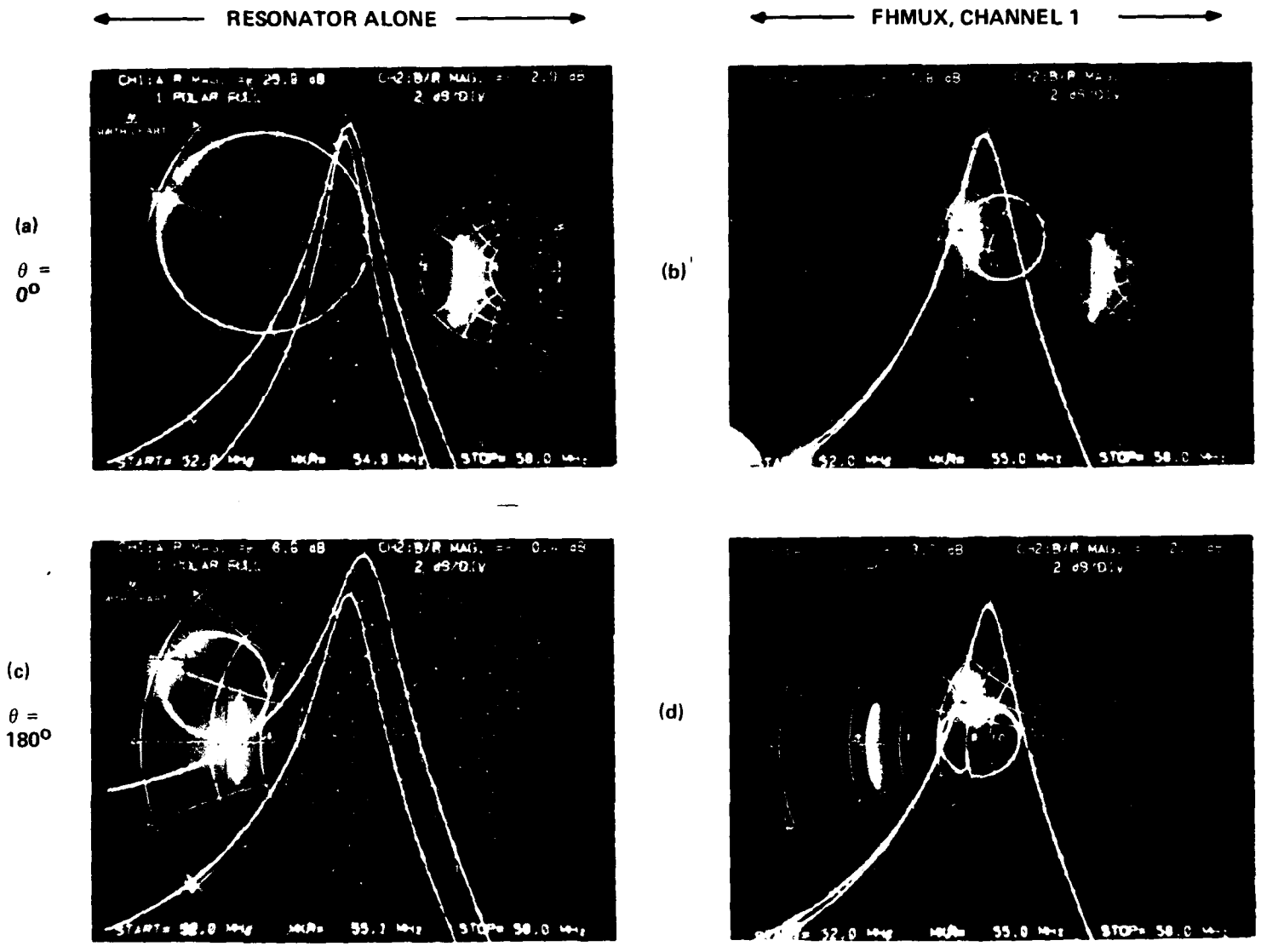

Figure 6-7. Load Pulling Data: VSWR = 4.0:1, 0 = 0, 180°

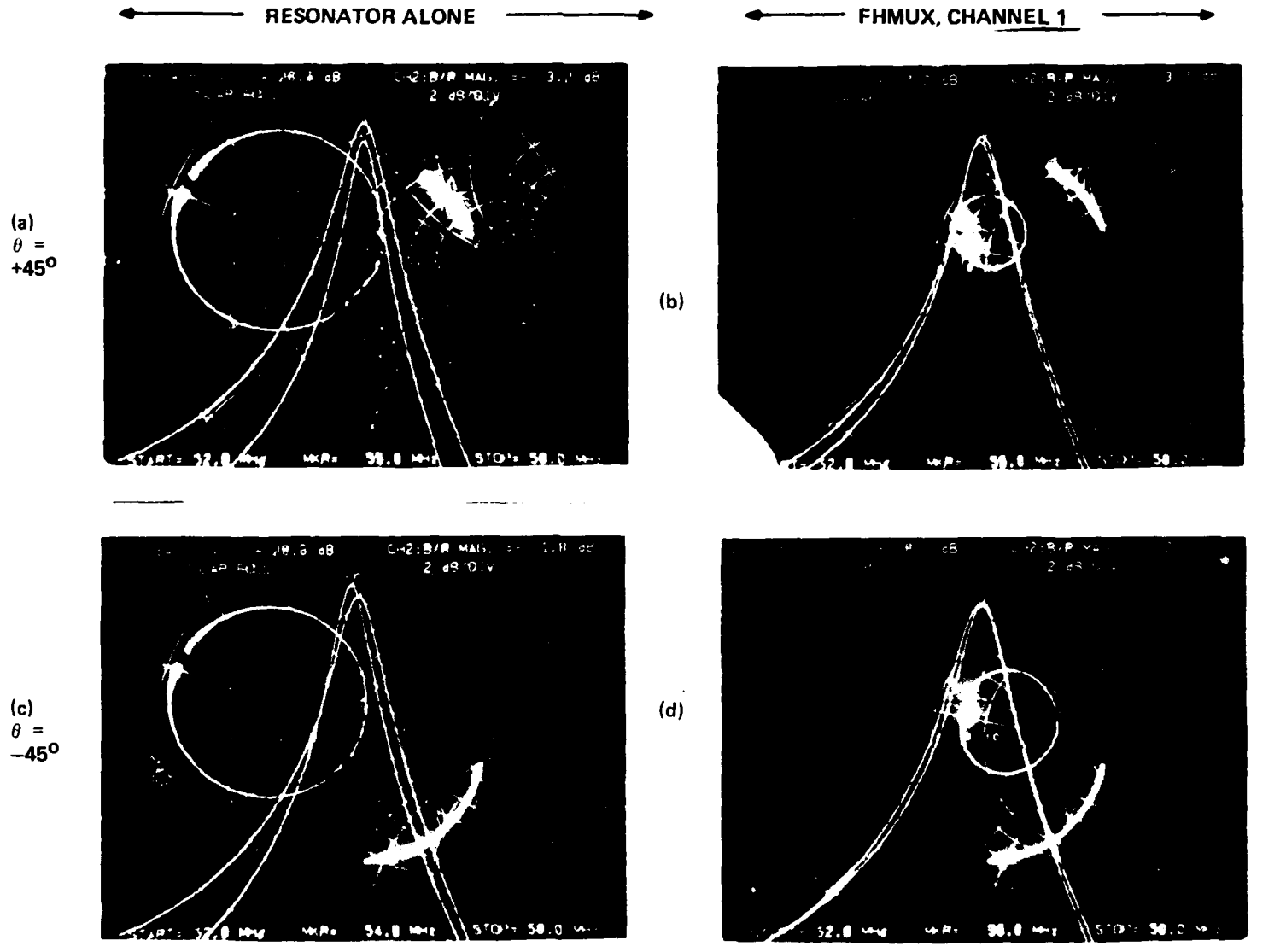

9738-82

Figure 6-8. Load Pulling Data: VSWR = 4.0:1, 0 = +/- 45°

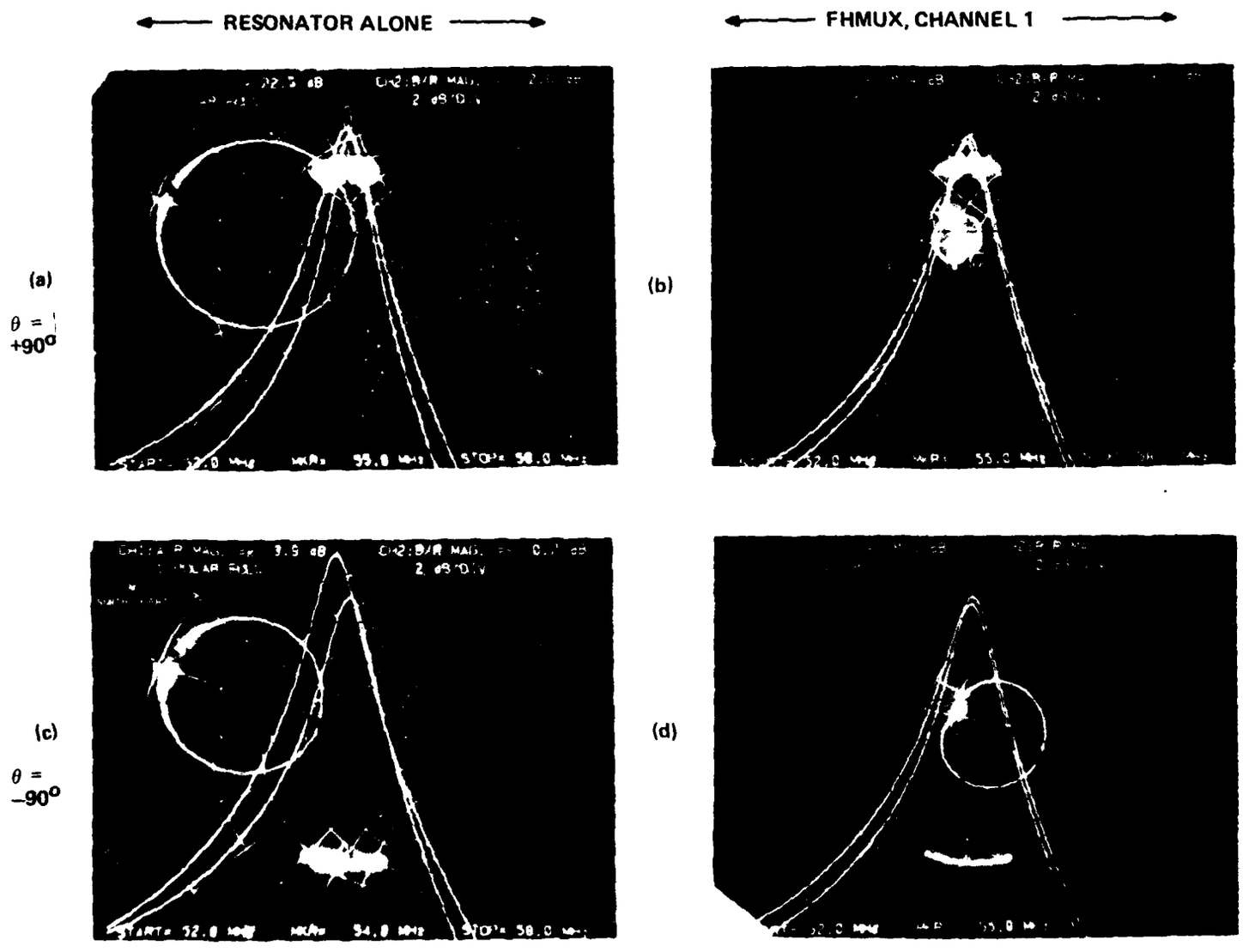

Figure 6-9. Load Pulling Data: VSWR = 4.0:1,, 0 = +/- 90°

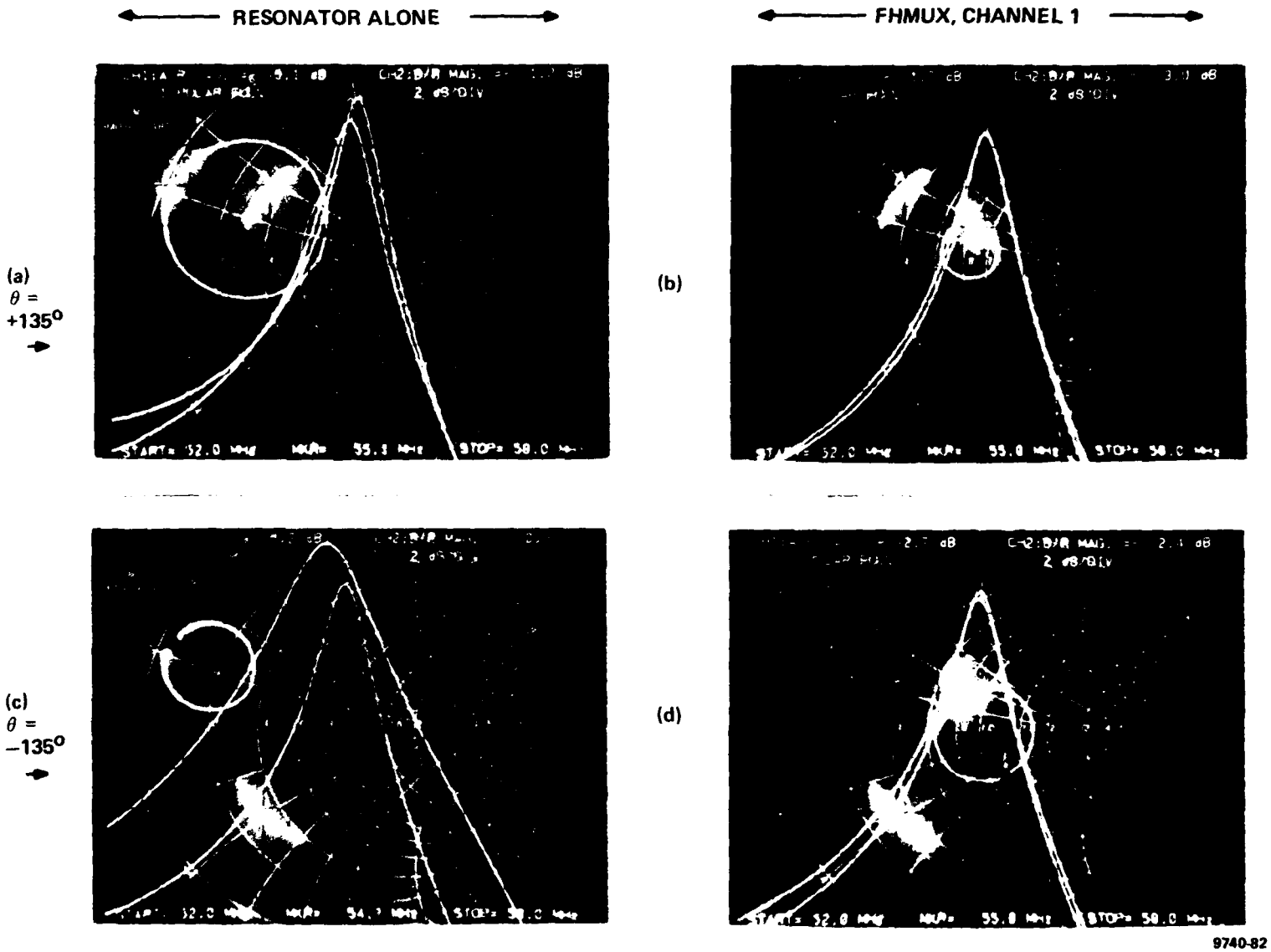

Figure 6-10. Load Pulling Data: VSWR = 4.0:1, 0 = +/- 135°

Figures 6-7 through 6-10 are organized as noted:

- Data with the resonator alone is on the left hand side, and data with the FHMUX is on the right hand side
- Data with similiar load phase angles are located side by side
- Thus a side by side comparison of the load-pulling of the resonator alone, and the FHMUX is possible.

6.3.3 Comments, Load Pulling Data

- The left hand photographs of Figures 6-7 through 6-10 show that the high Q resonator is severely affected by a 4:1 VSWR. Frequency pulling and skirt degradation are readily apparent
- The right hand photographs of Figures 6.7 through 6.10 show that the high Q resonators of the FHMUX are relatively unaffected by the 4:1 VSWR. The load VSWR is passed through the system, modified by the losses, and seen at the input port. However, since there is no multiple reflection between the load and the FHMUX output port, there is little interaction between the load VSWR, and the filters are not detuned
- This data is considered to be proof that the mathematical derivation of the Design Assessment is correct, and the FHMUX system does not require an antenna tuner

6.4 CHANNEL ISOLATION AND COMBINING LOSS

6.4.1 Combining Losses

The FHMUX Design Assessment Final Report derived the relationship between the off channel reflection coefficient of the band pass filters and the "combining loss." Figure 6-11 (a) illustrates this technique, and Figure 6-11 (b) and (c) display the data.

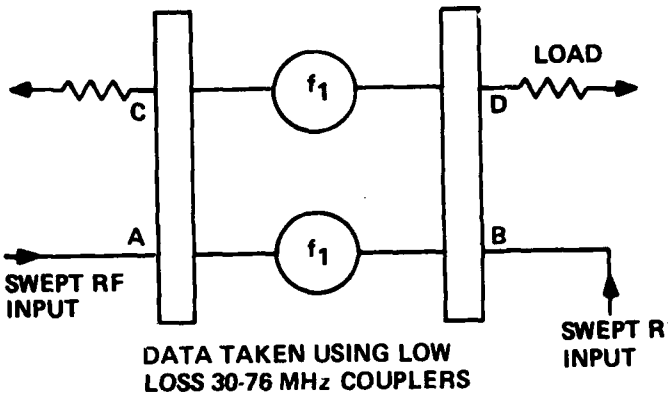

(a) BLOCK DIAGRAM

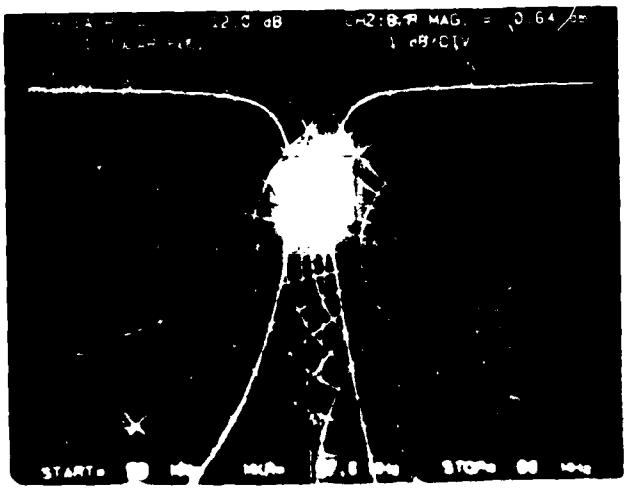

(b) SEPARATE INPUTS

- UPPER TRACE; SWEPT INPUT INCIDENT ON PORT B.
- 1dB/DIVISION.
- LOWER TRACE; SWEPT INPUT INCIDENT ON PORT A.
- RIGHT HAND MARKER IS AT 57.0 MHz +5%.

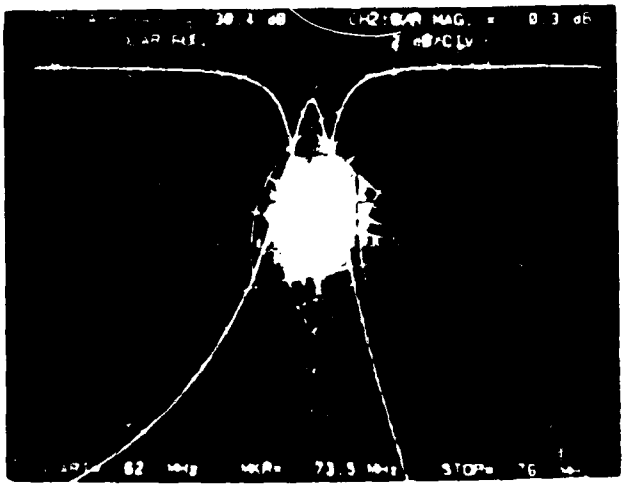

(c) SEPARATE INPUTS

- UPPER TRACE; SWEPT INPUT INCIDENT ON PORT B.
- LOWER TRACE; SWEPT INPUT INCIDENT ON PORT A.
- RIGHT HAND MARKER IS AT 73.5 MHz +5%.
- 2dB/DIVISION.

9741-82

Figure 6-11. Combining Loss Data

Figure 6-11 (a) is a simple block diagram showing a single channel of the feasibility mode. The normal RF input/output path is from Port A to Port D. A second channel can be combined and routed to Port D if the second channel signal is applied to Port B.

Figures 6-11 (b) and (c) show the results of these two separate inputs simultaneously. The upper trace shows how the Port B input is attenuated at the center frequency of the filters (57.0, or 73.5 MHz). The "normal" Port A to Port D response (lower trace) is shown merely as a reference. The markers at the right hand side of the upper traces are positioned +5% above the filter center frequency, and the insertion loss at these points is -0.64 and -0.3 dB, respectively. More precise, single frequency data is given later, but these photographs serve to clarify the combining process.

6.4.2 Channel Isolation

Figures 6-12 through 6-15 show system data pertaining to insertion loss, and channel isolation. The channel isolation data is given in two parts; with a 50 ohm "antenna" load, and with a 12.5 ohm (4:1 VSWR) " antenna" load. Also, Figures 6-12 and 6-13 show data taken with the 30-76 MHz low loss quadrature couplers, and Figures 6-14 and 6-15 show data taken with the higher loss 30-90 MHz quad-couplers.

6.4.3 Comments Regarding Systems Data

- The measured combining loss with the 30-76 MHz quad couplers is -0.62 and -0.69 dB and with the lossier 30-90 MHz couplers, the combining loss is -1.7 and -1.4 dB. The insertion loss of the 30-76 MHz quad-couplers was measured separately, and is close to -0.25 dB. If the Channel 1 filter is at the -14 dB point as far as the Channel 2 signals is concerned, the total "combining loss should be:

$$\begin{array}{l} -.250 \\ \underline{-.176} \\ -.426 \text{ dB} \end{array}$$

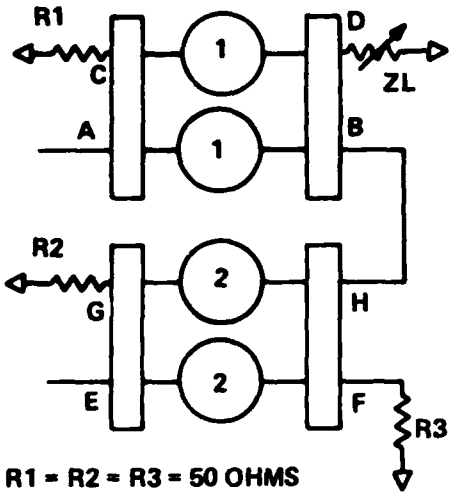

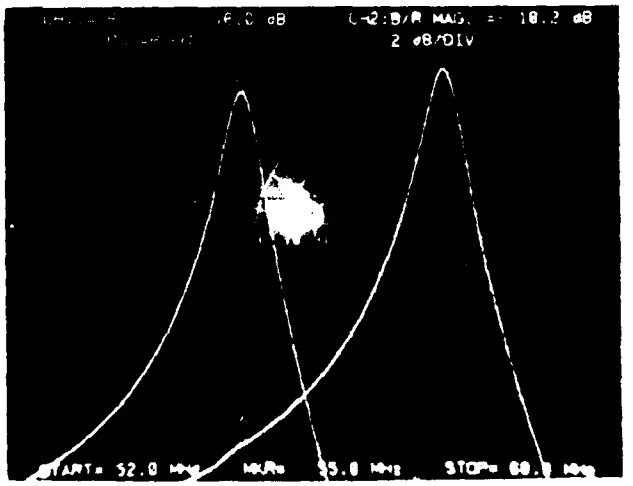

CHANNEL 1 TUNED TO 57.750 MHz

CHANNEL 2 TUNED TO 55.000 MHz

CHANNEL 2 ON LEFT
CHANNEL 1 ON RIGHT
SEPARATE INPUTS,
COMMON PORT D OUTPUT

SIGNAL FLOW PATH	FREQ. (MHz)	LOSS (dB)	
WITH 30-76 MHz LOW LOSS HYBRID COUPLERS		ZL = 50Ω	ZL = 12.5Ω (S = 4:1)
A → D E → H E → D (E - D) – (E - H)	57.75 55.00 55.00	–2.55 –2.83 –3.45 –0.62	—— —— —— ——
A → E E → A	57.75 55.00	–54.1 –34.9	–51.3 –24.2
INTERMOD OBSERVATION NONE VISIBLE –85 dBc (2) SIGNALS, 55 & 57.75 MHz, +20 dBm EACH			HARMONIC OBSERVATION NONE VISIBLE –85 dBc

9749-82

Figure 6-12. System Data

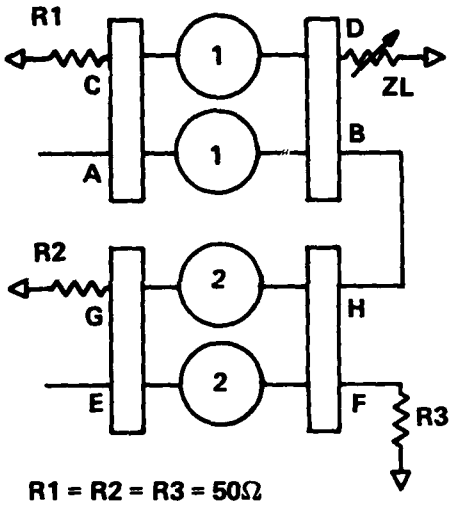

R1 = R2 = R3 = 50Ω

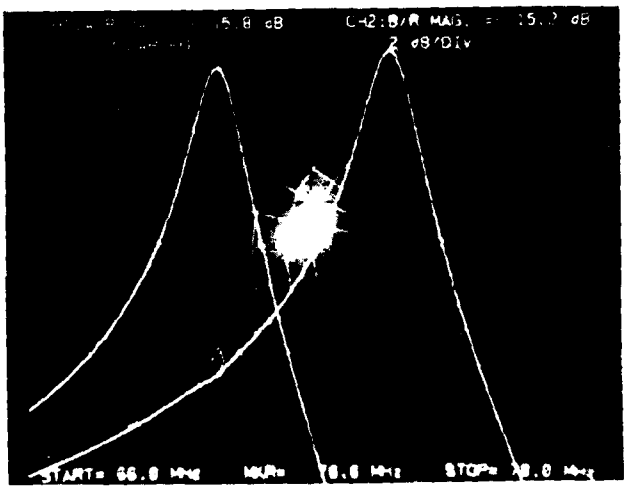

CHANNEL 1 TUNED TO 73.50 MHz

CHANNEL 2 TUNED TO 70.00 MHz

CHANNEL 2 ON LEFT
CHANNEL 1 ON RIGHT
SEPARATE INPUTS,
COMMON PORT D OUTPUT

SIGNAL FLOW PATH	FREQ. (MHz)	LOSS (dB)	
WITH 30-76 MHz LOW LOSS HYBRID COUPLERS		ZL = 50Ω	ZL = 12.5Ω (S = 4:1)
A → D E → H E → D (E - D) – (E - H)	73.50 70.00 70.00	–1.70 –1.81 –2.50 – .69	
A → E E → A	73.50 70.00	–61.4 –32.70	–51.70 –20.8
INTERMOD OBSERVATION NO INTERMOD PRODUCTS SEEN @ –85 dBc			HARMONIC OBSERVATION NONE VISABLE @ –85 dBc

9750-82

Figure 6-13. System Data

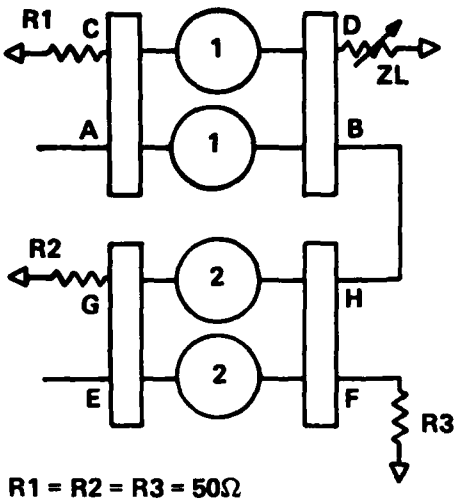

R1 = R2 = R3 = 50Ω

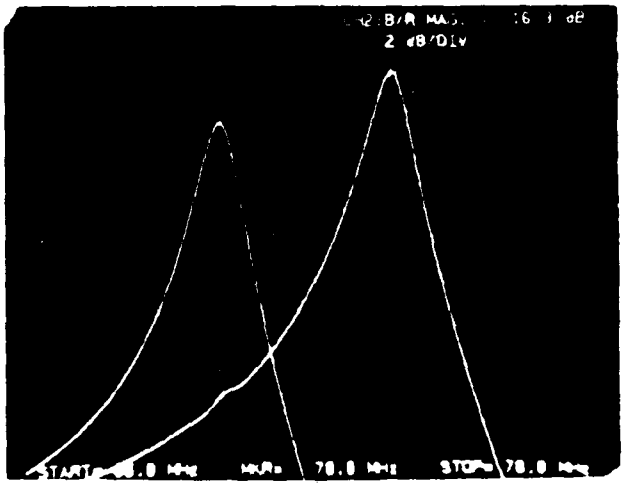

CHANNEL 1 TUNED TO 73.5 MHz

CHANNEL 2 TUNED TO 70.00 MHz

CHANNEL 2 ON LEFT,
CHANNEL 1 ON RIGHT
SEPARATE INPUTS,
COMMON PORT D
OUTPUT

SIGNAL FLOW PATH	FREQ. (MHz)	LOSS (dB)	
WITH WIDE BAND, LOSSY HYBRID COUPLERS		ZL = 50Ω	ZL = 12.5Ω (S = 4:1)
A → D E → H E → D (E - D) – (E - H)	73.50 70.00 70.00	– 2.7 – 2.9 – 4.6 – 1.7	
A → E E → A	73.50 70.00	–47.7 –31.4	–47.9 –32.9

9751-82

Figure 6-14. System Data

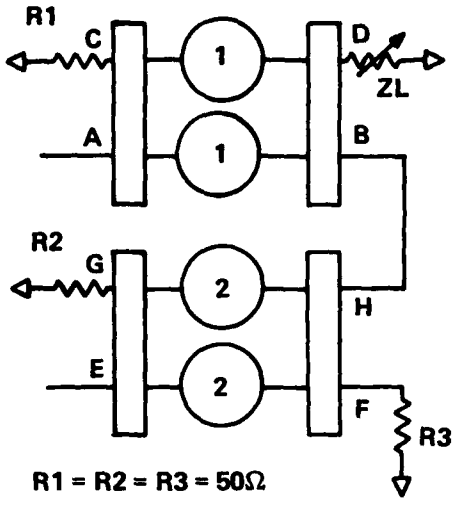

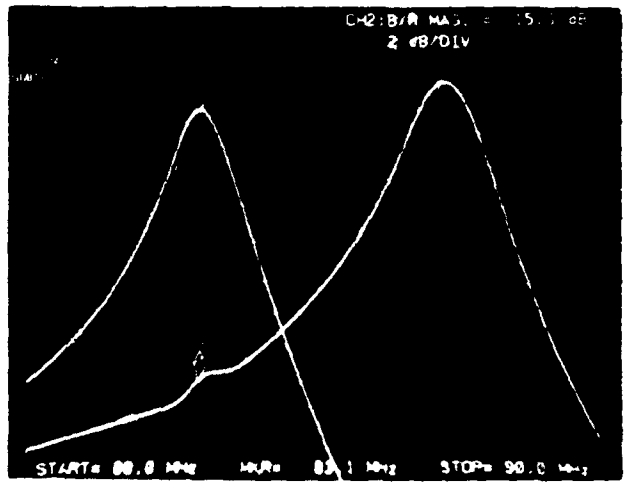

CHANNEL 1 TUNED TO 87.4 MHz

CHANNEL 2 TUNED TO 83.2 MHz

CHANNEL 2 ON LEFT
CHANNEL 1 ON RIGHT
SEPARATE INPUTS, COMMON PORT D OUTPUT

SIGNAL FLOW PATH	FREQ. (MHz)	LOSS (dB)	
WITH WIDE BAND, LOSSY QUAD. COUPLERS		ZL = 50Ω	ZL = 12.5 Ω (S = 4:1)
A → D E → H E → D (E - D) – (E - H)	87.4 83.2 83.2	– 3.4 – 3.0 – 4.4 – 1.4	— — — —
A → E E → A	87.4 83.2	–37.9 –28.8	–36.2 –23.5
INTERMOD OBSERVATION NO INTERMOD PRODUCTS SEEN @ –80 dBc			HARMONIC OBSERVATION NO HARMONIC PRODUCTS SEEN @ –80 dBc

9752-82

Figure 6-15. System Data

Thus, there is about .194 to .264 dB of "excess" loss involved. This excess is attributed to phase and amplitude imbalance (up to 1 dB) of the 30-76 MHz quad couplers, as shown in Figure 6-4 (b), and internal losses of the RF connecting cables (measured as being 0.10 to 0.15 dB). Thus, the measured combining losses appear to be reasonable.

The Design Assessment Final Report proved that the worst case channel isolation should be -14 dB for the recommended final system design as shown on Pages 69A of that report. This would give a minimum of 42 dB of attenuation to off channel signals that were +/-5% off frequency. It was also proved that this worst case condition existed when a high antenna VSWR existed; and the signal path was similiar to the E to D path shown in Figure 6-12. The antenna specified for use with the FHMUX has a specified maximum VSWR of 3:1. (Reflected power is 6 dB below incident power). The channel isolation tests were performed with a 50 ohm load, and a 12.5 ohm (4:1 VSWR) load. A 4:1 VSWR load will cause the reflected power to be 4 dB below the incident power, so this is a more rigorous test than required.

The data shows that the channel isolation of the A to E path is always higher than the E to A path, because of the isolation provided by the quadrature couplers.

The E to A isolation is affected by the load VSWR as predicted, but always is greater than the required 14 dB. The E to A isolation is predictable within a dB or so, as shown below. The data is taken from Figure 6-13.

- Insertion loss E-D	-2.5 dB
- Return loss, 4:1 VSWR	-4.5 dB
- Channel 1 Response at -5% of fo (From Photograph)	-15.2 dB
Total	-22.2 dB
- Measured Value	-20.8 dB
- "Error"	-1.4 dB

Observations of third order intermodulation and harmonic generation were made. Two signals separated in frequency by 5%, were introduced into ports A and E respectively, each at a power level of +20 dBm. The measuring system sensitivity limited the observation of intermod products to -85 dBc.

No intermod products were observed. Also, no harmonically related signals were observed.

6.4.4 Calibration Data

An advanced development model of the FHMUX would be automatically calibrated at the factory. Each bandpass filter would be individually tuned for PROM control of the PIN Diodes in the shunt capacitive bus.

This FHMUX Feasibility Model is manually tuned by four arrays of single pole double throw (SPDT) switches. Figure 6-1 shows a block diagram of the model, and denotes the two channels as Channel 1 and Channel 2. Figure 6-2 is a photograph of the model. Channel 1 is the upper unit, and Channel 2 is the lower unit.

Figure 6-2 shows the four arrays of SPDT switches used to control the unit. These switches are identified as shown in Figure 6-16. The two switches on the right hand side (S9 and S10) are not used.

Calibration data and single channel insertion loss data are given in Table 6-1 and Table 6-2 for Channel 1 and Channel 2 respectively. All data was taken using the Merrimac QHF-3-.060G 30 to 90 MHz quad hybrid couplers (higher loss coupler).

The Channel 2 insertion loss (Table 6-2) measured at 85.000 MHz was -3.95 dB, about 1 dB higher than other nearby data points. There is no circuit malfunction at this frequency. This high insertion loss value is attributed to the inability of the shunt capacitive busses to exactly tune to this frequency, and points out the need for capacitor trimming and/or a 9 or 10 bit shunt capacitive bus.

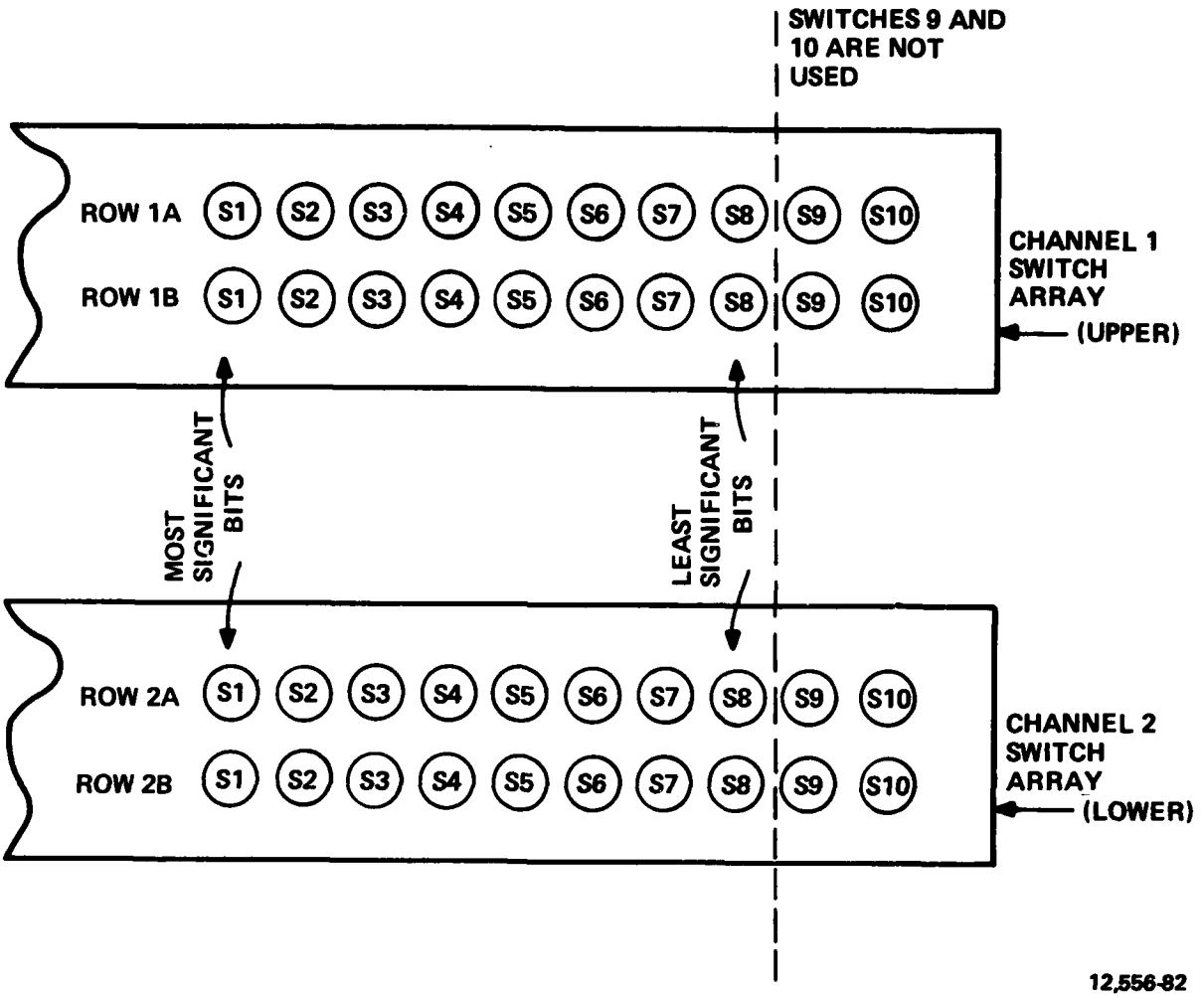

Figure 6-16. Switch Identification

TABLE 6-1. CHANNEL 1 CALIBRATION AND INSERTION LOSS DATA

Frequency (MHz)	Channel and Row	Switch Settings 1 2 3 4 5 6 7 8	Insertion Loss (dB)
55.000	1A	1 1 1 1 0 1 0 1	-2.90
	1B	1 1 1 1 1 0 1 0	
57.500	1A	1 1 0 1 0 1 0 0	-2.80
	1B	1 1 0 1 1 0 0 0	
60.000	1A	1 0 1 1 0 0 1 0	-2.80
	1B	1 0 1 1 1 0 0 0	
62.500	1A	1 0 0 1 1 1 0 0	-2.85
	1B	1 0 0 1 1 1 1 0	
65.000	1A	1 0 0 0 0 1 0 0	-2.85
	1B	1 0 0 0 0 1 1 1	
67.500	1A	0 1 1 0 1 1 1 0	-2.85
	1B	0 1 1 0 1 1 1 1	
70.000	1A	0 1 0 1 1 1 1 0	-2.95
	1B	0 1 0 1 1 1 1 0	
72.500	1A	0 1 0 0 1 1 1 1	-3.00
	1B	0 1 0 0 1 1 1 1	
75.000	1A	0 0 1 1 1 0 1 1	-3.05
	1B	0 0 1 1 1 1 0 1	
77.500	1A	0 0 1 0 1 1 1 0	-3.25
	1B	0 0 1 1 0 0 0 0	
80.000	1A	0 0 1 0 0 0 1 0	-2.65
	1B	0 0 1 0 0 1 0 1	
82.500	1A	0 0 0 1 1 0 1 0	-2.85
	1B	0 0 0 1 1 0 1 1	
85.000	1A	0 0 0 1 0 0 0 0	-3.00
	1B	0 0 0 1 0 0 0 1	
87.500	1A	0 0 0 0 0 1 1 1	-2.65
	1B	0 0 0 0 1 0 0 1	
88.000	1A	0 0 0 0 0 1 1 0	-2.65
	1B	0 0 0 0 1 0 0 0	
90.000	1A	0 0 0 0 0 0 0 1	-2.75
	1B	0 0 0 0 0 0 1 0	

NOTE: Switch up 1, Switch down 0

TABLE 6-2. CHANNEL 2 CALIBRATION AND INSERTION LOSS DATA

Frequency (MHz)	Channel and Row	Switch Settings 1 2 3 4 5 6 7 8	Insertion Loss (dB)
55.000	2A	1 1 1 1 0 1 0 0	-2.90
	2B	1 1 1 1 0 0 0 1	
57.500	2A	1 1 0 1 0 0 1 0	-3.20
	2B	1 1 0 1 0 0 0 0	
60.000	2A	1 0 1 1 0 0 0 1	-2.85
	2B	1 0 1 1 0 0 0 1	
62.500	2A	1 0 0 1 1 0 1 0	-2.90
	2B	1 0 0 1 1 0 0 1	
65.000	2A	1 0 0 0 0 1 0 1	-3.00
	2B	1 0 0 0 0 1 0 1	
67.500	2A	0 1 1 0 1 1 1 1	-2.80
	2B	0 1 1 0 1 1 0 0	
70.000	2A	0 1 0 1 1 1 1 0	-2.95
	2B	0 1 0 1 1 0 0 1	
72.500	2A	0 1 0 0 1 1 1 0	-3.20
	2B	0 1 0 0 1 0 1 1	
75.000	2A	0 0 1 1 1 0 1 1	-2.80
	2B	0 0 1 1 1 0 1 0	
77.500	2A	0 0 1 0 1 1 1 1	-2.70
	2B	0 0 1 0 1 1 1 1	
80.000	2A	0 0 1 0 0 1 0 0	-2.50
	2BB	0 0 1 0 0 1 0 0	
82.500	2A	0 0 0 1 1 0 0 1	-2.90
	2B	0 0 0 1 1 0 0 1	
85.000	2A	0 0 0 1 0 0 0 0	-3.95*
	2B	0 0 0 1 0 0 0 0	
87.500	2A	0 0 0 0 0 1 1 1	-2.65
	2B	0 0 0 0 1 0 0 0	
88.000	2A	0 0 0 0 0 1 1 0	-2.80
	2B	0 0 0 0 0 1 1 0	
90.000	2A	0 0 0 0 0 0 0 0	-2.40
	2B	0 0 0 0 0 0 0 0	

* See text.

SECTION 7

CONCLUSIONS AND RECOMMENDATIONS

7.1 CONCLUSIONS

- The practical results obtained from the FHMUX Feasibility Model have verified the findings of the FHMUX Design Assessment Program
- The feasibility of the FHMUX system is now proven. The areas of concern that have been identified are solveable
- The FHMUX system has now passed two milestones, design assessment and feasibility, and is now ready for further development via the design of an advanced development model
- Load pulling is not a problem
- Channel isolation is predictable, and better than expected
- Low power testing of the PIN Diodes and the shunt capacitive bus showed that the PIN Diodes are not as severe a problem as originally believed, but problems will arise when high power operation is attempted. Additional PIN Diode development will be needed. This additional PIN Diode work should not delay the next phase of this work, it will be best to perform further PIN Diode development concurrently with the next FHMUX hardware phase
- A 10 bit shunt capacitive bus may be needed instead of the 8 bit bus used herein
- Improved tuning and calibration techniques to provide more accurate filter frequency control are needed.

7.2 COMMENT

The FHMUX Design Assessment Final Report derived a baseline system with three cascaded building block bandpass filter-couplers per channel. These channels were then combined by use of load insensitive quadrature coupler circuitry. This FHMUX Feasibility model is a two channel system, which does not have any channel cascaded sections. It is thus, an abbreviated model.

The use of three cascaded filter-couplers was based on the need for approximately 40 dB of channel isolation at +/- 5% of the filter center frequency derived from practically realizable filter coupler sections with 14 dB of channel isolation at ±5% of filter center frequency. Measured values of channel isolation exceeded 14 dB at ± 5% of filter center frequency, and performance was shown to be predictable.

The measured values of insertion loss per filter coupler section were higher than anticipated, and were attributed to variations of loaded Q as the filter frequency was varied. Thus, without additional effort to reduce insertion losses, the -2 dB insertion loss per channel design goal will not be met. Additional effort aimed at reducing variations in loaded Q, and development of lower loss quadrature couplers, is required.

Thus, the channel isolation data, derived from this program and anticipated insertion loss improvements can be extended to a next generation FHMUX model which will probably consist of two cascaded filter-couplers in each channel, and the total channel insertion loss will be about 2.5 to 3.0 dB, plus the channel combining losses.

7.3 RECOMMENDATIONS

Several areas of concern (listed below) will need to be addressed in a future program.

- Resonator loss
- PIN Diode evaluation and test (high power levels)
- Component design and development
  - Bias choke
  - Tuning capacitor trimmers
  - Bypass capacitors
  - Low loss hybrid quadrature couplers

SECTION 8

BIBLIOGRAPHY

- Radio Engineers Handbook, by F.E. Terman.
- Microwave Filters, Impedance Matching Networks, and Coupling Structures, by G. Mathqei, L. Young, and E.M.T. Jones: Artech House.

SECTION 9

APPENDIX A

9.1 VENDOR DATA SHEETS

This appendix contains the following vendor data sheets:

ATC 100 Series Chip Capacitor
ATC 175 Series Ultra High Q Chip Capacitor
Microwave Associates MA4P506 PIN Diode
Unitrode UM6200 Series PIN Diode
Unitrode UM7200 Series PIN Diode

ATC 100

Specifications

ELECTRICAL CHARACTERISTICS:

QUALITY FACTOR: (Qcap): greater than 10,000 at 1 MHz.

CAPACITANCE VALUES AND TOLERANCES:

Case A: standard values and tolerances from 0.1 pF to 100 pF.
Case B: standard values and tolerances from 0.1 pF to 1000 pF.

TEMPERATURE COEFFICIENT OF CAPACITANCE: +90 ±20 PPM/°C (−55°C to 125°C).

DIELECTRIC TEST VOLTAGE: 250% of WVDC rating for 5 secs.

RETRACE: Less than ±0.02% or 0.02 pF, whichever is greater.

AGING EFFECTS: None.

PIEZOELECTRIC EFFECTS: None (No capacitance variation with voltage or pressure).

CAPACITANCE DRIFT: ±0.02% or 0.02 pF, whichever is greater.

CAPACITANCE RANGE, INSULATION RESISTANCE, AND OPERATING VOLTAGE (WVDC) BY CASE SIZE

Case A: 0.1 pF to 100 pF (50 WVDC); 10^5 Megohms Min @ 25°C, 10^3 Megohms Min @ 125°C

Case B: 0.1 pF to 100 pF (500 WVDC); 10^5 Megohms Min @ 25°C, 10^3 Megohms Min @ 125°C
110 pF to 300 pF (300 WVDC); 10^5 Megohms Min @ 25°C, 10^3 Megohms Min @ 125°C
220 pF to 470 pF (200 WVDC); 10^5 Megohms Min @ 25°C, 10^3 Megohms Min @ 125°C
510 pF to 820 pF (100 WVDC); 10^5 Megohms Min @ 25°C, 10^3 Megohms Min @ 125°C
680 pF to 1000 pF (50 WVDC); 10^5 Megohms Min @ 25°C, 10^3 Megohms Min @ 125°C

LIFE TEST: 150% rated voltage for 2000 hours at 125°C as per MIL-STD-202C, method 208A (test condition F).

CHANGE IN CAPACITANCE: At 25°C; ±0.02% or 0.02 pF, whichever is greater.

QUALITY FACTOR: greater than 10,000 at frequency of 1 MHz.

INSULATION RESISTANCE: See table above; no degradation. Standard frequency measurements, 1 MHz, unless otherwise noted.

MECHANICAL CHARACTERISTICS:

HERMETICITY: The porcelain dielectric is non-porous and impervious to moisture and commonly used cleaning solvents.

TERMINATION STYLES: available in Case A as chips and pellets; Case B units as chips, pellets, and leaded devices.

TERMINAL STRENGTH: Microstrip, Axial Ribbon, and Radial Ribbon leaded capacitors withstand a lead pull of 5 lbs. for 5 seconds in the axis of the lead per MIL-STD-202, method 211.

OUTLINE DIMENSIONS: *See Mechanical Configurations on page 7.*

MARKING: All ATC Case A and Case B capacitors may be laser marked with manufacturer's identification, capacity and tolerance code.

ENVIRONMENTAL CHARACTERISTICS:

TEMPERATURE RANGE: From −55°C to +125°C (no derating of working voltage); above 125°C, derate linearly to 50% DCWV @ 200°C.

ATC 100 porcelain capacitors are designed and manufactured to meet or exceed the requirements of MIL-C-11272C, according to the methods of MIL-STD-202. ATC 100 series capacitors are available in all CY80D styles. See QPL list of MIL-C-11272C:FSC-5910.

Barometric pressure	(method 105, cond. B)
Shock	(method 213, cond. J)
Vibration	(method 204, cond. B)
Temperature Cycling	(method 102, cond. C)
Immersion	(method 104, cond. B)
Moisture resistance	(method 106)
Solderability	(method 208)
Terminal Strength	(method 211)
Salt Spray	(method 101, cond. B)

ATC SW 100 BOILING SALT WATER TEST:

Thermal Shock and Hermeticity Test

PURPOSE: To provide a non-destructive simulation of the thermal shock and degradation caused by contaminant absorption experienced during normal circuit mounting and cleaning.

PROCEDURE: With plastic tweezers, drop capacitors into a boiling salt water solution. Remove after two hours, wash thoroughly (distilled water), then dry at 150°C for 10 minutes

MEASURE: I.R., capacity, and Q shall be within published specifications.

MILITARY SPECIFICATIONS:

ATC is on the QPL List for MIL-C-55681/4 and /5, BG (+90 ±20 PPM/°C) characteristic, and the QPL List for MIL-C-11272. Refer to the ATC Military Products Manual.

Capacity Values

CASE A mini-cube® capacitors are available only as chips and pellets from 0.1 pF through* 100 pF in the values and tolerances listed below; working voltages 50 VDC.

CASE B MAXI-"Q"-UBE®* capacitors are available in all values and tolerances at the working voltages shown in the table below. The Case B size may be ordered with a rating of 1000 WVDC, 0.1 pF to 47 pF, or with a rating of 100 WVDC, 680 pF to 1000 pF. To order, specify new WVDC in the ordering code.

CAP CODE	CAP (pF)	TOL	WVDC 125°C
0R1	0.1	B	500
0R2	0.2		
0R3	0.3	BC	500
0R4	0.4		
0R5	0.5	BCD	500
0R6	0.6		
0R7	0.7		
0R8	0.8		
0R9	0.9		
1R0	1.0		
1R1	1.1		
1R2	1.2		
1R3	1.3		
1R4	1.4		
1R5	1.5		
1R6	1.6		
1R7	1.7		
1R8	1.8		
1R9	1.9		
2R0	2.0		
2R1	2.1		
2R2	2.2		
2R4	2.4		
2R7	2.7		
3R0	3.0		
3R3	3.3		
3R6	3.6		
3R9	3.9		

CAP CODE	CAP (pF)	TOL	WVDC 125°C
4R3	4.3	BCD	500
4R7	4.7		
5R1	5.1		
5R6	5.6		
6R2	6.2		
6R8	6.8	BCJKM	500
7R5	7.5		
8R2	8.2		
9R1	9.1		
100	10	FGJKM	500
110	11		
120	12		
130	13		
150	15		
160	16		
180	18		
200	20		
220	22		
240	24		
270	27		
300	30		
330	33		
360	36		
390	39		
430	43		
470	47		
510	51		
560	56		
600	62		

CAP CODE	CAP (pF)	TOL	WVDC 125°C
680	68	FGJKM	500
750	75		
820	82		
910	91		
101	100		
111	110	FGJKM	500
121	120		
131	130		
151	150		
161	160		
181	180		
201	200		
221	220	FGJKM	500
241	240		
271	270		
301	300		
331	330		
361	360		
391	390		
431	430		
471	470		
511	510	FGJKM	100
561	560		
621	620		
681	680	FGJKM	50
751	750		
821	820		
911	910		
102	1000		

TOLERANCE CODE:

B = ±0.1 pF
C = ±0.25 pF
D = ±0.5 pF
F = ±1%
G = ±2%
J = ±5%
K = ±10%
M = ±20%

*MAXI-"Q"-UBE® and mini-cube® are registered trademarks of ATC.

Figure 9-1. ATC 100 Chip Capacitor Data Sheet

ATC 175 ULTRA HIGH Q PORCELAIN CAPACITORS

ULTRA HIGH "Q's" UP TO 4X HIGHER THAN BEST INDUSTRY STANDARD (ATC 100).

MICROWAVE POWER, CURRENT, AND Q RATINGS FIED AT UHF/MICROWAVE FREQUENCIES FOR ALL CAPACITANCE VALUES. (CONTACT FACTORY.)

NO DERATING FOR OPERATION UP TO 175°C.

ATC 175 capacitors are designed for use with today's higher power, higher frequency transistors. The low loss ATC 175 capacitors reduce circuit loss by as much as a factor of 4, and permit reliable operation up to 175°C case temperature.

ATC 175 Series utilizes a unique internal construction* while retaining the ruggedness that is inherent in all ATC UHF/Microwave capacitors.

The ATC 175 power handling capability equals or exceeds the power capability of transistors presently available.

* Patent Pending

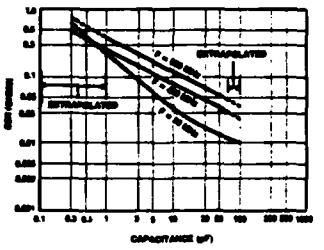

Specifications

ELECTRICAL CHARACTERISTICS:

CAPACITANCE VALUES AND TOLERANCES: Case B-standard values and tolerances from 1.0 pF to 100 pF. See table for standard ATC 175 Capacity Values.

WORKING VOLTAGE: See table of Capacity Values below.

QUALITY FACTOR: See curve entitled, "Equivalent Series Resistance (Ohms) versus Capacitance (pF)".

INSULATION RESISTANCE: 10^4 Megohms Min @ 25°C, 10^3 Megohms Min @ 175°C at rated voltage.

TEMPERATURE COEFFICIENT OF CAPACITANCE: +90 ±30 PPM/°C (−55°C to +175°C).

DIELECTRIC TEST VOLTAGE: 250% of WVDC rating for 5 secs.

RETRACE: Less than ±0.02% or 0.02 pF, whichever is greater.

AGING EFFECTS: None.

PIEZOELECTRIC EFFECTS: None (No capacitance variation with voltage or pressure).

CAPACITANCE DRIFT: ±0.02% or 0.02 pF, whichever is greater.

LIFE TEST:

150% rated voltage for 2000 hours at 175°C as per MIL-STD-202C, method 208A (test condition F).

CHANGE IN CAPACITANCE: At 25°C; less than 0.02% or 0.02 pF, whichever is greater.

QUALITY FACTOR: No degradation.

INSULATION RESISTANCE: No degradation.

Standard frequency of measurements, 1 MHz, unless otherwise noted.

MECHANICAL CHARACTERISTICS:

HERMETICITY: The porcelain dielectric is impervious to moisture and commonly used cleaning solvents.

TERMINATION STYLES: Available as chips, pellets, and microstrip leaded devices.

TERMINAL STRENGTH: Microstrip leaded capacitors withstand a lead pull of 5 lbs. for 5 seconds in the axis of the lead per MIL-STD-202, Method 211.

OUTLINE DIMENSIONS: See Mechanical Configurations on page 7.

MARKING: All ATC 175 Capacitors are laser marked permanently with manufacturer's identification, capacity code, and tolerance code.

ENVIRONMENTAL CHARACTERISTICS:

MILITARY SPECIFICATIONS: All ATC 175 Series Capacitors meet *MIL-C-11272C, MIL-C-55681, and MIL-C-23269.*

TEMPERATURE RANGE: From −55°C to +175°C (NO DERATING OF WORKING VOLTAGE).

ATC 175 porcelain capacitors are designed and manufactured to exceed the following requirements of MIL-STD-202:

Barometric pressure	(method 105, cond. B)
Shock	(method 213, cond. J)
Vibration	(method 204, cond. B)
Temperature Cycling	(method 102, cond. C)
Immersion	(method 104, cond. B)
Moisture Resistance	(method 106)
Solderability	(method 208)
Terminal Strength	(method 211)
Salt Spray	(method 101, cond. B)

Capacity Values

CAP CODE	CAP (pF)	TOL	WVDC 175°C
1R0	1.0		
1R1	1.1		
1R2	1.2		
1R3	1.3		
1R4	1.4		
1R5	1.5		
1R6	1.6		
1R7	1.7		
1R8	1.8		
1R9	1.9		
2R0	2.0		
2R1	2.1		
2R2	2.2		
2R4	2.4		
2R7	2.7		
3R0	3.0		
3R3	3.3		
3R6	3.6		
3R9	3.9		

CAP CODE	CAP (pF)	TOL	WVDC 175°C
4R3	4.3		
4R7	4.7		
5R1	5.1		
5R6	5.6		
6R2	6.2		
6R8	6.8		
7R5	7.5		
8R2	8.2		
9R1	9.1		
100	10		
110	11		
120	12		
130	13		
150	15		
160	16		
180	18		
200	20		

CAP CODE	CAP (pF)	TOL	WVDC 175°C
220	22		
240	24		
270	27		
300	30		
330	33		
360	36		
390	39		
430	43		
470	47		
510	51		
560	56		
620	62		
680	68		
750	75		
820	82		
910	91		
101	100		

TOLERANCE CODE:

B = ±0.1 pF
C = ±0.25 pF
D = ±0.5 pF
F = ±1%
G = ±2%
J = ±5%
K = ±10%
M = ±20%

Figure 9-2. ATC 175 Ultra High Q Capacitor Data Sheet

PIN specification and switch performance selection guide

10.13 MA-4P506 SPECIFICATIONS AND SWITCHING PERFORMANCE

Voltage Breakdown (V_b)	= 500 volts (MIN) @ 10μA
Junction Capacitance (C_j)	= .70 pF (MAX) @ 100 volts
Series Resistance (R_s)	= 0.3Ω (MAX) @ 100 mA
Carrier Lifetime (τ_L)	= 3.0μs (TYP)
Reverse Recovery Time (T_{rr})	= .350 μs (TYP)
Thermal Resistance (θ_{jc})	= 10°C/W (MAX)
Power Dissipation @ 25°C	= 15W (MAX)
Standard Case Styles[1]	= 30, 4 and 131[2]

The MA-4P506 PIN diode is specifically designed for use as a moderate to high power switching diode. The low R_s, low thermal resistance and CERMACHIP™ construction of this diode make it an excellent choice for many medium power , low-loss applications. Switching speeds of 200 ns are typical.

NOTES:
1. Custom packaging is available upon request.
2. Case style 131 is a CERMACHIP™ (hermetically sealed chip).

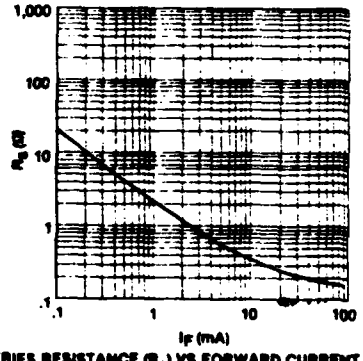

SERIES RESISTANCE (R_s) VS FORWARD CURRENT (I_F) FOR AN MA-4P506 PIN DIODE

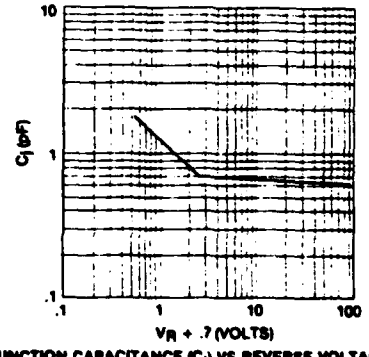

JUNCTION CAPACITANCE (C_j) VS REVERSE VOLTAGE (V_R) FOR AN MA-4P506 PIN DIODE

Figure 9-3. Microwave Associates 4P506 PIN Diode Data Sheet

PIN DIODE

UM6000 SERIES
UM6200 SERIES
UM6600 SERIES

Features

- Capacitance specified as low as 0.4 pF (UM6600)
- Resistance specified as low as 0.4Ω (UM6200)
- Voltage ratings to 1000V
- Power dissipation to 6W

Description

These series of PIN diodes are designed for applications requiring small package size and moderate average power handling capability. The low capacitance of the UM6000 and UM6600 allows them to be used as series switching elements to 1 GHz. The low resistance of the UM6200 is useful in applications where forward bias current must be minimized.

Because of its thick I-region width and long lifetime the UM6000 and UM6600 have been used in distortion sensitive and high peak power applications, including receiver protectors, TACAN, and IFF equipment. Their low capacitance allows them to be useful as attenuator diodes at frequencies greater than 1 GHz. The UM6200 has been used successfully in switches in which low insertion loss at low bias current is required.

The "A" style package for this series is the smallest Unitrode PIN diode package. It has been used successfully in many microwave applications using coaxial, microstrip, and stripline techniques at frequencies beyond X-Band. The "B" and "E" style, leaded packages offer the highest available power dissipation for a package this small. They have been used extensively as series switch elements in microstrip circuits. The "C" style package duplicates the physical outline available in conventional ceramic-metal packages but incorporates the many reliability advantages of the Unitrode construction.

MAXIMUM RATINGS

Average Power Dissipation and Thermal Resistance Ratings

Package	Condition	UM6000 UM6200		UM6600	
		P_D	θ	P_D	θ
A&C	25°C Pin Temperature	6W	25°C/W	4W	37.5°C/W
B&E (Axial Leads)	½ in. Total Lead Length to (12.7mm) to 25°C Contact	2.5W	60°C/W	2.0W	75°C/W
B&E (Axial Leads)	Free Air	0.5W	—	0.5W	—

Peak Power Dissipation Rating

All Packages	1 μs Pulse (Single) at 25°C Ambient	UM6000 - 25 KW UM6200 - 10 KW	UM6600 - 13 KW

Operating and Storage Temperature Range: −65°C to +175°C

UNITRODE

Figure 9-4. Unitrode UM6200 Series PIN Diode Data Sheet

Voltage Ratings (25 °C)

Reverse Voltage (V_R) — Volts (I_R = 10 μA)	Types		
100V	UM6001	UM6201	UM6601
200V	UM6002	UM6202	UM6602
400V	—	UM6204	—
600V	UM6006	—	UM6606
1000V	UM6010	—	UM6610

Electrical Specifications (25 °C)

Test	Symbol	UM6600	UM6000	UM6200	Conditions
Total Capacitance (Max)	C_T	0.4 pF	0.5 pF	1.1 pF	0V, 1 GHz
Series Resistance (Max)	R_S	2.5Ω	1.7Ω	0.4Ω	100 mA, 1 GHz
Parallel Resistance (Min)	R_P	10 KΩ	15 KΩ	10 KΩ	100V, 1 GHz
Carrier Lifetime (Min)	τ	1.0 μs	1.0 μs	0.6 μs	I_F = 10 mA
Reverse Current (Max)	I_R	10 μA	10 μA	10 μA	V_R = Rating
I-Region Width (Min)	W	150 μm	150 μm	40 μm	—

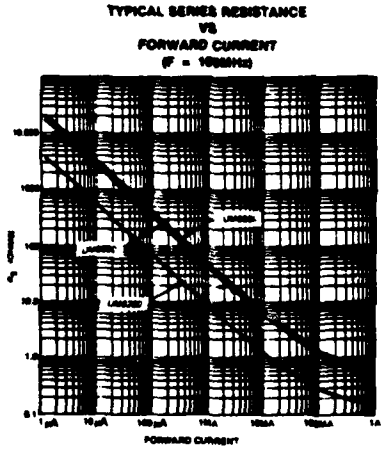

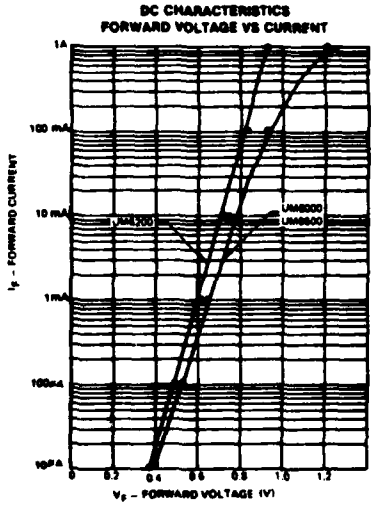

UNITRODE CORPORATION • 5 FORBES ROAD
LEXINGTON, MA 02173 • TEL. (617) 861-6540
TWX (710) 326-6509 • TELEX 95-1064

Figure 9-5. Unitrode UM6200 Series PIN Diode Data Sheet (Cont.)

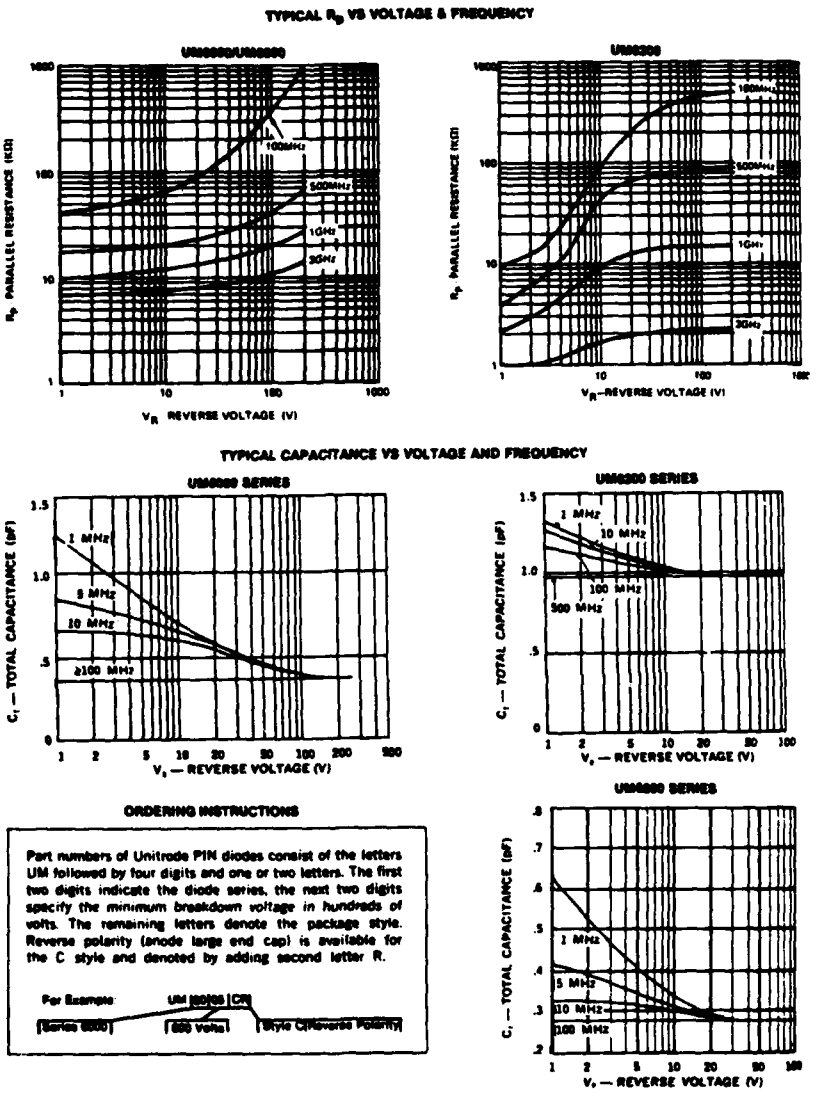

Figure 9-6. Unitrode UM6200 Series PIN Diode Data Sheet (Cont.)

PIN DIODE

UM7000 SERIES
UM7100 SERIES
UM7200 SERIES

Features

- Voltage ratings to 1000V (UM7000)
- Wide variety of package styles
- Rated average power dissipation to 10W
- Cost effective in volume applications

Description

The UM7000 and UM7100 series offer moderately high power handling in combination with reasonably low levels of both series resistance and capacitance. The UM7200 series offers the lowest series resistance, but the highest capacitance of the group. The differences in specified performance, for each of the series, results from different I-region thicknesses. The three series have broad applicability in many RF and microwave switch and attenuator circuits. Additionally, the UM7100 in leaded versions, is usually the most cost-effective diode choice in high volume usage.

MAXIMUM RATINGS

Average Power Dissipation and Thermal Resistance Ratings

Package	Condition	P_D	θ
A	25 °C Pin Temperature	10W	15 °C/W
B&E (Axial Leads)	½ in.(12.7 mm) Lead Length to 25 °C Contact	5.5W	27.5 °C/W
B&E (Axial Leads)	Free Air	1.5W	—
C (Studded)	25 °C Stud Temperature	10W	15 °C/W
D (Insulated Stud)	25 °C Stud Temperature	7.5W	20 °C/W

Peak Power Dissipation Rating

All Packages	1 μs Pulse (Single) at 25 °C Ambient	UM7000 - 60 KW UM7100 - 35 KW UM7200 - 20 KW

Operating and Storage Temperature Range: −65 °C to +175 °C

UNITRODE

Figure 9-7. Unitrode UM7200 Series PIN Diode Data Sheet

Voltage Ratings (25 °C)

Reverse Voltage (V_R) — Volts (I_R = 10 μA)	Types		
100V	UM7001	UM7101	UM7201
200V	UM7002	UM7102	UM7202
400V	—	UM7104	UM7204
600V	UM7006	—	—
800V	—	UM7108	—
1000V	UM7010	—	—

Electrical Specifications (25 °C)

Test	Symbol	UM7000	UM7100	UM7200	Conditions
Total Capacitance (Max)	C_T	0.9 pF	1.2 pF	2.2 pF	0V, 1 GHz
Series Resistance (Max)	R_S	1.0Ω	0.6Ω	0.25Ω	100 mA, 1 GHz
Parallel Resistance (Min)	R_P	10 KΩ	8 KΩ	7 KΩ	100V, 1 GHz
Carrier Lifetime (Min)	τ	2.5 μs	2.0 μs	1.5 μs	I_F = 10 mA
Reverse Current (Max)	I_R	10 μA	10 μA	10 μA	V_R = Rating
I-Region Width (Min)	W	150 μm	80 μm	40 μm	—

TYPICAL FORWARD RESISTANCE VS FORWARD CURRENT (F = 100 MHz)

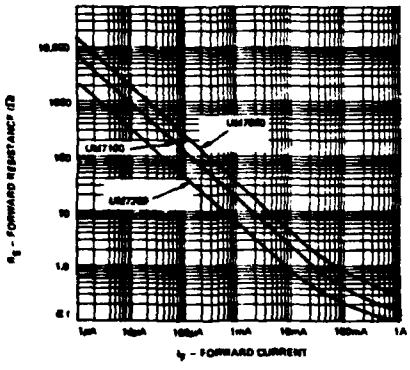

TYPICAL DC CHARACTERISTIC FORWARD VOLTAGE VS FORWARD CURRENT UM7000/UM7100/UM7200

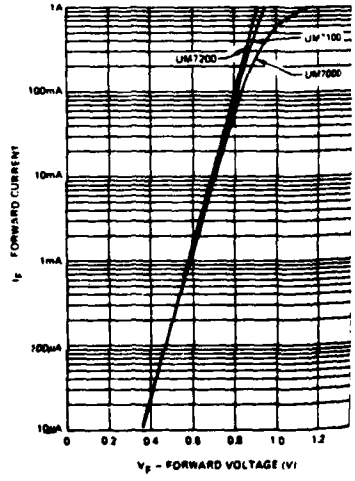

UNITRODE CORPORATION • 5 FORBES ROAD
LEXINGTON, MA 02173 • TEL. (617) 863-8300
TWX (710) 326-6509 • TELEX 95-1064

Figure 9-8. Unitrode UM7200 Series PIN Diode Data Sheet (Cont.)

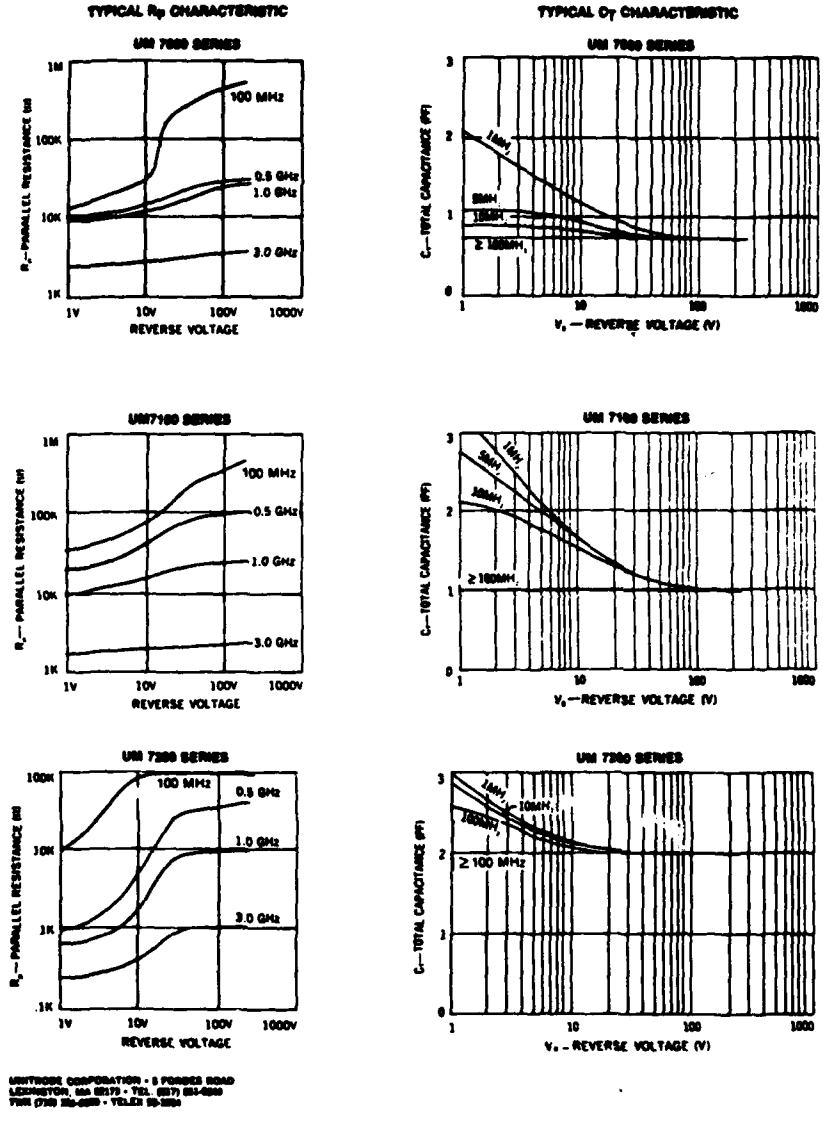

Figure 9-9. Unitrode UM7200 Series PIN Diode Data Sheet (Cont.)

FREQUENCY HOPPING MULTIPLEXER DESIGN ASSESSMENT

REFERENCE DOCUMENT

AUGUST 1982

PREPARED FOR
USA CORADCOM
CONTRACT NO.
DAAK80-80-C-0588

Systems

Communication Systems Division
GTE Communications Products Corporation
77 "A" Street
Needham Heights, MA 02194
Area Code 617 449-2000
TELEX: 922497

FREQUENCY HOPPING MULTIPLEXER

DESIGN ASSESSMENT

REFERENCE DOCUMENT

AUGUST 1982

Prepared for:

USA CORADCOM
Contract No. DAAK80-C-0588

Communication Systems Division
GTE Communications Products Corporation
77 "A" Street
Needham Heights, MA 02194

ABSTRACT

This GTE Sylvania Reference Document is in support of the Final Report for a Frequency Hopping Multiplexer (FHMUX) Design Assessment.

The Final Report and this document complete a 12 month study to investigate its concept and feasibility.

The results of the study are positive. The FHMUX can perform as desired and also enhance certain transceiver performance parameters such as broadband transmitter noise rejection, more constant transmitter loading, and increased receiver selectivity. These positive results should encourage the design and development of an advanced engineering model.

This reference document describes work performed early in the FHMUX program, and is in separate form to increase the readability and utility of the Final Report.

TABLE OF CONTENTS

		Page
APPENDIX A	CIRCULATOR CIRCUIT TECHNIQUES	A-1
A.1	Circulator Multiplexing Schemes	A-1
APPENDIX B	DISCUSSION OF DUAL ANTENNA SYSTEMS	B-1
B.1	Circulator Discussion	B-1
B.2	Switching Considerations	B-4
B.3	Active Circulator	B-4
B.4	Two Antenna Systems with Linear Amplifiers	B-4
B.5	Alternate Approaches	B-14
B.6	Hybrid Two Antenna System	B-16
B.7	System Requirement	B-19
APPENDIX C	LOAD PULLING STUDY	C-1
C.1	Filter Application & Load Pulling Study	C-1
C.2	Load Pulling	C-3
APPENDIX D	ANTENNA STUDY	D-1
D.1	Antenna Description	D-1
D.2	Antenna Impact on System Design	D-8
D.3	Analysis of Antenna Parameter Variation	D-9
D.4	Possible Value of Phase Correction	D-12
D.5	The Self-Calibrating Single Antenna FHMUX	D-16
D.6	Advantage of Self-Calibration	D-16
D.7	Block Diagram Description	D-17
D.8	Alignment Procedure	D-19

TABLE OF CONTENTS (Cont.)

		Page
D.9	Impedance Measurement Techniques	D-21
D.10	Operational Scenario	D-21

LIST OF FIGURES

Figure	Title	Page
A-1	Summation of 3 Transmitters	A-2
A-2	Summation cf 4 Transmitters	A-5
A-3	5 Way Combiner	A-7
A-4	9 Way Combiner	A-8
A-5	16 Way Combiner	A-9
B-1	3 Port Circulator Preliminary Specification	B-2
B-2	Specification Response	B-3
B-3	Switching Considerations	B-5
B-4	Active 3 Port Circulator	B-6
B-5	Alternate Circuit - Transmit Multi - Coupler	B-7
B-6	IMD analysis	B-10
B-7	Noise Floor Analysis	B-11
B-8	Channelized Amplifier	B-15
B-9	Hybrid 2 Antenna RF Block Diagram	B-17
B-10	Dual Antenna System Model Derivation	B-20
C-1	Tuned Circuit Response	C-5
C-2	Range of Element Values	C-6
C-3	Loads 3 and 4	C-8
C-4	Loss (vs) Bandwidth, Load #3	C-9
C-5	Loss (vs) Bandwidth, Load #4	C-10
C-6	Impedance (vs) Frequency, Loads 5 and 6	C-11
C-7	Loss (vs) % Bandwidth Load #5	C-12
C-8	Loss (vs) % Bandwidth Load #6	C-13
C-9	Antenna Load #1 impedance (vs) Frequency	C-15

LIST OF FIGURES (Cont.)

Figure	Title	Page
C-10	Impedance (vs) Frequency Load #2	C-17
C-11	Locus Points for Load 3,4,5, and 6. Taken every 10 degrees	C-20
D-1	Antenna Characteristic	D-2
D-2	As 3166/GRC Antenna Impedance	D-3
D-3	Antenna Group OE-254/GRC R + JS at Input to 50 ft. Cable. Resistance (vs) Frequency	D-6
D-4	Antenna Group OE-254/GRC Reactance (vs) Frequency	D-7
D-6	Variation in Input Impedance for +/-10% Variation in Load Impedance	D-10
D-7	Variation in Input Impedance as Length is Varied from 80'-2% to 80"+2%	D-11
D-8	Block Diagram, FHMUX Single Antenna Scheme with Antenna Phase Correction	D-15
D-9	Block Diagram, Self Calibrating FHMUX	D-18

APPENDIX A CIRCULATOR CIRCUIT TECHNIQUES

A.1 CIRCULATOR MULTIPLEXING SCHEMES

An extension of the "Stites Coupler" (discussed in GTE Proposal) permits easy connection of three or four transmitters into a common antenna circuit. The basic Stites coupler permits low loss connection of two transmitters to a common antenna; these variations permit additional transmitters to be so connected with little, if any, added complexity or loss.

Extension of the original Stites circuit to accomodate more transmitters to a common antenna is limited to growth in a binary fashion i.e., 2, 4, 8, 16, etc. This extended concept permits much greater flexibility in this regard. In addition, the circuit bandwidth is limited only by the circulators and the power combiner.

When the four (4) port combiner is used, the combining efficiency is higher than that obtained in building a tree of three (3) of the original Stites couplers.

As in the original circuit, use is made of the non-reciprocal properties of ferrite circulators. It uses the energy reflected at the juncture of three (or four) transmitters, so that it can be equally divided, and made available in segments of equal power and phase for recombining.

Figure A-1 shows how the summation of three transmitters is accomplished.

The circuit shown makes use of a deliberate 3 to 1 VSWR. The ratio of power reflected to incident power, is determined by the following relationship:

$$\frac{Pr}{Pi} = \left(\frac{s - 1}{s + 1}\right)^2$$

Where Pr = Reflected Power
Pi = Incident Power
s = VSWR

For a 3:1 VSWR

$$\frac{Pr}{Pi} = \left(\frac{3 - 1}{3 + 1}\right)^2 = \left(\frac{2}{4}\right)^2 = 0.25$$

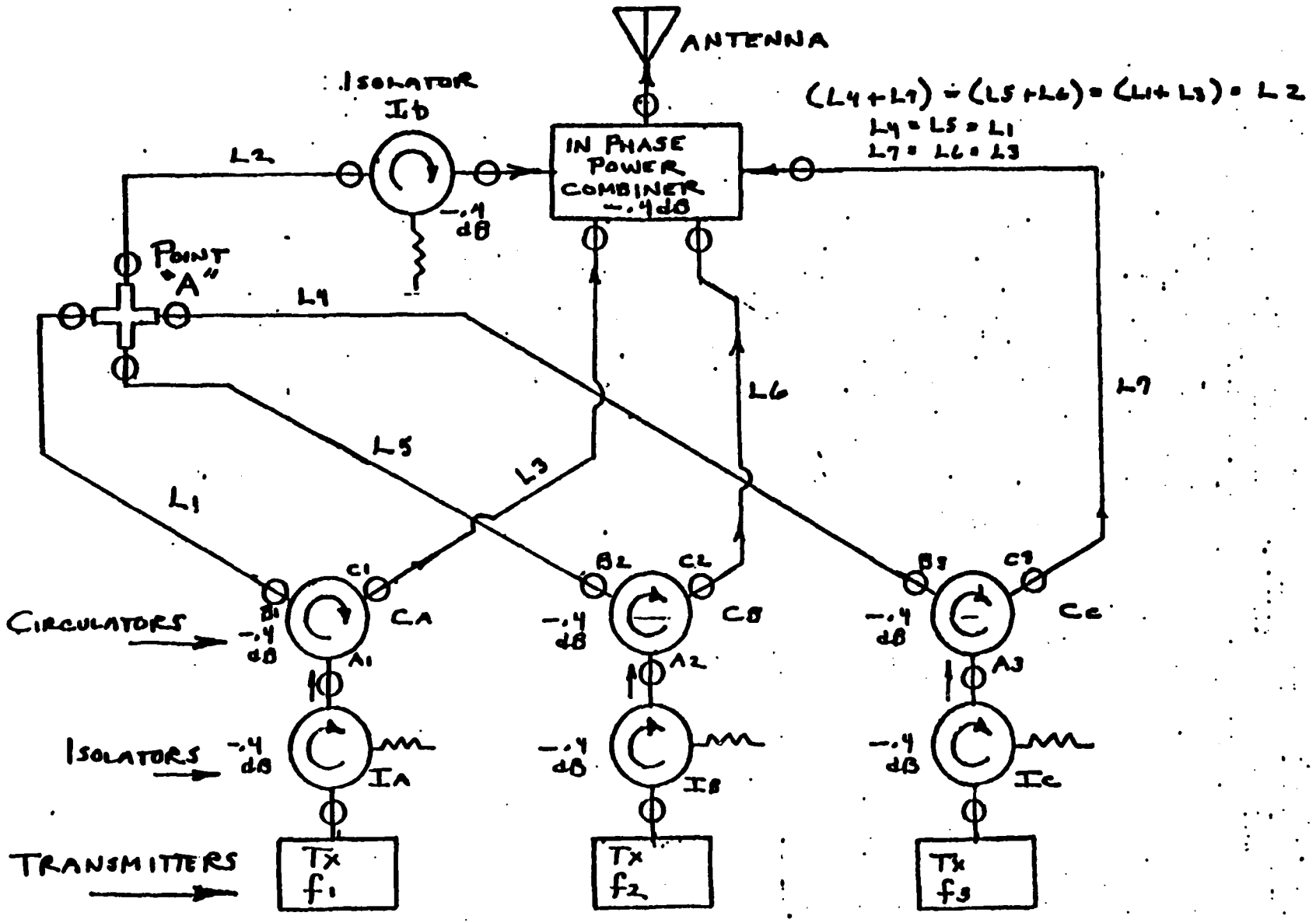

Figure A-1 - Summation of 3 Transmitters

Thus a 3:1 VSWR reflects 25 percent of the incident power, leaving 75 percent to travel to the load(s). A 3:1 VSWR is created by the connection of RF transmission lines L1, L2, L4, and L5 at point A, which is a four way "T" connection. Thus, if transmitter F1 is on line, RF power will flow to point A, and at Point A, the impedance presented to transmission line L1 will consist of L2, L4, and L5 in parallel. All of the Rf transmission lines (L1 through L7) are of the same characteristic impedance (Zo). Thus the impedance seen by L1 at Point A is Zo/3, which corresponds to a 3:1 VSWR, as described above. The same situation exists when transmitters f2 and f3 are on line.

The output power of transmitter f1 (or f2, or f3), is split equally four ways, both in amplitude and phase, and combined in a four way in-phase combiner, as described below.

RF power leaves transmitter F1 and passes through its associated ferrite isolator, to Port A1 of circulator CA. It leaves Port B1 of CA, and flows to point A. At point A, the load is now Zo/3, as described above. This is a deliberate 3:1 VSWR, and 25% of the power incident upon point A is reflected back to Port B1 of Circulator CA. The action of circulator CA is to allow this power to flow with low loss out of Port C1, to the four way in phase power combiner. Very little of this energy will leak through to Port A of CA; what does leak through, will be dissipated in the load resistor of isolator IA.

The remaining 75% of the power at point A is divided equally, and flows to the in phase power divider via three equal paths. One path is through L2 and circulator C4; another is through L5 and circulator CB, and L6 and finally L4, circulator CC, and L7. Circulators CB and CC provide isolation to transmitters f2 and f3 in the same fashion as circulator A.

Thus, we have four inputs to the in-phase power divider which are of equal power and phase, resulting in recombination of the output of transmitter f1 for connection to the antenna.

It has been shown that the RF power flowing through lines L4 and L5 is not allowed to get back into transmitters f2 and f3. In similar fashion, transmitters f2 and f3 are coupled to this single antenna, and each transmitter is so isolated from the other transmitters by circulator action.

Isolator C4 is needed to separate point A from any undesirable effects resulting from a less than ideal antenna VSWR. It may not always be necessary.

The transmission line length relationships shown in Figure 2.2.1 are necessary to guarantee maximum summing efficiency of the in phase power divider.

The summation of four transmitters to a single antenna is shown in Figure A-2.

Circuit action is very similar to the three way combiner previously described. Again, a deliberate 3:1 VSWR is created at Point A by the parallel combination of three of the four transmission lines. Thus, the "driving" transmission line (from CA, or CB, or Cc, or Cd) sees an impedance which is one third of its own characteristic impedance.

Of interest is that we can combine four transmitters with the number and kind of components as in the three way combiner. Again, the line length relationships needed to insure optimum power recombination are shown in Figure A-2.

With this added capability of being able to combine three or four transmitters to a single antenna, we can now construct trees of a non-binary form thus providing great flexibility.

It is not necessary that all of the transmitters be energized at the same time, or that they have equal output power.

A loss analysis can be performed on both the three and four port models. The values assumed for the original Stites coupler (two port design) are : 0.3 dB for the power combiner, and 0.4 dB for the isolators and circulators.

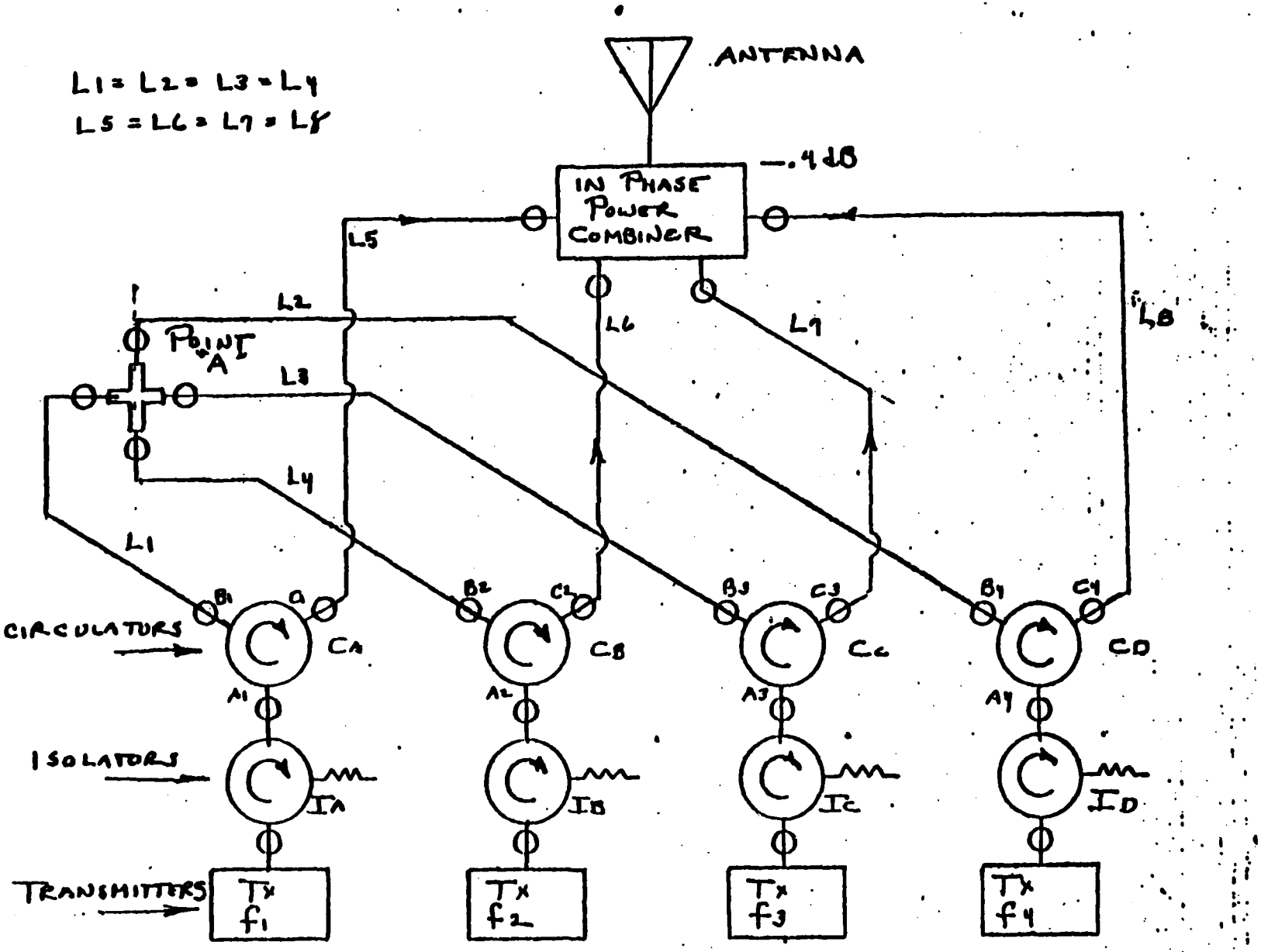

Figure A-2 Summation of 4 Transmitters.

The three (3) and four (4) port modules use a slightly more complex combiner, so our loss model will assume a 0.4 dB loss for the power combiner.

Thus, a typical combining path (including the isolators at the output of each transmitter), has the following loss:

3 Port			4 Port		
Isolator Ia	-.4		Isolator Ia	-.4	
Circulator Ca	-.4	dB	Circulator Ca	-.4	dB
Circulator C4	-.4		Circulator Cb	-.4	
Combiner	-.4		Combiner	-.4	
	-1.6	dB		-1.6	dB

The losses are the same for each combiner. Thus the efficiency of these combiners is 69%. Of great interest is the improvement in efficiency realized by using the above described four way combiner over the use of a four way combiner constructed from a "tree" using three of the orignal Stites couplers. This is an improvement of from 57 to 69 percent.

In all of the previous and following examples, it is to be understood that the transmission media may be coaxial, waveguide, balanced stripline, or microstrip.

Figures A-3, A-4, and A-5 show practical examples of 5, 9, and 16 way combiners and demonstrate the high efficiency obtainable with this technique.

5 way combiner

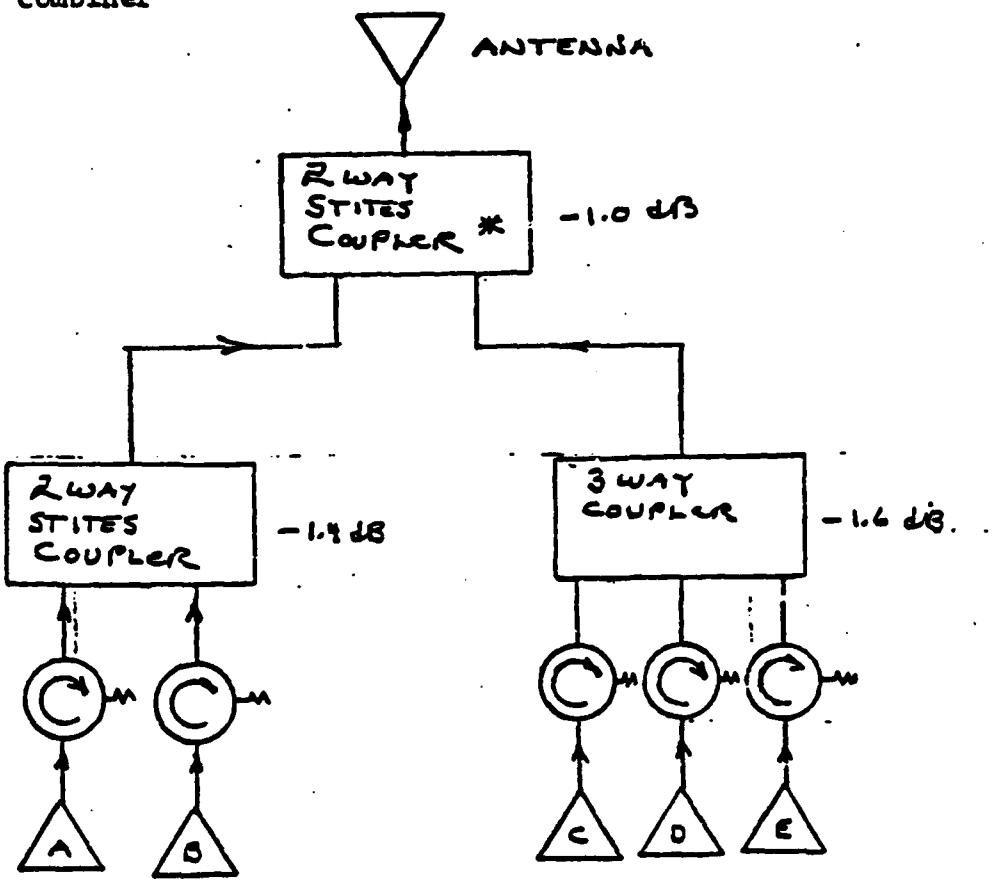

Total Losses, Transmitter A or B

= -2.4 dB , or 57.5% EFFICIENCY

Total Losses Transmitter C, or, D, or E

= -2.6 dB = 55% EFFICIENCY

* This element does not need circulators on its input port, hence the loss is -1.0 dB instead of -1.4 dB.

Figure A-3 - Five Way Combiner.

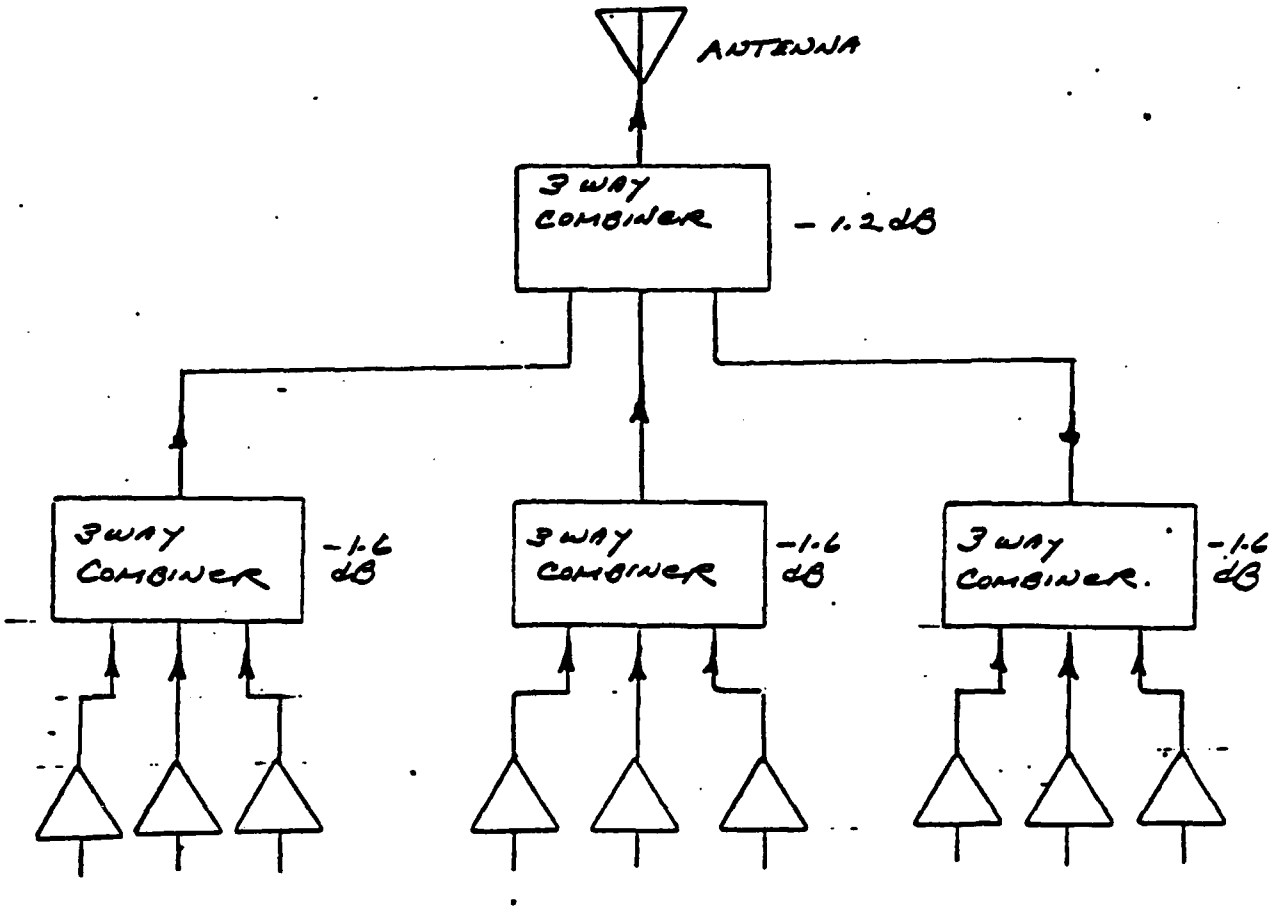

All 3 Port Combiners

Total Loss in any one Path = (-1.6) + (-1.2),

= - 2.8 dB, or an

efficiency of 52.4 %

A conventional linear 9 way combiner would have a combining loss of -9.54 dB for each independent frequency, or an efficiency of only 11 percent.

Figure A-4 - Nine Way Combiner

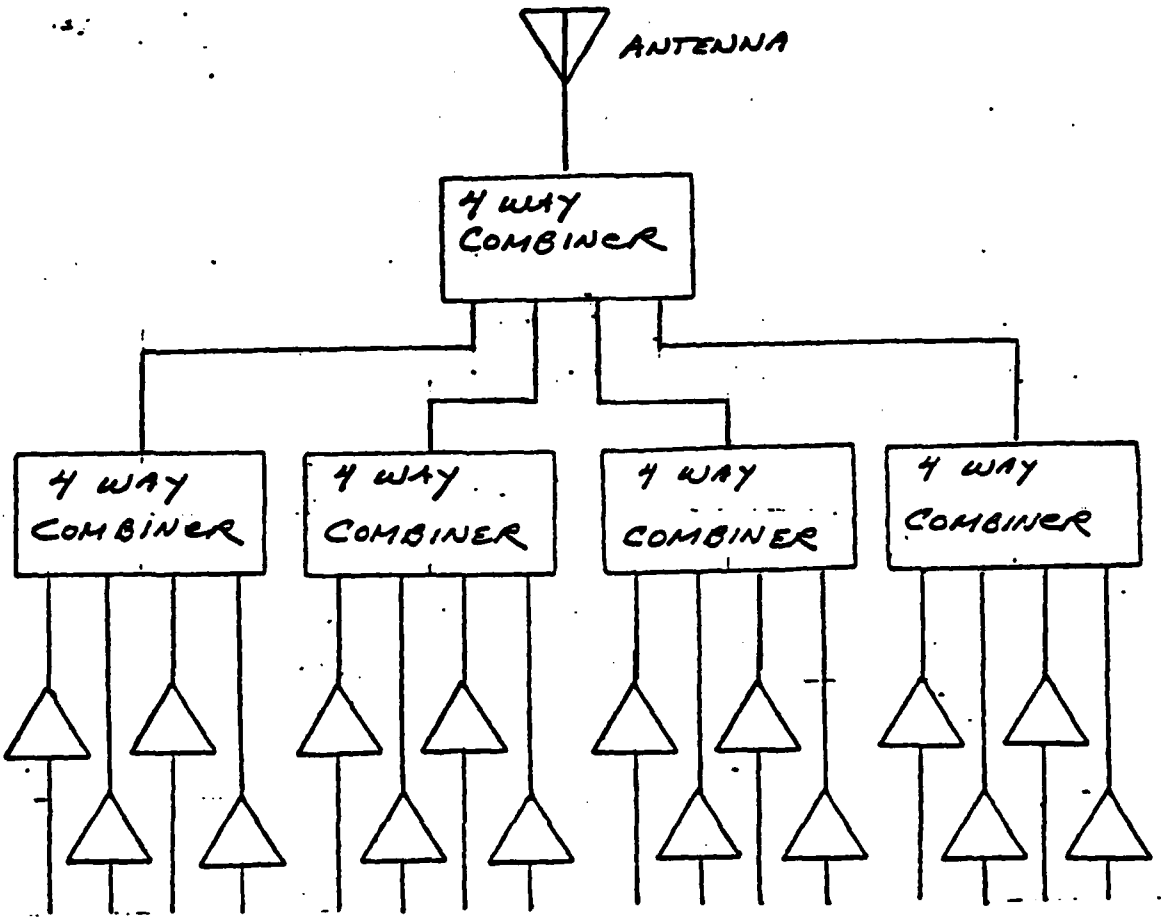

All 4 Port Combiners.

Total Loss in Any one Path = - 2.8 dB, or 52.4% efficiency.

Figure A-5 - 16 Way Combiner

APPENDIX B DISCUSSION OF DUAL ANTENNA SYSTEMS

B.1 CIRCULATOR DISCUSSION

A three (3) port circulator specification was prepared and sent out to 15 vendors. The specification is shown in Figure B-1.

Nine of the fifteen queried vendors responded, and all have indicated that the specification is beyond their capability. Of particular interest is the response from MICON, Inc., shown herein as Figure B-2. We are no longer pursuing the circulator search. The circulator method of combining transmitters remains ideal for frequency ranges where ferrite circulators are available.

A literature search (New England Research Application Center) has been conducted on the following topics:

Ferrite Circulators
Active Circulators
Distortion Products

The ferrite circulator search showed that very little work is in progress in the 30 - 88 MHz band, and that these circulators offer only about 5% bandwidth and fairly high insertion loss.

The literature search regarding active circulators produced numerous abstracts. The active circulator is a circuit developed for use in the telephone industry, and originally operated at audio to video frequencies. Isolation of up to 50 dB has been reported. The adaptability of this circuit to high powered, wide band RF use is debatable, and is not under consideration.

The literature search yield regarding distortion products was small. "A study of Non-Linearities and Intermodulation Characteristics of 3 Port Distributed Circulators" by You-SunWu, Walter H. Ku, and John E. Erickson, IEEE Trans., MTT, No. 2, Feb 1976, stated that for a particular ferrite, used in a distributed circulator, the dominating distortion term is 86-91 dB down. Other VHF and UHF distributed circulators were also tested, and intermodulation products in the range of 80 - 100 dB below the main signal of 50 to 100 watts were produced with an interfering signal

3 PORT CIRCULATOR

PRELIMINARY SPECIFICATION

FREQUENCY	30 to 88 MHz
INSERTION LOSS	1.0 dB max.
ISOLATION	25 dB min.
TECHNOLOGY	FERRITE OR ACTIVE
VSWR	1:15 :1
INPUT RF POWER	60 WATTS C.W.
TEMPERATURE	N/A
IMD PRODUCTS	-120 dBc max.
SIZE	N/A
TUNING	- PREFER BROAD BAND OPERATION - IF TUNING IS NECESSARY, IT WILL BE NECESSARY TO MAINTAIN SPECIFIED ISOLATION TO ALL OTHER FREQUENCIES. - TUNING, IF ANY, MUST BE ELECTRONIC

Figure B-1 - 3 Port Circulator Preliminary Specification

Figure ~~2.3.2~~

MICON INC.
FERRITE CONTROL CO. DIVISION
1105 INDUSTRIAL PARKWAY, BRICKTOWN, NEW JERSEY 08723 • (201) 458-3333 TELEX 642-651

November 26, 1980

Sylvania Systems Group
Eastern Division
GTE Sylvania Incorporated
77 "A" Street
Needham Heights, MA 01294

Attn: Mr. Colin B. Weir
Advanced Development Engineer

Dear Mr. Weir:

I spent many hours examining feasibility of a ferrite circulator or an active gyrator to approach the broad band requirements of 30 to 88 MHz. I believe it to be very difficult to even approach your requirements.

The best I feel could be accomplished with an electronically tuned ferrite circulator would use a unit with 3 to 5% instantaneous bandwidth to the 20 db return and isolation points. Insertion loss would be of the order of 1½ db. Isolation would drop to 5 or 6 db, 10% away from the operating band. Matching-using LC networks along with change of magnetic bias (coil current) would be digitally controlled, probably by a microprocessor. Pin Diode switches used in the LC matching networks would probably reduce the IMD products typically to the order of 80 dbc.

One active type approach would require 9 approximate unity gain amplifiers. Each amplifier probably needs to have meet the 120 dbc specification. Phase and amplifier balance would be critical. Amplitude balance of ½ db could result in isolation of 10 db, instead of the desired 25 db. I do not believe better tolerance or controls can be met at this time.

Should you basically modify the preliminary specifications or change approach, Ferrite Control would appreciate the opportunity to be of service.

Very truly yours,

FERRITE CONTROL COMPANY

H. Ward Hurd

HWH/sad

Figure B-2 - Specification Response

20 dB below tne main signal. Tne authors conclude that since distributed circulators are of larger volume than the lumped type, tne intermodulation noise will, in general, be less tnan that produced in a lumped element circulator.

B.2 SWITCHING CONSIDERATIONS

This section contains preliminary concepts which help to illustrate and clarify various system problems. FigureB-3 shows now a two antenna scheme could be greatly simplified if the receiver inputs and tne transmitter outputs could be individually accessed. This would probably mean modification of equipment in tne field, wnicn is to be avoided. However, tne benefits are large, and tne concept will be held in reserve.

B.3 ACTIVE CIRCULATOR

FigureB-4 snows some of tne design requirements of a 3 port active circulator to implement tne 2 antenna approacn. As shown, a large number of class A amplifiers are needed (18) to implement tnis approacn, and nence, it does not seem workable at tnis time.

B.4 TWO ANTENNA SYSTEMS WITH LINEAR AMPLIFIERS

It is still felt tnat a two antenna system would be more versatile than tnat of a single antenna. Consideration was given to alternate circuitry wnicn could retain tne two antenna adaptability.

The circuit shown in FigureB-5 is an early model of sucn a circuit. The circuit snown represents a complete transmitter multiplexer. It consists of 5 class A linear cascode RF amplifiers. The cascode circuit is cnosen to provide about 40 dB of isolation between tne power combiner port and tne transceivers.

The cascode amplifiers are combined in a linear five way in phase-power combiner, wnicn will incur about 7 dB of loss in each forward path. The summed outputs are routed to a linear, nign power output amplifier capable of nandling five simultaneous inputs and driving eacn one up to 60 watts witn little or no intermodulation.

Under normal operations, eacn transceiver will probably operate on a five minute receive - 1 minute transmit duty cycle. To reduce tne neat dissipation, tne non-used cascodes could be disabled

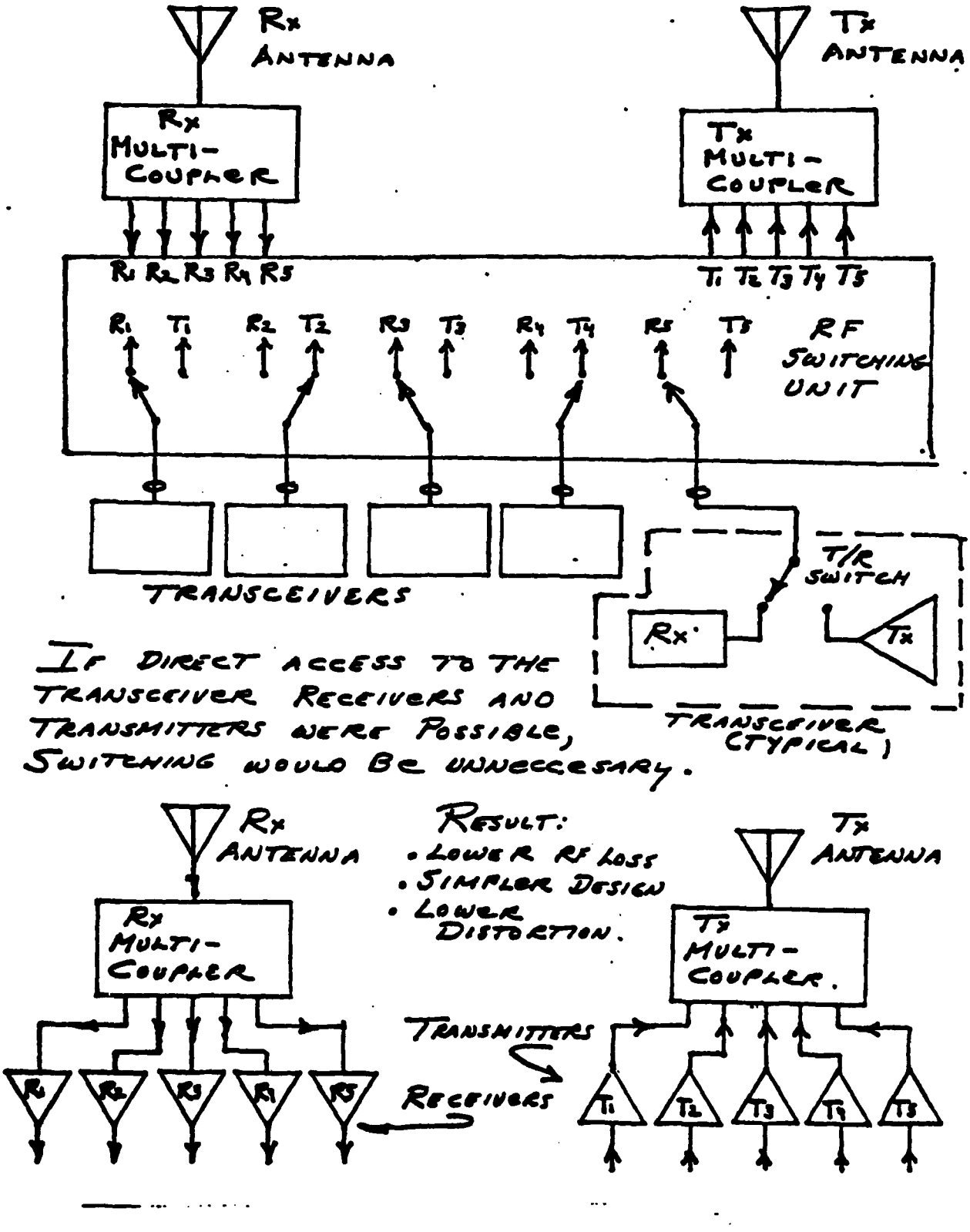

Figure B-3 - Switching Considerations

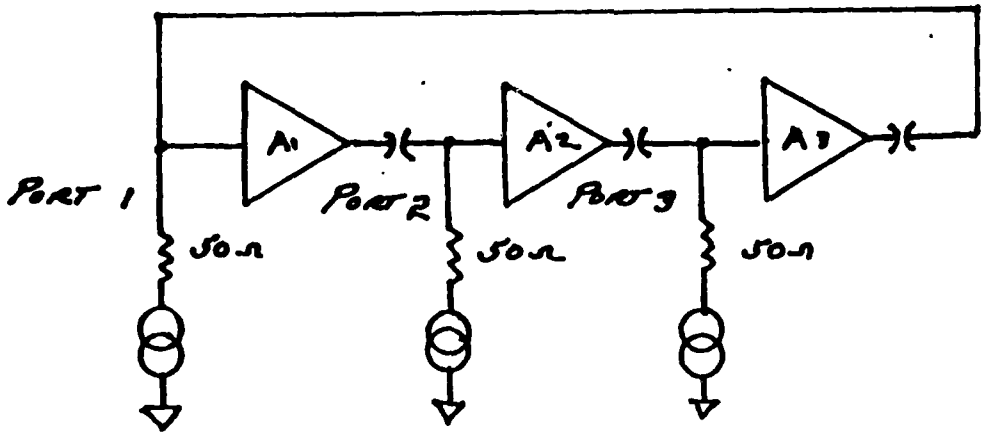

ILLUSTRATION OF SIGNAL CIRCULATION.

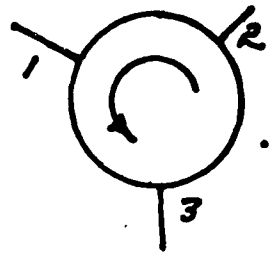

FOR 60 WATT CW OPERATION:
EACH AMPLIFIER MUST BE CAPABLE OF 60 WATT CW, WOULD BE PUSH PULL, CLASS A, PRECISELY MATCHED, AND WOULD HAVE EXCELLENT IMD & HARMONIC PERFORMANCE (-120 dBc).

FOR A 3 PORT COMBINER, 4 CIRCULATORS AND 3 ISOLATORS ARE NEEDED. TOTAL — (12+6) 18 CLASS "A" AMPLIFIER ARE NEEDED. ALSO, "BACK INTERMOD." WOULD BE A SEVERE PROBLEM. EX: HIGH POWER INTO PORT 2 WOULD INTERMOD WITH OUTPUT OF A1. CONSENSUS OF DESIGNERS IS THAT THE ACTIVE CIRCULATOR CAN BE BUILT AT VHF, BUT "BACK INTERMOD" IS A LIMITATION.

REF: "ACTIVE CIRCULATORS: THE REALIZATION OF CIRCULATOR USING TRANSISTORS." S. TANAKA PROC IEEE MARCH 1965, PPES 260-266

Figure B-4 - Active 3 Port Circulator

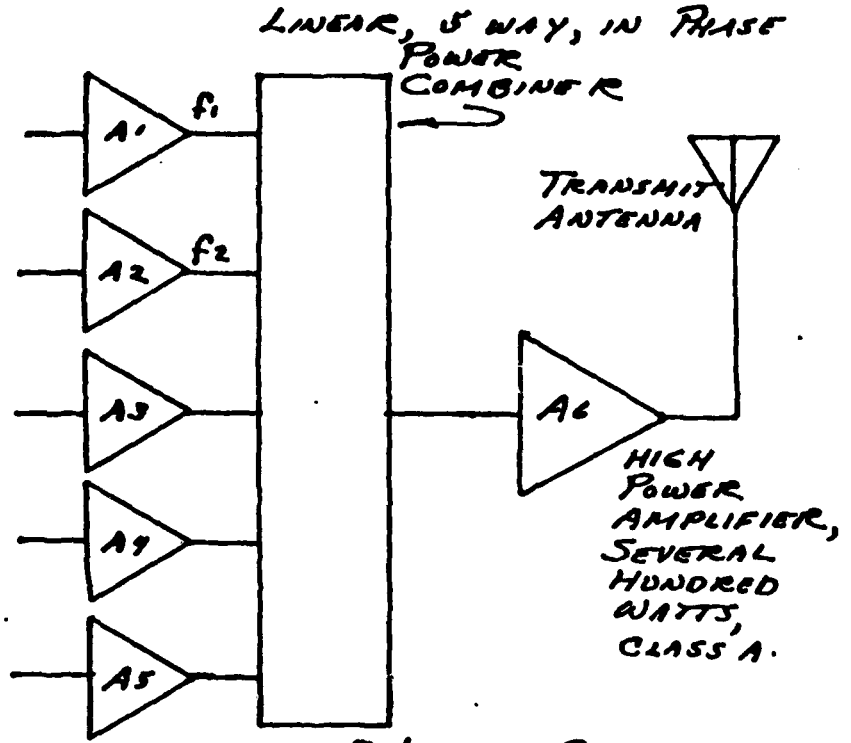

- CASCODES WILL PROVIDE ABOUT 40 dB OF ISOLATION.
- 5 WAY POWER COMBINER WILL PROVIDE ABOUT 14-20 dB OF ISOLATION.
- PROBLEM "BACK INTERMOD" PERFORMANCE OF AMPLIFIERS WITH AN OFF FREQUENCY SIGNAL — dB BELOW AMPLIFIER OUTPUT.

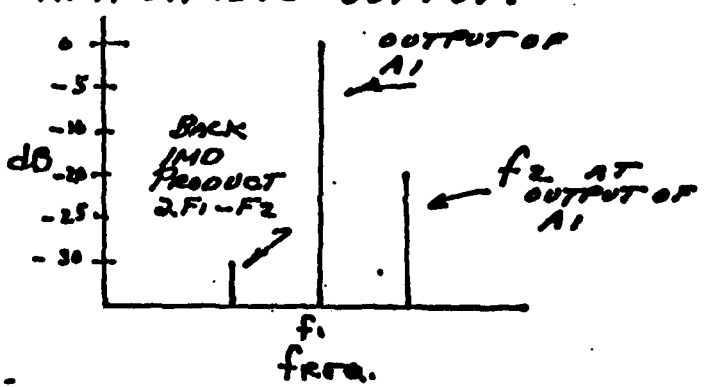

30-88 MHZ ULTRA-LINEAR AMPLIFIERS, -140 dB IMD & HARMONIC PERFORMANCE (INPUT). PROBABLY FEED FORWARD. HF AMPLIFIERS OF THIS QUALITY ARE NOW IN CONCEPT STAGE (NAVY HF IMP).

ACTION: INVESTIGATE STATE OF THE ART "BACK IMD" ACTIVITY & PERFORMANCE.

Figure B-5 - Alternate Circuit - Transmit Multi-Coupler

wnen the associated transceiver is in the receive mode. The output amplifier would be active as long as one of tne transceivers is in tne transmit mode.

The total isolation from one transceiver output to another transceiver output would be sum of tne cascode isolation plus about fourteen to twenty dB of isolation provided by the power combiner, giving a total of about 54 to 60 dB isolation. This is generally more isolation than provided by either the circulator or single antenna approach.

It is felt tnat this circuit would not suffer adversely from antenna impedance variations in any way.

There are two areas of concern with this circuit, back intermodulation of tne cascode amplifiers, and an increase in the broadband noise floor. The neat dissipation and linearity problems can probably be overcome. As noted in Figure B-5, much effort is being expended in the design of ultra linear power amplifiers in the HF band by most of the military services.

Figure B-5 illustrates now tne cascode amplifiers will be subject to back intermodulation. A search for applicable literature was made in tne GTE library with little success. One excellent reference is available however, wnicn documents tne causes of back intermod. It is "If Back Intermodulation is a Problem", by Dieter R. Lonrmann; found in Electronic Design 23, November 11, 1971.

Back intermod occurs when tne output of one transmitter enters a second transmitter, and mixes witn tne second transmitters second harmonic, and is retransmitted. A mathematical analysis snows that if tne interference source looking back into tne output of tne amplifier sees a load that does not vary over time, no back intermod will occur. The approach described in tne reference is slanted toward class D amplifiers, and results in equal on/off impedances. Amplifiers of this type are not applicable herein because of their high harmonic output, but tne text does offer an implied solution to our problem . A class A amplifier does not switch on or off; it is always in conduction, and tne collector impedance tends to be relatively constant with time. Careful RF design can greatly reduce

harmonic generation, so the only significant amount of second harmonic present will be that delivered by the driving transceiver itself, which would be faithfully reproduced by the cascode amplifiers, except for some rolloff at the high end of the band. Thus, if the driving transceiver second harmonic is running at -80 dBc or so, if the cascodes are class A, and if additional input filtering is provided, considerable progress can be made toward resolving the back intermod problem.

In order to provide a meaningful IMD analysis, the block diagram shown in Figure B-5 was increased in detail and is shown in Figure B-6. The input power level of 60 watts is tentatively attenuated by 10 dB, to 6 watts. Overall gain is 0 dB. These parameters are also used in the noise floor analysis to follow.

Figure B-6 assumes the second harmonic content of the transceiver to be -80 dBc, and that no significant harmonic enhancement occurs in the cascode amplifiers. Thus, three signals are shown at the output of A1; +47 dBm at f1, -33 dBm at 2f1, and +27 dBm at f2. The 2 f1 signal at -33 dBm will mix with the +27 dBm f2 signal to produce the IMD signal (2f1-f2) at 45 MHz.

If we assume little or no IMD enhancement from A6, the IMD product at 45 MHz must be 120 dB below the +47 dBm f1 signal, or -73 dBm. This means that the IMD signal must be 100 dB below the jamming signal (+27 dbm f2). The cited reference shows that the switching amplifier provided about 65 dB of IMD supression. It is unknown at this time how well a class A amplifier will suppress back IMD, but it is clear that reduction of the input second harmonic, and increased isolation to the jamming signal would greatly improve performance.

Figure B-7 shows a noise model of the previously discussed circuit, and the effects of this circuit on the system broad band noise floor are shown below:

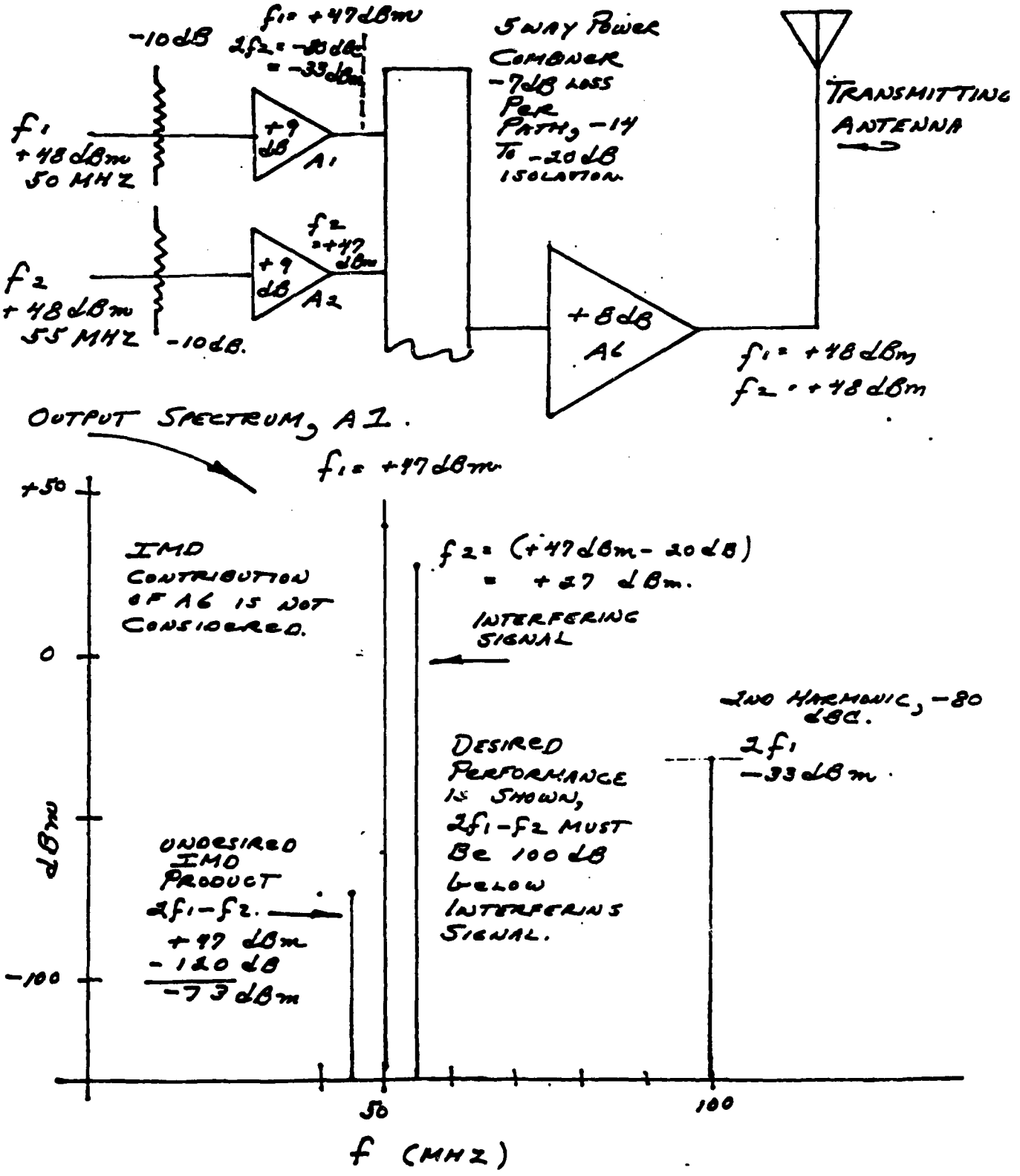

Figure B-6 - IMD Analysis

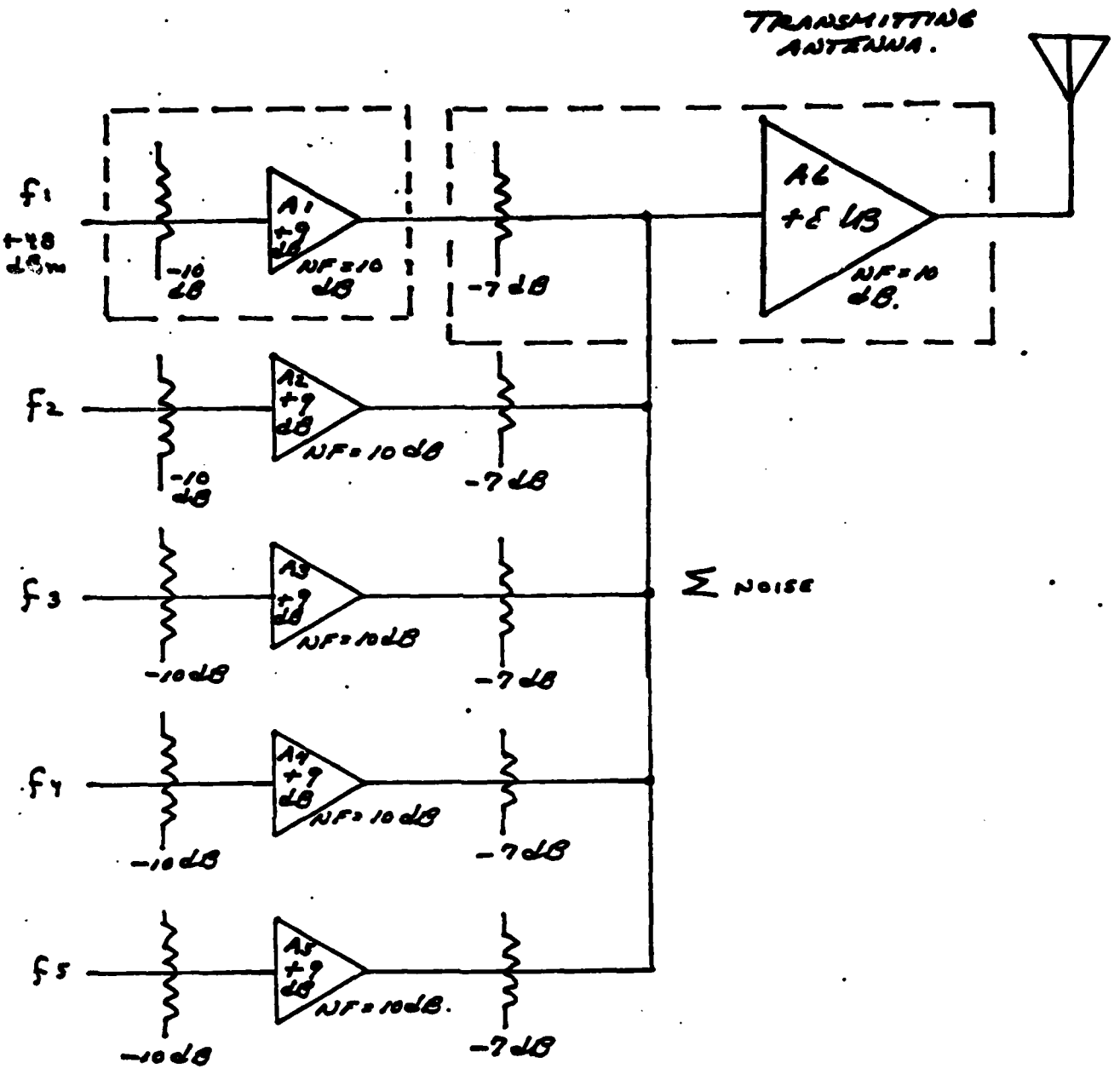

Figure B-7 - Noise Floor Analysis

The input noise figure of a typical cascode stage (A1) is calculated with the following assumptions:

NFA1 = (10 + 10) = 20 dB

NFA6 = (7 +10) = 17 dB

Ga1 = (-10 + 9) = 1 dB

$$NF = F1 + \frac{F2-1}{G1}$$

NF_1 = 22.1 dB

The noise generated by A1 and A6 is:

N = NF + G KTB + NE

NF = 21.1 dB

Where G = 0 dB

KTB = -174 dBm/Hz

NE = Noise enchancement of the final amplifier which is estimated to be 6 dB.

thus: N = 22.1 + 0 - 174 + 6

= -145.9 dBm/Hz

This noise is summed with the noise generated from each of the four input cascodes (A2 AS) which is summed and then amplified by A6:

N = NF + G + KTB + NE

= 22.1 + (-10 + 9 - 7) - 174 + 6

= -153.9 dBm/Hz

Since we are summing four of these amplifiers, the level is increased by 6 dB. The amplification of A6 raises this level by an additional 8 dB

$$\begin{aligned} & -153.9 \\ & + \ 6.0 \\ & \underline{+ \ 8.0} \\ N= \ & -139.9 \quad \text{dBm/Hz} \end{aligned}$$

Now, assume the input noise to be -147 dBc (in a 20 KHz bandwidth) on each of the 5 channels:

	+ 48 dBm in each channel
	-147 dB
	- 99 dBm/20 KHz
	- 43 (Normalize 20 KHz to Hz)
	-142 dBm/Hz
	+ 7 (There are 5 channels)
Total Noise Due To Input =	-135 dBm/Hz

Since the channels have 0 dB gain, this is the total noise related to the input.

The summation of these 3 noise sources is shown.

Noise from A1	-145.9 dBm/Hz
Noise from (A2 + A3 + A4 + A5) + A6	-139.9 dBm/Hz
Summation of input Noise	-135.0 dBm/Hz
Total Noise =	-133.5 dBm/Hz

If we consider channel A1 alone, the input noise is about -142 dBm/Hz, and the total output noise is -133.5 dBm/Hz, or 8.5 dB higher. This is a severe degradation in the noise floor. However, if we were to connect each transmitter to a separate antenna and energize them simultaneously, the noise would be:

	-142 dBm/Hz
	+ 7 dB
N=	-135 dBm/Hz

Thus, for this point of view, the noise of the multicoupler is only 1.5 dB higher.

One goal of the design assessment is to improve performance. The IMD Noise and analysis show that both of these parameters could be improved if some selectivity could be added to the cascode amplifier stages.

B.5 ALTERNATE APPROACHES

the FQR briefly discussed an early version of an alternate, non-ferrite, broadband circuit for the transmit section (page 20), and some of the difficulties arising from its use, namely back intermodulation, and enchancement of the noise floor. An increase in the selectivity of the amplifiers was needed but in that scheme, each amplifier had to cover the full 30 - 88 MHz bandwidth.

An interim scheme was then devised to provide the necessary selectivity, but at the expense of frequency coverage. The approach was that of a channelized amplifier array, and is shown in Figure B-8.

This arrangement would take the 5 transmitter RF input lines and switch them to 10 available narrow band amplifiers. The narrow band feature of the amplifiers is obtained by fixed tuned filters in the amplifier output network. The amplifiers are Class A push-pull cascades. Each channel will have 2 pole response with an effective loaded Q of 121 to provide about 40 dB of isolation at +/- 6.4% of center frequency. This isolation will prevent signals from adjacent channels from generating excessive back intermod products. Also, the use of push-pull circuitry, and Class A operation will reduce the back intermod problem to an acceptable level.

The 10 way combiner will incur a 10 dB forward loss, and provide about 20 to 25 dB isolation between channels.

The main disadvantage of this scheme is the severe loss of channel space. At 30 MHz, the 3 dB bandwidth is 30/121, = +/-124 KHz. With 25 KHz spacing, this allows use of only 4 to 5 channels.

If the isolation requirements can be eased, such that 20 dB isolation is provided by the filters (QL = 78), then the 3 dB bandwidth is increased to

$$\frac{30}{78} = +/- 192 \text{ KHz at } 30 \text{ MHz}$$

With this degree of isolation, about 7 channels are available at 30

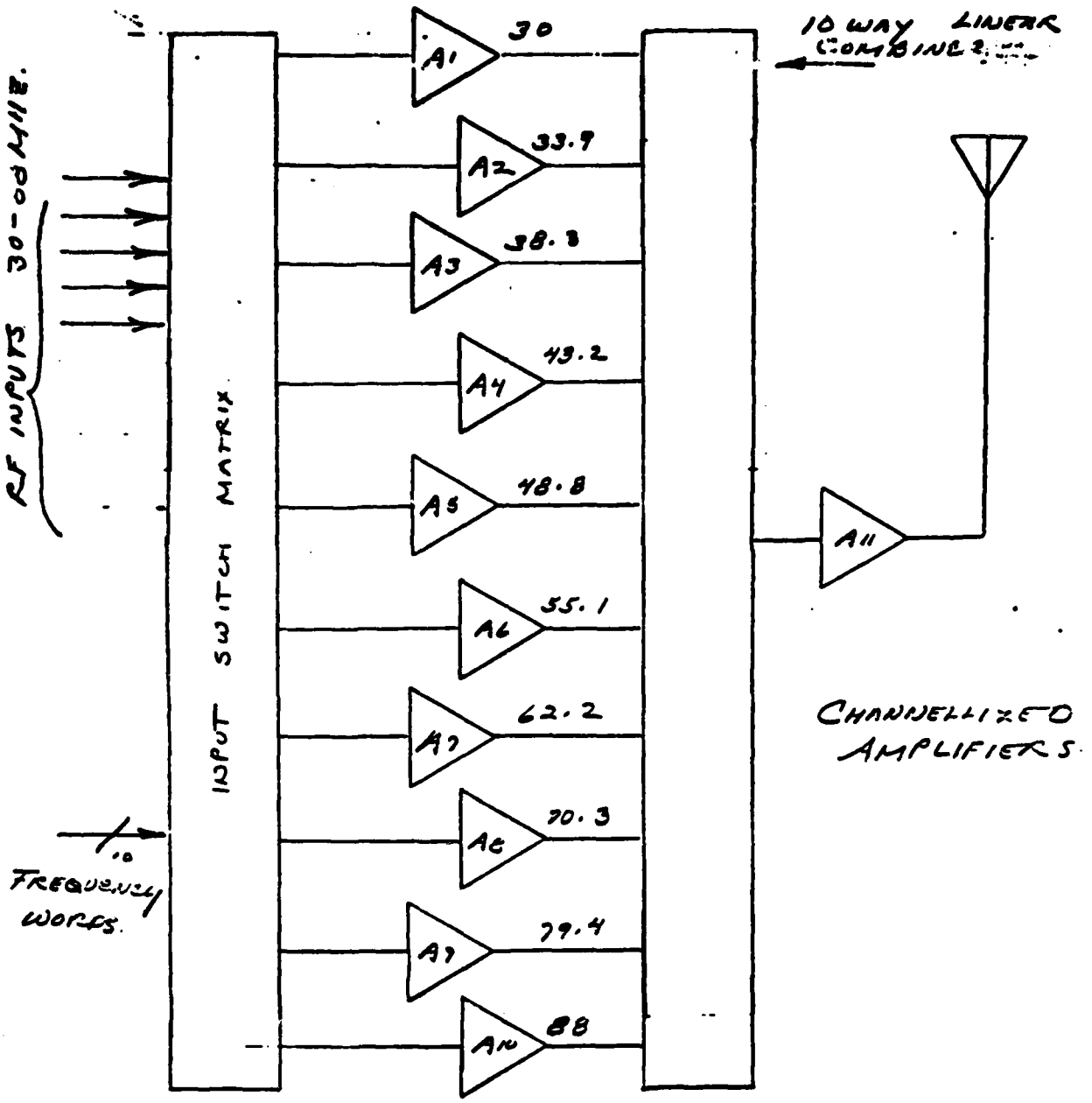

$A_1 \rightarrow A_{10}$
TUNEABLE OVER 10% R.W.

FIGURE B-9
CHANNELIZED AMPLIFIER.

MHz. Now, as frequency is increased, the number of channels available for each amplifier is increased also, since the bandwidth is increased. The total number of channels available with this scheme is 221, out of a possible 2320. However, more flexibility could be obtained with the use of snap in filters to move the channels about as desired.

B.6 HYBRID TWO ANTENNA SYSTEM

The system described in B5 is not flexible enough, in that too many channels are lost. However, this led to another concept, which is shown in Figure B-9.

This circuit combines some features of the single antenna scheme. It uses an ultra linear isolation amplifier after the transmit combiner to eliminate the need for any antenna isolation or tuning compensation whatsoever. The receiving section could use combining circuitry similar to that of the TD1288. The rationale for the receiving section is that antenna pulling is a much less severe problem in the receive mode than in transmit.

A 2 pole helical filter is used in the receiving multiplexer instead of the 3 pole filter used in the TD1288. The antenna isolation (nominal - 20 dB), and the use of physically larger resonators, could provide more than enough isolation.

The T/R switching units are shown as separate units to emphasize the need for shielding between units. The RF switch used for the T/R function has an additional set of contacts to short the receive port when the transceiver is in the transmit mode. For example, let transceiver #1 be transmitting at 30.000 MHz, and transceiver #1 receiving at 30.750 MHz (+ 2.5%). The 2 pole helical filter associated with transceiver #1's receiver multiplexer is tuned to 30.000 MHz, even in the transmit mode. Any leakage in the transceiver #1 T/R switch will pass through this filter, to the summing point, and cause possible interference or IMD distortion for the other channels.

In the transmit mode, RF power is passed through the quad-coupled filters as in the single antenna circuit. The compensating networks are still used, but not shown herein.

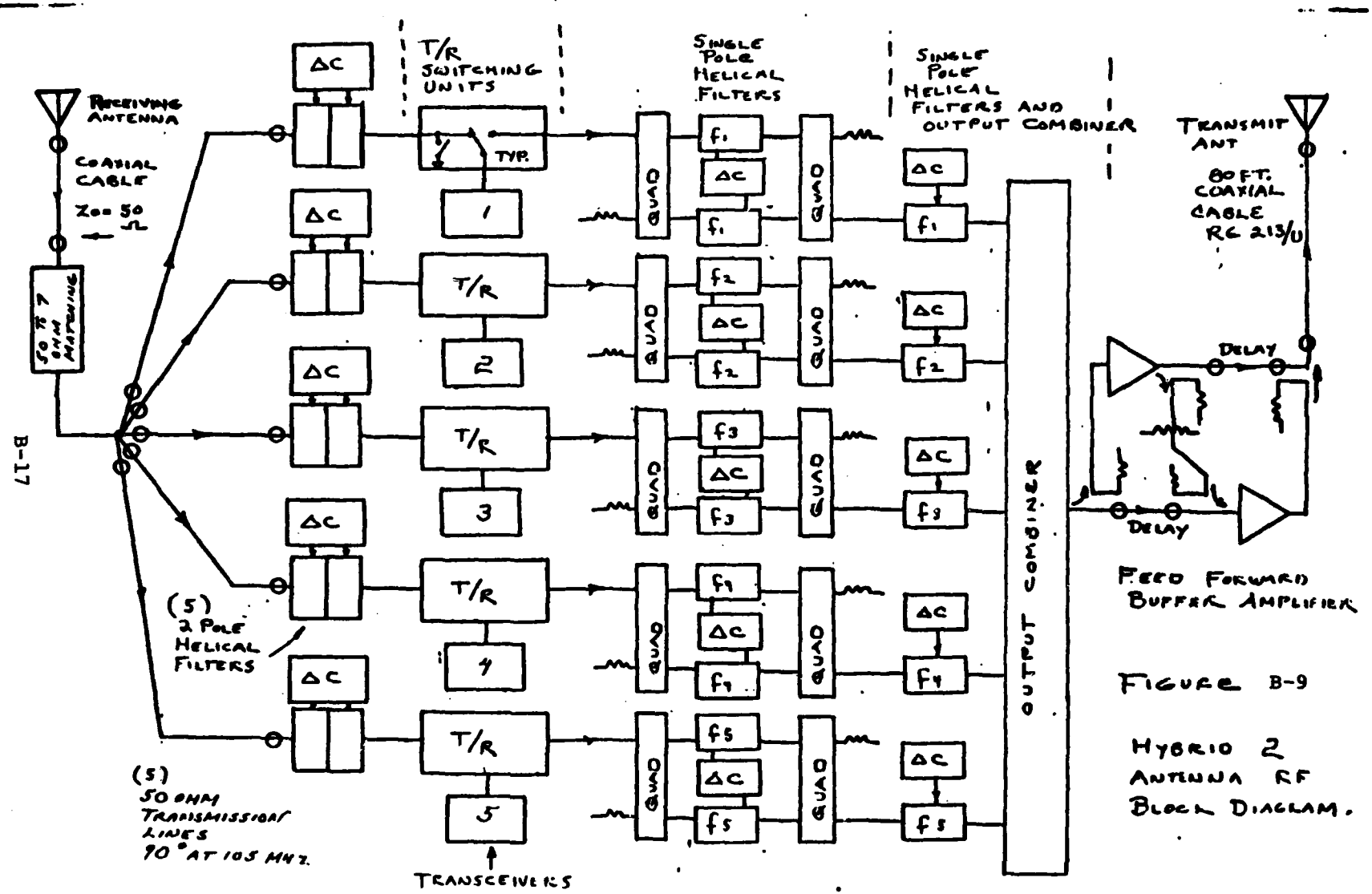

FIGURE B-9

HYBRID 2 ANTENNA RF BLOCK DIAGRAM.

The ouput resonator and combining scheme is like that shown for the single antenna circuit. Thus, with this combining scheme, the back intermod problem is not present.

The combiner now operates into a low gain, ultralinear feed forward R.F. amplifier. This amplifier isolates the combiner from the antenna VSWR. It simplifies the combiner and compensating network design by the virtue of its well controlled input impedance. There is no need to measure the antenna impedance and compute the needed correction factors.

The main disadvantage to this scheme is the need for 2 sets of RF filters, one for receive and one for transmit. However, it extremely flexible.

The linearity requirements of the amplifier are indeed rigorous, the IMD required performance would be -120 dBc. Feed forward techniques will provide about 20 dB of improvement, hence the amplifiers themselves must have IMD performances of -100 dBc. The linearity requirements will result in low efficiency, about 10 percent or so, and the need for a feed-forward type circuit will cut this in half, to about 5 percent. Thus the RF and DC power requirements for the amplifier are large, as shown in TableB-1:

NO. of Simultaneous Channels in Transmit	RF Power Per Channel (watts)	Required Peak RF Power (Watts)	Required DC Power @ 5% Efficiency (Watts)
5	60	3000	60 KW
5	40	2000	40 KW
3	40	720	14.4 KW

TableB-1 Power Requirements

An amplifier with the above D.C. power requirement is not practical for field operation. Future effort on the two antenna approach will be limited to those which do not require amplifiers to buffer the variations in antenna impedance.

Note: The above was written prior to the development of the single antenna output combiner.

B.7 SYSTEM REQUIREMENTS

FigureB-10 shows the system requirements for the Dual Antenna FHMUX.

A minimum antenna isolation of -15 is assumed. The power level of Fo is scaled down by the value of the antenna isolation to +33 dBm, or 2 watts. Curve A is also scaled down by 15 dB, but any noise filtering action as a result of the transmitter FHMUX is not shown.

As shown, at +2% of Fo, about -26 dB of filtering is needed, and at 1%, about -38 dB is needed. These filtering requirements are less than those for the single antenna system.

FIGURE B-10
DUAL ANTENNA SYSTEM MODEL DERIVATION.

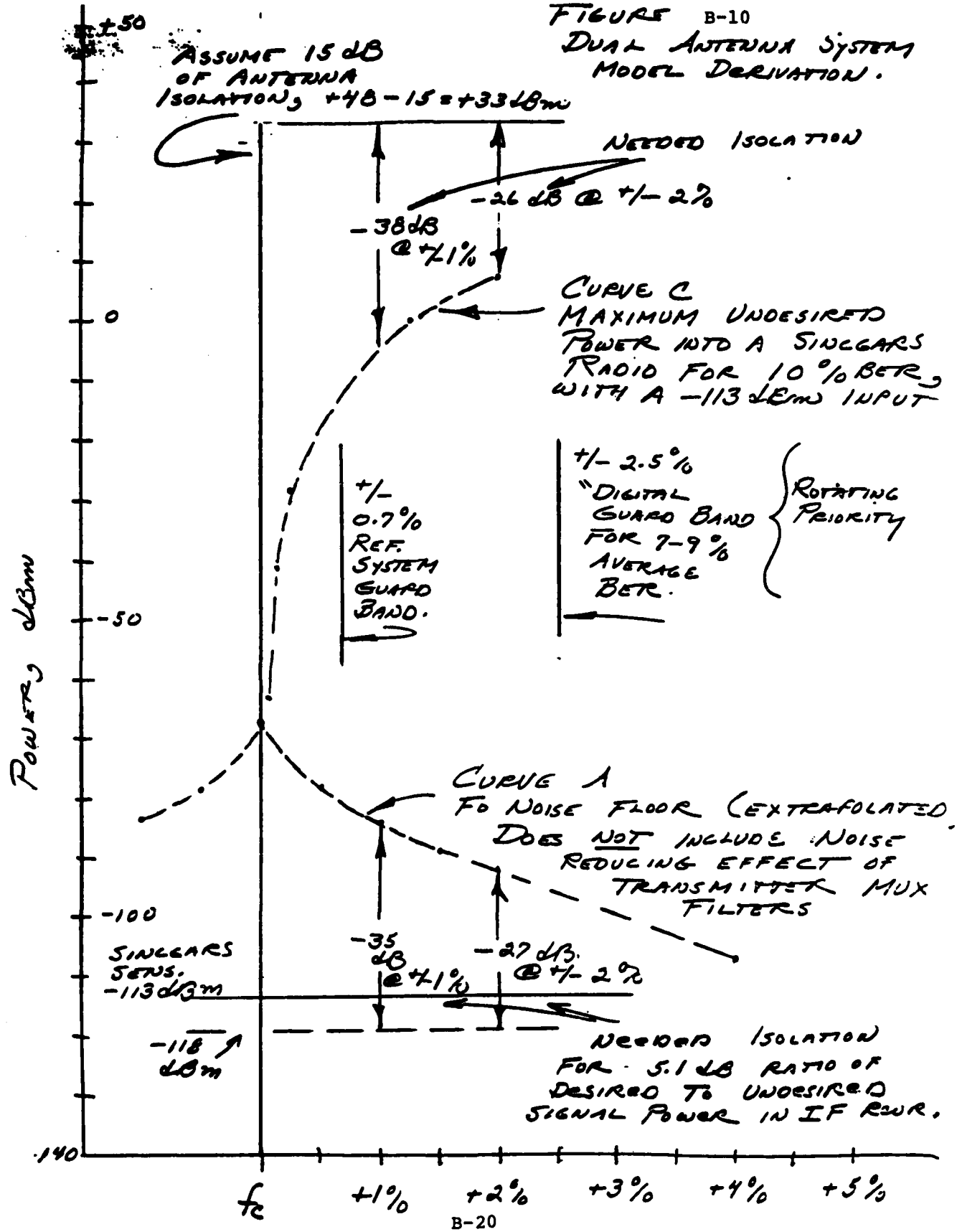

APPENDIX C LOAD PULLING STUDY

C.1 FILTER APPLICATION & LOAD PULLING STUDY

A single tuned, high Q filter was computer analyzed and optimized, using a GTE program called "NET ADJUST". The output section of the circuit was composed of an all inductive "T" circuit which will later be modelled into a transformer to provide the output power combining function.

A total of twenty optimization runs were made to achieve the desired response according to the frequency versus attenuation weighting values assigned. Three center frequencies were used, and three values of "Q" were assigned to element , (Fig C-2); which will be modelled into the transformer previously mentioned.

The center frequencies, "Q", frequency range, and attenuation goals are listed below, in Tables C-1 and C-2. These initial goals were derived from previous work on an agile HF band antenna (single channel) tuner. Thus, two of these circuits would present -35 dB of isolation at ±5% of the channel center frequency. These were initial goals used to evaluate the tradeoff between insertion loss at mid-band and off frequency isolation.

Table C-1 Frequencies and Element Ω

CENTER FREQUENCIES (MHz)	"Q" ELEMENT L3
30.0	1130
51.0	1130
51.0	1473
88.0	1130
88.0	1935

TABLE C-2

FREQUENCY AND ATTENUATION GOALS

FREQUENCY RANGE	ATTENUATION GOAL (dB)
Fo	0
Fo +/-.375%	-1.5
Fo +/-.75%	-5.0
Fo +/- 5%	-17.5
Fo +/- 10%	-22.5
Fo +/- 15%	-27.0
Fo +/- 20%	-30.0

A typical result of the optimization process is Run 17, shown in Figure C-1. This run is for a "Q" of 1130, at a center frequency of 51 MHz. The mid-band insertion loss is 0.54 dB, and the +/-5% insertion loss is in excess of 17.5 dB. The loaded Q was calculated to be 78.5. This run was typical, in that the filter skirts were close to this design goal, and the mid-band insertion loss varied between .5 and 1.0 dB. The weighting value assigned to each frequency was equal. Five runs were made under the conditions of geometric symmetry about the center frequency, and equal attentuation weighting. These results are shown in Figure C-2. This figure showed the spread of values for each element in the circuit. It was encouraging to note that the three elements to be modelled into the transformer did not vary appreciably. Element L5 changed by a factor of about 1.7, and element C4 changed by factor of 8.5. C4 is performing a dual function, that of impedance matching and resonating the filter.

C.2 LOAD PULLING

A brief investigation was performed to determine the effect on the filter performance, and verify the need for compensating networks which correct for antenna VSWR.

The antenna VSWR is specified at 3.5:1 which will incur a 1.6 dB loss in transmitted power, even if the filter performance is unaffected. Four computer runs were made using the COMPACT Microwave Analysis program, with a 3.5:1 load VSWR. Two earlier runs were made with lesser VSWR, and are not significant.

Load 3 was rotated from +120 to +120 degrees (Figure C-3)
Load 4 was rotated from + 60 to - 60 degrees (Figure C-3)
Load 5 was rotated from +150 to + 30 degrees (Figure C-6)
Load 6 was rotated from - 30 to - 15 degrees (Figure C-6)

The data is tabulated in Table C-3. The optimization was only effective in one case. Load 5 had the most severe effect on mid band insertion loss, and load 6 had the most effect on the skirts. This data points out the need for specific antenna VSWR data.

Thus, a more complex tuned circuit seems to be needed.

The addition of a closed loop frequency hoppable antenna tuning capability for each channel, with the attendant impedance measuring circuitry is (at this time), an unwanted complication. It may be sufficient for the system to operate on a - priori antenna impedance data as reflected back into the tuned circuits, and use the data to compute a "best fit" solution for each channel.

	S21 (dB) Center frequency is 51 MHz				
%	Run 17 Control	Load 3	Load 4	Load 5	Load 6
-20	-27.8	-26.2	-32.8	-32.4	-27.3
-15	-26	-25.9		-31	-23.9
-10	-23.2	-24.3		-28.4	-19.4
- 5	-19	-20.3	-21.3	-23.4	-12.5
-.75	- 4.4	- 7.2		- 9.1	- 2
-.38	- 1.9	- 4.3		- 5.38	- 1.7
0	- .54	- 1.64	- 1.86	- 2.7	- 1.18
+.38	- 1.8	- 4.3		- 5.1	- .82
+.75	- 4.3	- 8.5		- 8.7	- 2.04
+ 5	-19.3	-24.7	-18.2	-24	-18.4
+10	-26	-31.7		-30.3	-26.6
+15	-30.2	-36.1		-33.9	-32
+20	-33.5	-39.4	-28.1	-36.4	-36.1

TABLE C-3 TABULATION OF DATA, CIRCUIT OPTIMIZED FOR EACH LOAD

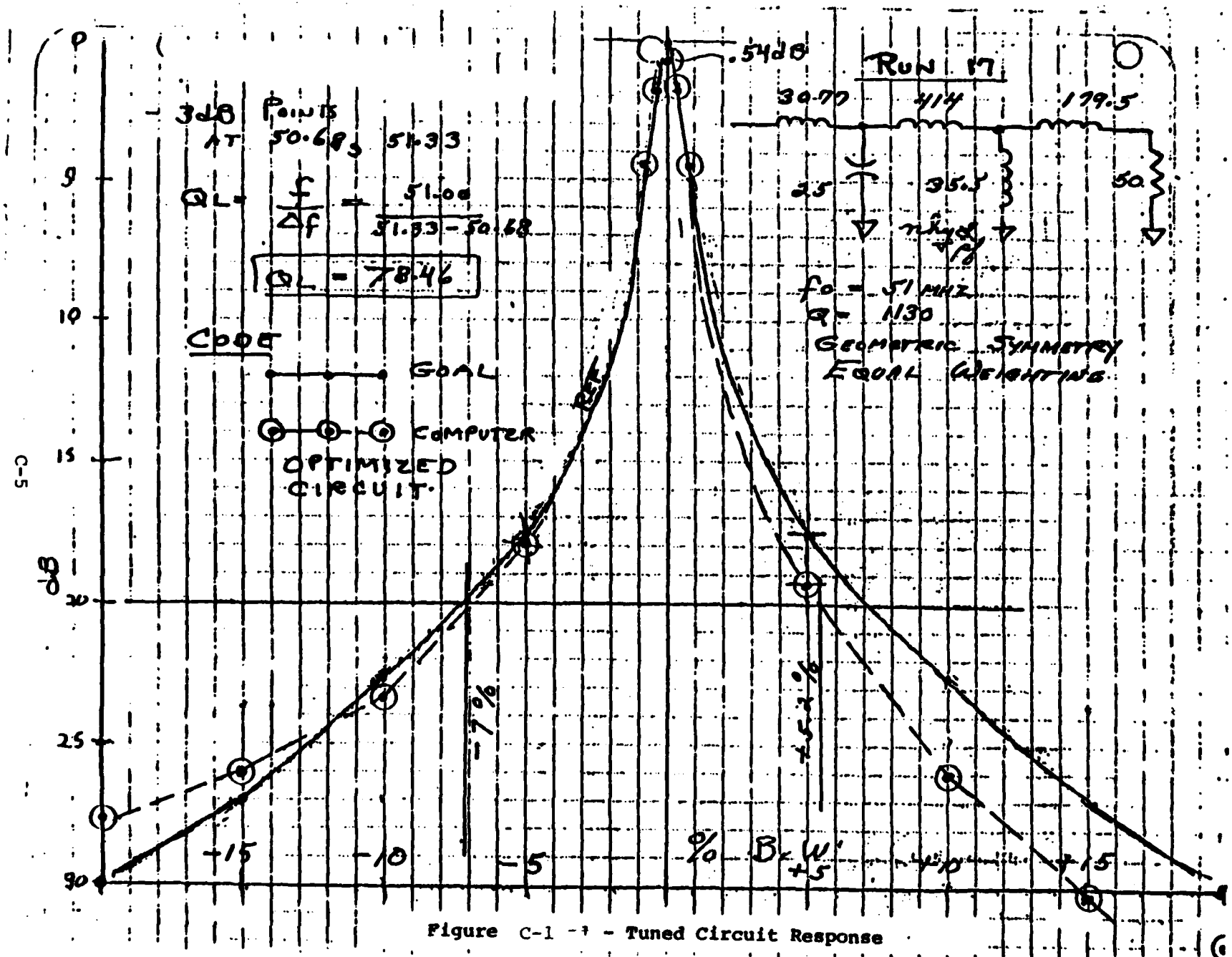

Figure C-1 - Tuned Circuit Response

RUNS 16 — 20 GEOMETRIC SYMMETRY EQUAL WEIGHTING

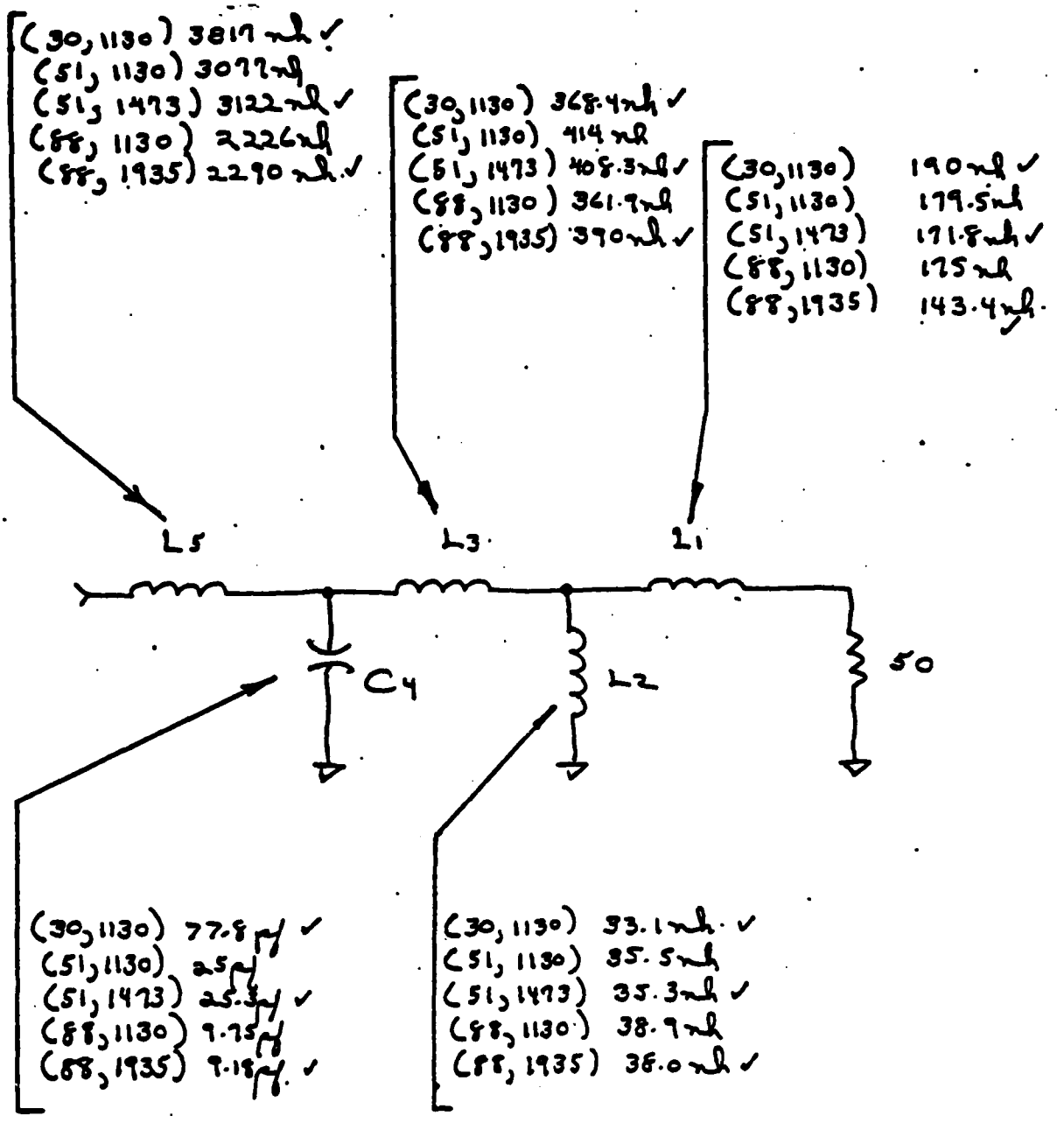

Figure C-2 - Range of Element Values

TABLE C-4

MAGNITUDE OF OPTIMIZATION CHANGES

Element	Load 3	Load 4	Load 5	Load 6
C4	−.352%	+.488%	−.052%	+.43%
LS	+5.7%	−.11%	−.005%	−.089%

TABLE C-5

MID BAND INSERTION LOSS WITH AND WITHOUT OPTIMIZATION.

Control	With	Without −.54dB	ΔdB
Load 3	−1.64 dB	−2.45 dB	+.81
Load 4	−1.86 dB	−1.86 dB	0
Load 5	−2.7 dB	−2.71 dB	0
Load 6	−1.18 dB	−1.56 dB	+.38

- IN ONLY ONE CASE DOES OPTIMIZATION SEEM TO BE WORTHWHILE.
- LOAD 5 HAD THE MOST SEVERE EFFECT ON MID BAND LOSS, OPTIMIZATION DID NOT HELP
- LOAD 6 HAD THE MOST EFFECT ON THE SKIRTS.
- THE TRANSFORMER CAN NOT BE INCLUDED IN THE OPTIMIZATION ; . . IT THUS APPEARS THAT THERE ARE NOT ENOUGH ELEMENTS TO ~~COMPENSATE~~ COMPENSATE FOR THE ANTENNA PULLING at any/all phase angles.

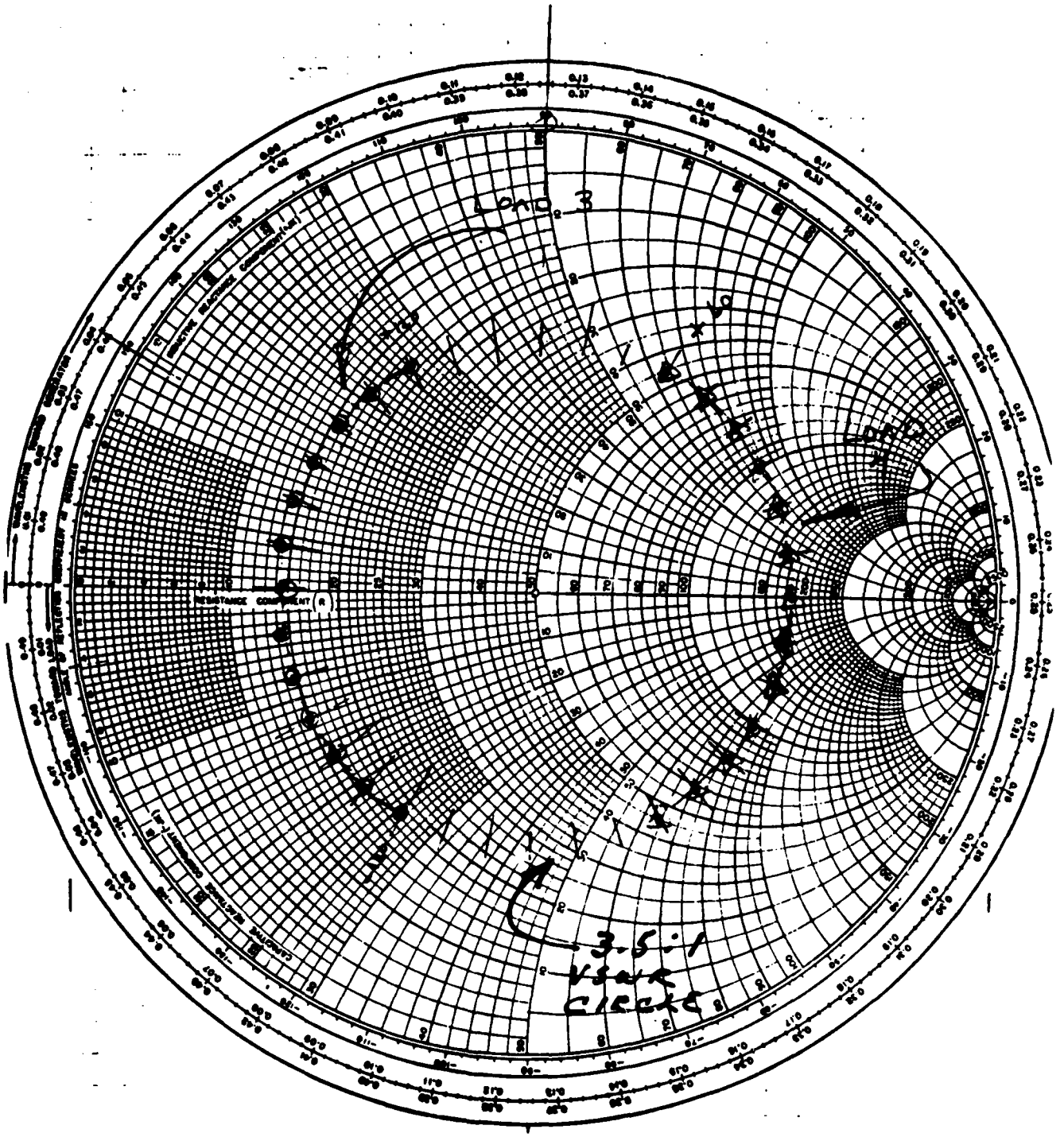

FIGURE C-3
LOADS 3 and 4

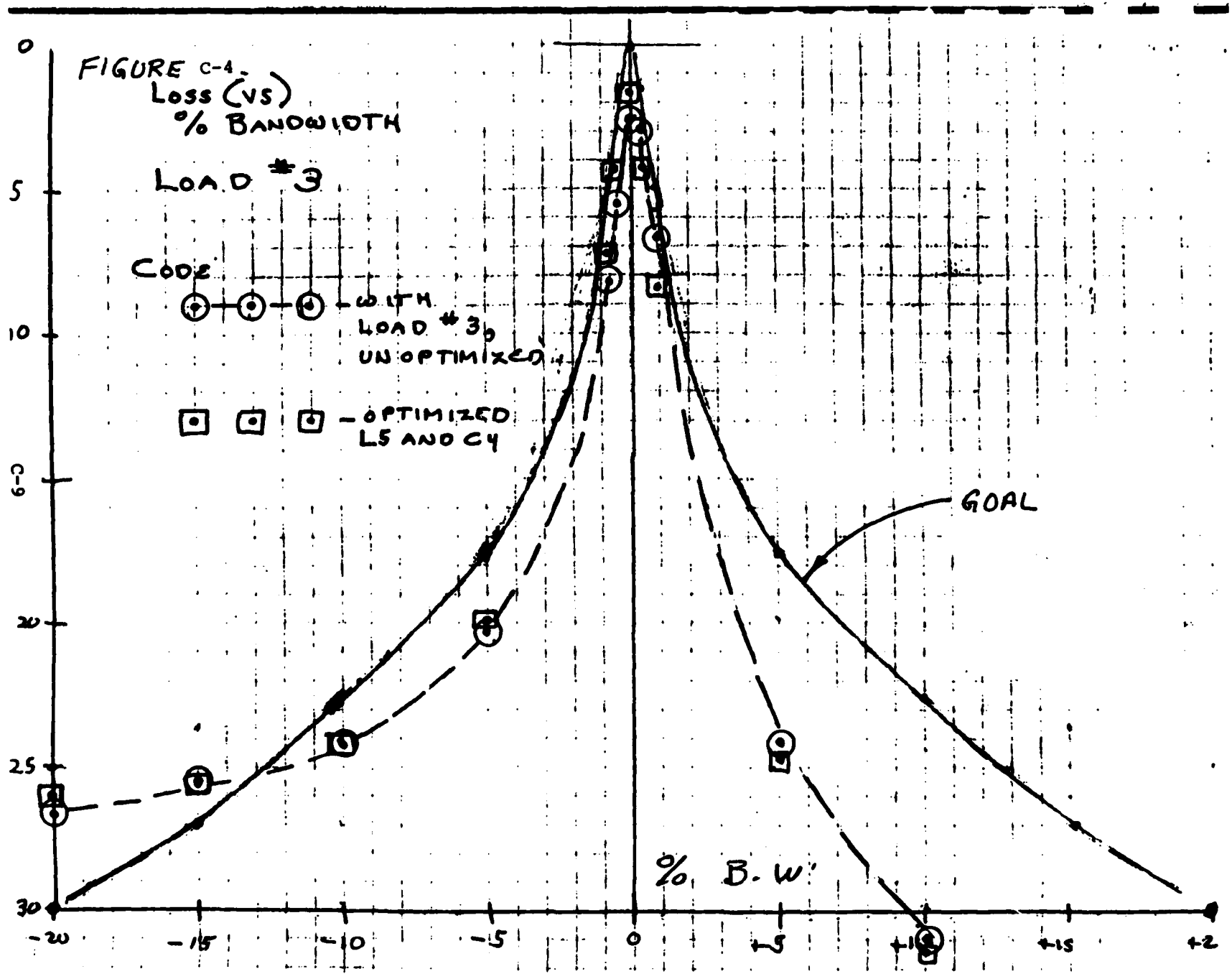
FIGURE C-4.
Loss (VS)
% BANDWIDTH
LOAD #3
CODE
WITH LOAD #30 UNOPTIMIZED
OPTIMIZED L5 AND C4
GOAL
% B.W.
0
5
10
C-9
20
25
30
-20
-15
-10
-5
0
+5
+10
+15
+20

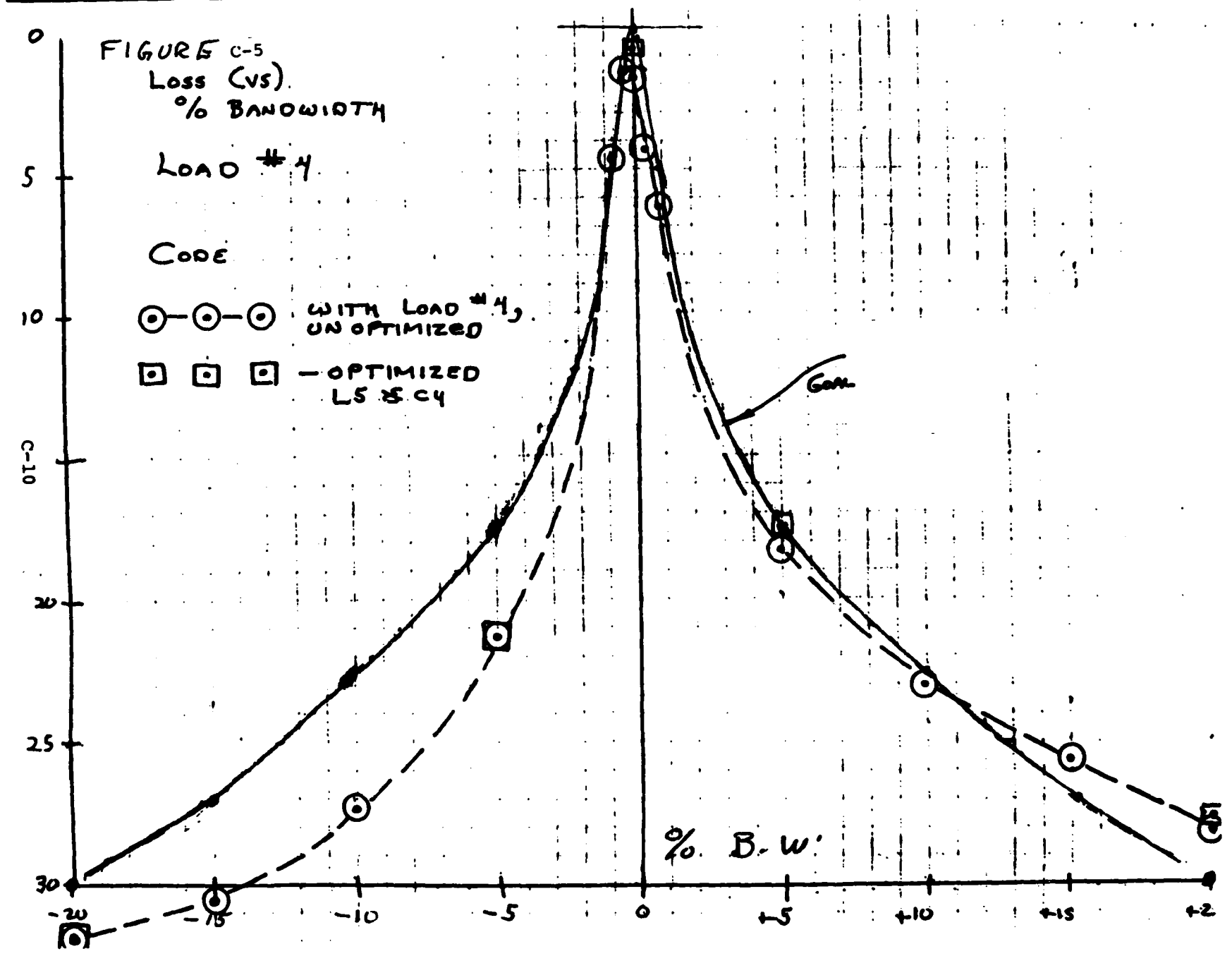
FIGURE C-5
Loss (vs)
% BANDWIDTH
LOAD #4
CODE
WITH LOAD #4, UN OPTIMIZED
OPTIMIZED L5 & C4
GAIN
0
5
10
C-10
20
25
30
-20
-15
-10
-5
0
+5
+10
+15
+20
% B.W.

TITLE DATE

IMPEDANCE COORDINATES—50-OHM CHARACTERISTIC IMPEDANCE

FIGURE C-6
IMPEDANCE (VS) FREQUENCY, LOADS 5 & 6.

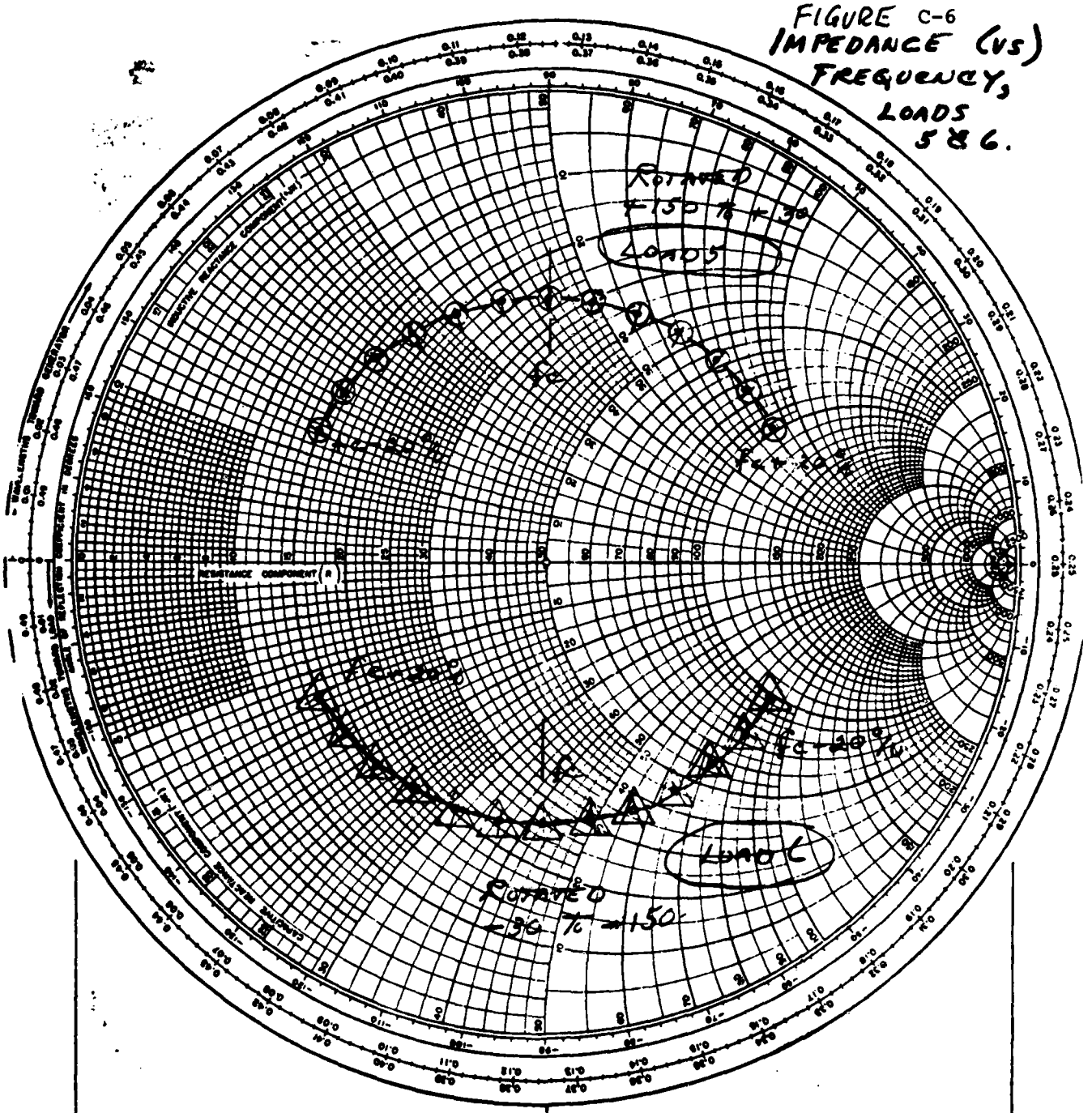

Electronics - VOL. 17, NO. 1, PP - 130 - 133, 348 - 325, JAN 1944

GENERAL RADIO COMPANY
WEST CONCORD, MASS.
FORM 0301-7002Z
Printed in USA

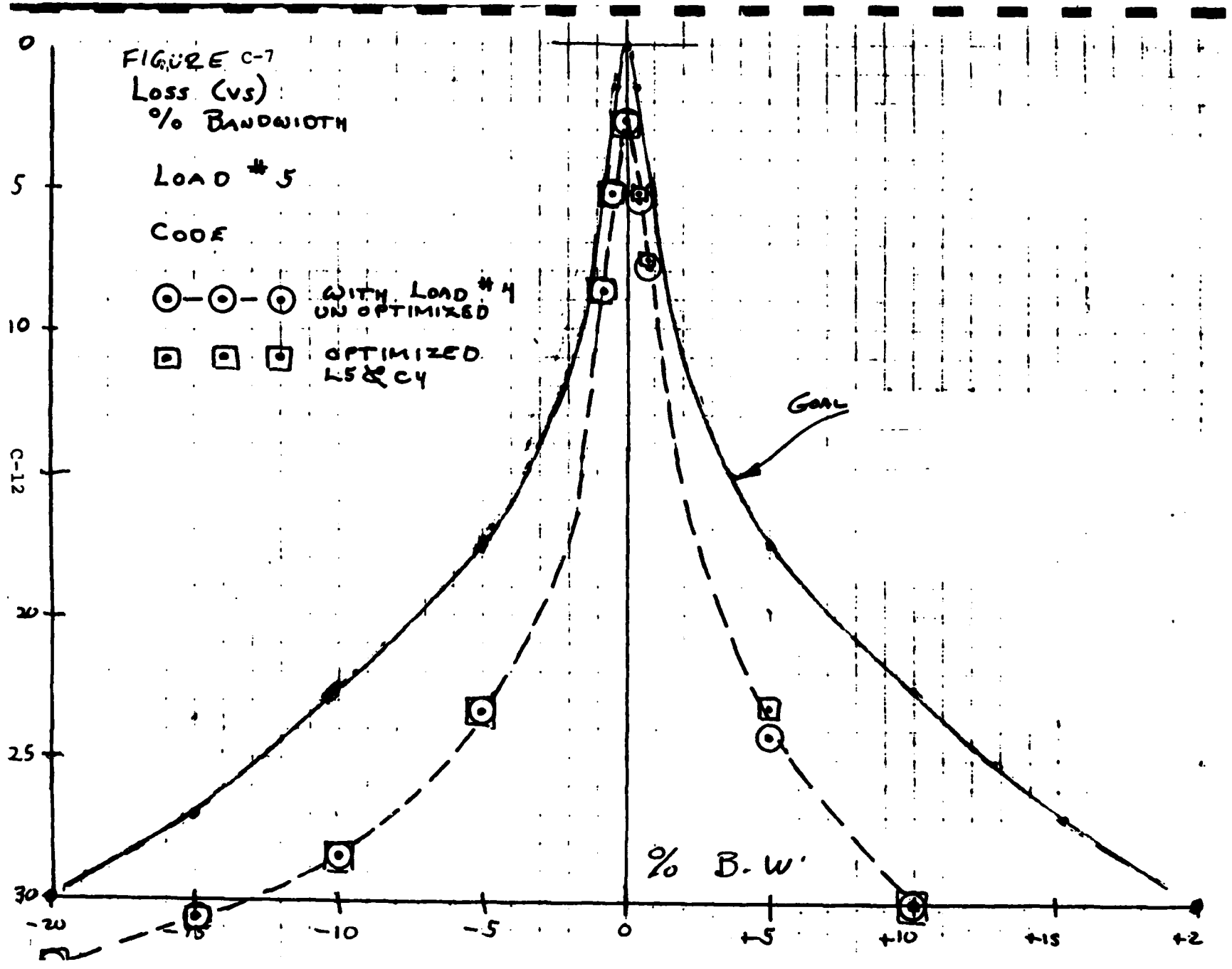
FIGURE C-7
Loss (vs)
% BANDWIDTH
LOAD #5
CODE
WITH LOAD #4 UN OPTIMIZED
OPTIMIZED L5 & C4
GOAL
% B.W.
0
5
10
20
25
30
-20
-15
-10
-5
0
+5
+10
+15
+20

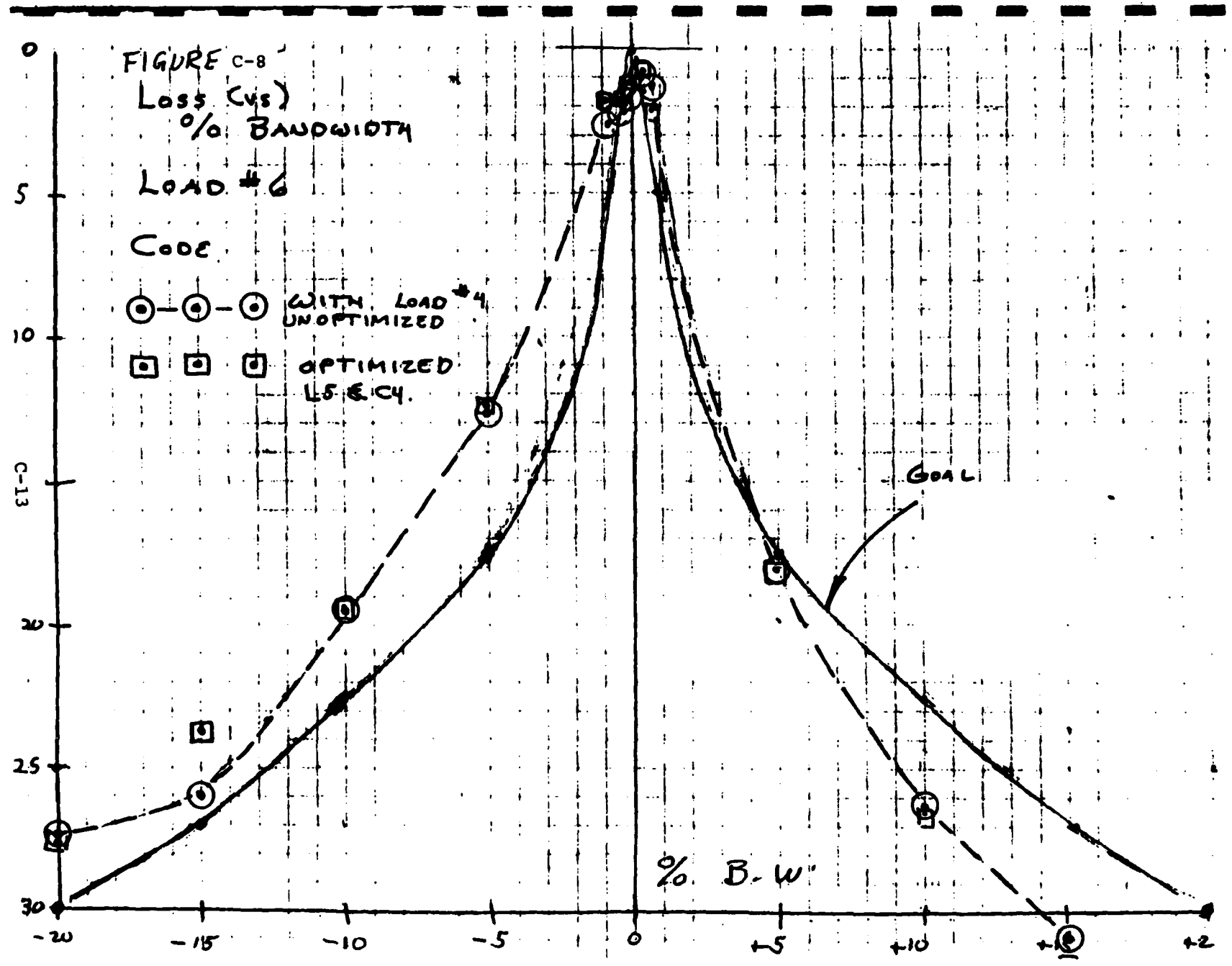
FIGURE C-8
Loss (vs)
% BANDWIDTH
LOAD #6
CODE
WITH LOAD #4 UNOPTIMIZED
OPTIMIZED L5 & C4.
GOAL
% B.W.
0
5
10
C-13
20
25
30
-20
-15
-10
-5
0
+5
+10
+15
+20

The following pages show the actual compute data files, analysis, and optimization, for loads 1 through 6.

TITLE

DATE

IMPEDANCE COORDINATES—50-OHM CHARACTERISTIC IMPEDANCE FIGURE C-9

ANTENNA LOAD #1 IMPEDANCE (VS) FREQUENCY

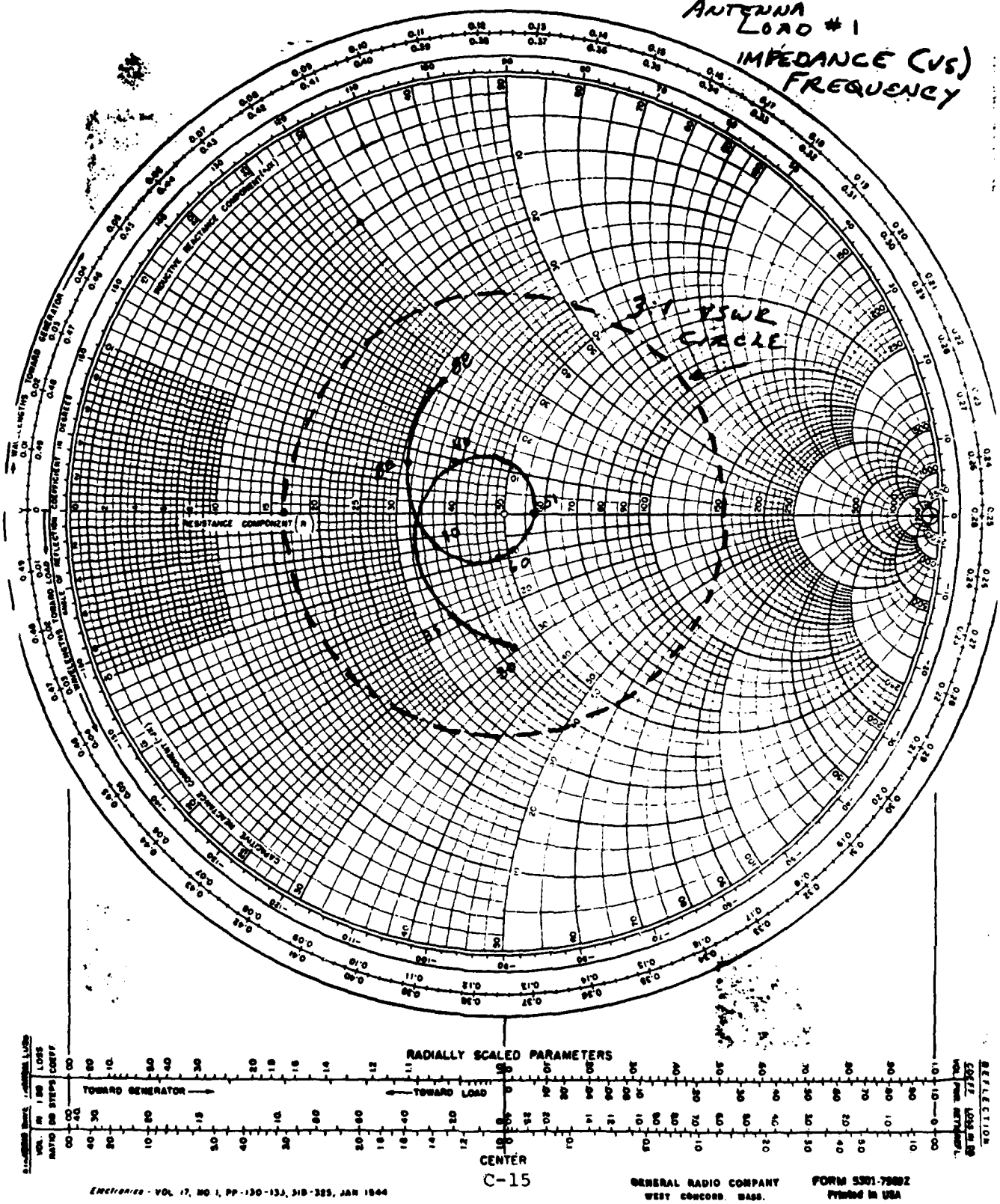

Electronics - VOL. 17, NO. 1, PP. 130-133, 318-325, JAN 1944

GENERAL RADIO COMPANY
WEST CONCORD, MASS.

FORM 5301-7502Z
Printed in USA

TABLE C-6

BASELINE: RUN 17 WITH 50 OHM LOAD.

POLAR S-PARAMETERS IN 50.0 OHM SYSTEM

F MHZ	S11 (MAGN<ANGL)	S21 (MAGN<ANGL)	S12 (MAGN<ANGL)	S22 (MAGN<ANGL)	S21 DB
41.8	(1.00< 4)	(0.04< -47)	(0.041< -47)	(1.00< 81)	-27.80
43.9	(1.00< 3)	(0.05< -49)	(0.050< -49)	(1.00< 78)	-25.98
46.1	(1.00< 1)	(0.07< -51)	(0.069< -51)	(1.00< 74)	-23.17
48.1	(0.99< 0)	(0.11< -55)	(0.112< -55)	(0.99< 70)	-19.00
50.6	(0.77< -35)	(0.60< -90)	(0.603< -90)	(0.77< 39)	-4.40
50.8	(0.52< -54)	(0.80<-109)	(0.801<-109)	(0.54< 26)	-1.93
51.0	(0.03<-116)	(0.94<-139)	(0.940<-139)	(0.13< 62)	-0.54
51.2	(0.49< 67)	(0.82<-170)	(0.818<-170)	(0.50< 119)	-1.75
51.4	(0.76< 47)	(0.61< 169)	(0.612< 169)	(0.76< 106)	-4.26
53.6	(0.99< 12)	(0.11< 134)	(0.109< 134)	(0.99< 75)	-19.25
56.4	(1.00< 8)	(0.05< 129)	(0.050< 129)	(1.00< 70)	-25.98
59.2	(1.00< 6)	(0.03< 126)	(0.031< 126)	(1.00< 66)	-30.24
62.2	(1.00< 5)	(0.02< 124)	(0.021< 124)	(1.00< 63)	-33.47

****

TABLE C-7 ANALYSIS WITH LOAD 1

POLAR S-PARAMETERS WITH COMPLEX LOAD AND SOURCE

F MHZ	SOURCE IMP. (R,JX) OHMS	LOAD #1 IMP. (R,JX) OHMS
41.810	(50.00, 0.0)	(39.00, 10.00)
43.920	(50.00, 0.0)	(45.00, 11.00)
46.150	(50.00, 0.0)	(48.00, 12.00)
48.510	(50.00, 0.0)	(52.00, 9.00)
50.620	(50.00, 0.0)	(54.00, 6.00)
50.810	(50.00, 0.0)	(56.00, 3.00)
51.000	(50.00, 0.0)	(59.00, 0.0)
51.190	(50.00, 0.0)	(56.00, -3.00)
51.380	(50.00, 0.0)	(54.00, -6.00)
53.610	(50.00, 0.0)	(52.00, -9.00)
56.350	(50.00, 0.0)	(48.00, -12.00)
59.220	(50.00, 0.0)	(45.00, -11.00)
62.210	(50.00, 0.0)	(44.00, -10.00)

F MHZ	S11 (MAGN<ANGL)	S21 (MAGN<ANGL)	S12 (MAGN<ANGL)	S22 (MAGN<ANGL)	S21 DB
41.8	(1.00< 4)	(0.04< -57)	(0.035< -57)	(1.00< 59)	-29.08
43.9	(1.00< 3)	(0.04< -56)	(0.044< -56)	(1.00< 63)	-27.09
46.1	(1.00< 1)	(0.06< -57)	(0.062< -57)	(1.00< 63)	-24.22
48.5	(0.99< -1)	(0.12< -59)	(0.118< -59)	(0.99< 64)	-18.56
50.6	(0.77< -36)	(0.60< -90)	(0.599< -90)	(0.78< 41)	-4.45
50.8	(0.49< -57)	(0.82<-109)	(0.816<-109)	(0.51< 30)	-1.76
51.0	(0.05< 95)	(0.94<-138)	(0.941<-138)	(0.12< 100)	-0.53
51.2	(0.51< 63)	(0.81<-166)	(0.813<-166)	(0.51< 132)	-1.79
51.4	(0.75< 45)	(0.63< 175)	(0.630< 175)	(0.75< 120)	-4.01
53.6	(0.99< 12)	(0.12< 139)	(0.119< 139)	(0.99< 86)	-18.48
56.4	(1.00< 8)	(0.06< 133)	(0.056< 133)	(1.00< 77)	-25.01
59.2	(1.00< 6)	(0.03< 128)	(0.034< 128)	(1.00< 69)	-29.48
62.2	(1.00< 6)	(0.02< 124)	(0.023< 124)	(1.00< 63)	-32.90

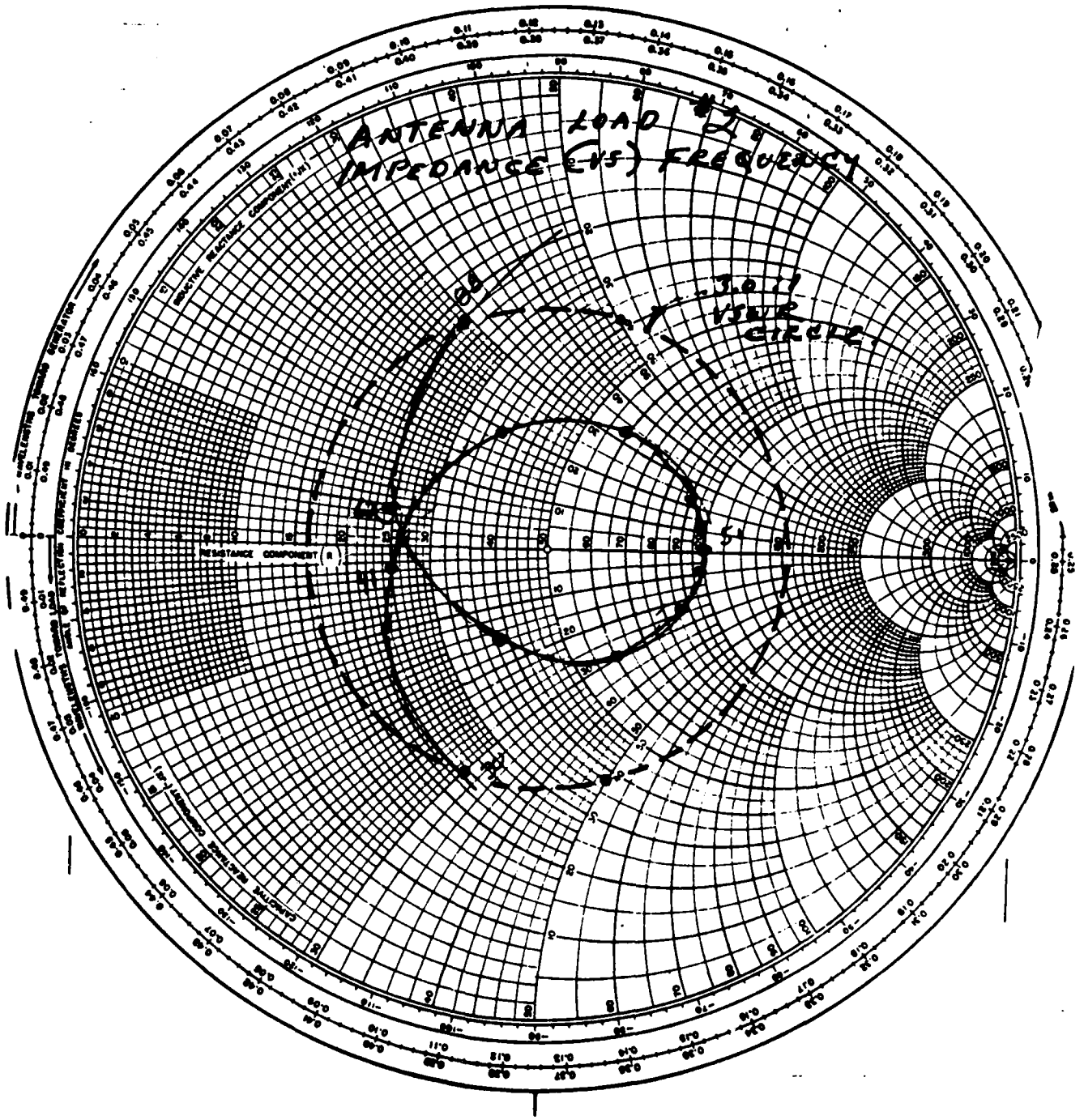

FIGURE C-10
IMPEDANCE - VS - FREQUENCY
LOAD # 2

ANALYSIS WITH LOAD 2

TABLE C-8

DATA FILE

```
LIST
00010 IND AA SE 3077  L5
00020 CAP BB PA 25    C4
00030 IND CC SE 414 1130 51 L3
00040 IND DD PA 35.5  L2
00050 IND EE SE 179.5  L1
00060 CAX AA EE
00070 PRI AA S3
00080 END
00090 41.81 43.92 46.15 48.51 50.62
00100 50.81 51 51.19 51.38 53.61
00110 56,35 59.22 62.21
00120 END
00130 50 0 25 -3
00140 50 0 26 0
00150 50 0 39 20
00160 50 0 60 33
00170 50 0 90 21
00180 50 0 98 10
00190 50 0 100 0
00200 50 0 98 -10
00210 50 0 90 -21
00220 50 0 60 -33
00230 50 0 39 -20
00240 50 0 26 0
00250 50 0 25 3
00260 END
```

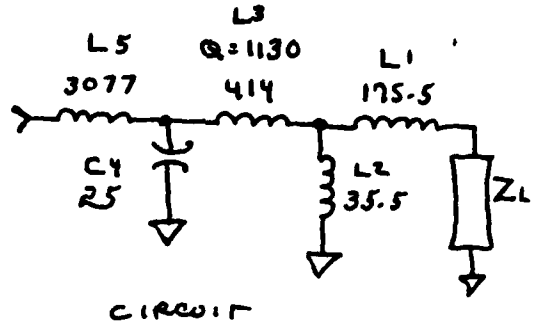

CIRCUIT

POLAR S-PARAMETERS WITH COMPLEX LOAD #2.

F MHZ	SOURCE IMP. (R,JX) OHMS	LOAD IMP. (R,JX) OHMS
41.810	(50.00, 0.0)	(25.00, -3.00)
43.920	(50.00, 0.0)	(26.00, 0.0)
46.150	(50.00, 0.0)	(39.00, 20.00)
48.510	(50.00, 0.0)	(60.00, 33.00)
50.620	(50.00, 0.0)	(90.00, 21.00)
50.810	(50.00, 0.0)	(98.00, 10.00)
51.000	(50.00, 0.0)	(100.00, 0.0)
51.190	(50.00, 0.0)	(98.00, -10.00)
51.380	(50.00, 0.0)	(90.00, -21.00)
53.610	(50.00, 0.0)	(60.00, -33.00)
56.350	(50.00, 0.0)	(39.00, -20.00)
59.220	(50.00, 0.0)	(26.00, 0.0)
62.210	(50.00, 0.0)	(25.00, 3.00)

F MHZ	S11 (MAGN<ANGL)	S21 (MAGN<ANGL)	S12 (MAGN<ANGL)	S22 (MAGN<ANGL)	S21 DB
41.8	(1.00< 4)	(0.04< -63)	(0.037< -63)	(1.00< 49)	-28.74
43.9	(1.00< 3)	(0.04< -65)	(0.043< -65)	(1.00< 46)	-27.32
46.1	(1.00< 1)	(0.05< -64)	(0.054< -64)	(1.00< 49)	-25.39
48.5	(0.99< -2)	(0.10< -61)	(0.101< -61)	(0.99< 59)	-19.89
50.6	(0.73< -44)	(0.64< -85)	(0.637< -85)	(0.74< 60)	-3.92
50.8	(0.34< -76)	(0.88<-106)	(0.879<-106)	(0.38< 60)	-1.12
51.0	(0.27< 86)	(0.90<-136)	(0.904<-136)	(0.30< 158)	-0.88
51.2	(0.65< 54)	(0.72<-158)	(0.719<-158)	(0.65< 161)	-2.87
51.4	(0.80< 39)	(0.57<-167)	(0.570<-167)	(0.80< 160)	-4.88
53.6	(0.99< 12)	(0.14< 158)	(0.143< 158)	(0.99< 125)	-16.88
56.4	(1.00< 8)	(0.06< 131)	(0.060< 131)	(1.00< 74)	-24.44
59.2	(1.00< 6)	(0.03< 112)	(0.025< 112)	(1.00< 37)	-32.00
62.2	(1.00< 6)	(0.02< 109)	(0.016< 109)	(1.00< 33)	-35.77

The effects of loads 1 & 2 were not severe, because the VSWR was low at the center frequency. Also, the load impedances were real at the center frequencies.

It was thus decided to investigate the effects of a "worst case" AS 3166/GRC antenna, namely a "constant 3.5:1 VSWR. The "VSWR" circle is divided into 4 cases.

Load 3	-120 to +120 degrees
Load 4	+60 to -60 degrees
Load 5	+150 to +30 degrees
Load 6	-30 to -150 degrees

The following table was derived to provide accurate load data for this investigation.

Locus of ... for S = 3.5:1, every 10°

50.	ZO
9.5555556	MAGI
180.	DEG
14.28571245	R
0.	JX
3.50000045	VSWR
170.	DEG
14.38607013	R
4.014828068	JX
3.50000045	VSWR
160.	DEG
14.69258184	R
8.076149532	JX
3.50000045	VSWR
150.	DEG
15.22216397	R
12.2320979	JX
3.50000045	VSWR
140.	DEG
16.00511964	R
16.5341156	JX
3.50000045	VSWR
130.	DEG
17.08670632	R
21.03864188	JX
3.50000045	VSWR
120.	DEG
18.5430441	R
25.80870485	JX
3.50000045	VSWR
110.	DEG
20.47055532	R
30.91505254	JX
3.50000045	VSWR
100.	DEG
23.02094867	R
36.43587669	JX
3.50000045	VSWR
[illegible]	

70.	DEG
37.22503627	R
56.21801333	JX
3.50000045	VSWR
60.	DEG
45.90163576	R
63.88712464	JX
3.50000045	VSWR
50.	DEG
58.15267485	R
71.59426099	JX
3.50000045	VSWR
40.	DEG
75.56131006	R
78.05873769	JX
3.50000045	VSWR
30.	DEG
99.79430459	R
80.19186405	JX
3.50000045	VSWR
20.	DEG
130.6722069	R
71.82728633	JX
3.50000045	VSWR
10.	DEG
161.2225239	R
44.99357418	JX
3.50000045	VSWR
0.	DEG
175.0000225	R
0.	JX
3.50000045	VSWR
-10.	DEG
161.2225839	R
-44.99357418	JX
3.50000045	VSWR
-20.	DEG
130.6722069	R
71.82728633	JX
[illegible]	VSWR
[illegible]	DEG
[illegible]	R
[illegible]	JX
[illegible]	VSWR

-40.	DEG
75.56131006	R
-78.05873769	JX
3.50000045	VSWR
-50.	DEG
58.15267485	R
-71.59426099	JX
3.50000045	VSWR
-60.	DEG
45.90163576	R
-63.88712464	JX
3.50000045	VSWR
-50.	DEG
58.15267485	R
-71.59426099	JX
3.50000045	VSWR
-70.	DEG
37.22503627	R
-56.21801333	JX
3.50000045	VSWR
-80.	DEG
30.98315988	R
-49.03788324	JX
3.50000045	VSWR
-90.	DEG
26.41509146	R
-42.45283198	JX
3.50000045	VSWR
-100.	DEG
23.02094867	R
-36.43587669	JX
3.50000045	VSWR
-110.	DEG
20.47055532	R
-30.91505254	JX
3.50000045	VSWR
-120.	DEG
18.5430441	R
25.80870485	JX
3.50000045	VSWR
-130.	DEG
17.08670632	R
-21.03864188	JX
[illegible]	VSWR

FIGURE C-11
LOCUS POINTS FOR LOADS 3, 4, 5, and 6

```
      -140.        DEG
16.00511964         R
-16.5341156        JX
 3.50000045      VSWR

      -150.        DEG
15.22216397         R
-12.2320979        JX
 3.50000045      VSWR

      -160.        DEG
14.69258184         R
-8.076149532       JX
 3.50000045      VSWR

      -170.        DEG
14.38607013         R
-4.014828066       JX
 3.50000045      VSWR

      -180.        DEG
14.28571245         R
          0.       JX
 3.50000045      VSWR
```

Figure C-11

Locus of points for loads 3, 4, 5, and 6. Taken every 10 degrees.

Figure C-11 (Continued)

ANALYSIS WITH LOAD #3 TABLE C-9

DATA FILE

```
00010 IND AA SE-3077
00020 CAP BB PA-25
00030 IND CC SE 414 1130 51
00040 IND DD PA 35.5
00050 IND EE SE-179.5
00060 CAX AA EE
00070 PRI AA S3
00080 END
00090 41.81 43.92 46.15 48.51 50.62
00100 50.81 51 51.19 51.38 53.61
00110 56.35 59.22 62.21
00120 END
00130 50 0 18.5 -25.8
00140 50 0 17.1 -21
00150 50 0 16 -16.5
00160 50 0 15 -12.2
00170 50 0 14.7 -8.1
00180 50 0 14 -4
00190 50 0 14.3 0
00200 50 0 14.4 4
00210 50 0 14.7 8.1
00220 50 0 15.2 12.2
00230 50 0 16 16.5
00240 50 0 17.1 21
00250 50 0 18.5 25.8
00260 END
```

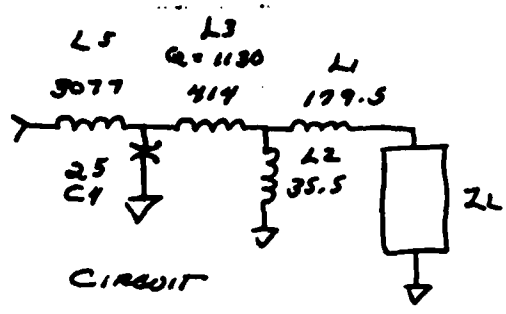

POLAR S-PARAMETERS WITH COMPLEX LOAD #3

F MHZ	SOURCE IMP. (R+JX) OHMS	LOAD IMP. (R+JX) OHMS
41.810	(50.00, 0.0)	(18.54, -25.81)
43.920	(50.00, 0.0)	(17.09, -21.04)
46.150	(50.00, 0.0)	(16.00, -16.53)
48.510	(50.00, 0.0)	(15.22, -12.23)
50.620	(50.00, 0.0)	(14.70, -8.08)
50.810	(50.00, 0.0)	(14.39, -4.01)
51.000	(50.00, 0.0)	(14.30, 0.0)
51.190	(50.00, 0.0)	(14.90, 4.00)
51.380	(50.00, 0.0)	(14.70, 8.10)
53.610	(50.00, 0.0)	(15.20, 2.23)
56.350	(50.00, 0.0)	(16.00, 16.50)
59.220	(50.00, 0.0)	(17.10, 21.00)
62.210	(50.00, 0.0)	(18.50, 25.80)

F MHZ	S11 (MAGN<ANGL)	S21 (MAGN<ANGL)	S12 (MAGN<ANGL)	S22 (MAGN<ANGL)	S21 DD
41.8	(1.00< 4)	(0.05< -57)	(0.051< -57)	(1.00< 60)	-25.81
43.9	(1.00< 3)	(0.05< -65)	(0.053< -65)	(1.00< 46)	-25.53
46.1	(1.00< 2)	(0.06< -71)	(0.063< -71)	(1.00< 36)	-24.03
48.5	(0.99< -1)	(0.10< -77)	(0.098< -77)	(0.99< 27)	-20.14
50.6	(0.90< -28)	(0.39<-100)	(0.394<-100)	(0.91< 12)	-8.09
50.8	(0.80< -48)	(0.53<-113)	(0.526<-113)	(0.83< 6)	-5.58
51.0	(0.50<-103)	(0.75<-142)	(0.754<-142)	(0.61< 7)	-2.45
51.2	(0.55< 112)	(0.72< 169)	(0.722< 169)	(0.65< 37)	-2.65
51.4	(0.84< 59)	(0.46< 140)	(0.459< 140)	(0.87< 35)	-6.76
53.6	(1.00< 12)	(0.06< 107)	(0.063< 107)	(1.00< 22)	-24.03
56.4	(1.00< 8)	(0.03< 104)	(0.028< 104)	(1.00< 20)	-31.13
59.2	(1.00< 6)	(0.02< 103)	(0.017< 103)	(1.00< 19)	-35.59
62.2	(1.00< 5)	(0.01< 102)	(0.011< 102)	(1.00< 19)	-38.92

TABLE C-10

OPTIMIZATION OF L5 AND C4, WITH LOAD #3

```
00010 IND AA SE -3077  L5
00020 CAP BB PA -25    C4
00030 IND CC SE 414 1130 51
00040 IND DD PA 35.5
00050 IND EE SE 179.5
00060 CAX AA EE
00070 PRI AA S3
00080 END
00090 41.81 62.21
00100 48.51 53.61
00110 51
00120 END
00130 50 0 18.5 -25.8
00140 50 0 18.5 25.8
00150 50 0 15 -12.2
00160 50 0 15.2 12.2
00170 50 0 14.3 0
00180 END
00190 .1
00200 0 0 1 -30 LT
00210 0 0 1 -17.5
00220 0 0 10 0
00230 END
```

CIRCUIT OPTIMIZATION WITH 2 VARIABLES

INITIAL CIRCUIT ANALYSIS:
POLAR S-PARAMETERS WITH COMPLEX LOAD

F MHZ	SOURCE IMP. (R,JX) OHMS	LOAD IMP. (R,JX) OHMS
41.810	(50.00, 0.0)	(18.50, -25.80)
62.210	(50.00, 0.0)	(18.50, 25.80)
48.510	(50.00, 0.0)	(15.00, -12.20)
53.610	(50.00, 0.0)	(15.20, 12.20)
51.000	(50.00, 0.0)	(14.30, 0.0)

F MHZ	S11 (MAGN<ANGL)	S21 (MAGN<ANGL)	S12 (MAGN<ANGL)	S22 (MAGN<ANGL)	S21 DB
41.8	(1.00< 4)	(0.05< -57)	(0.051< -57)	(1.00< 60)	-25.81
62.2	(1.00< 5)	(0.01< 102)	(0.011< 102)	(1.00< 19)	-38.92
48.5	(0.99< -1)	(0.10< -77)	(0.098< -77)	(0.99< 27)	-20.14
53.6	(1.00< 12)	(0.06< 107)	(0.063< 107)	(1.00< 22)	-24.03
51.0	(0.50<-103)	(0.75<-142)	(0.754<-142)	(0.61< 7)	-2.45

OPTIMIZATION BEGINS WITH FOLLOWING VARIABLES AND GRADIENTS

VARIABLES:		GRADIENTS:
(1):	3077.001	(1): -377.805
(2):	25.000	(2): -2911.366
ERROR FUNCTION =	25.460	
----	****	----
(1):	3078.377	(1): -10.928
(2):	25.087	(2): 1.378
ERROR FUNCTION =	20.488	
----	****	----
(1):	3252.118	New L5 (1): -26.607
(2):	24.912	New C4 (2): -207.950
ERROR FUNCTION =	20.374 (WANTED 0.1)	
----	****	----

FRACTIONAL TERMINATION WITH ABOVE VALUES. FINAL ANALYSIS FOLLOWS

41.8	(1.00< 4)	(0.05< -57)	(0.049< -57)	(1.00< 60)	-26.17
62.2	(1.00< 5)	(0.01< 102)	(0.011< 102)	(1.00< 19)	-39.43
48.5	(0.99< -1)	(0.10< -77)	(0.097< -77)	(0.99< 27)	-20.30
53.6	(1.00< 11)	(0.06< 107)	(0.058< 107)	(1.00< 22)	-24.74
51.0	(0.32<-158)	(0.83<-161)	(0.828<-161)	(0.48< 19)	-1.64

TABLE C-11 ANALYSIS OF OPTIMIZED CIRCUIT. WITH LOAD 3

```
00010 IND AA SE 3252  NEW L5
00020 CAP BB PA 24.912  NEW C4
00030 IND CC SE 414 1130 51
00040 IND DD PA 35.5
00050 IND EE SE 179.5
00060 CAX AA EE
00070 PRI AA S3
00080 END
00090 41.81 43.92 46.15 48.51 50.62
00100 50.81 51 51.19 51.38 53.61
00110 56.35 59.22 62.21
00120 END
00130 50 0 18.5 -25.8
00140 50 0 17.1 -21
00150 50 0 16 -16.5
00160 50 0 15 -12.2
00170 50 0 14.7 -8.1
00180 50 0 14 -4
00190 50 0 14.3 0
00200 50 0 14.4 4
00210 50 0 14.7 8.1
00220 50 0 15.2 12.2
00230 50 0 16 16.5
00240 50 0 17.1 21
00250 50 0 18.5 25.8
```

COMPLETE ANALYSIS, WITH "NEW" VALUES OF L5 & C4.

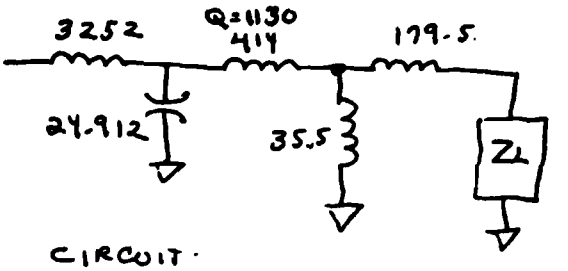

CIRCUIT

POLAR S-PARAMETERS WITH COMPLEX LOAD #3.

F MHZ	SOURCE IMP. (R,JX) OHMS	LOAD IMP. (R,JX) OHMS
41.810	(50.00, 0.0)	(18.50, -25.80)
43.920	(50.00, 0.0)	(17.10, -21.00)
46.150	(50.00, 0.0)	(16.00, -16.50)
48.510	(50.00, 0.0)	(15.00, -12.20)
50.620	(50.00, 0.0)	(14.70, -8.10)
50.810	(50.00, 0.0)	(14.00, -4.00)
51.000	(50.00, 0.0)	(14.30, 0.0)
51.190	(50.00, 0.0)	(14.40, 4.00)
51.380	(50.00, 0.0)	(14.70, 8.10)
53.610	(50.00, 0.0)	(15.20, 12.20)
56.350	(50.00, 0.0)	(16.00, 16.50)
59.220	(50.00, 0.0)	(17.10, 21.00)
62.210	(50.00, 0.0)	(18.50, 25.80)

F MHZ	S11 (MAGN<ANGL)	S21 (MAGN<ANGL)	S12 (MAGN<ANGL)	S22 (MAGN ANGL)	S21 DB
41.8	(1.00< 4)	(0.05< -57)	(0.049< -57)	(1.00 60)	-26.17
43.9	(1.00< 3)	(0.05< -65)	(0.051< -65)	(1.00 46)	-25.84
46.1	(1.00< 2)	(0.06< -71)	(0.061< -71)	(1.00< 36)	-24.34
48.5	(0.99< -1)	(0.10< -77)	(0.097< -77)	(0.99< 27)	-20.30
50.6	(0.87< -31)	(0.44<-103)	(0.435<-103)	(0.89< 9)	-7.22
50.8	(0.72< -56)	(0.61<-120)	(0.612<-120)	(0.76< 2)	-4.27
51.0	(0.32<-157)	(0.83<-161)	(0.828<-161)	(0.48 19)	-1.64
51.2	(0.70< 76)	(0.61< 153)	(0.611< 153)	(0.76< 41)	-4.28
51.4	(0.90< 45)	(0.38< 132)	(0.376< 132)	(0.92< 33)	-8.50
53.6	(1.00< 11)	(0.06< 107)	(0.058< 107)	(1.00< 22)	-24.74
56.4	(1.00< 7)	(0.03< 104)	(0.026< 104)	(1.00 20)	-31.71
59.2	(1.00< 6)	(0.02< 103)	(0.016< 103)	(1.00 19)	-36.12
62.2	(1.00< 5)	(0.01< 102)	(0.011< 102)	(1.00 19)	-39.43

ANALYSIS WITH LOAD #4 TABLE C-12

DATA FILE

```
00010 IND AA SE 3077
00020 CAP BB PA 25
00030 IND CC SE 414 1130 51
00040 IND DD PA 35.5
00050 IND EE SE 179.5
00060 CAX AA EE
00070 PRI AA S3
00080 END
00090 41.81 43.92 46.15 48.51 50.62
00100 50.81 51 51.19 51.38 53.61
00110 56.35 59.22 62.21
00120 END
00130 50 0 45.9 64
00140 50 0 58.2 71.6
00150 50 0 75.6 78.16
00160 50 0 100 80.2
00170 50 0 130.7 72
00180 50 0 161.2 45
00190 50 0 175 0
00200 50 0 161.2 -45
00210 50 0 130.7 -72
00220 50 0 100 -80.2
00230 50 0 75.6 -78
00240 50 0 58.2 -71.6
00250 50 0 45.7 -64
00260 END
```

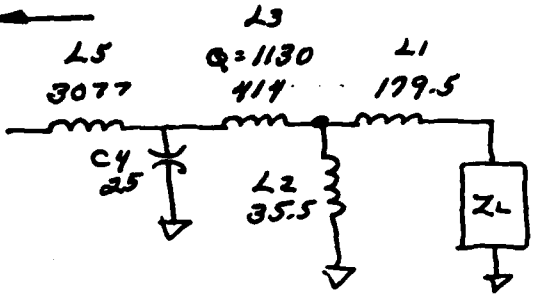

IN BAND INSERTION LOSS IS -1.9 dB.

Z_{IN} IS $33 + j41.3$

VSWR = 2.85:1

POLAR S-PARAMETERS WITH COMPLEX LOAD #4.

F MHZ	SOURCE IMP. (R,JX) OHMS	LOAD IMP. (R,JX) OHMS
41.810	(50.00, 0.0)	(45.90, 64.00)
43.920	(50.00, 0.0)	(58.20, 71.60)
46.150	(50.00, 0.0)	(75.60, 78.16)
48.510	(50.00, 0.0)	(100.00, 80.20)
50.620	(50.00, 0.0)	(130.70, 72.00)
50.810	(50.00, 0.0)	(161.20, 45.00)
51.000	(50.00, 0.0)	(175.00, 0.0)
51.190	(50.00, 0.0)	(161.20, -45.00)
51.380	(50.00, 0.0)	(130.70, -72.00)
53.610	(50.00, 0.0)	(100.00, -80.20)
56.350	(50.00, 0.0)	(75.60, -78.00)
59.220	(50.00, 0.0)	(58.20, -71.60)
62.210	(50.00, 0.0)	(45.70, -64.00)

F MHZ	S11 (MAGN<ANGL)	S21 (MAGN<ANGL)	S12 (MAGN<ANGL)	S22 (MAGN<ANGL)	S21 DB
41.8	(1.00< 4)	(0.02< -67)	(0.023< -67)	(1.00< 41)	-32.80
43.9	(1.00< 3)	(0.03< -64)	(0.030< -64)	(1.00< 47)	-30.59
46.1	(1.00< 1)	(0.04< -61)	(0.043< -61)	(1.00< 53)	-27.25
48.5	(1.00< -2)	(0.09< -58)	(0.087< -58)	(1.00< 66)	-21.20
50.6	(0.76< -52)	(0.58< -86)	(0.579< -86)	(0.79< 65)	-4.75
50.8	(0.34<-113)	(0.85<-107)	(0.853<-107)	(0.44< 90)	-1.38
51.0	(0.48< 86)	(0.81<-135)	(0.807<-135)	(0.52< 170)	-1.86
51.2	(0.76< 50)	(0.60<-144)	(0.603<-144)	(0.77<-165)	-4.39
51.4	(0.86< 35)	(0.48<-145)	(0.479<-145)	(0.86<-149)	-6.39
53.6	(0.99< 11)	(0.12<-164)	(0.124<-164)	(0.99<-161)	-18.15
56.4	(1.00< 8)	(0.07<-170)	(0.071<-170)	(1.00<-169)	-22.99
59.2	(1.00< 6)	(0.05< 178)	(0.052< 178)	(1.00< 170)	-25.70
62.2	(1.00< 5)	(0.04< 162)	(0.040< 162)	(1.00< 139)	-28.06

OPTIMIZATION OF L5 AND C4 WITH LOAD #4. TABLE C-13

```
00010 IND AA SE -3077 L5
00020 CAP BB PA -25   C4
00030 IND CC SE 414 1130 51
00040 IND DD PA 35.5
00050 IND EE SE 179.5
00060 CAX AA EE
00070 PRI AA S3
00080 END
00090 41.81 62.21
00100 48.51 53.61
00110 51
00120 END
00130 50 0 45.9 64
00140 50 0 45.9 -64
00150 50 0 100 82
00160 50 0 100 -82
00170 50 0 175 0
00180 END
00190 .1
00200 0 0 1 -30 LT
00210 0 0 1 -17.5
00220 0 0 10 0
```

DATA FILE

CIRCUIT OPTIMIZATION WITH 2 VARIABLES

INITIAL CIRCUIT ANALYSIS:
POLAR S-PARAMETERS WITH COMPLEX LOAD #4

F MHZ	SOURCE IMP. (R,JX) OHMS	LOAD IMP. (R,JX) OHMS
41.810	(50.00, 0.0)	(45.90, 64.00)
62.210	(50.00, 0.0)	(45.90, -64.00)
48.510	(50.00, 0.0)	(100.00, 82.00)
53.610	(50.00, 0.0)	(100.00, -82.00)
51.000	(50.00, 0.0)	(175.00, 0.0)

F MHZ	S11 (MAGN<ANGL)	S21 (MAGN<ANGL)	S12 (MAGN<ANGL)	S22 (MAGN<ANGL)	S21 DB
41.8	(1.00< 4)	(0.02< -67)	(0.023< -67)	(1.00< 41)	-32.80
62.2	(1.00< 5)	(0.04< 162)	(0.039< 162)	(1.00< 139)	-28.07
48.5	(1.00< -2)	(0.09< -58)	(0.086< -58)	(1.00< 65)	-21.27
53.6	(0.99< 11)	(0.12<-163)	(0.123<-163)	(0.99<-159)	-18.18
51.0	(0.48< 86)	(0.81<-135)	(0.807<-135)	(0.52< 170)	-1.86

OPTIMIZATION BEGINS WITH FOLLOWING VARIABLES AND GRADIENTS

VARIABLES:		GRADIENTS:	
(1):	3077.001	(1):	299.464
(2):	25.000	(2):	2277.981
ERROR FUNCTION =	10.597		
----****----			
(1):	3074.921	(1):	-2.979
(2):	24.873	(2):	-30.738
ERROR FUNCTION =	5.874		
----****----			
(1):	3073.593 NEW L5	(1):	1.454
(2):	24.878 NEW C4	(2):	3.929
ERROR FUNCTION =	5.870 (WANTED .1)		
----****----			

FRACTIONAL TERMINATION WITH ABOVE VALUES. FINAL ANALYSIS FOLLOWS

41.8	(1.00< 4)	(0.02< -67)	(0.023< -67)	(1.00< 41)	-32.88
62.2	(1.00< 6)	(0.04< 162)	(0.040< 162)	(1.00< 139)	-27.93
48.5	(1.00< -1)	(0.08< -58)	(0.082< -58)	(1.00< 65)	-21.68
53.6	(0.99< 11)	(0.13<-163)	(0.130<-163)	(0.99<-159)	-17.74
51.0	(0.18< 165)	(0.91<-111)	(0.905<-111)	(0.30< 144)	-0.87

TABLE C-14 ANALYSIS WITH LOAD #5.

Data File

```
00010 IND AA SE 3077
00020 CAP BB PA 25
00030 IND CC SE 414 1130 51
00040 IND DD PA 35.5
00050 IND EE SE 179.5
00060 CAX AA EE
00070 PRI AA S3
00080 END
00090 41.81 43.92 46.15 48.51 50.62
00100 50.81 51 51.19 51.38 53.61
00110 56.35 59.22 62.21
00120 END
00130 50 0 15.2 12.2
00140 50 0 16 16.6
00150 50 0 17.1 21
00160 50 0 18.5 25.8
00170 50 0 20.5 30.9
00180 50 0 23 36.4
00190 50 0 26.4 42.5
00200 50 0 31 49
00210 50 0 37.2 56.2
00220 50 0 45.9 63.9
00230 50 0 58.1 71.6
00240 50 0 75.6 78
00250 50 0 99.8 80.2
00260 END
```

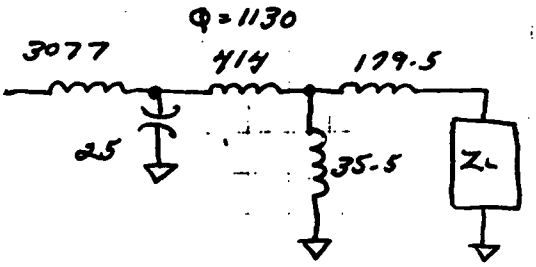

CIRCUIT

POLAR S-PARAMETERS WITH COMPLEX LOAD #5

F MHZ	SOURCE IMP. (R,JX) OHMS	LOAD IMP. (R,JX) OHMS
41.810	(50.00, 0.0)	(15.20, 12.20)
43.920	(50.00, 0.0)	(16.00, 16.60)
46.150	(50.00, 0.0)	(17.10, 21.00)
48.510	(50.00, 0.0)	(18.50, 25.80)
50.620	(50.00, 0.0)	(20.50, 30.90)
50.810	(50.00, 0.0)	(23.00, 36.40)
51.000	(50.00, 0.0)	(26.40, 42.50)
51.190	(50.00, 0.0)	(31.00, 49.00)
51.380	(50.00, 0.0)	(37.20, 56.20)
53.610	(50.00, 0.0)	(45.90, 63.90)
56.350	(50.00, 0.0)	(58.10, 71.60)
59.220	(50.00, 0.0)	(75.60, 78.00)
62.210	(50.00, 0.0)	(99.80, 80.20)

F MHZ	S11 (MAGN<ANGL)	S21 (MAGN<ANGL)	S12 (MAGN<ANGL)	S22 (MAGN<ANGL)	S21 DB
41.8	(1.00< 4)	(0.02< -75)	(0.024< -75)	(1.00< 24)	-32.41
43.9	(1.00< 3)	(0.03< -76)	(0.028< -76)	(1.00< 23)	-30.97
46.1	(1.00< 1)	(0.04< -78)	(0.038< -78)	(1.00< 22)	-28.41
48.5	(1.00< -1)	(0.07< -80)	(0.068< -80)	(1.00< 21)	-23.32
50.6	(0.90< -39)	(0.36<-105)	(0.362<-105)	(0.92< 13)	-8.84
50.8	(0.74< -72)	(0.55<-124)	(0.554<-124)	(0.81< 12)	-5.13
51.0	(0.47< 176)	(0.73<-166)	(0.732<-166)	(0.64< 28)	-2.71
51.2	(0.77< 77)	(0.54< 154)	(0.537< 154)	(0.82< 42)	-5.40
51.4	(0.91< 47)	(0.36< 137)	(0.358< 137)	(0.93< 43)	-8.93
53.6	(1.00< 12)	(0.06< 116)	(0.063< 116)	(1.00< 39)	-24.07
56.4	(1.00< 8)	(0.03< 116)	(0.031< 116)	(1.00< 44)	-30.29
59.2	(1.00< 6)	(0.02< 119)	(0.020< 119)	(1.00< 52)	-33.94
62.2	(1.00< 5)	(0.02< 124)	(0.015< 124)	(1.00< 63)	-36.46

OPTIMIZATION OF L5 & C4 WITH LOAD # 5.

TABLE C-15

```
00010 IND AA SE -3077    % L5
00020 CAP BB PA -25      % C4
00030 IND CC SE 414 1130 51
00040 IND DD PA 35.5
00050 IND EE SE 179.5
00060 CAX AA EE
00070 PRI AA S3
00080 END
00090 41.81 62.21
00100 48.51 53.61
00110 51
00120 END
00130 50 0 15.2 12.2
00140 50 0 99.8 80.2
00150 50 0 18.5 25.8
00160 50 0 58.1 71.6
00170 50 0 26.4 42.5
00180 END
00190 .1
00200 0 0 1 -30 LT
00210 0 0 1 -17.5
00220 0 0 10 0
00230 END

                CIRCUIT OPTIMIZATION WITH  2 VARIABLES

 INITIAL CIRCUIT ANALYSIS:
           POLAR S-PARAMETERS WITH COMPLEX LOAD # 5

   F MHZ    SOURCE IMP. (R,JX) OHMS     LOAD IMP. (R,JX) OHMS
    41.810  (     50.00,       0.0 )     (     15.20,      12.20)
    62.210  (     50.00,       0.0 )     (     99.80,      80.20)
    48.510  (     50.00,       0.0 )     (     18.50,      25.80)
    53.610  (     50.00,       0.0 )     (     58.10,      71.60)
    51.000  (     50.00,       0.0 )     (     26.40,      42.50)

   F          S11           S21           S12           S22          S21
   MHZ   (MAGN<ANGL)  ( MAGN<ANGL)  ( MAGN<ANGL)  (MAGN<ANGL)    DB

   41.8 (1.00<   4) ( 0.02< -75) (0.024< -75) (1.00<  24) -32.41
   62.2 (1.00<   5) ( 0.02< 124) (0.015< 124) (1.00<  63) -36.46
   48.5 (1.00<  -1) ( 0.07< -80) (0.068< -80) (1.00<  21) -23.32
   53.6 (1.00<  12) ( 0.06< 119) (0.065< 119) (1.00<  46) -23.76
   51.0 (0.47< 176) ( 0.73<-166) (0.732<-166) (0.64<  28)  -2.71
OPTIMIZATION BEGINS WITH FOLLOWING VARIABLES AND GRADIENTS

     VARIABLES:                    GRADIENTS:

 ( 1):    3077.001              ( 1):    66.286
 ( 2):      25.000              ( 2):   632.529
   ERROR FUNCTION =     29.296
        ----****----
 ( 1):    3076.833  New L5      ( 1):   -12.820
 ( 2):      24.987  New C4      ( 2):     4.736
   ERROR FUNCTION =     29.165
        ----****----            (WANTED 0.1)
FRACTIONAL TERMINATION WITH ABOVE VALUES. FINAL ANALYSIS FOLLOWS

   41.8 (1.00<   4) ( 0.02< -75) (0.024< -75) (1.00<  24) -32.42
   62.2 (1.00<   5) ( 0.02< 124) (0.015< 124) (1.00<  63) -36.44
   48.5 (1.00<  -1) ( 0.07< -80) (0.068< -80) (1.00<  21) -23.36
   53.6 (1.00<  12) ( 0.07< 119) (0.065< 119) (1.00<  46) -23.72
   51.0 (0.47<-172) ( 0.73<-163) (0.733<-163) (0.63<  26)  -2.70
```

TABLE C-16

USE OF COMPACT "SWEEP" OPTION

L5 & C4 ARE VARIED SIMULTANEOUSLY.

SHOWS PATH OF ERROR FUNCTION.

VERIFIES OPTIMIZATION PREVIOUSLY PERFORMED.

(Load 5)

ERROR FUNCTION VALUES WITH TWO COMPONENTS VARYING

VAR.1	VAR.2						
	250.00	62.50	31.25	25.00	20.00	10.00	2.50
*******	*******	*******	6615.76	4290.91	3815.64	7264.62	8402.82
7692.50	*******	6796.64	3773.79	1808.92	2359.43	4591.71	5445.69
3846.25	9314.82	5295.97	2508.26	431.80	1941.13	3575.16	4273.63
3077.00	8741.80	4842.49	2108.89	29.30	1843.21	3296.23	3943.00
2461.60	8186.13	4402.30	1707.38	316.05	1764.43	3041.19	3635.80
1230.80	6572.00	3111.97	392.16	947.90	1693.56	2399.31	2834.60
307.70	3964.27	1093.87	1117.94	1299.90	1440.44	1706.22	1888.64

TABLE C-17

ANALYSIS OF "OPTIMIZED" CIRCUIT, LOAD # 5.

```
00010 IND AA SE 3076.833  L5
00020 CAP BB PA 24.987    C4
00030 IND CC SE 414 1130 51
00040 IND DD PA 35.5
00050 IND EE SE 179.5
00060 CAX AA EE
00070 PRI AA S3
00080 END
00090 41.81 43.92 46.15 48.51 50.62
00100 50.81 51 51.19 51.38 53.61
00110 56.35 59.22 62.21
00120 END
00130 50 0 15.2 12.2
00140 50 0 16 16.6
00150 50 0 17.1 21
00160 50 0 18.5 25.8
00170 50 0 20.5 30.9
00180 50 0 23 36.4
00190 50 0 26.4 42.5
00200 50 0 31 49
00210 50 0 37.2 56.2
00220 50 0 45.9 63.9
00230 50 0 58.1 71.6
00240 50 0 75.6 78
00250 50 0 99.8 80.2
00260 END
```

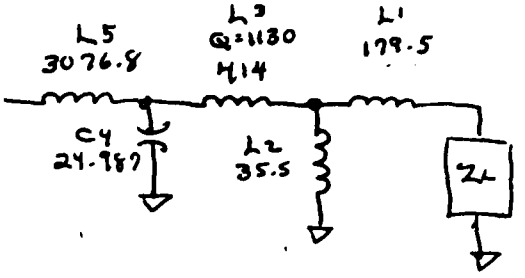

LITTLE IMPROVEMENT

$Z_L = 18 - j3$, VSWR = 2.8:1 AT MIDBAND.

POLAR S-PARAMETERS WITH COMPLEX LOAD AND SOURCE

F MHZ	SOURCE IMP. (R,JX) OHMS	LOAD IMP. (R,JX) OHMS
41.810	(50.00, 0.0)	(15.20, 12.20)
43.920	(50.00, 0.0)	(16.00, 16.60)
46.150	(50.00, 0.0)	(17.10, 21.00)
48.510	(50.00, 0.0)	(18.50, 25.80)
50.620	(50.00, 0.0)	(20.50, 30.90)
50.810	(50.00, 0.0)	(23.00, 36.40)
51.000	(50.00, 0.0)	(26.40, 42.50)
51.190	(50.00, 0.0)	(31.00, 49.00)
51.380	(50.00, 0.0)	(37.20, 56.20)
53.610	(50.00, 0.0)	(45.90, 63.90)
56.350	(50.00, 0.0)	(58.10, 71.60)
59.220	(50.00, 0.0)	(75.60, 78.00)
62.210	(50.00, 0.0)	(99.80, 80.20)

F MHZ	S11 (MAGN<ANGL)	S21 (MAGN<ANGL)	S12 (MAGN<ANGL)	S22 (MAGN<ANGL)	S21 DB
41.8	(1.00< 4)	(0.02< -75)	(0.024< -75)	(1.00< 24)	-32.42
43.9	(1.00< 3)	(0.03< -76)	(0.028< -76)	(1.00< 23)	-30.99
46.1	(1.00< 1)	(0.04< -78)	(0.038< -78)	(1.00< 22)	-28.43
48.5	(1.00< -1)	(0.07< -80)	(0.068< -80)	(1.00< 21)	-23.37
50.6	(0.90< -37)	(0.35<-104)	(0.353<-104)	(0.93< 14)	-9.06
50.8	(0.76< -69)	(0.54<-122)	(0.538<-122)	(0.82< 12)	-5.38
51.0	(0.47<-172)	(0.73<-163)	(0.733<-163)	(0.63< 26)	-2.70
51.2	(0.75< 81)	(0.55< 155)	(0.553< 155)	(0.81< 42)	-5.14
51.4	(0.90< 48)	(0.37< 138)	(0.367< 138)	(0.92< 43)	-8.70
53.6	(1.00< 12)	(0.06< 116)	(0.063< 116)	(1.00< 39)	-24.02
56.4	(1.00< 8)	(0.03< 116)	(0.031< 116)	(1.00< 44)	-30.26
59.2	(1.00< 6)	(0.02< 119)	(0.020< 119)	(1.00< 52)	-33.92
62.2	(1.00< 5)	(0.02< 124)	(0.015< 124)	(1.00< 63)	-36.44

TABLE C-18 ANALYSIS WITH LOAD #6.

```
00010 IND AA SE 3077
00020 CAP BB PA 25
00030 IND CC SE 414 1130 51
00040 IND DD PA 35.5
00050 IND EE SE 179.5
00060 CAX AA EE
00070 PRI AA S3
00080 END
00090 41.81 43.92 46.15 48.51 50.62
00100 50.81 51 51.19 51.38 53.61
00110 56.35 59.22 62.21
00120 END
00130 50 0 99.8 -80.2
00140 50 0 75.6 -78
00150 50 0 58.2 -71.6
00160 50 0 45.9 -63.9
00170 50 0 37.2 -56.2
00180 50 0 31 -49
00190 50 0 26.4 -42.5
00200 50 0 23 -36.4
00210 50 0 20.5 -30.9
00220 50 0 18.5 -25.8
00230 50 0 17.1 -21
00240 50 0 16 -16.5
00250 50 0 15.2 -12.2
00260 END
```

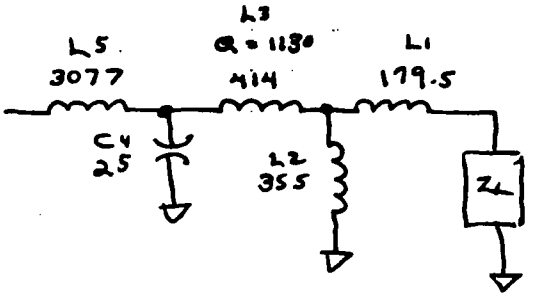

POLAR S-PARAMETERS WITH COMPLEX LOAD #6

F MHZ	SOURCE IMP. (R,JX) OHMS	LOAD IMP. (R,JX) OHMS
41.810	(50.00, 0.0)	(99.80, -80.20)
43.920	(50.00, 0.0)	(75.60, -78.00)
46.150	(50.00, 0.0)	(58.20, -71.60)
48.510	(50.00, 0.0)	(45.90, -63.90)
50.620	(50.00, 0.0)	(37.20, -56.20)
50.810	(50.00, 0.0)	(31.00, -49.00)
51.000	(50.00, 0.0)	(26.40, -42.50)
51.190	(50.00, 0.0)	(23.00, -36.40)
51.380	(50.00, 0.0)	(20.50, -30.90)
53.610	(50.00, 0.0)	(18.50, -25.80)
56.350	(50.00, 0.0)	(17.10, -21.00)
59.220	(50.00, 0.0)	(16.00, -16.50)
62.210	(50.00, 0.0)	(15.20, -12.20)

F MHZ	S11 (MAGN<ANGL)	S21 (MAGN<ANGL)	S12 (MAGN<ANGL)	S22 (MAGN<ANGL)	S21 DB
41.8	(1.00< 4)	(0.04< 14)	(0.043< 14)	(1.00<-154)	-27.34
43.9	(1.00< 3)	(0.06< 14)	(0.063< 14)	(1.00<-154)	-24.01
46.1	(0.99< 1)	(0.11< 6)	(0.105< 6)	(0.99<-168)	-19.55
48.5	(0.97< -2)	(0.23< -12)	(0.228< -12)	(0.97< 157)	-12.85
50.6	(0.64< -12)	(0.75< -76)	(0.752< -76)	(0.61< 42)	-2.48
50.8	(0.61< -12)	(0.78< -94)	(0.778< -94)	(0.57< 7)	-2.18
51.0	(0.52< -13)	(0.84<-112)	(0.836<-112)	(0.47< -25)	-1.56
51.2	(0.33< -3)	(0.92<-136)	(0.916<-136)	(0.26< -84)	-0.76
51.4	(0.40< 47)	(0.88<-169)	(0.881<-169)	(0.37< 142)	-1.10
53.6	(0.99< 12)	(0.13< 122)	(0.126< 122)	(0.99< 51)	-17.97
56.4	(1.00< 8)	(0.05< 113)	(0.048< 113)	(1.00< 37)	-26.35
59.2	(1.00< 6)	(0.03< 108)	(0.026< 108)	(1.00< 29)	-31.82
62.2	(1.00< 6)	(0.02< 105)	(0.016< 105)	(1.00< 24)	-36.03

OPTIMIZATION OF L5 & C4, WITH LOAD #6

TABLE C-19

```
LIST
00010 IND AA SE -3077 L5
00020 CAP BB PA -25  C4
00030 IND CC SE 414 1130 51
00040 IND DD PA 35.5
00050 IND EE SE 179.5
00060 CAX AA EE
00070 PRI AA S3
00080 END
00090 41.81 62.21
00100 48.51 53.61
00110 51
00120 END
00130 50 0 99.8 -80.2
00140 50 0 15.2 -12.2
00150 50 0 45.9 -63.9
00160 50 0 17.1 -21
00170 50 0 26.4 -42.5
00180 END
00190 .1
00200 0 0 1 -30 LT
00210 0 0 1 -17.5
00220 0 0 10 0
00230 END
```

CIRCUIT OPTIMIZATION WITH 2 VARIABLES

INITIAL CIRCUIT ANALYSIS:

POLAR S-PARAMETERS WITH COMPLEX LOAD AND SOURCE

F MHZ	SOURCE IMP. (R,JX) OHMS	LOAD IMP. (R,JX) OHMS
41.810	(50.00, 0.0)	(99.80, -80.20)
62.210	(50.00, 0.0)	(15.20, -12.20)
48.510	(50.00, 0.0)	(45.90, -63.90)
53.610	(50.00, 0.0)	(17.10, -21.00)
51.000	(50.00, 0.0)	(26.40, -42.50)

F MHZ	S11 (MAGN<ANGL)	S21 (MAGN<ANGL)	S12 (MAGN<ANGL)	S22 (MAGN<ANGL)	S21 DB
41.8	(1.00< 4)	(0.04< 14)	(0.043< 14)	(1.00<-154)	-27.34
62.2	(1.00< 6)	(0.02< 105)	(0.016< 105)	(1.00< 24)	-36.03
48.5	(0.97< -2)	(0.23< -12)	(0.228< -12)	(0.97< 157)	-12.85
53.6	(0.99< 12)	(0.11< 118)	(0.112< 118)	(0.99< 43)	-19.05
51.0	(0.52< -13)	(0.84<-112)	(0.836<-112)	(0.47< -25)	-1.56

OPTIMIZATION BEGINS WITH FOLLOWING VARIABLES AND GRADIENTS

VARIABLES:		GRADIENTS:	
(1):	3077.001	(1):	-55.143
(2):	25.000	(2):	-492.936
ERROR FUNCTION =	11.069		
----****----			
(1):	3078.430	(1):	0.620
(2):	25.104	(2):	-0.586
ERROR FUNCTION =	10.061		
----****----			
(1):	3074.261 NEW L5	(1):	-0.229
(2):	25.108 NEW C4	(2):	-1.867
ERROR FUNCTION =	10.059		
----****----			

RADIENT TERMINATION WITH ABOVE VALUES. FINAL ANALYSIS FOLLOWS

41.8	(1.00< 4)	(0.04< 14)	(0.043< 14)	(1.00<-154)	-27.26
62.2	(1.00< 6)	(0.02< 105)	(0.016< 105)	(1.00< 24)	-36.14
48.5	(0.97< -2)	(0.24< -13)	(0.238< -13)	(0.97< 156)	-12.49
53.6	(0.99< 12)	(0.11< 118)	(0.107< 118)	(0.99< 42)	-19.44
51.0	(0.45< -5)	(0.87<-122)	(0.873<-122)	(0.39< -56)	-1.18

TABLE C-20

- USE OF COMPACT "SWEEP" OPTION
- L5 & C4 ARE VARIED SIMULTANEOUSLY
- SHOWS PATH OF ERROR FUNCTION.
- VERIFIES PREVIOUS OPTIMIZATION.
  (Load 6)

ERROR FUNCTION VALUES WITH TWO COMPONENTS VARYING

VAR.1	VAR.2						
	250.00	62.50	31.25	25.00	20.00	10.00	2.50
*******	*******	7518.02	4437.41	2570.13	2347.13	5024.96	5967.15
7692.50	8338.49	4606.12	2196.04	776.23	1223.07	2854.04	3526.46
3846.25	6719.60	3388.85	1274.55	53.47	915.81	2067.00	2598.33
3077.00	6234.45	3028.91	1002.57	11.07	846.63	1856.72	2342.53
2461.60	5766.82	2683.93	744.07	70.44	793.83	1667.13	2107.84
1230.80	4427.25	1713.26	96.34	324.76	785.38	1204.25	1511.96
307.70	2349.50	409.61	422.19	513.01	589.04	745.94	860.64

****

TABLE C-21
ANALYSIS OF "OPTIMIZED" CIRCUIT, LOAD #6.

```
00010 IND AA SE 3074.261   L5
00020 CAP BB PA 25.108     C4
00030 IND CC SE 414 1130 51
00040 IND DD PA 35.5
00050 IND EE SE 179.5
00060 CAX AA EE
00070 PRI AA S3
00080 END
00090 41.81 43.92 46.15 48.51 50.62
00100 50.81 51 51.19 51.38 53.61
00110 56.35 59.22 62.21
00120 END
00130 50 0 99.8 -80.2
00140 50 0 75.6 -78
00150 50 0 58.2 -71.6
00160 50 0 45.9 -63.9
00170 50 0 37.2 -56.2
00180 50 0 31 -49
00190 50 0 26.4 -42.5
00200 50 0 23 -36.4
00210 50 0 20.5 -30.9
00220 50 0 18.5 -25.8
00230 50 0 17.1 -21
00240 50 0 16 -16.5
00250 50 0 15.2 -12.2
00260 END
```

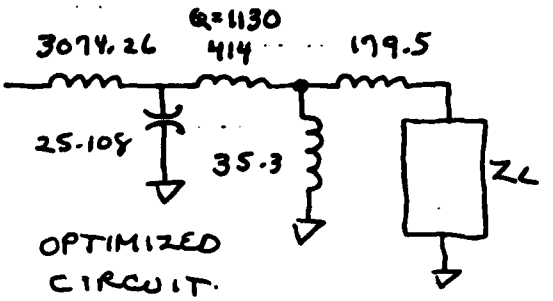

POLAR S-PARAMETERS WITH COMPLEX LOAD #6.

F MHZ	SOURCE IMP. (R,JX) OHMS	LOAD IMP. (R,JX) OHMS
41.810	(50.00, 0.0)	(99.80, -80.20)
43.920	(50.00, 0.0)	(75.60, -78.00)
46.150	(50.00, 0.0)	(58.20, -71.60)
48.510	(50.00, 0.0)	(45.90, -63.90)
50.620	(50.00, 0.0)	(37.20, -56.20)
50.810	(50.00, 0.0)	(31.00, -49.00)
51.000	(50.00, 0.0)	(26.40, -42.50)
51.190	(50.00, 0.0)	(23.00, -36.40)
51.380	(50.00, 0.0)	(20.50, -30.90)
53.610	(50.00, 0.0)	(18.50, -25.80)
56.350	(50.00, 0.0)	(17.10, -21.00)
59.220	(50.00, 0.0)	(16.00, -16.50)
62.210	(50.00, 0.0)	(15.20, -12.20)

F MHZ	S11 (MAGN<ANGL)	S21 (MAGN<ANGL)	S12 (MAGN<ANGL)	S22 (MAGN<ANGL)	S21 DB
41.8	(1.00< 4)	(0.04< 14)	(0.043< 14)	(1.00<-154)	-27.26
43.9	(1.00< 3)	(0.06< 13)	(0.064< 13)	(1.00<-155)	-23.90
46.1	(0.99< 1)	(0.11< 6)	(0.108< 6)	(0.99<-168)	-19.36
48.5	(0.97< -2)	(0.24< -13)	(0.238< -13)	(0.97< 156)	-12.49
50.6	(0.58< -9)	(0.80< -84)	(0.797< -84)	(0.54< 24)	-1.97
50.8	(0.55< -8)	(0.82<-102)	(0.820<-102)	(0.50< -13)	-1.72
51.0	(0.45< -5)	(0.87<-122)	(0.873<-122)	(0.39< -56)	-1.18
51.2	(0.35< 21)	(0.91<-149)	(0.910<-149)	(0.28<-146)	-0.82
51.4	(0.57< 45)	(0.79< 178)	(0.791< 178)	(0.55< 123)	-2.04
53.6	(0.99< 12)	(0.12< 122)	(0.121< 122)	(0.99< 51)	-18.36
56.4	(1.00< 8)	(0.05< 113)	(0.047< 113)	(1.00< 37)	-26.55
59.2	(1.00< 6)	(0.03< 108)	(0.025< 108)	(1.00< 29)	-31.96
62.2	(1.00< 6)	(0.02< 105)	(0.016< 105)	(1.00< 24)	-36.14

****

APPENDIX D ANTENNA STUDY

D.1 ANTENNA DESCRIPTION

Antenna Group OE-254/GRC is a VHF-FM antenna system designed for broadband operations without field adjustment from 30 to 88 MHz. It is designed for use with:

AN/VRC-12
AN/VRC-43→49
AN/VRC-53
AN/VRC-64
AN/GRC-125
AN/GRC-160
AN/PRC-25
AN/PRC-77

Its primary function is to extend the range of coverage of portable and mobile radios beyond that available from low elevation whip antennas.

The Principal Components are:

Antenna	A5-3166/GRC
Mast	AB-1244/GRC
Cable Assy	GC-1889 B/U (80 feet)

Comments on the Antenna are:

- The data provided shows the impedance as measured at the input to a 50 foot length of RG 213/U coaxial cable which is connected to the erected antenna. Fielded antennas will use an 80 foot length with an equivalent in air of 116 feet, because of the dielectric constant of 2.06. Thus the fielded cable is 3.5 wavelengths at 30 MHz, and 10.4 wavelengths long at 88 MHz.
- Figure D-1 shows the electrical performance parameters, and a mechanical sketch of the erected antenna.
- Figure D-2 is a Smith Chart compilation of points of the impedance measured at the input of a 50 foot cable.

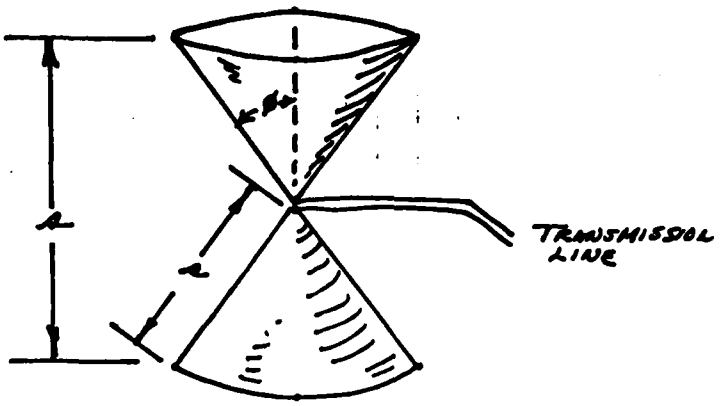

CHARACTERISTICS

- 30 – 88 MHz
- 50 OHMS NOMINAL
- 3.5:1 VSWR 30-35 MHz,
- 3.0:1 VSWR 35-88 MHz
- OMNIDIRECTIONAL
- 350 WATTS CONTINUOUS DUTY

AS 3166/GRC IS A BROADBAND, OMNIDIRECTIONAL BICONICAL ANTENNA, CONSISTING OF 3 UPWARD & 3 DOWNWARD EXTENDED RADIALS WHICH SIMULATE THE TWO CONES.

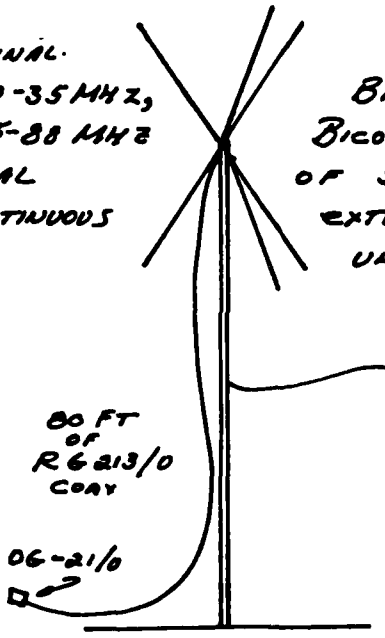

FIGURE D-1
ANTENNA CHARACTERISTIC

TITLE FIGURE D-2 AS 3166/GRC ANTENNA IMPEDANCE DATE

IMPEDANCE COORDINATES—50-OHM CHARACTERISTIC IMPEDANCE

CORADCOM DATA, MEASURED WITH 50 FT CABLE.

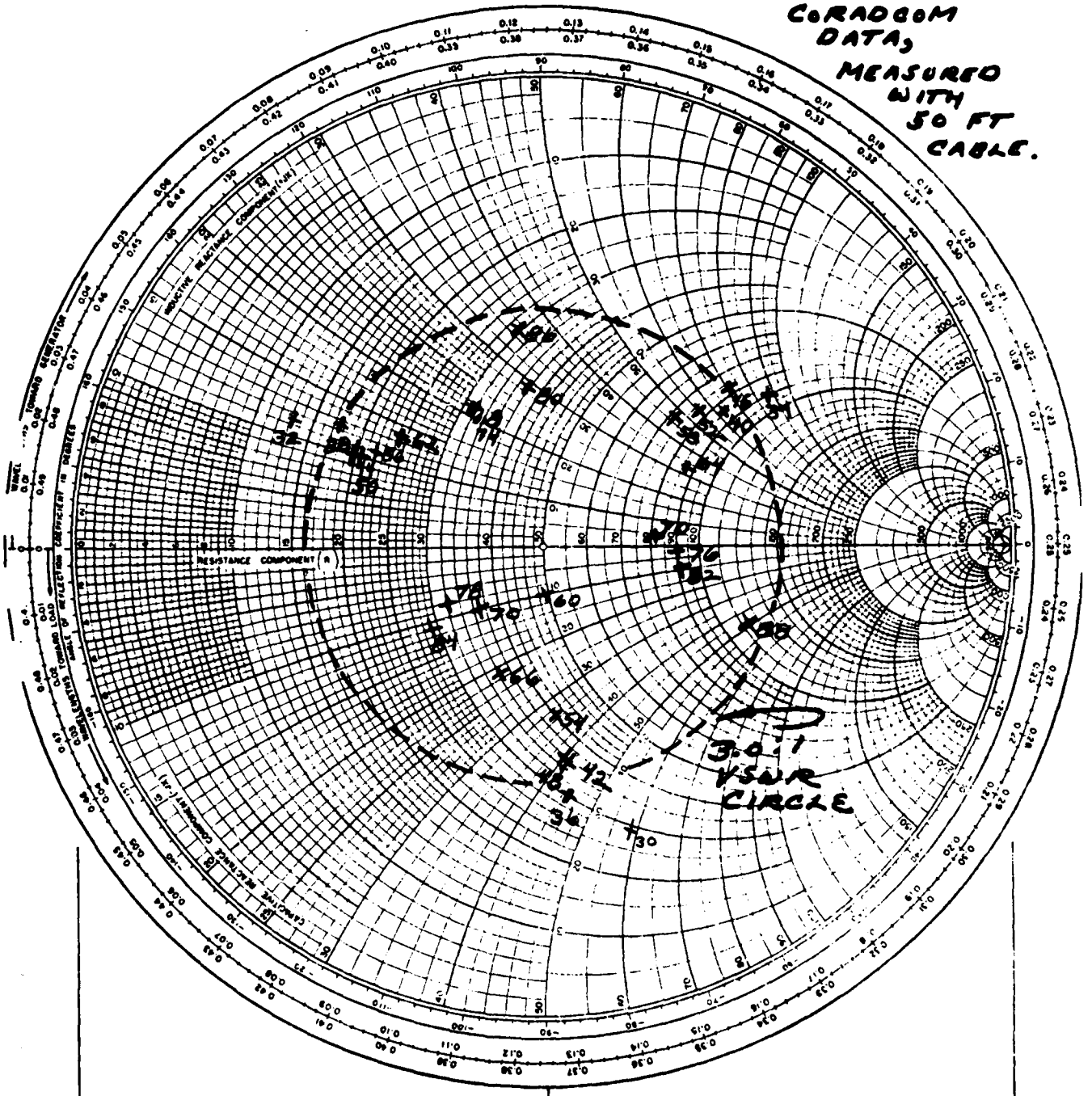

RADIALLY SCALED PARAMETERS

TOWARD GENERATOR → ← TOWARD LOAD

CENTER

D-3

Electronics - VOL 17, NO 1, PP-130-133, 518-525, JAN 1944

GENERAL RADIO COMPANY
WEST CONCORD, MASS.

FORM 5301-7502
Printed in USA

- Table D-1 is a compliation of the above data All of the above except Figure D1 were supplied by CORADCOM.

- The data from Table D-1 is plotted in Figures D-3 and D-4. These figures show a definite periodicity approximately every 6 MHz. This periodicity is not entirely due to the antenna itself, but is enhanced by the cable. Figure D-3 shows that the average resistance is indeed close to 50 ohms. Figure D-4 shows that the reactive component changes rapidly from inductive to capacitive, indicating rapid revolution around the Smith Chart.

A 3.5:1 VSWR will have a severe effect on the performance of a high Q tuned circuit.

Freq. MHz	F (ohms)	θ degrees	R (ohms)	X (ohms)	Unloaded Q
30	65	-63	29.5	57.9	1.95
32	17.5	+40	13.4	11.24	.84
34	125	+44	89.91	86.83	.97
36	54	-56	30.2	-44.17	4.48
38	21.5	+35	17.6	12.33	.70
40	105	+37	83.86	63.19	.75
42	54	-49	35.42	-40.75	1.15
44	20	+32	16.96	10.59	.62
46	104	+43	76.06	70.93	.93
48	54	.50	34.71	-41.37	1.19
50	22.5	+28	19.87	10.56	.53
52	92	+36	77.43	54.08	.70
54	52	-40	39.83	33.42	.84
56	25	+22	23.18	9.365	.40
58	86	+33	72.02	46.84	.65
60	50	-41	49.08	-9.54	.194
62	28	+29	24.49	13.57	.55
64	92	+20	86.45	31.46	.36
66	42	-30	36.37	-21	.58
68	37	+34	30.67	20.69	.67
70	80	+2	79.45	2.79	.035
72	39	-16	37.49	40.79	.29
74	39	+34	32.33	21.81	.67
76	90	-1	90	-1.57	.02
78	33	-15	31.88	-8.54	.26
80	43	+17	37.54	28.29	.75
82	41	-5	90.65	-7.93	.09
84	30	-21	28	-10.75	.39
86	45	+50	28.92	34.47	1.19
88	120	-19	113.5	-39.1	.344

TABLE D-1 AN 3166/GRC Antenna Impedance

FIGURE D-3

ANTENNA GROUP OE-254/GRC

R + jX AT INPUT TO 50 FT CABLE.

RESISTANCE (VS) FREQUENCY

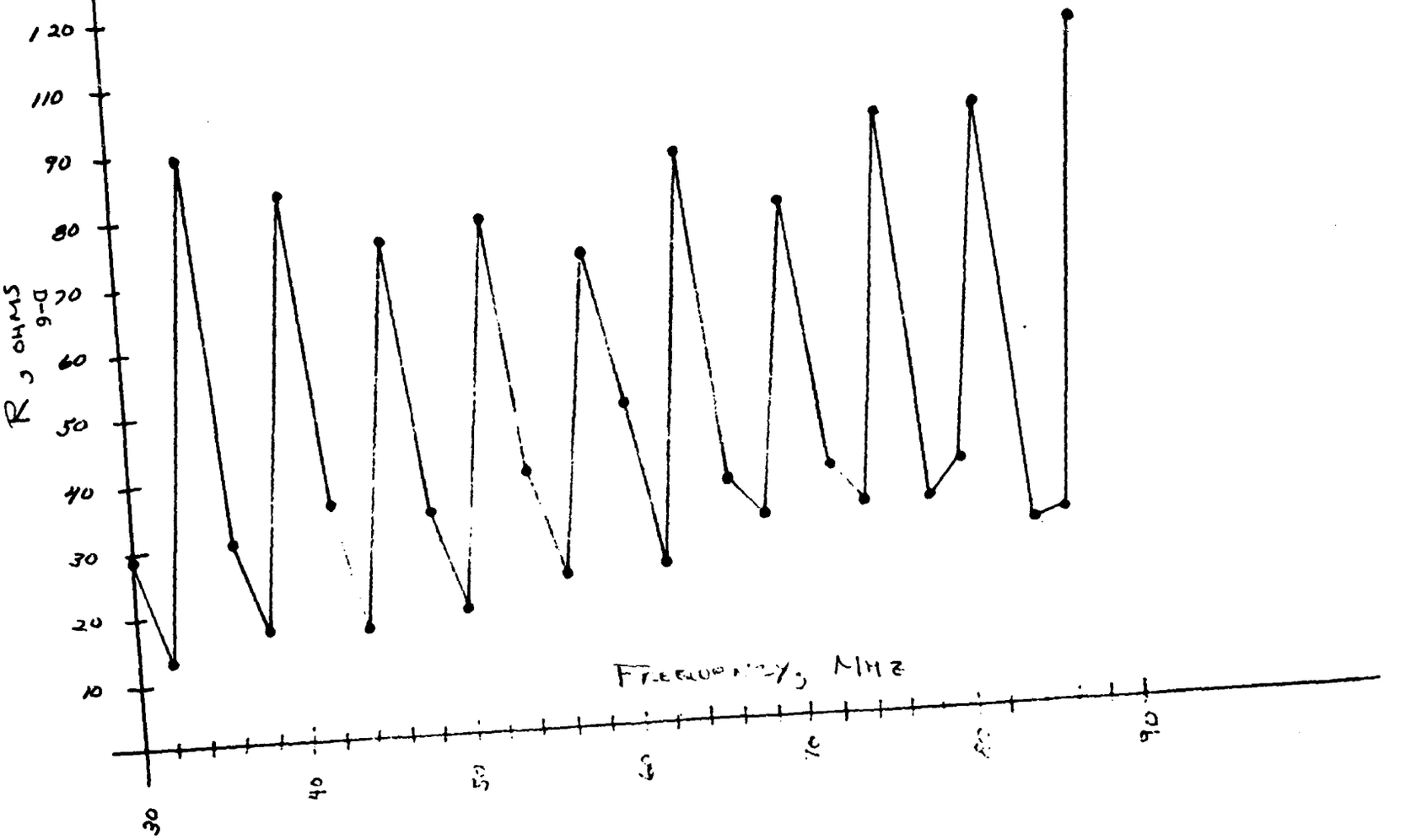

FIGURE D-4

ANTENNA GROUP OE-254/GRC

REACTANCE (VS) FREQUENCY

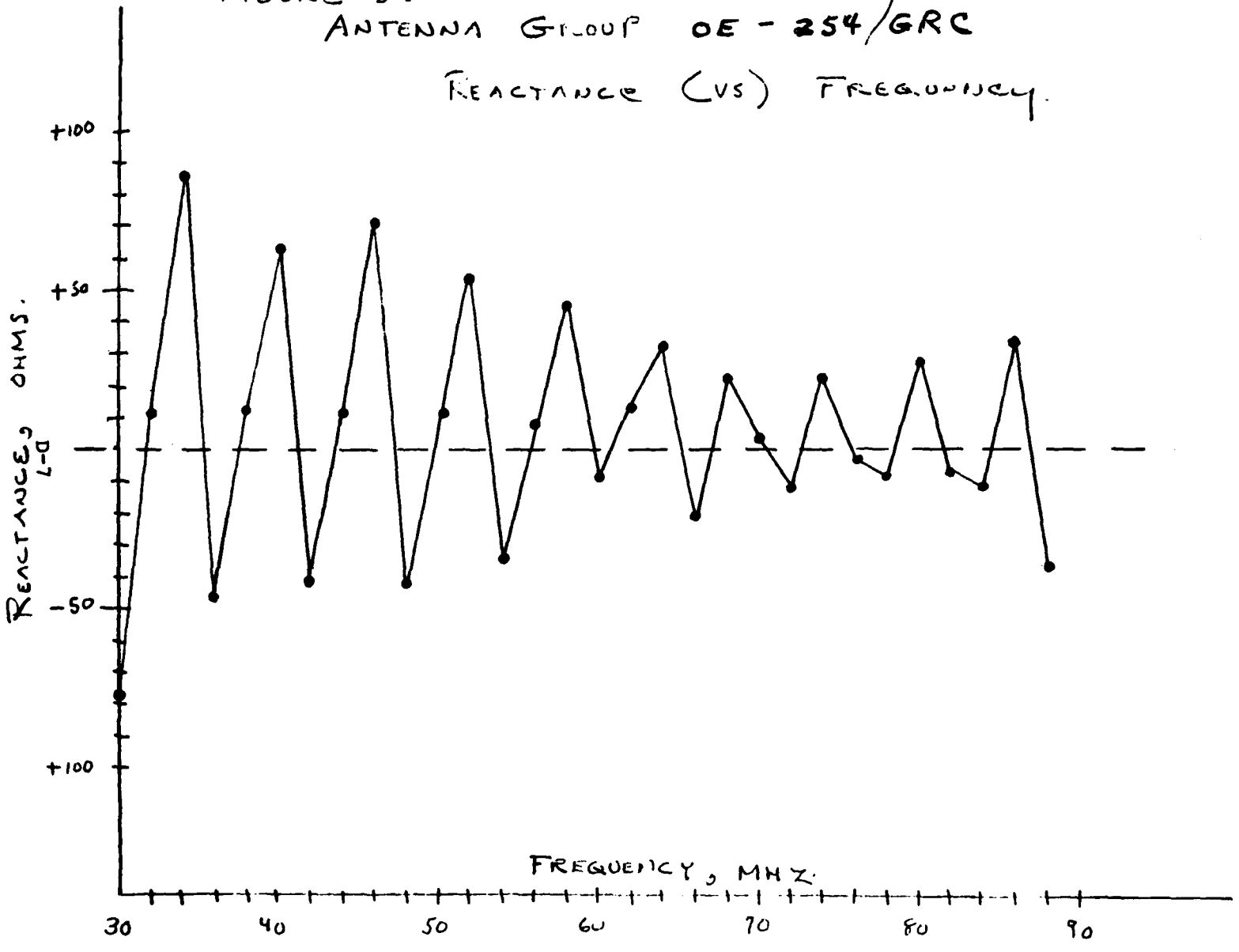

D.2 ANTENNA IMPACT ON SYSTEM DESIGN

- The first quarterly report described a potentially serious degradation of performance caused by load (antenna + cable) VSWR's of about 3.5:1. This problem was recognized in the proposal, which described the use of compensating networks to maintain the proper impedance level at the filter terminals. At that time, the antenna characteristics were unknown, it had been merely described as a broadband antenna.
- The description of the antenna characteristics in the previous section has raised several important issues which are listed below:
    - Need to include VSWR measuring circuits
    - If so, what tuning philosophy is best?
- The TD1288 system is manually tuned by the operator whenever necessary. This automatically corrects for the above antenna problem by minimizing the reflected RF power in each of the 5 channels. In a later analysis, it is shown that the complex nature of the antenna itself, and the multiplying effect of the cable, produce severe impedance changes at the cable input for relatively small changes in the cable length.

- Knowledge of the actual channel to channel isolation of the TD1288, when operated into the AS-3166/GRC antenna would be desirable.

D.3 ANALYSIS OF ANTENNA PARAMETER VARIATION

Figure D-6, shows that changes of ±10% in the antenna impedance do not cause severe variations in the impedance measured at the input of the cable. These input variations are generally within ±10% of the original value. The critical parameter regarding the variation of the input impedance of the cable is Bl, the phase angle of lag, or the cable delay, in degrees.

$$Bl = \frac{2\pi l\sqrt{k}}{\lambda\,(air)}$$

The physical length, and the square root of the dielectric constant are the only two variables involved. Dimensional tolerance variations in either of these parameters has a severe effect on the cable input impedance, and, therefore, on the performance of the single antenna FHMUX. This is vividly shown in Figure D-7, which plots impedance variations caused by a ± 2% change in the physical length of the cable. Thus, the electrical length of the cable is critical to the operation of the single antenna FHMUX.

Some factors which affect the electrical length are listed below:

- Temperature coefficient. As the temperature rises, the electrical length decreases and there may be a hysterisis effect when the temperature falls.

FIGURE D-6.

TITLE VARIATION IN INPUT IMPEDANCE FOR +/- 10% DATE 1/22/81
VARIATION IN LOAD IMPEDANCE

IMPEDANCE COORDINATES—50-OHM CHARACTERISTIC IMPEDANCE

$Z_0 = 50\Omega$
$L = 80'$
$K = 2.06$
$F = 52\,MHz$

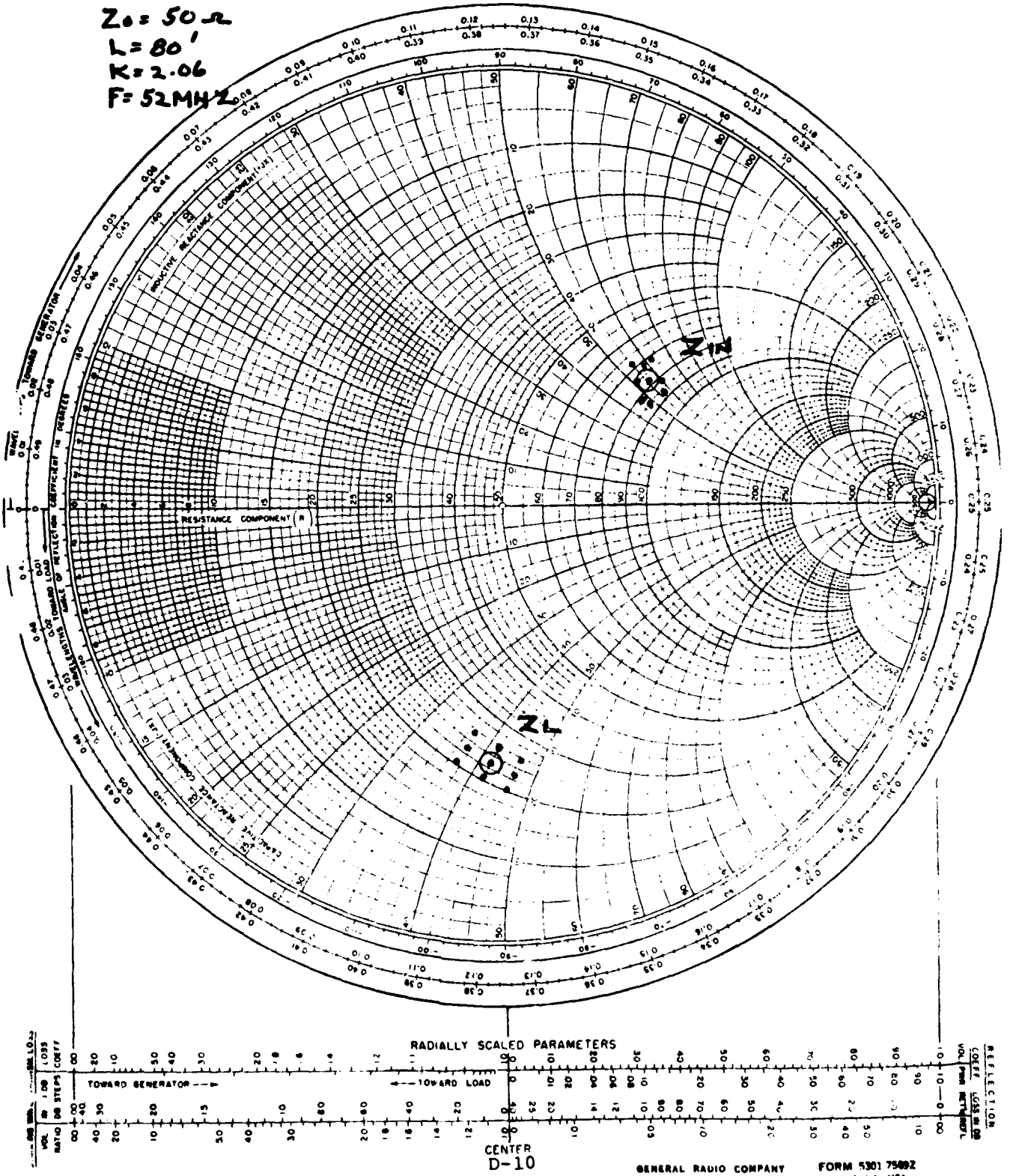

D-10

Electronics - VOL 17, NO 1, PP 130-133, 318 325, JAN 1944

GENERAL RADIO COMPANY
WEST CONCORD MASS.

FORM 5301 7508Z
Printed in USA

TITLE VARIATION IN INPUT IMPEDANCE AS LENGTH IS VARIED FROM 80-2% TO 80+2%.

DATE 1/22/81

IMPEDANCE COORDINATES—50-OHM CHARACTERISTIC IMPEDANCE

Z0 = 50Ω
K = 2.06
RL = 23Ω
jXL = -42
F = 52MHZ

FIGURE
D-7

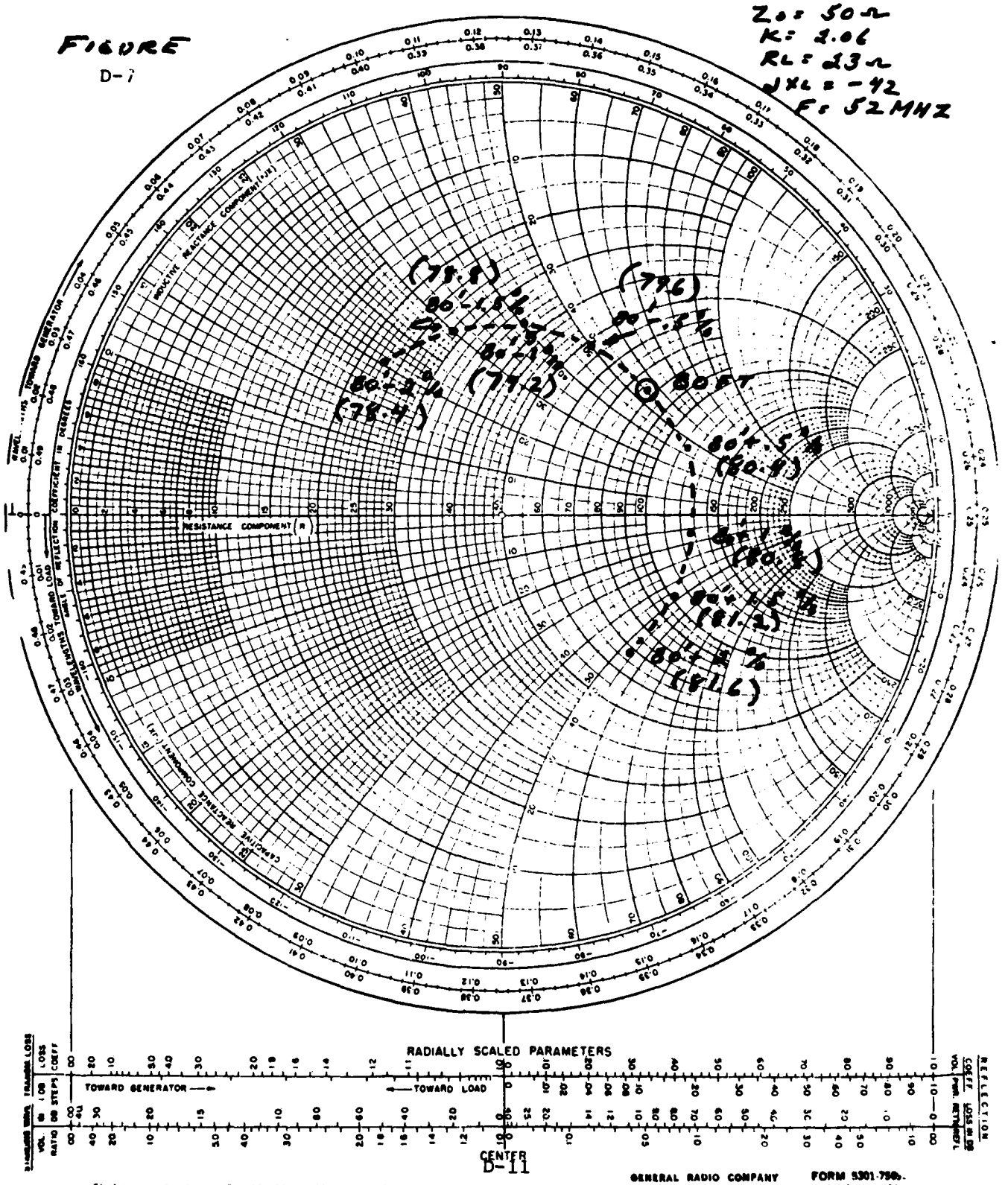

D-11

Electronics - VOL 17, NO 1, PP 130-133, 318-325, JAN 1944

GENERAL RADIO COMPANY
WEST CONCORD, MASS.

FORM 5301-750b
Printed in USA

RG 223/U (solid polyethylene) will change by 3600 parts per million in length as temperature is varied from 50 to 90 degrees, farenheit. This is a change of -0.34 percent, a significant amount, as shown in the previous figure. This is the normal variation of temperature experienced on a summer day, and may have some implications for practical operation of the TD 1288 system.

- Temperature stability, change with time or storage.
- Flexure
- Frequency, or non-linear change over bandwidth.
- Humidity
- Tension
- Cutting, or error due to variation of dielectric constant
- Measurement error

Phase compensated cables exhibit much better performance in this regard, namely only 300 parts per million variation in electrical length from +50 to +70 degrees Farenheit, or .03%. These are usually semi-flexible, and cut to precise lenghts.

ANTENNA COMPENSATION

D.4 POSSIBLE VALUE OF PHASE CORRECTION

In a previous section, doubts were placed on the actual cable length used in the measurement. The actual antenna impedance rotates clockwise around the Smith Chart about 4-1/2 times, as the frequency is varied from 30 to 88 MHz. Also, the actual antenna VSWR is about 9:1, and its effect is softened by the cable attenuation.

The antenna itself, is center fed, and is thus reasonably unaffected by nearby loading effects, as compared to an end fed ground plane antenna.

Variations in the phase shift of the cable have profound effect on the impedance at the input of the cable. It is interesting to note that if a more stable cable were used, and if it had a lower loss, this could result in a higher VSWR at the cable input, and the 3.5:1 VSWR specification might not be met.

Initial consideration was given to greatly reduce the unit to unit variations of the cable and antenna assembly, and thus enable a simpler single antenna FHMUX. Namely, the antenna impedance might not have to be rigorously measured. A preliminary procedure to accomplish this was determined as follows:

- Collect statistical data on as many antennas as possible, review, final reports, and determine as accurately as possible, the average values of the antenna impedances, including weather effects.
- Ascertain the possibility of field retrofit of the antennas to add a small trimmer element which could make the antennas more alike.
- Determine whether it is possible to replace the RG 213 with a more stable cable, and compensate for the difference in loss.

Calibrate the FHMUX's in production against a "standard load" and provide means to correct for phase differences in the cable.

A block diagram of a possible phase correcting FHMUX is shown in FigureD-8. From early discussion, we can assume that the adjustable length of air line is to be manually adjusted. When properly set, it is left untouched until calibration is needed again.

At band edges and at mid-band, the adjustable air line can be set, and at these frequencies an indication of forward and reflected power can be read by the reflectometer, in one of the channels, and VSWR computed by the computations and control circuit.

During tuneup, it is desirable to protect the transmitter. If the filters inside the quadrature couplers are correctly, tuned, this assembly will only provide load isolation caused by the loss of the assembly. The quad coupled filter assembly is a reciprocal circuit in this regard. If the filters are off frequency, but similar in impedance, the load isolation is proportional to the off frequency isolation.

Thus, in the tuneup mode, it is desirable to slightly detune the first filter section to provide load isolation, but still allow enough RF energy into the output section to allow accurate calibration.

This scheme provides a means of standardizing the antenna load, and effects a simple way to accomplish it. It does not afford great precision, or optimum performance, but is simple.

Recent information tends to disallow this approach, in that field operation often calls for widely varying cable lengths. Also, this approach tends to limit the FHMUX to operation with one antenna type.

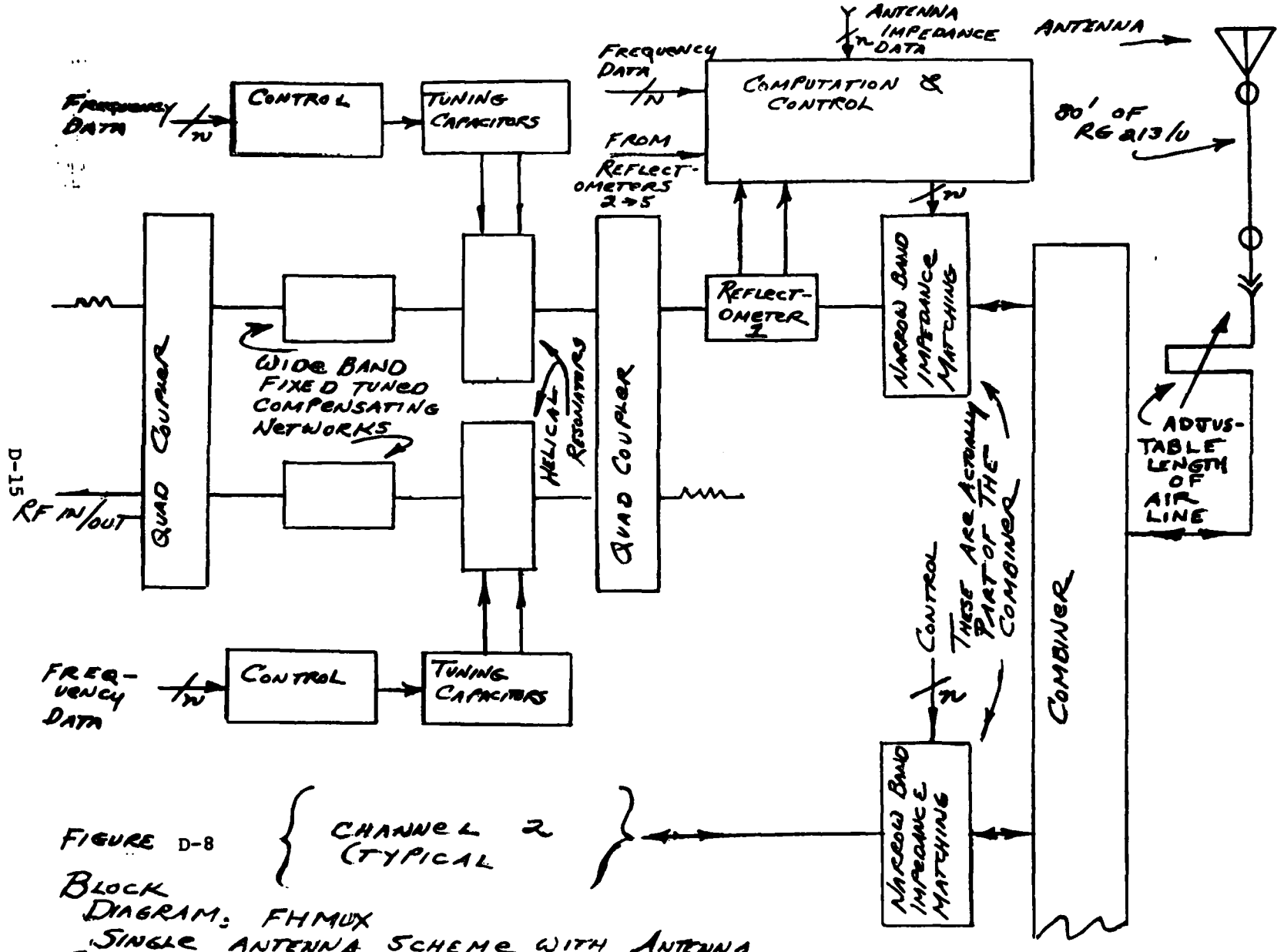

FIGURE D-8

BLOCK DIAGRAM: FHMUX SINGLE ANTENNA SCHEME WITH ANTENNA PHASE CORRECTION

D.5 THE SELF-CALIBRATING SINGLE ANTENNA FHMUX

The following discussion presents a preferred alternate to the antenna standardization/phase correction scheme previously discussed. For various reasons the phase correction scheme is not acceptable. The self-calibrating approach is more complex, but would provide optimum performance of a single antenna FHMUX despite antenna loading.

As mentioned, relatively small variations in the cable delay can cause severe changes in the impedance seen by the FHMUX. Thus a system with two modes of operation seems most feasible. These modes are calibrate and operate. Circuitry would be provided to measure impedance, and use the data to correct the output resonator such that an acceptable impedance match is obtained.

An additional consideration was the need for a +2%, -40 dB RF system bandwidth. As discussed earlier, 3 cascaded, high Q resonators will provide this selectivity. If the output resonator is not precisely aligned, the RF insertion loss will be unacceptably high.

The scheme presented will retain the frequency hopping features of the proposal.

D.6 ADVANTAGE OF SELF-CALIBRATION

The addition of low loss coaxial switches, and a 30 - 88 MHz low power synthesizer can greatly increase the utility of the FHMUX. Some of these advantages are listed:

- The FHMUX can stand alone regarding alignment and calibration, and not require "handshaking" with the driving transceivers. This will eliminate many troublesome interface problems.

- It may be possible to calibrate a given channel (or channels) while other channels are in use by the driving transceivers.
- The self-calibrate sequence can be relatively simple, because the input filter section does not have to be "pulled" off frequency to provide isolation for the driving transmitter.
- There is never any danger of damaging the transmitters in the calibrate mode because they are not required.
- The cost impact of this added utility is low.

The procedure described in the next section is preliminary in nature, but will serve to illustrate the flexibility that can be added to the FHMUX.

D.7 BLOCK DIAGRAM DESCRIPTION

Figure D-9 is a preliminary block diagram of a self-calibrating FHMUX.

The two input filter sections will be factory aligned and need not be compensated for variations in antenna impedance. It is not intended that these units be aligned or calibrated in the field.

As shown in Figure D-9, each channel output resonator/combiner section is preceeded by a low loss coaxial switch. In the "operate" mode, the RF path between the input filters and the output resonator/combiner is closed, and the FHMUX is functional. In the "calibrate" mode, the switch connects the VCO section of a low power synthesizer to the output resonator/combiner. Thus, there are 5 of these VCO's; the tuning voltage and the RF sample are "time shared" with the phase locked loop. The use of a single phase locked loop with switched multiple VCO's greatly simplifies the RF switching scheme.

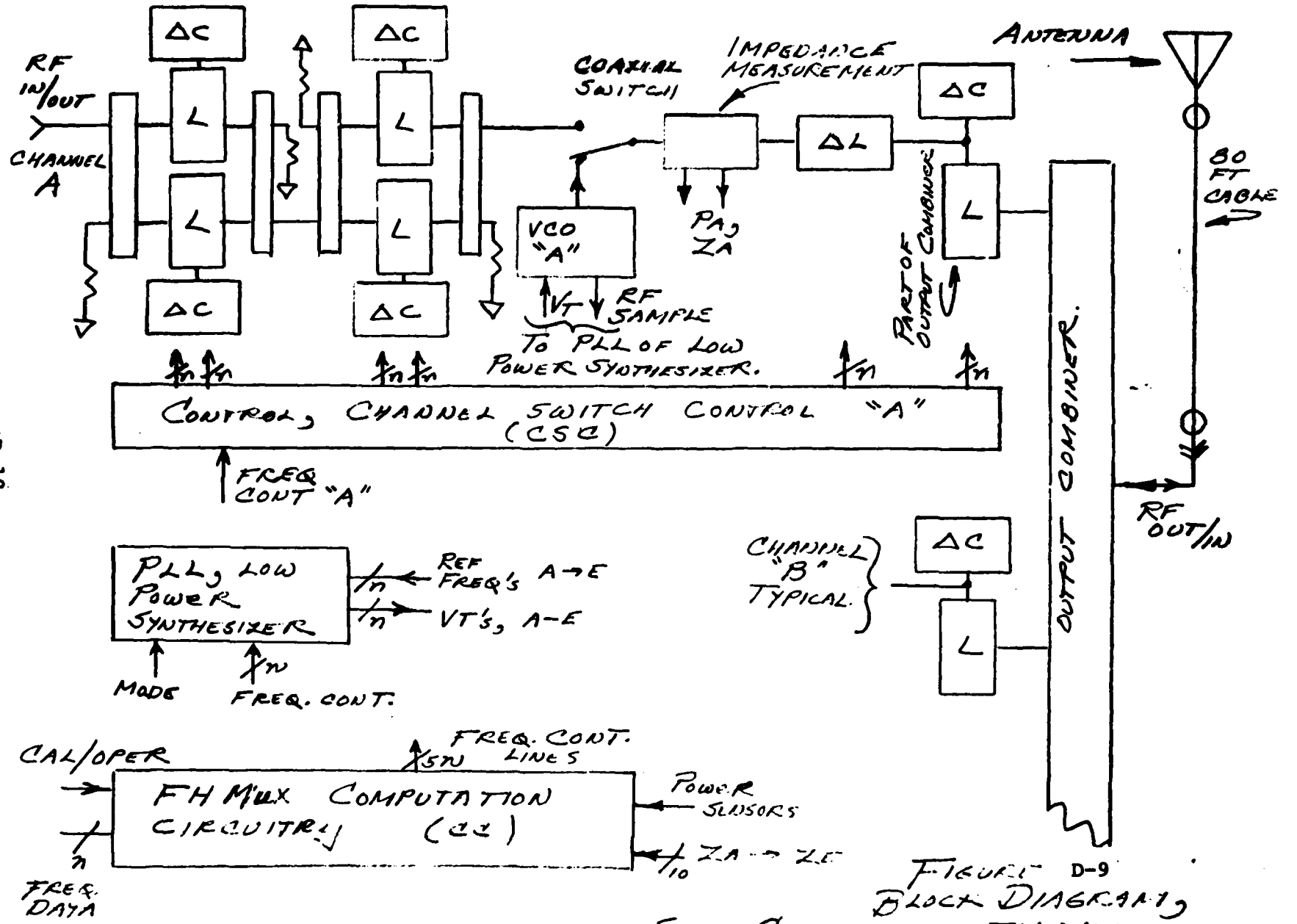

FIGURE D-9
BLOCK DIAGRAM, SELF CALIBRATING FH MUX

The use of the low loss coaxial switches will enable calibration to proceed without the need to add or remove any cables.

Thus, in the calibrate mode, a low level RF signal, at the desired frequency, is injected into one channel of the FHMUX, and enters an RF impedance measuring circuit which measures the impedance of the output resonator/combiner and the antenna, and provides an indication of whether the output resonator/combiner is properly aligned to match the antenna. The impedance of the antenna itself is not measured, but circuit action will tune the output resonator and combiner such that the impedance seen by the filter sections is acceptably close to 50 ohms.

D.8 ALIGNMENT PROCEDURE

There are two modes of operation; operate and calibrate. Once the calibration is performed, the alignment data for each frequency channel is stored and made ready for instant use in the operate mode. No alignment or optimization is performed when in the operate mode.

The need to calibrate the system may occur fairly often. As mentioned, temperature effects can cause the phase shift of the 80 foot cable to vary considerably during the course of the day. When calibration is deemed necessary, the command is given to the computational circuitry (CC), along with the identity of the FHMUX channel to be calibrated, and the frequency information relevant to the particular transceiver NET used with this FHMUX channel. This frequency data is changed into the identical format as that received from the transceivers when the FHMUX is in the operate mode. After the frequency data is logged in, the following events occur, all under control of the CC.

- The appropriate coaxial switch is placed in the calibrate position, enabling the VCO signal to enter the chosen FHMUX channel.
- The low power synthesizer and the desired VCO are locked up on the correct frequency.

The CC provides initial data to the channel switch control (CSC) to preset the output resonator/combiner to a nominal value. The combined action of the CC and CSC will then iteratively adjust the output section for the best possible impedance match.

The above process will be repeated for each frequency to be used in the channel. The data obtained is then stored in the CC for use in the operate mode.

Because of the narrow system RF bandwidth and expected manufacturing tolerances individual calibration of each of the FHMUX channels will be required rather than using the calibration data for any of the channels.

It may be desirable to calibrate more than one channel at a time, if so, the flexibility of this system enables. the following:

- The CC could arrange the desired frequencies in any desired order, along with the associated FHMUX channel I.D. Calibration could begin, and the CC could align the FHMUX channels in a random or other pattern, such that a particular set of frequencies could never be identified as being part of a particular net. This would be an additional safeguard for network security.

Alternate configurations undoubtedly exist which offer advantages over the scheme outlined above. The main point herein is that a programmable signal source can enable the FHMUX to stand alone to provide a necessary calibration operation.

D.9 IMPEDANCE MEASUREMENT TECHNIQUES

There are two basic methods of measuring impedance, namely, the well known reflectometer method and that of an EI cos ϕ sensor. The reflectometer method makes use of relatively large expensive directional couplers, and computes the complex reflection coefficient. The reflected RF voltage is divided by the incident RF voltage, and the phase angle between them is also measured. An important disadvantage is that under nearly matched conditions, the reflected voltage is very low, and may even be in the noise level. Thus fine tuning in the near matched case is difficult.

The EI cos ϕ technique was fully described in an appendix to the proposal, and is the favored approach for use in the calibrate mode. It is more accurate in the near match case than the reflectometer, can be made smaller, and will cost less. It also enables easy computation of the real power delivered to any load to which it is connected. This is of great importance in any antenna matching scheme.

D.10 OPERATIONAL SCENARIO

This scenario is based on the following FHMUX capabilities;

- A single antenna FHMUX is used, but this need not be firm at this time.

- All FHMUX calibrate circuits are internal to the FHMUX, including a low level programmable synthesizer.
- No high power emissions occur in the calibrate mode, typical calibrate emissions may be -20 to 0 dBm. If desired, some form of modulation could be used as a means of deception.

The FHMUX is installed at the site, or, in some form of vehicle. The antenna is connected to the FHMUX. Any antenna cable length is acceptable, the only requirement is that the VSWR looking "into" the cable be about 3.5.1, or less, and a center-fed antenna is preferred to reduce loading effects.

Up to 5 frequency hopping transceivers are put in place, and the 5 RF input/output cables from the transceivers are connected to the RF connectors on the FHMUX. Next, the cables which carry the frequency word data, and the transmit - receive status, are connected between the transceivers and the correct FHMUX receptacle. The system is now ready for calibration. The transceivers are not needed for this operation and are best left in an unpowered state. The FHMUX is energized and antenna calibration action begins. At some RF frequency in the band, a low level programmable synthesizer is energized and performs an RF impedance measurement. In an iterative manner the reactive elements in the FHMUX are configured for optimum match to the antenna in use. The digital control information thus obtained for the best match, is stored along with the associated digital RF frequency word. The calibration process continues until all programmed frequencies have been covered and stored.

Whether this channel calibration is suitable to the remaining four channels will depend primarily on manufacturing tolerances. Thus the remaining four channels can be likewise calibrated even in random manner if desired for security reasons. In any event only low level signals are radiated, and the FHMUX operates independently from the transceivers.

When calibration is complete, a set of calibration data is stored alongside the digital frequency word, for each RF frequency that is to be used in a any of the 5 transceiver channels.

With the microprocessor techniques currently available, this function could be accomplished in a manner of minutes. Once calibrated, the system is operable, and only need be recalibrated if the antenna is changed, or as a routine performance check.

To operate the system, the FHMUX is placed in the operate mode, and the transceivers are energized. Each transceiver will provide the FHMUX with a digital word (which identifies the next frequency to be used) during the dwell period. During this dwell time the FHMUX looks up the desired control data, and up on command aligns the FHMUX for this new frequency. No optimization or calibration occurs during the operate mode. Thus, each transceiver can operate in a frequency hopping mode into an antenna circuit that is now well matched.

If the system is installed in a vehicle and the antenna properly calibrated the use of a center fed antenna will serve to reduce the effects of a changing near field environment. The short duration perturbations of antenna characteristics caused by near field changes due to vehicle motion will most likely cause some detuning effects, but in the major portion of time the antenna will remain tuned and over all systems performance enhanced.

The matter of frequency collision avoidance, channel priority, and guard bandwidth are discussed in other sections, as well as the means of combining the transceivers to common antenna.

Thus it is seen that use of low RF level calibrating signals can extend the use of the FHMUX to accommodate many different antenna systems and environments.

Only a short period of time is needed for calibration, and once this is performed the only a-prior knowledge required from the transceivers is the next frequency word, the "hop command", and an indication of transmit/receive state.

101 Defense Technical Info Ctr
ATTN: DTIC-TCA
Cameron Station (Bldg 5)
*012 Alexandria, VA 22314

102 Director
National Security Agency
ATTN: TDL
001 Fort George G. Meade, MD 20755

103 Code R123, Tech Library
DCA Defense Comm Engrg Ctr
1860 Wiehle Ave
001 Reston, VA 22090

104 Defense Comm Agency
Tech Library Ctr
Code 205 (P.A. Tolovi)
002 Washington, DC 20305

200 Office of Naval Research
Code 427
001 Arlington, VA 22217

205 Commanding Officer
Naval Research Lab
ATTN: Code 2627
001 Washington, DC 20375

206 Commander
Naval Oceans Systems Ctr
ATTN: Library
001 San Diego, CA 92152

207 CDR, Naval Surface Weapons Ctr
White Oak Lab
ATTN: Library, Code WX-21
001 Silver Springs, MD 20910

210 Commandant, Marine Corps
HQ, US Marine Corps
ATTN: Code LMC
002 Washington, DC 20380

211 HQ, US Marine Corps
ATTN. Code INTS
001 Washington, DC 20380

212 Command, Control & Comm Div
Development Ctr
Marine Corps Development &
Education Command
001 Quantico, VA 22134

*Reduce to 2 copies if report bears a limited distribution statement.

215 Naval Telecommunications Cmd
Tech Library, Code 91L
4401 Massachusetts Avenue, NW
001 Washington, DC 20390

217 Naval Air Systems Comd
Code: Air-5332
004 Washington, DC 20360

219 Dr. T.G. Berlincourt
Ofc of Naval Research
(Code 420)
800 N. Quincy Street
001 Arlington, VA 22217

300 AUL/LSE 64-285
001 Maxwell AFB, AL 36112

301 Rome Air Development Ctr
ATTN: Documents Library (TSLD)
001 Griffiss AFB, NY 13441

302 USAFETAC/CBTL
ATTN: Librarian
Stop 825
001 Scott AFB, IL 62225

304 Air Force Geophysics Lab
L.G. Hanscom AFB
ATTN: LIR
001 Bedford, MA 01730

307 AFGL/SULL
S-29
001 HAFB, MA 01731

312 HQ, AFEWC
ATTN: EST
002 San Antonio, TX 78243

314 HQ, Air Force Systems Cmd
ATTN: DLWA/Mr. P. Sandler
Andrews AFB
001 Washington, DC 20331

403 Commander, MICOM
Redstone Scientific Info Center
ATTN: Chief, Document Section
002 Redstone Arsenal, AL 35809

404 Commander, MICOM
ATTN: DRSMI-RE (Mr. Pittman)
001 Redstone Arsenal, AL 35809

406 Commandant
US Army Aviation Ctr
ATTN: ATZQ-D-MA
001 Fort Rucker, AL 36362

408 Commandant
US Army Military Police School
ATTN: ATZN-CDM-CE
003 Fort McClellan, AL 36205

417 Commander
US Army Intelligence Ctr & School
ATTN: ATSI-CD-MD
003 Fort Huachuca, AZ 85613

418 Commander
HQ Fort Huachuca
ATTN: Technical Ref Div
001 Fort Huachuca, AZ 85613

419 Commander
US Army Elct Proving Ground
ATTN: STEEP-MT
001 Fort Huachuca, AZ 85613

422 Commander
US Army Yuma Proving Ground
ATTN: STEYP-MTD (Tech Library)
001 Yuma, AZ 85364

432 Dir, US Army Air Mobility R&D Lab
ATTN: T. Gossett, Bldg 207-5
NASA AMES Research Ctr
001 Moffett Field, CA 94035

436 HQDA (DAMO-TCE)
002 Washington, DC 20310

437 Deputy for Science & Tech
Office, Asst Sec Army (R&D)
002 Washington, DC 20310

438 HQDQ (DAMA-ARZ-D/Dr. F. D. Verderme)
001 Washington, DC 20310

455 Commandant
US Army Signal School
ATTN: ATZH-CD
001 Fort Gordon, GA 30905

456 Commandant
US Army Infantry School
ATTN: ATSH-CD-MS-E
001 Fort Benning, GA 31905

462 CDR, ARRCOM
ATTN: Systems Analysis Ofc, DRSAR-PE
001 Rock Island, IL 61299

470 Dir of Combat Developments
US Army Armor Ctr
ATTN: ATZK-CD-MS
002 Fort Knox, KY 40121

474 Commander
US Army Test & Evaluation Cmd
ATTN: DRSTE-CT-C
001 Aberdeen Proving Ground, MD 21005

475 CDR, Harry Diamond Lab
ATTN: Library
2800 Powder Mill Road
001 Adelphi, MD 20783

477 Director
US Army Ballistic Research Lab
ATTN: DRXBR-LB
001 Aberdeen Proving Ground, MD 21005

479 Director
US Army Human Engineering Lab
001 Aberdeen Proving Ground, MD 21005

482 Director
US Materiel Systems Analysis Activity
ATTN: DRXSY-T
001 Aberdeen Proving Ground, MD 21005

483 Director
US Army Materiel Systems
Analysis Activity
ATTN: DRXSY-MP
001 Aberdeen Proving Ground, MD
21005

503 Director
US Army Engr Waterways Exper
Station
ATTN: Research Ctr Library
002 Vicksburg, MS 39108

504 Chief, CERCOM Aviation Elct Ofc
ATTN: DRSEL-MME-LAF(2)
001 St. Louis, MO 63166

507 CDR, AVRADCOM
ATTN: DRSAV-E
PO Box 209
001 St. Louis, MO 63166

512 Commander
ARRADCOM
ATTN: DRDAR-LCN-S (Bldg 95)
001 Dover, NJ 07801

513 Commander
ARRADCOM
ATTN: DRDAR-TSS, #59
001 Dover, NJ 07801

514 Director
Joint Comm Ofc (TRI-TAC)
ATTN: TT-AD (Tech Doc Cen)
001 Fort Monmouth, NJ 07703

515 PM, FIREFINDER/ REMBASS
ATTN: DRCPM-FER
BLDG 2539
001 Fort Monmouth, NJ 07703

516 Project Manager, NAVCON
ATTN: DRCPM-NC-TM
Bldg 2539
001 Fort Monmouth, NJ 07703

517 Commander
US Army Satellite Comm Agcy
ATTN: DRCPM-SC-3
002 Fort Monmouth, NJ 07703

518 TRI-TAC Office
ATTN: TT-DA
001 Fort Monmouth, NJ 07703

519 CDR, US Army Avionics Lab
AVRADCOM
ATTN: DAVAA-D
001 Fort Monmouth, NJ 07703

529 CDR, US Army Research Ofc
ATTN: Dr. Horst Wittmann
PO Box 12211
001 Research Triangle Park, NC
27709

531 CDR, US Army Research Ofc
ATTN: DRXRO-IP
PO Box 12211
002 Research Triangle Park, NC
27709

533 Commandant
US Army Inst for Military Asst
ATTN: ATSU-CTD-MO
002 Fort Bragg, NC 28307

536 Commander
US Army Arctic Test Ctr
ATTN: STEAC-TD-MI
002 APO Seattle 98733

542 Commandant
USAFAS
ATTN: ATSF-CD-DE
001 Fort Sill, OK 73503

554 Commandant
US Army Air Defense School
ATTN: ATSA-CD-MS-C
001 Fort Bliss, TX 79916

563 Commander, DARCOM
ATTN: DRCDE
5001 Eisenhower Ave
001 Alexandria, VA 22333

565 CDR, US Army Signals Warfare Lab
ATTN: DELSW-SO
Vint Hill Farms Station
002 Warrenton, VA 22186

566 CDR, US Army Signals Warfare Lab
ATTN: DELSW-AQ
Vint Hill Farms Station
001 Warrenton, VA 22186

567 Commandant
US Army Engineer School
ATTN: ATZA-TDL
002 Fort Belvoir, VA 22060

569 Commander
US Army Engineer Topographic Labs
ATTN: ETL-TD-EA
001 Fort Belvoir, VA 22060

572 Commander
US Army Logistics Ctr
ATTN: ATCL-MC
002 Fort Lee, VA 22801

575 Commander
TRADOC
ATTN: ATDOC-TA
001 Fort Monroe, VA 23651

577 Commander
US Army Training & Doctrine Cmd
ATTN: ATCD-TM
001 Fort Monroe, VA 23651

578 CDR, US Army Garrison
Vint Hill Farms Station
ATTN: LAVAAF
001 Warrenton, VA 22186

579 Proj Mgr, Control & Analysis Ctrs
Vint Hill Farms Station
001 Warrenton, VA 22186

602 CDR, Night Vision & Electro-Optics Laboratory
ERADCOM
ATTN: DELNV-D
001 Fort Belvoir, VA 22060

603 CDR, Atmospheric Sciences Lab
ERADCOM
ATTN: DELAS-SY-S
001 White Sands Missile Range, NM 88002

604 Chief
Ofc of Missile Electronic Warfare
Electronic Warfare Lab
ERADCOM
001 White Sands Missile Range
NM 88002

606 Chief
Intel Materiel Dev & Support Office
Electronic Warfare Lab
ERADCOM
001 Fort Meade, MD 20755

608 Commander
US Army Ballistic Rsch Lab/ARRADCOM
ATTN: DRDAR-TSB-S (STINFO)
001 Aberdeen Proving Ground, MD 21005

612 CDR, ERADCOM
ATTN: DRDEL-CT
2800 Power Mill Road
002 Adelphi, MD 20783

619 CDR, ERADCOM
ATTN: DRDEL-PA
2800 Powder Mill Road
001 Adelphi, MD 20783

622 HQ, Harry Diamond Lab
ATTN: DELHD-TD (Dr. W.W. Carter)
2800 Powder Mill Road
001 Adelphi, MD 20783

680 Commander
ERADCOM
Fort Monmouth, NJ 07703
1 DELEW-D
1 DELCS-D
1 DELET-D
1 DELSD-L
1 DELSD-D
*2 DELSD-L-S

*Furnish only unclassified reports.

681 Commander, CECOM
Fort Monmouth, NJ 07703

1 DRSEL-PPA-S
1 DRSEL-COM-D
1 DRSEL-TCS-B
1 DRSEL-PL-ST
1 DRSEL-MA-MP
1 DRSEL-LE-RI
1 DRSEL-PA
1 DRSEL-LE-C
3 DRSEL-COM
25 DRSEL-COM-RN

701 MIT-Lincoln Lab
ATTN: Library (Rm A-082)
PO Box 73
002 Lexington, MA 02173

703 NASA Scientific & Tech Info Facility
Baltimore/Washington Intl Airport
001 PO Box 8757, MD 21240

704 National Bureau of Standards
Bldg 225, RM A-331
ATTN: Mr. Leedy
001 Washington, DC 20231

706 Advisory Group on Electron Devices
ATTN: Secy, Working Grp D (Lasers)
201 Varick Street
002 New York, NY 10014

707 TACTEC
Battelle Memorial Inst
505 King Ave
001 Columbus, OH 43201

709 Plstics Tech Eval Ctr
Picatinny Arsenal, Bldg 176
ATTN: Mr. A.M. Anzalone
001 Dover, NJ 07801

710 Ketron, Inc.
1400 Wilson Blvd, Architect Bldg
002 Arlington, VA 22209

712 R. C. Hansen, Inc.
PO Box 215
001 Tarzana, CA 91356

714 Dynalectron Corp
GIDEP Engineering & Support
Department
PO Box 398
001 Norco, CA 91760